ELECTRO-ASSISTED PHYTOREMEDIATION (EAPR) OF HEAVY METALS IN SYNTHETIC WASTEWATER USING *Pistia stratiotes*: PHYSIOLOGICAL AND TRANSCRIPTOMIC ANALYSES

CHAN MUN YEE

DOCTOR OF PHILOSOPHY (SCIENCE)

FACULTY OF SCIENCE
UNIVERSITI TUNKU ABDUL RAHMAN
OCTOBER 2025

ELECTRO-ASSISTED PHYTOREMEDIATION (EAPR) OF HEAVY METALS IN SYNTHETIC WASTEWATER USING *Pistia stratiotes*: PHYSIOLOGICAL AND TRANSCRIPTOMIC ANALYSES

By

CHAN MUN YEE

A thesis submitted to the Department of Chemical Science
Faculty of Science
Universiti Tunku Abdul Rahman,
in partial fulfillment of the requirements for the degree of
Doctor of Philosophy in Science
October 2025

This thesis is submitted in partial fulfilment of the requirements for the degree of Doctor of Philosophy in Science at Universiti Tunku Abdul Rahman (UTAR). This thesis represents the work of the author, except where due acknowledgment has been made in the text. No part of this thesis may be reproduced, stored, or transmitted in any form or by any means, whether electronic, mechanical, photocopying, recording, or otherwise, without the prior written permission of the author or UTAR, in accordance with UTAR's Intellectual Property Policy.

ABSTRACT

ELECTRO-ASSISTED PHYTOREMEDIATION (EAPR) OF HEAVY METALS IN SYNTHETIC WASTEWATER USING *Pistia stratiotes*: PHYSIOLOGICAL AND TRANSCRIPTOMIC ANALYSES

Chan Mun Yee

Landfilling is the most common solid waste disposal approach, yet leachate treatment remains challenging due to the presence of toxic heavy metals (HMs) that pose long-term environmental and health risks. Electro-Assisted Phytoremediation (EAPR) is an electrical enhancement of phytoremediation designed to improve leachate remediation. EAPR overcomes mass-transfer limitations by driving mobilization of dissolved metals and charged contaminants toward the rhizosphere. The primary aim of this study was to evaluate the HM removal from synthetic leachate between EAPR and non-EAPR, alongside changes in leachate physicochemical parameters, *P. stratiotes's* physiological responses, and Pb-induced molecular responses.

EAPR significantly reduced Biochemical Oxygen Demand, colour and turbidity ($p < 0.05$) with minimal impact on growth. HMs accumulated more in roots, with Pb and Fe displaying the highest Bioconcentration Factor and removal efficiency, while translocation factor values less than one implied restricted root transport. Antioxidative enzyme assays revealed increased activity of superoxide

dismutase, ascorbate peroxidase, and glutathione reductase in leaves and root peroxidase, suggesting enhanced reactive oxygen species scavenging.

RNA-Sequencing revealed Pb stress upregulated root differentially expressed genes (DEGs), but downregulated leaf DEGs, while EAPR reversed this trend. Functional enrichment analysis revealed distinct tissue-specific expression profiles, with Pb stress upregulated DEGs enriched in the Mitogen Activated Protein Kinase (MAPK)-plant, Ras and cyclic adenosine monophosphate (cAMP) signalling pathwayin root, which EAPR suppressed. Ten key regulatory genes were identified through which EAPR reverses Pb-induced transcription across MAPK, hormone and metal-homeostasis signaling networks. Quantitative Reverse Transcription-Polymerase Chain Reaction confirmed MAPK pathway involvement.

Overall, EAPR enhanced leachate remediation by improving HM removal and water quality, while maintaining plant growth. Electro-assisted increased root accumulation and antioxidant defenses, while transcriptomic regulation alleviated Pb-induced stress. These findings demonstrate that EAPR is an effective, mechanistically driven strategy for accelerating phytoremediation and support its practical application for leachate treatment.

Keywords: EAPR; wastewater; *P. stratiotes;* heavy metal; transcriptome

Subject Area: QK710-899 Plant physiology

ACKNOWLEDGEMENTS

First and foremost, I am deeply indebted to God for His grace, strength and sustenance, so that I have been finally able to accomplish this doctoral level.

I am deeply indebted to my supervisors for this research, Assoc. Prof. Dr. Chai Tsun Thai and Dato' Dr. Sim Yoke Leng, for their guidance, advice and supervision. I wish to thank my former supervisor, Asst. Prof. Dr. Tee Chong Siang for his mentorship and support throughout this research. Further acknowledgement to the financial support provided by UTARRF grants (IPSR/RMC/UTARRF/2017-C2/C01 and IPSR/RMC/UTARRF/2021-C2/C02).

I would like to express my deepest appreciation to the lab officers for all their kind assistance. I am grateful to the Department of Chemical Science and Department of Allied Health Sciences of UTAR for the laboratory facilities, instruments and equipments which have been provided.

This endeavor would not have been possible without the unwavering support of my husband, Tan Gim Cheong, children (Tan Janie and Tan Jaron), family members, church members and colleagues throughout this research. Dedicating this thesis, especially to my late father, Mr. Chin Chong @ Chan Chor.

TABLE OF CONTENTS

LIST OF TABLES

LIST OF FIGURES

LIST OF ABBREVIATIONS

ABA	Abscisic acid
ABC transporters	ATP-binding cassette transporters
AC	Alternate current
ACs	Adenylyl cyclases
ADP	Adenosine diphosphate
AIK1	ABA-insensitive protein kinase 1
AKAPs	A-kinase anchoring proteins
AMP	Adenosine monophosphate
ANOVA	Analysis of variance
AOPs	Advanced oxidation processes
APX	Ascorbate peroxidase
Arf/Sar	Adenosine diphosphate-ribosylation factor / Secretion-associated and Ras-related protein
ASA	Ascorbic acid
AsA	Reduced ascorbate
AsA-GSH	Ascorbate-glutathione
AtCNGC1	*Arabidopsis thaliana* cyclic nucleotide-gated channel 1
AtMKK	*Arabidopsis thaliana* Mitogen-activated protein kinase kinase
ATMYC2/JIN1	Transcription factor MYC2/ JASMONATE INSENSITIVE 1 (JIN1)
ATP	Adenosine triphosphate
BCF	Bioconcentration factor
bHLH	Basic helix-loop-helix.

BOD_5	Biochemical oxygen demand over 5 days
BP	Biological process
bp	Base pair
$C_2H_3NaO_2$	Sodium acetate
C_3H_5NaO2	Sodium propanoate
$C_9H_8Na_2O_4$,	Humic acid sodium salt/ Sodium bicyclo(2.2.1)hept-5-ene-2,3-dicarboxylate
CA	Calmodulin
CA5	Calmodulin 5
$CaCl_2.2H_2O$	Calcium chloride dihydrate
CAL	Calcium-binding protein NCS-1-like
cAMP	Cyclic AMP
$Ca(NO_3)_2.4H_2O$	Calcium nitrate tetrahydrate
CAT/HAC	Catalase
Cat. No.	Catalogue Number
CC	Cellular component
$CdCl_2 \cdot 2.5H_2O$	Cadmium chloride hemipentahydrate
cDNA	Complementary DNA
CDPKs	Calcium-dependent protein kinases
cGMP- PKG	Cyclic guanosine monophosphate (cGMP)-dependent protein kinase
CNGCs	Cyclic nucleotide-gated channels
COD	Chemical oxygen demand
Cr(VI)	Hexavalent chromium

CREB	cAMP response element binding protein
Cu/Zn-SOD	Copper/zinc SOD
CuO-NPs	Copper oxide nanoparticles
DAsA	dehydroascorbate
DC	Direct current
DEGs	Differentially expressed genes
DHAR	Dehydroascorbate reductase
DNA	Deoxyribonucleic acid
DO	Dissolved oxygen
DTT	Dithiothreitol
EAPR	Electro-assisted phytoremediation
E.C.	Enzyme commission
EDTA	Ethylenediaminetetraacetic acid
e.g.	Exempli gratia
Epac	Exchange protein
ERK	Extracellular signal-regulated kinase
ESTs	Expressed sequence tags
et al.	et alia
FAAS	Flame atomic adsorption spectrophotometer
$FeCl_3 \cdot 6H_2O$)	Iron(III) chloride hexahydrate
Fe-SOD	Iron SOD
FPKM	Fragments per kilobase of transcript per million mapped reads

GA	Gibberellins
GC content	Guanine-cytosine content
GDIs	Guanine nucleotide dissociation inhibitors
GDP	Guanosine diphosphate.
GEFs	Guanine nucleotide exchange factors
GO	Gene ontology
GOseq	Gene ontology (GO) analysis of RNA-seq data
GPOX	Glutathione peroxidase
GR	Glutathione reductase
GSH	Reduced glutathione
GSSG	Oxidized glutathione
GT	GTP-binding protein rhoA-like
GTP	Guanosine triphosphate.
GTPases	Guanosine triphosphatase
GUA	Guanine nucleotide-binding protein subunit beta-like
HFA	Humic and fluvic acids
HMs	Heavy metals
HNO_3	Nitric acid
HSD	Honestly significant difference
IAA	Auxin
IP	Iron plaque
IRT	Iron-regulated transporter
JA	Jasmonic acid

KAS	Ketoacyl-acyl carrier protein synthase I
KCl	Potassium chloride
KEGG	Kyoto encyclopedia of genes and genomes
KH_2PO_4	Potassium dihydrogen phosphate
KNO_3	Potassium nitrate
MAPK	Mitogen-activated protein kinase
MAPKK	Mitogen-activated protein kinase kinase
MAPKKK	Mitogen-activated protein kinase kinase kinase
MDAsA	Monodehydroascorbate
MDHAR	monodehydroascorbate reductase
MEKK1	Mitogen-activated protein kinase kinase kinase 1
MF	Molecular function
$MgCl_2.2H_2O$	Magnesium dichloride dihydrate
$MgCl_2.6H_2O$	Magnesium chloride hexahydrate
MIR genes	miRNA genes
MKK	Mitogen-activated protein kinase kinase
$MnCl_2 \cdot 4H_2O$	Manganese(II) chloride tetrahydrate
Mn-SOD	Manganese SOD
MPK	Mitogen-activated protein kinase
mRNA	Messenger ribonucleic acid
MSW	Municipal solid waste
MT	Metal transporters
MYB	Myeloblastosis

N50	Spliced transcripts are sorted by length from long to short, and the length of spliced transcripts is N50
N90	Spliced transcripts are sorted by length from long to short, and the length of spliced transcripts is N90
$NADP^+$	Nicotinamide Adenine Dinucleotide Phosphate
NADPH	Reduced nicotinamide adenine dinucleotide phosphate
NBT	Nitroblue tetrazolium
NH_3–N	Ammonia nitrogen
NH_4Cl	Ammonium Chloride
$NiCl_2 \cdot 6H_2O$	Nickel(II) chloride hexahydrate
NRAMP	Natural resistance-associated macrophage proteins
NtCBP4	Nicotiana tabacum Calmodulin-Binding Protein 4
NTU	Nephelometric Turbidity Unit
ORP	Oxidation-Reduction Potential
OsRac1	Rac-like GTP-binding protein 1 from *Oryza sativa*
P. stratiotes	*Pistia stratiotes*
$Pb(NO_3)_2$	Lead(II) nitrate
PC	Phytochellatins
PDEs	Phosphodiesterases
PfbZIP85	*Perilla frutescens* basic-leucine zipper (bZIP) transcription factor 85
PKA	Protein kinase A
PMSF	Phenylmethylsulphonyl fluoride
Popdcs	Popeye domain-containing proteins
POX	Peroxidase

PP2C	Protein Phosphatase 2C
ppm	Parts per million
ppt	Parts per thousand
PSI	Photosystem I
PSII	Photosystem II
Pt/Co	Platinum Cobalt
PVPP	Polyvinylpolypyrrolidone
PYR/PYL/RCAR	Pyrabactin Resistance/Pyrabactin Resistance-Like/Regulatory Components of Abscisic Acid Receptor
Q20	The percentage of the bases whose Q Phred values is greater than 20
Q30	The percentage of the bases whose Q Phred values is greater than 30
qRT-PCR	Quantitative Reverse Transcription-Polymerase Chain Reaction
Q score	Phred quality score
Rab	Ras-like in brain
RAB	Rab5b rab family GTPase
RabE1c	Ras-related protein RABE1c
raf	Rapidly accelerated fibrosarcoma
Ran	Ras-like nuclear protein
Rap1	Ras-proximate-1
RAS	Rat sarcoma
RBOH	Respiratory burst oxidase homolog

Rho	Ras homolog
RNA	Ribonucleic acid
RNA-Seq	RNA sequencing
ROPs	Rho-like GTPases from Plants
ROS	Reactive oxygen species
RPs	Ribosomal proteins
rRNA	Ribosomal ribonucleic acid
RSEM	RNA-Seq by Expectation-Maximization
sAC	Soluble ACs
SE	Standard error
-SH	–Sulfhydryl group
SnRK2	SNF1-related protein kinase 2
SOD	Superoxide dismutase
TDS	Total dissolved solids
TF	Translocation factor
TFs	transcription factors
TmAC	Transmembrane ACs
tris-HCl	Tris(hydroxymethyl)aminomethane hydrochloride
U/g fw	Units per gram fresh weigh
UV-VIS	Ultraviolet-visible
VFA	Volatile fatty acids
WRI1	WRINKLED1
ZIP	Zrt-/Irt-like protein

ZmMPK	*Zea mays* mitogen-activated protein kinase
$ZnSO_4 \cdot 7H_2O$	Zinc sulfate heptahydrate

CHAPTER 1

INTRODUCTION

1.1 Background of Study

The overcrowding of solid waste systems is a persistent challenge worldwide. Human activities, such as household, commercial and industrial contribute to the generation of solid waste (Zulkipli, et al., 2020). Nearly 60 tonnes of domestic waste are generated globally per second, which amounts to approximately 2 billion tonnes/annum (Cheng, et al., 2022). By 2050, global waste production is projected to reach 3.40 billion metric tonnes. In Malaysia, the continuous population growth has caused tremendous solid waste (40,000 tonnes/day), of which approximately 95 percent will end up in landfills (Taib, et al., 2021; Bernama, 2022).

Effective solid waste management is essential for environmental protection and the sustainability of community life (Zulkipli, et al., 2020). Proper waste treatment is crucial for environmental protection, public health, resource conservation (Abubakar, et al., 2022), prevention of pollution (Abdullah, Salleh and Ismail, 2017) and disease outbreaks (Choon, Tan and Chong, 2017). In developing countries, besides open burning of waste, open dumping (Yukalang,

Clarke and Ross, 2017; Vaccari, Vinti and Tudor, 2018) and incineration, the most common alternative for waste disposal is landfilling (Siddiqua, et al., 2022). Numerous gas emissions and ash residues are released during open burning, which could endanger both the environment and humans (Powrie, et al., 2021). This practice is usually undertaken with open dumping on the water surface or open ground (Reyna-Bensusan, et al., 2019). Incineration involves burning waste in a furnace to recover energy released during combustion, while substantially reducing the amount of solid waste generated. This approach can significantly reduce waste volume (Traven, 2023; Maphuhla and Oyedeji, 2025).

On the other hand, a landfill is where the final-stage waste is disposed of, from collection to transportation and finally disposal (Abidin, et al., 2024). It is a standard method adopted by lower and upper-middle-income countries to curb waste disposal problems (Aziz and Ariffin, 2024). Three classes of landfills are class I (municipal solid waste), II (industrial waste) and II (hazardous waste landfills) (Butti, Peres and Lops, 2018; Siddiqua, et al., 2022). Microorganisms present in the land will decompose the organic contents of the dumped materials (Yaashikaa, et al., 2022), producing greenhouse gases and liquid (leachate) as by-products (Anqi, et al., 2020). Landfill leachate often contains high amounts of organic pollution [e.g. BOD_5 (Biochemical Oxygen Demand 5) and Chemical oxygen demand (COD)], along with variable pH (often mildly acidic to neutral/alkaline), high ammoniacal nitrogen and total dissolved solids (TDS). Studies report BOD_5 can range from hundreds to over 20 000 mg/L and COD from

several thousand to tens of thousands mg/L (Saghi, et al., 2024; Sharma, et al., 2026). Notorious contaminants, such as heavy metals (HMs), organic carbons and microplastics are also present in leachate (Gunarathne, et al., 2024). According to Yusof, et al. (2009) and Hussein, et al. (2021), at a leachate discharge flow rate of 400 mm/year, HMs can persist in landfill sites for as long as 150 years.

HMs in landfills are from industrial wastes, mining wastes, incinerator ashes and domestic hazardous items (Erses and Onay, 2003). These include co-disposed batteries, paints and dyes (Erses and Onay, 2003). HMs, such as lead (Pb), are commonly found in batteries, cans and paint. Cadmium (Cd), ferum (Fe), and cuprum (Cu) are elements present in iron-based and electric waste tools (Santoso, et al., 2016). In addition, HMs in landfills are likely created via leaching from natural soils under certain circumstances (Hussein, et al., 2021). As these ubiquitous metals do not decompose, they pose a severe environmental and human health hazard due to their toxicity and carcinogenicity properties (Abu-Rukah and Abu-Aljarayesh, 2002). They are well known for their long-term existence in the environment and ability to accumulate within living organisms (Oladimeji, et al., 2024).

It is critical to handle waste appropriately, as HMs pose serious hazards, inflicting harm to human health, disrupting aquatic habitats, and disturbing the delicate biological balance of natural systems (Gworek, et al., 2016; Oladimeji, et

al., 2024). There are many ways to remediate landfill leachate, which generally can be categorized into biological, physical and chemical methods (Mojiri, et al., 2021; Hussein, et al., 2021). Malaysia has employed biological techniques, such as anaerobic-aerobic treatment (Er, et al., 2017) and biofilter system (Nik Daud, et al., 2015), as well as physical and chemical methods (electrocoagulation, coagulation-flocculation) (Taib, et al., 2021). Er, et al. (2017) study employed *Brevibacillus panacihumi* strain ZB1 in a 42-day combined anaerobic-aerobic process to treat leachate. This technique reduced approximately 40% of COD, 50% of ammonia nitrogen and varying contents of HMs. On the other hand, Taib et al. (2021) demonstrated that via utilizing aluminium electrodes, electrocoagulation is able to moderately reduce total suspended solids (44.38%), COD (42.88%), BOD_5 (25.88%), ammonia–nitrogen (13.54%) and colour (31.21%). This highlights the potential of electrochemical method as an enhancement treatment for landfill leachate.

Under many controlled laboratory conditions, synthetic wastewater is commonly adopted to simulate contaminated wastewater. Researchers can control physicochemical parameters, including ionic and pollutant concentrations. This enables the reproducible evaluation of treatment technologies before their application to complex environmental matrices. The formulation of synthetic wastewater often resembles real effluents for the mechanistic study of contaminant removal processes (Grossule, et al., 2022; Xiang, et al., 2025). However, real leachate exhibits much greater chemical complexity than synthetic systems, thereby

affecting treatment efficacy. Nevertheless, results from the synthetic wastewater treatment ought to be cautiously interpreted when applied to real leachate environments, despite the preliminary insights provided (Sossou, et al., 2024). In this context, while preserving experimental control, synthetic leachate formulations are often used to mimic the composition of landfill leachate. Such an approach enables remediation strategies to be systematically evaluated prior to field-scale testing. However, leachate treatment efficiency may decline in aging landfills due to the presence of stabilized, refractory compounds that challenge conventional purification technologies (Teng, et al., 2021). Hence, new techniques are needed to effectively remediate the hazardous environmental impact of landfill leachates (Putra and Hastika, 2018).

Although primary biological and physicochemical treatments effectively remove bulk organic load and suspended solids in landfill leachate, the presence of persistent HMs and residual nutrients often exceeds permissible discharge limits. These recalcitrant contaminants present continuous environmental threats, which include increasing amounts of COD, ammonia and HM content (Xiang, et al., 2025). Phytoremediation offers an economical and sustainable tertiary treatment to further eradicate such residual pollutants from wastewater. However, its efficacy is restricted by factors such as slow mass transfer and HM uptake rates. Thus, in this study, electro-assisted phytoremediation (EAPR) was adopted to improve pollutant transport toward the rhizosphere and enhance plant accumulation. EAPR increases the feasibility of phytoremediation as a secondary or tertiary leachate treatment

strategy (Putra and Hastika, 2018; Bayuo, et al., 2024). In phytoremediation, researchers have explored many plant species such as *Typha angustifolia*, *Acorus calamus* (Bhagwat, Boralkar and Chavhan, 2018), *Alcea rosea* (hollyhock), *Cynodon dactylon* (Bermuda grass), *Melilotus officinalis* (yellow melilot) (Erdogan and Zaimoglu, 2015) and *Pistia stratiotes* for potential leachate remediation. Among these plant species, *P. stratiotes*, also known as water lettuce or water cabbage, from the Araceae family, has great potential for phytoremediation. According to Quattrocchi (2017), it is primarily found in lakes, streams, and ponds. This plant is well recognized for its capability to eliminate HMs from the contaminated environment based on high bioconcentration and translocation capacities (Wibowo, Nugraha and Rohman, 2023). Nevertheless, there are numerous setbacks to phytoremediation (Schwitzguébel, 2017), such as the need for an adequate site size for the application of farming techniques, and particularly, the requirement that contaminants be within the root zones of plants used for phytoremediation (Tripathi, et al., 2020).

Electro-assisted phytoremediation, also known as EAPR, is a method used to overcome the shortcomings of phytoremediation with the addition of electrical input (Putra, Annisa and Budiarjo, 2022). The electric field applies a direct or alternating current to electrodes inserted into polluted sources. This method mobilizes metal ions from a polluted source and improve uptake by the plant roots (Akemoto, Tanaka and Putra, 2022). Proton is then produced around the anode via the effect of water electrolysis. Therefore, more metals and metaloids can be

demobilized around the anode electrode under an acidic condition (Thangavel and Subbhuraam, 2004), which are subsequently transported to the cathode (Dermont, et al., 2008). The HM ions will then be transported to the shoot of plants via adsorption process (Putra, Ohkawa and Tanaka, 2013; Putra and Hastika, 2018) and subsequenly extracted through phytoremediation (O'Connor, et al., 2003). Phytoremediation alone is often limited by slow mass transfer in water environments. Hence, EAPR enables greater uptake and removal of HMs (eg. Fe, Cu, Cd, and Pb), increases dissolved oxygen and further supports plant growth. The application of an electrical field can enhance pollutant removal, while concurrently maintaining the physiological stability of aquatic macrophytes (Putra and Hastika, 2018). Floating aquatic plants, such as *P. stratiotes* is able to eradicate organic and inorganic pollutants such as HMs, TDS, BOD and COD. This plant is pertinent as a biofilter in water treatment due to its extensive root systems, large biomass and easy to harvest (Pang, et al., 2023). The combination of these characteristics makes EAPR a polishing method for phytoremediation alone in the remediation of aquatic systems, such as residual leachate contaminants.

An increase in HM concentrations in plants can lead to increased plant stress, decreased plant growth and alterations in nutrient uptake (Bibi, et al., 2024). In response to HM stress, plants employ changes in gene expression (Li, et al., 2017a; Cong, et al., 2019) involved in regulating transporters or metal chelators that favour the detoxification or exclusion of HMs (Gulli, et al., 2018; Zhang, et al., 2019). These responses include the activation of metal transporter genes [e.g.

heavy-metal ATPases (HMA family), natural resistance-associated macrophage protein (NRAMP), Zinc-regulated/Iron-regulated transporter-like Protein (ZIP) (Zhu, et al., 2022)], chelation and vacuolar sequestration systems (e.g. phytochelatin synthase and metallothioneins) (Raza, et al., 2022), antioxidant defense genes [e.g. superoxide dismutase (SOD), catalase (CAT) and ascorbate peroxidase (APX)] (Tyagi, et al., 2024) and stress-signaling pathways that are controlled by transcription factors, such as WRKY (Wang, et al., 2023), NAC, MYB, and bZIP (Jamla, et al., 2021). Transcriptome analysis enables the identification of genes that are differentially expressed under various conditions. The study of gene expression via sequencing technology offers a rapid and efficient way to understand genes or metabolic pathways associated with tolerance or hyperaccumulation of HMs in plants (Ge, et al., 2022).

1.2 Project Rationale

Poorly managed landfills are waste disposal sites with insufficient engineering controls, including liners, leachate collection systems and improper waste containment. For example, municipal landfills with inadequate leachate containment can cause toxic pollutants (e.g. organic compounds, HMs, and microplastics) to migrate into the surrounding surface and groundwater (Gunarathne, 2024). This can negatively impact the environment, humans and aquatic ecosystem (Siddiqua, Hahladakis and Al-Attiya, 2022). Leachate generated from these landfills contains harmful contaminants threatening human and aquatic

ecosystems (Essein, et al., 2022). Landfill leachate can be classified as young, intermediate and old based on age. The HM content in the young leachate is the highest among the three mentioned groups (Tejera, et al., 2019). The treatment of leachate is crucial to ensure future safety and sustainability. Remediation of leachate with current technologies, such as nanofiltration and reverse osmosis (Wang and Qiao, 2024) to overcome the adversity of leachate is often costly, has limited potential and requires subsequent treatment (Younas, et al., 2021; Siddiqi, et al., 2022).

The sole phytoremediation method is ineffective. Hence, EAPR may overcome this setback (Mao, et al., 2016; Bu, et al., 2024). Based on the effectiveness of the EAPR-water lettuce approach to remediate HM-contaminated waterways (Putra, Cahyana and Novarita, 2015; Putra, Novarita and Cahyana, 2016), this strategy is applied to treat HM-abundant synthetic leachate. This study aimed to evaluate the potential of *P. stratiotes* to remove HMs from synthetic young leachate via EAPR. Nonetheless, the efficacy of HM removal alone is insufficient for assessing EAPR performance. This is because the physiological responses of plants under electro-assisted conditions determine their tolerance, survival, and sustainability of the remediation process. EAPR offers an environmentally friendly approach (Putra, Ohkawa and Tanaka, 2013) that can be established to remediate HMs from leachate. Moreover, there is limited information on *P. stratiotes'* molecular response to HM stress, which hinders a better understanding of its stress signals. Hence, the transcriptomic study of *P. stratiotes* in this model may help

enhance our understanding of the molecular response of these HM hyperaccumulators, which is crucial for the future development of phytoremediation applications. Data from transcriptomic analysis of this plant allows the identification of key regulatory differentially expressed genes (DEGs) (e.g. stress signaling, metal transport and detoxification processes) involved in phytoremediation processes (El-Sappah, et al., 2024; Razalli, et al., 2025). This information provides guidance to select genetically improved plant species with enhanced HM accumulation capability. Hence, systems such as EAPR could benefit from integrating phytoremediation strategies with transcriptomic knowledge.

1.3 Research Objectives

The purpose of this study is to evaluate the potential of EAPR using *P. stratiotes* for treating HM-contaminated synthetic young leachate and to understand the associated physiological and molecular responses of the plant under metal stress. The aim of this study is to:

- evaluate the removal efficiencies of heavy metals from synthetic young leachate by *P. stratiotes* via EAPR.
- determine the physiological changes of *P. stratiotes* in response to EAPR in synthetic young leachate.
- elucidate the transcriptomic responses and cellular pathways involved in Pb stress response in *P. stratiotes* roots and leaves.

CHAPTER 2

LITERATURE REVIEW

2.1 The Global Crisis of Waste Management: Impacts and Sustainable Solutions

Globalization, rapid urbanization and population growth have caused the rise of municipal solid waste (MSW) generation. Open burning, terrestrial dumping, and informal recycling sector activities are the dominant contributors to the rapid increase in waste statistics (Kaza, et al., 2018). As these processes are challenging to handle, approximately 93% of waste in developing nations is burned or dumped openly, while a minority, 3%, is landfilled (Lei, et al., 2023). As many countries rise to high-income levels, urbanization and population expansion make solid waste management even more challenging (Kumar, et al., 2023). Close to 3.5 billion of the 7.6 billion world's population are without basic waste collection services (Aslam, et al., 2022).

MSW management's primary objective is to manage garbage to support sustainability, while protecting the environment and public health (Munguía-López, et al., 2020). Trash is divided into four categories: recyclables, inorganic materials, organic materials and other miscellaneous items. According to Özmen and Özsoy

(2020), MSW management entails transporting, processing, recycling and disposing of solid waste produced by metropolitan populations. Over the years, the management of MSW has shifted to sustainable and environmentally friendly treatment, recovery and recycling methods. Most developed countries practice advanced technologies, such as thermal and biological treatment, as well as sanitary landfills for appropriate treatment of MSW (Kumar, et al., 2023). Waste-to-energy technologies can produce heat and electricity through the conversion of waste via biochemical or thermochemical processes. Recently, they have received increased attention to reduce environmental pressures, enhance resource efficiency and produce impactful economic benefits (Liang, et al., 2022). Typical examples include sanitary landfills, comprehensive resource treatment, biodegradation (aerobic composting and anaerobic fermentation) and heat treatment (pyrolysis, gasification, incineration and preparation of waste-derived fuel). Among them, composting, sanitary landfill and incineration power generation are usually adopted to dispose of urban domestic waste (Zhao, 2021).

In developing nations like Malaysia, landfilling is the most common and broadly accepted way to dispose of MSW. This is primarily due to its innate ability to save costs and more straightforward operating mechanisms (Kamaruddin, et al., 2017). In contrast, burning waste, incineration [(Rawang (Selangor), Sungai Udang (Melaka), Jedok (Kelantan)] (Yusof, 2024) and dumpsites can cause air pollution, the release of harmful toxins and long-term health problems for organisms living near these sites (Rosenberg and Hoover, 2021; Vinti, et al., 2021).

2.2 Landfill Types and Challenges in Urbanisation

The landfill is a pit specifically constructed to hold compacted solid waste with a covering to dispose of waste. It has a lining at the bottom to prevent waste from contaminating underground water. Siddiqua, Hahladakis and Al-Attiya (2022) stated that there are three customary landfills, namely municipal, industrial and hazardous waste. A new type of landfill, known as a "green waste landfill," is occasionally utilized. Municipal waste (garbage or trash) refers to all solid or semi-solid state waste, mostly household or domestic. Municipal landfills are recommended strategies to address the rapidly expanding solid waste problem (Krčmar, et al., 2018). An industrial waste landfill is a facility designed for the disposal of industrial waste. These landfills typically dispose of construction and demolition waste, such as concrete, bricks, asphalt and gypsum (United States Environmental Protection Agency, 2011).

Hazardous waste landfills are specifically engineered to contain hazardous waste by precluding the possibility of it being leached or released into the environment. Dual leachate collection and removal approaches, dual liners, leak detection systems and dispersal controls are some design criteria for hazardous waste landfills. Hazardous waste dumps are inspected numerous times a year to ensure that the facility meets the latest high standards (Hazardous Waste Experts, 2019; United States Environmental Protection Agency, 2022). Green waste landfills are used to store organic waste for decomposition. Composting sites are becoming

increasingly popular as conventional landfills and transfer stations are unable to accept organic waste, such as vegetables and fruits. Examples of green waste include leaves, weeds, flowers, tree branches, grass trimmings and biodegradable food waste (Siddiqua, Hahladakis and Al-Attiya, 2022).

According to Siddiqua, Hahladakis and Al-Attiya, (2022), all the landfills mentioned earlier should be sanitary. Within the sanitary landfills, four layers are critical for the whole waste decomposition process (Figure 2.1). The landfill's base layer is compacted dense clay, preventing waste seepage and underground pollution (Rajaeifar, et al., 2015). The drainage system, the second landfill layer, shields against decomposition of waste-generated liquids by removing toxins from waste, rain and snow to protect the liner system. Perforated pipes in the upper section collect leachate, preventing liquids from seeping into the landfill bottom (Adamcová, et al., 2017). The third layer of sanitary landfills is the gas collection system, where natural gases such as methane, are produced. The fourth and largest waste storage layer is collected by various companies and compacted daily. Finally, a compacted soil layer covers the surface to minimize odor and harmful microorganism growth (Siddiqua, Hahladakis and Al-Attiya, 2022).

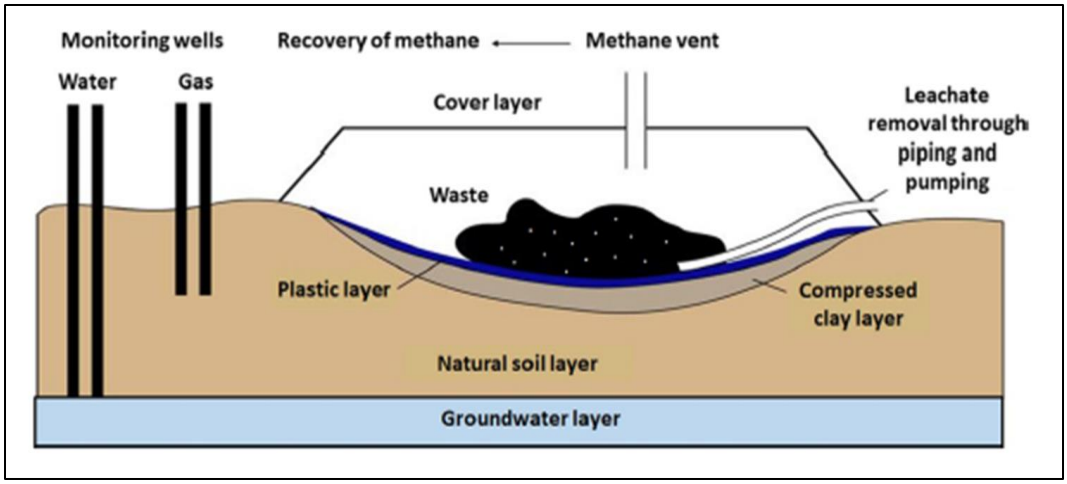

Figure 2.1: Layout of a typical waste landfill (adopted from Siddiqua, Hahladakis and Al-Attiya, 2022).

Landfilling is the standard method practiced in Malaysia to dispose of municipal solid waste (Kamaruddin, et al., 2017). Of 165 operating landfills in Malaysia, only eight [Pulau Burung (Pulau Pinang), Selong (Johor), Bukit Tagar (Selangor), Jeram (Selangor), Kuching, Miri (Sarawak), Kota Kinabalu (Sabah) (Malek and Shaban, 2008), Tanjung Duabelas – Kuala Langat, (Selangor), Sabak Bernam (Selangor) (Worldwide Environment, n.d.) are considered sanitary landfills provided with a leachate treatment system (Taib, et al., 2021). Several existing landfills, such as Taman Beringin Landfill (Kuala Lumpur) (Chin, et al., 2020) and Kayu Madang Landfill (Selangor) (Manaf, Samah and Zukki, 2009), have reached their maximum design capacity more quickly than anticipated due to rapid urbanization. Hence, the construction of new landfill sites has become increasingly challenging due to land scarcity, urban expansion and public opposition (The Malaysian Reserve, 2024).

In addition to disposal availability, the focus has increasingly shifted to the environmental by-products generated during landfill operations. The decomposition of municipal solid waste in landfills generates numerous waste products that adversely affect the environment and pose management challenges (Virdi, Sharma and Devi, 2021; Kafle, et al., 2025). Landfills generate a complex mixture of wastes, including liquid (leachate), gases (e.g. methane and carbon dioxide) (Anqi, et al., 2020), and solids/residuals that remain after biological and chemical transformations (Gunarathne, 2024).

2.2.1 Characteristics of Young, Intermediate and Old Leachates

Landfill leachate is an intensely black coloured liquid generated through the percolation of precipitation through solid waste in landfills (Taib, et al., 2021). It is produced from liquids in the waste and outside water, including rainwater (Jayawardhana, et al., 2017). Leachates are comprised of numerous chemicals, which are affected by factors such as weather conditions, landfill design, operational procedures and waste decomposition (Singh, et al., 2016a; Naveen, et al., 2017). The production of leachates also relies on the water balance at the landfill site. The water balance effect of leachate in a landfill refers to the accounting of water inputs (precipitation, waste moisture and high rate of rainfall) and outputs (leachate, runoff and evapotranspiration) to determine leachate generation and potential groundwater contamination (Bengtsson, et al., 1994; Taib, et al., 2021).

Landfill leachate can be categorized into three key groups based on its age, namely young (0-5 years old), intermediate (5-10 years old) and old (more than 10 years old) (Table 2.1). Young landfills (acetogenic) have been observed to produce leachate from the fresh waste discarded there, which contributes to the waste's rapid degradation. The leachate is distinguished by low pH, high load of volatile acids and degraded organic matter. The Biochemical Oxygen Demand over 5 days (BOD_5)/Chemical Oxygen Demand (COD) ratio is highest compared to intermediate and old landfills because of a readily biodegradable organic matter abundance, leading to a rapid decrease in BOD levels compared to COD (Lindamulla, et al., 2022). In contrast, a significant level of biodegradable organic materials in the intermediate landfills actively participates in the anaerobic digestion of waste.

Leachate from an intermediate landfill (acetogenic) is identified by a pH between 6.5 and 7.5, a lower COD value (5,000-10,000 mg/L) than young leachate, a BOD_5/COD ratio of 0.1-0.5 and reduction in volatile fatty acids (Tejera, et al. 2019). As for old landfills from the methanogenic phase, both pH and leachate methane production are high, and the primary organic materials present are humic and fulvic fractions (Aziz, et al., 2012; Tejera, et al., 2019). Leachate generated from these landfills contains high ammonia nitrogen levels from hydrolysis and fermentation of biodegradable materials with nitrogenous compounds (Lindamulla, et al., 2022).

Table 2.1: Leachate characteristics based on the landfill age (adopted from Aziz, et al., 2012; Yadav and Dikshit, 2017; Tejera, et al., 2019; Arat, et al., 2024)

	Young	Intermediate	Old
Age (years)	0–5	5–10	>10
pH	< 6.5	6.5 – 7.5	7.5
Biological Oxygen Demand (BOD_5) (mg/L)	>4000	1000–4000	<400
Chemical Oxygen Demand (COD) (mg/L)	>10,000	5,000–10,000	<5,000
BOD_5/COD	0.5 – 1.0	0.1 – 0.5	> 0.1
Total Organic Carbon (mg/L)	>2500	1000–2500	<1000
NH_3–N (mg/L)	< 400	-	> 400
HMs levels	Medium to low	Low	Low
Volatile Fatty Acids (VFA)/ Humic and Fluvic Acids (HFA)	VFA (80%)	VFA (5–30%) + HFA	HFA (80%)
Biodegradability	High	Medium	Low
Microplastics	High	Medium	Low

2.2.2 Heavy Metals (HMs) in Landfill Leachate: Toxicity and Environmental Risks

Pollutants, such as HMs, plastics, organic and inorganic compounds, inorganic salts, nitrogenous components and xenobiotic pollutants are present in the leachate (Dagwar and Dutta, 2024). Before disposal in a landfill, separating non-hazardous from hazardous waste is uncommon for most developing countries. Hence, failure to properly segregate waste in landfills leads to severe environmental and public health consequences. Some of the key impacts include the leaching of HMs from mixed-waste landfills (Dagwar and Dutta, 2024), soil and groundwater pollution (Zhang, et al., 2023) and higher toxicity threat to human health (causing cancer, organ damage and weakening immune systems) (Radfard, et al., 2023) and ecosystems (Rahman and Singh, 2019).

The continuous percolation of landfill leachate to the surrounding aquatic and soil area is a hazardous contamination source of various pollutants (Hussein, et al., 2021; Hredoy, et al., 2022; Beinabaj, et al., 2023). HMs are one of the most noxious pollutants found in landfill leachate (Edokpayi, et al., 2018). The most common HMs found in landfill leachate are lead (Pb), cadmium (Cd), manganese (Mn), zinc (Zn), nickel (Ni) and iron (Fe). Non-threshold HM pollutants, such as Pb, Cd, chromium (Cr), arsenic (As) and mercury (Hg) can be harmful even at very low concentrations (Jayanthi, et al., 2016; Rahman and Singh, 2019). It was

reported that the metal contents in young (acetogenic) leachate are comparatively higher than those found in old leachate (Dan, et al., 2017).

2.2.2.1 Lead

Pb appears to be a silvery-white and highly malleable metal. In nature, it is rarely found in its native form but in combination with other elements, forming interesting minerals (Johnson, 1998). Pb has been widely applied in numerous anthropogenic activities, such as leaded paints, fossil fuels, molten Pb as a coolant, and vehicle batteries (as lead oxide) (Pinho and Ladeiro, 2012). Humans can be exposed to Pb (release to the environment via mining, industrial processes and fossil fuel combustion) (Abdulaziz, et al., 2022; Ghosh, et al., 2023) through inhalation or by consuming polluted water and soil (Jyothi, 2021). Pb toxicity was reported in pregnant women (Forsyth, et al., 2018) and children (Dong, Taylor and Gulson, 2020). Pb produces reactive oxygen species (ROS) that inhibit crucial metabolic processes in plants (Aslam, et al. 2021; Khaliq, et al., 2021). Additionally, Pb inhibits enzyme activity by reacting with the enzyme–SH groups of numerous plant enzymes, such as those involved in chlorophyll biosynthesis and α-amino levulinate dehydrogenase (Konuk, Ciğerci, and Korcan, 2010; Kumar, et al., 2020).

2.2.2.2 Cadmium

Cd is widely distributed as a non-essential trace element in the environment. It is usually incorporated into phosphorites, sulphides and carbonates in soils and rocks (Kubier, Willkin and Pichler, 2019). Cd exposure increases in the environment due to mining activities, waste burning, combustion of fossil fuels, and recycling of electronic waste, in addition to the use of Cd-containing colourant in paints, Cd-containing stabilizers in plastics and Ni-Cd batteries (Genchi, et al., 2020).

Cd can be easily absorbed by crops, which increases the probability of Cd toxicity in humans and livestock after consuming the crops (Cai, et al., 2019; Hou et al., 2023a). In the human body, Cd stimulates the production of ROS and metallothionein, subsequently causing oxidative damage to cells and lipid peroxidation (Patra, Rautray and Swarup, 2011). On the other hand, a high level of Cd inhibits plant nutrient absorption and translocation, increases oxidative damage and disrupts growth and metabolism (Haider, et al., 2021). Further Cd toxicity leads to chlorosis, stunted growth, reduced chlorophyll content, compromised carbon fixation and subsequent necrosis. Besides, Cd is also known to induce osmotic stress, reducing stomatal conductance, water content and transpiration rate in plants (Soni, et al., 2024).

2.2.2.3 Ferum

Fe is the fourth-most prevalent element in the Earth's crust, widely utilized in life and industry. Regarding the number, density and atomic weight, Fe is considered a HM. It is present in landfill waste, usually from metal containers, construction debris, household appliances and natural soil beneath the landfill. This HMs has the potential to mobilize and leach into the leachate (Li, et al., 2011). Fe is an element required for photosynthesis and chlorophyll synthesis in plants, besides being important for human body building.

In plants, Fe deficiency will lead to chlorosis and slow growth (Santos, et al., 2015). However, excessive use of iron fertilizer in soil might generate pollution and cell toxicity in plants. For example, damage to biomolecules occurs when excessive Fe in cells reacts with hydrogen peroxide (H_2O_2) (Schmidt, Thomine and Buckhout, 2020), which will form hydroxyl radicals through Fenton chemistry. Plant toxicity is visible in stunted root systems and leaf bronzing (Li, Kronzucker, and Shi, 2016).

2.2.2.4 Zinc

Zn is one of the most abundant elements in the environment and an essential trace element for all living organisms (Guarino, et al., 2020a). Its occurrence on Earth is due to the weathering of rocks (Hussain, et al., 2022), while through mining, its concentration increases (International Lead and Zinc Study Group, 2020). Most of the Zn in landfill waste originates mainly from industrial activities, such as mining, smelting and waste disposal, which are the primary industrial sources. Zn is also found in everyday home objects that wind up in landfills, such as paints, musical instruments and several types of plastics (Ng, et al., 2016).

Typically found in nature as divalent cations, Zn is involved in nucleic acid metabolism, chromatin structure, gene expression, regulation and enzyme activity (Meng, et al., 2023). Hence, it is an essential trace element that plants need for various metabolic and regulatory functions (Ganie, et al., 2020). Factors such as external bioavailable concentration, plant species and exposure time determine the toxic effects of Zn. For instance, excessive Zn in most vascular plants is toxic and negatively impacts their development and growth (Kaur and Garg, 2021). This results from cytostructural disturbance, nitrogen metabolism imbalance and alterations in enzyme function brought on by Zn (Meng, et al., 2023). The most apparent Zn toxicity symptoms in plants are growth inhibition, young leaves

chlorosis (due to lower uptake of Fe^{2+} and Fe^{3+}) and even cell death (Sturikova, et al., 2018).

2.2.2.5 Manganese

Mn is crucial for carbohydrate, lipid and protein metabolism in humans and animals. It functions as an enzyme cofactor and is embodied in several metalloenzymes (Horning, et al., 2015; Balachandran, et al., 2020). Mn is well known for its application in steel production (Marsidi, Hasan and Abdullah, 2018), textile dyeing mills (Mamun, et al., 2022), entrainment of soils containing Mn and combustion of fossil fuels (Men, et al., 2021). Wastes such as insecticides, paint, pigments, bottle caps and blades are examples of the source of Mn in landfill leachate (Kanmani and Gandhimathi, 2013).

Exposure to excessive amounts (more than 150 mg per kg dry weight) (Millaleo, et al., 2010; Li, et al., 2019a) of Mn in plants can decrease photosynthetic rate (Alejandro, et al., 2020), production and quality of crops worldwide (Liu, Li and Xu, 2019). Being a toxic metal, excessive Mn can generate ROS, trigger oxidative stress and finally poison plants. ROS could lead to lipid peroxidation and damage photosynthetic pigments if not well scavenged (Li, et al., 2019a). In general, the most apparent effects of plant exposure to high soil Mn concentration are brown spots, chlorosis and leaf necrosis, which can reduce the photosynthetic efficiency

(Faria, et al., 2020; Garcia, et al., 2020). Hence, addressing Mn pollution is vital to safeguard plant/agricultural productivity and ecosystem health, focusing on pollution control measures and sustainable waste management (Singh, Chakraborty and Sehgal, 2023).

2.2.2.6 Nickel

Ni, along with Cd and As, is known to impede deoxyribonucleic acid (DNA) repair mechanisms in plants (Briffa, Sinagra and Blundell, 2020). Hence, it is a well-known carcinogenic toxic metal (Haque, 2016). Ni is a transition element widely distributed in the environment. The environment can acquire it through anthropogenic activities, such as the use of liquid and solid fuels, as well as the disposal of municipal and industrial waste. Ni can also originate from natural sources (Genchi, et al., 2020). Approximately half of the Ni used in the global production of Ni-Cd batteries, colour ceramics and electroplating is discarded in landfills and other waste disposal sites (Agency for Toxic Substances and Disease Registry, 2024).

While Ni is an essential micronutrient for some plants, high concentrations (more than 10 mg per kg for sensitive plants, more than 50 mg per kg for tolerant plants) (Gerendas and Sattelmacher, 1999) can disrupt metabolic processes, impair nutrient uptake and cause oxidative stress (Hassan, et al., 2019). High Ni levels

suppressing enzymatic activity, chlorophyll biosynthesis and photosynthetic electron transport (Sreekanth, et al., 2013). Elevated levels of Ni can lead to alterations in the activities of plant enzymes, such as catalase (CAT) and superoxide dismutase (SOD) (Gupta, et al., 2017).

2.3 Type of Landfill Leachate Treatments

Leachate from landfills has a high potential for pollution due to its significant levels of inorganic and organic pollutants. Hence, reducing environmental hazards and public health in landfills is a significant concern (Xaypanya, et al., 2018). Three main approaches frequently used to treat landfill leachate are physical (e.g. physical separation or filtration) (Renou, et al., 2008), chemical (e.g. coagulation-flocculation, precipitation) (Sengupta and Pal, 2021) and biological (e.g. microorganism treatments and phytoremediation (Mojiri, et al., 2021).

2.3.1 Chemical Methods

Chemical approaches for treating landfill leachate entail adding chemical reagents or agents to help pollutants in the leachate to precipitate, coagulate, flocculate, oxidize or neutralize (Aziz, et al., 2022). These techniques aim to improve the eradication of organic compounds, dissolved metals and other contaminants via chemical reactions that change them into insoluble aggregates or

precipitates that can be removed from the liquid phase (El-Saadony, et al., 2023; Chen, et al., 2024). Standard chemical treatment methods include advanced oxidation processes (AOPs), coagulation-flocculation, oxidation-reduction and precipitation (Sengupta and Pal, 2021). Precipitation and coagulation-flocculation directly remove metals, whereas oxidation-reduction and AOPs primarily alter metal speciation or organic complexation to facilitate subsequent removal. They are frequently used in hybrid systems to enhance the removal efficiencies of organics and HMs by integrating radical oxidation with particle destabilization and precipitation processes (Zazouli, et al., 2024; Wang and Qiao, 2024).

AOPs employ powerful oxidants to combine with catalysts or ultraviolet (UV) radiation, producing highly reactive hydroxyl radicals which can mineralize organic pollutants into less harmful and simpler compounds (Pandis, et al., 2022). In coagulation-flocculation, flocculants (e.g. cationic polymer flocculants, natural polymer flocculants and polyelectrolytes) (Ahmadli and Mammadova, 2024; Tsoutsa, et al., 2024) are added after coagulants (e.g. aluminum sulfate or ferric chloride) to enhance the aggregation of colloidal particles and suspended solids into bigger flocs for easier separation from the leachate (Abujazar, et al., 2022). Oxidation-reduction methods, such as chlorination or ozonation, involve the addition of oxidizing agents to reduce organic contaminants or lessen the number of toxic compounds (Wang and Chen, 2020). The main purpose of chlorination is microbiological disinfection. However, chlorine also functions as an oxidant and can eliminate or aid in the chemical conversion of certain chemicals, such as

oxidation of manganese (II) to insoluble products that can be eliminated by further filtration (World Health Organization, 2022). Precipitation methods involve adding chemicals that react with dissolved pollutants to form insoluble precipitates, which can be removed by sedimentation or filtration (Pohl, 2020).

Chemical treatment processes can attain significant removal efficiency for organic compounds, dissolved metals and recalcitrant contaminants that might not be adequately addressed by biological or physical techniques alone (Nidheesh, et al., 2022). Besides, by adjusting dosage and type of chemical additives, these processes are often tailored to specific treatment objectives and leachate compositions (Khoo, et al., 2020). Sludge generation is a key drawback of chemical treatments like precipitation and coagulation-flocculation. It contains excess chemical reagents and aggregated pollutants, posing major disposal challenges (Sharma, et al., 2022). In addition to increasing operating expenses, the improper use of chemical reagents can pose a risk to operators' health and safety if not handled correctly. Chemical sludge typically requires dewatering and often requires additional treatment/stabilization before disposal in landfills/utilisation in other applications (Hou, et al., 2023b).

2.3.2 Physical Methods

Physical techniques for treating landfill leachate involve physical separation or filtration processes to remove particulate matter and suspended solids (Renou, et al., 2008). Sedimentation and filtration are the commonly applied physical methods (Bashir, et al., 2016). Sedimentation allows suspended solids to sink to the bottom under the influence of gravity, which facilitates the removal of the solids from the leachate (Wang, et al., 2021). Simultaneously, HM concentrations are reduced by settling particle-bound metals formed via adsorption (Bakhtiyari-Ramezani, et al., 2025) and co-precipitation processes (Kowalik-Klimczak, 2025). Filtration methods, including activated carbon or sand filtration, use porous material to trap organic compounds and suspended solids as the leachate flows through the filter bed (Loh, et al., 2021). For instance, sand filtration prior to adsorbent columns (e.g. activated carbon or calcined materials) can enhance HM removal by reducing particulates, that might otherwise obstruct adsorption (Jaradat, Telfah and Ismail, 2024).

Membrane technologies, such as microfiltration, nanofiltration, ultrafiltration and reverse osmosis, employ semi-permeable membranes to eradicate pollutants based on charge selectively and molecular size (Rai and Shrivastav, 2022). These methods are often investigated for HM removal in wastewater treatment (Castro and Abejón, 2024). Air stripping is another physical

process that eliminates volatile pollutants, such as ammonia and volatile organic compounds from leachate. This is done via the passing of air through the liquid (De, Hazra and Dutta, 2019; 2022). It is routinely used as a pretreatment step preceding processes able to target non-volatile pollutants, including HMs (Wang and Qiao, 2024).

The main benefit of physical treatment techniques is their capacity to remove contaminants at high levels, especially for larger organic molecules and suspended particles (Saravanan, et al., 2021). The treated leachate's visual clarity and general quality are improved by these techniques, which are frequently successful in lowering turbidity and eliminating colloidal particles (Zakaria, et al., 2023). Physical treatment processes typically require comparatively low energy inputs and few chemical additions (Nyabadza, et al., 2023). Nevertheless, in membrane-based processes, membrane fouling or blockage can reduce treatment effectiveness and increase operating costs (Asif and Zhang, 2021). While simple physical separation processes (eg. sedimentation, air stripping) (Verma and Kuila, 2019) are ineffective for dissolved HMs, advanced physical techniques (e.g. membrane filtration and adsorption) require high energy input, frequent maintenance (Mannaf, et al., 2025) and generate secondary pollutants (Shofia, et al., 2025), necessitating further treatment stages (Saleh, Mustaqeem and Khaled, 2022). Moreover, in areas with low financial resources, membrane technologies may not be widely adopted due to their high operating and capital costs (Othman, et al., 2022).

2.3.3 Biological Methods or Bioremediation

According to Moris, et al. (2018), bioremediation eliminates environmental pollutants by biological means. Its advantages include environmentally friendly techniques and cost-effectiveness. In general, biological treatment methods for landfill leachate can be grouped into two main categories, namely microorganism treatments and phytoremediation (Mojiri, et al., 2021).

2.3.3.1 Microorganism Treatments

Landfill leachate can be remediated using various bacteria, microalgae and fungi (Moris, et al., 2018; Spina, et al., 2018). Microorganism treatments employ the metabolic activity of microbes to break down organic contaminants and eliminate nutrients from leachate (Wu, et al., 2015). These techniques, which use various environmental conditions and microbial communities to promote the leachate's biodegradation and transformation of toxins, usually include aerobic treatment, anaerobic treatment and constructed wetlands (Kurniawan, et al., 2010). Aerobic bacteria, such as *Brevibacillus panacihumi* strain ZB1 and *Pseudomonas putida* (Michalska, et al., 2020; Mojiri, et al., 2021) can break down organic compounds and oxidize them into less toxic, simpler forms by subjecting the leachate to oxygen-rich environments (Bhambore and Suresh Kumar, 2022). On the

other hand, anaerobic bacteria, such as *Syntrophomonas, Syntrophobacter* and *Smithella* (Hori, et al., 2011), break down organic matter through fermentation and methanogenesis in anaerobic treatment methods, which perform without oxygen and produce methane as a byproduct (Zamri, et al., 2021).

Utilizing wetland microbial communities, plants and soil, constructed wetlands are engineered systems that replicate natural wetland ecosystems. These systems use biological, physical and chemical processes to extract pollutants from the leachate (Hassan, et al., 2021). Bakhshoodeh, et al. (2020) stated that these systems foster wetland plants and microorganisms, which enhance leachate quality by adsorbing, absorbing and metabolizing contaminants. In addition, constructed wetlands can improve nutrient removal and groundwater recharge via retention in the soil and facilitating water infiltration (Chand, Kumar and Suthar, 2022).

2.3.3.2 Phytoremediation

Phytoremediation is a plant-based approach to inactivate and degrade potential toxic contaminants in leachate (Table 2.2) (Song, et al., 2018). It is an effective and economical alternative to remove elemental pollutants or lower their bioavailability (Eid, et al., 2020). Phytoremediation plants are classified as terrestrial plants and aquatic macrophytes. Terrestrial plants are effective in soil remediation via phytoextraction and phytostabilization. Aquatic macrophytes are

well-suited to aquatic and sediment environments due to their extensive root systems and high uptake capacities. Recently, numerous studies have highlighted that aquatic macrophytes are effective HM removal, thus making them potentially useful in wastewater and wetland remediation applications (El-Amier, et al., 2021; Bayuo et al., 2024).

Macrophyte plants are classified into four categories, namely free-floating, submerged, emergent and floating-leaved (Kochi, et al., 2020). Free-floating and submerged macrophytes are effective for rhizofiltration and direct uptake of dissolved HMs from water, whereas emergent and rooted species enhance metal stabilization and sediment interaction (Nadi, et al., 2025). They have been employed to treat leachate (Song, et al., 2018) and eutrophic rivers in stormwater detention ponds (Saha, et al., 2022). Plants with an exceptional capacity to accumulate metals are known as hyperaccumulators (Tangahu, et al., 2011). This ability is crucial for phytoremediation to be successful (Alaboudi, Ahmed and Brodie, 2018). At low HM levels, these hyperaccumulators can sequester metal ions via metallothioneins and phytochelatins. The complex procedure of metal sequestration include transportation across plasma membrane, translocation, xylem loading and detoxification process by the plant (Rascio and Navari-Izzo, 2011) (Figure 2.2).

Table 2.2: Summary of plant species used in phytoremediation (adopted from Sharma, et al., 2023a)

Mechanism	Plant	HMs	BCF / TF
Phytoextraction	*Brassica juncea, Sinapis arvensis, Brassica campestris*	Zn, Cu, Ni	BCF > 1; TF > 1
Phytoextraction	*Tagetes erecta*	Cd, Zn	High BCF (Cd, Zn); TF varies by metal
Rhizofiltration	*Eichhornia crassipes, Typha angustifolia*	Pb, Ni	BCF variable; TF > 1
Phytostabilization	*Brachiaria mutica, Leptochloa fusca*	Cr	BCF > 1; TF < 1
Phytovolatilization / phytoextraction	*Pteridium aquilinum* (fern species)	As	BCF > 1; TF < 1

Hyperaccumulators are plants with a Translocation Factor (TF) value of more than one or a Bioconcentration Factor (BCF) value greater than two (Mellem, Baijnath and Odhav, 2009). The BCF and TF values are the indicators used to identify the hyperaccumulator plants. The plant's ability to translocate metals from its root to shoot is indicated by TF (Ndimele, et al., 2014), while BCF illustrates the buildup of metals in plant tissues. Ornamental plants, which include *Helianthus annus* (sunflower) and *Impatiens glandulifera* have been demonstrated with elevated BCF values for Cd, indicating significant root accumulation (Deepika and Haritash, 2023). Besides, *Atractylis gummifera* has shown remarkably increased (eg. TF > 9 for Pb and Zn) (Chafik, et al., 2026), implying its phytoextraction capability. In addition, several aquatic and wetland flora, such as *Eichornia*

crassipes (Hidayati and Rini, 2020) and *P. stratiotes* have demonstrated elevated BCF under field and lab applications, respectively. This enables them as promising candidates for water-based remediation systems.

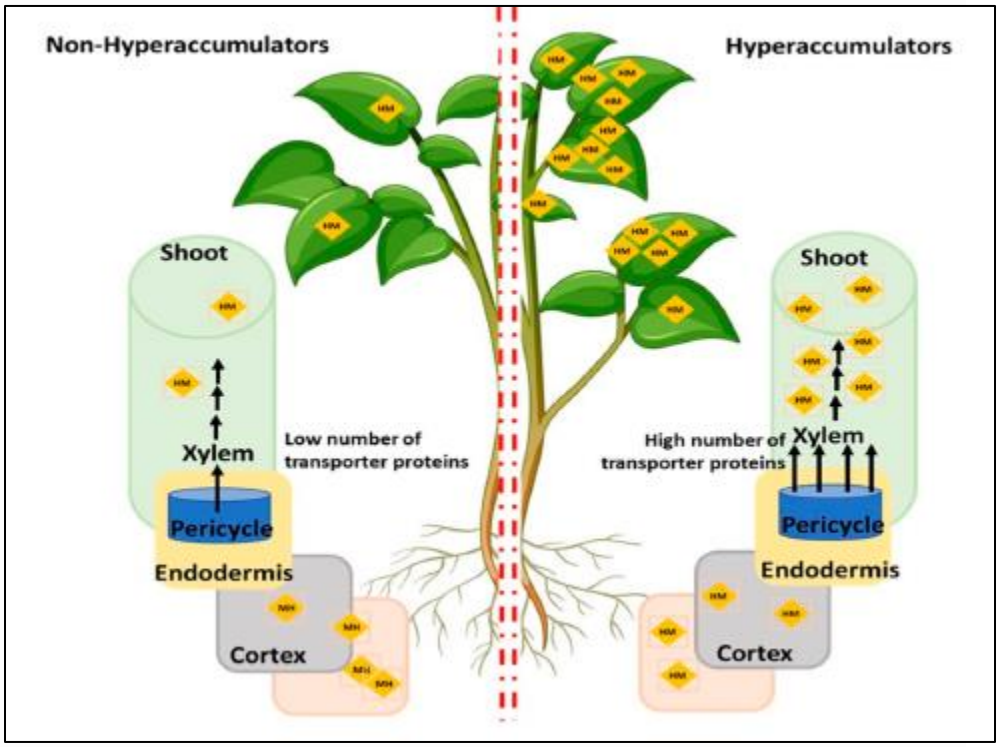

Figure 2.2: Mechanisms of HM resistance to stress in non-hyperaccumulators and hyperaccumulators plants (adopted from Tyagi, et al., 2024).

Phytoextraction, phytostabilization, phytodegradation, phytovolatilization and rhizofiltration or phytofiltration are among the various phytoremediation techniques (Wei, et al., 2021). Phytoextraction involves the uptake and transfer of toxins from plant roots into shoots. Roots and shoots will be harvested to eradicate

soil toxins (Ali, Khan and Sajad, 2013). This method is preferred because harmful components may be extracted from plant shoots (Jeyasundar, et al., 2021). During phytoremediation of specific metals, some plant species are better adapted for phytoextraction (Kafle, et al., 2022), such as *Nicotiana tabacum* for Cd (Yang, et al., 2019), *Sedum alfredii* for Pb (Ning, et al., 2019) and *Arundo donax* for As (Guarino, et al., 2020b).

In phytostabilization, plants such as *Eupatorium cannabinum* (González, et al., 2019), *Salix* spp. (Yang, et al., 2019) and *Solanum nigrum* (Li, et al., 2019b) are employed to lessen the mobility and bioavailability of pollutants. This strategy prevents their spread into the ecosystem and reduces the chances of metals from entering the food chain (Marques, Rangel and Castro, 2009; Yan, et al., 2020). However, its application is limited since metals are only confined and immobilized momentarily (Radziemska, 2018). Phytodegradation is frequently used against organic contaminants, but is rarely used and less effective against inorganic contaminants (Alsafran, et al., 2022). Phytodegradation is like phytostabilization, in which plant enzyme activities and rhizosphere bacteria transform contaminants metabolically into inactive forms. *Phragmites australis* (He, et al., 2017), *Pontederia crassipes* (Gong, Chen and Pu, 2019) and *Spirodela polyrhiza* (Singh, Pandey and Suthar, 2019) are examples of plants applied in phytodegradation.

Phytovolatilization plants, including *Polypogon monspeliensis* (Ruppert, et al., 2013) and *Juncus effusus (*Wiessner, et al., 2013) convert metal pollutants into a gaseous form, which is subsequently released into the air (Aweng, et al., 2018). However, pollutants are only shifted to different areas of the environment and they may still return to the soil after precipitation. Hence, phytovolatilization is less popular compared to phytofiltration and phytoextraction (Bisht, Chanyal and Srivastava, 2020). In rhizofiltration strategies, plant roots are utilized to absorb pollutants, particularly metals, from contaminated water and soil (Mahajan and Kaushal, 2018). Sunflower, tobacco, Indian mustard, spinach and rye are a few examples of plants employed for rhizofiltration (Suriya, et al., 2015). Phytofiltration involves the active absorption and adsorption of contaminants by the roots, shoots or seedling plants (Mesjasz-Przybyłowicz, et al., 2004). Phytofiltration plants, such as *Phragmites australis*, *Spartina alterniflora* and water hyacinth have a high rate of pollutant absorption (Park and Oh, 2023). However, both rhizofiltration and phytofiltration need to be used alongside suitable biomass disposal options (Yadav, Siebel and van Bruggen, 2011).

2.3.4 Emerging of Hybrid Methods for Leachate Remediation

Hybrid methods are frequently employed to treat landfill leachate to tackle the high levels of pollutants and limited biodegradability (Mojiri, et al., 2021). The hybrid methods include chemical and physical methods (Xiang, et al., 2019), such

as AOPs combined with membranes that indirectly remove HMs. AOPs degrade organic matter, whereas the membrane component separates the dissolved metal ions (Castro and Abejón, 2024; Shulin, et al., 2026). While effectively reducing the membrane-fouling problems and improving overall separation performance (Pan, et al., 2019), the potential drawbacks include degradation of membrane structure and reduction of photocatalytic activity in nanoparticles during operation (Regmi, Kshetri and Wickramasinghe, 2025). On the other hand, combining membrane filtration with coagulation improves HM removal (Kowalik-Klimczak, 2025), can also present challenges like increased chemical costs (Das, et al., 2023), the potential for membrane fouling (Wu, et al., 2009) and adverse effects on the environment and human health and due to aluminium (Al) residues (Ragio, et al., 2022).

Researchers have proposed the integration of biological, chemical and physical techniques to enhance biodegradability ratios and improve the biological method's performance (Wu, et al., 2010; Mojiri, et al., 2016). Biological methods have been integrated with membrane, AOP and coagulation methods (Mojiri, et al., 2021). The membrane bioreactor is a significant advancement in wastewater treatment, offering advantages over the traditional activated sludge process (Iorhemen, Hamza and Tay, 2016). Abuabdou, et al. (2020), however, mentioned that this integration caused a reduction in biomass growth, thereby affecting a longer time for stabilization.

AOP techniques are integrated as a pre-treatment (He, Ma and Liu, 2020), while coagulation can either be applied as pre- or post-treatment with biological treatment techniques (Niazi, 2018; Güvenç and Güven, 2019). Both integrations offer the generation of more easily biodegradable intermediates, with the latter integration lessening the colour, COD and metals in leachate. Hybrid methods may be longer and more costly due to chemical and energy demands (Qian, Sun and Liu, 2013; Aravind, et al., 2016), with additional toxicity risks from breakdown products.

2.4 Electro-assisted Phytoremediation (EAPR): Concepts and Applications

Phytoremediation utilizes various plant species to remove, remediate or transform contaminants from water and soil (Tejeda and Mallarino, 2022). However, phytoremediation has numerous drawbacks (Schwitzguébel, 2017), including the requirement for pollutants to be present in the root zones of the plants used for phytoremediation and the site must be sufficiently large to accommodate the use of farming methods (Tripathi, et al., 2020).

This study discussed electro–phytoremediation techniques under two configurations: (i) electrokinetic remediation combined with phytoremediation (EKR–PR) and (ii) EAPR (Figure 2.3). Both systems operate in soil or aquatic environments and use external electric fields to enhance pollutant mobility, bioavailability, and subsequent plant uptake. EKR–PR focuses on electrokinetic

transport mechanisms, which include electromigration, electroosmosis and electrophoresis. These processes mobilize contaminants and enhance plant uptake by modifying pollutant speciation and solubility in electric fields. In ryegrass and other plants, EKR–PR increased bioavailability and phytoextraction of HMs and organic pollutants from soils and mining tailings (Mulati, et al., 2023; Fan, et al., 2024). In contrast, EAPR employs milder electrochemical stimulation to enhance rhizosphere environments and the effectiveness of plant-based extraction in both soil and aquatic environments (Putra, Ohkawa and Tanaka, 2013; Putra and Hastika, 2018). Recent studies indicate that EAPR can markedly enhance the removal efficiencies of HMs and other pollutants when integrated with plant uptake, exemplified by Pb and Fe in synthetic leachate treated with *P. stratiotes*.

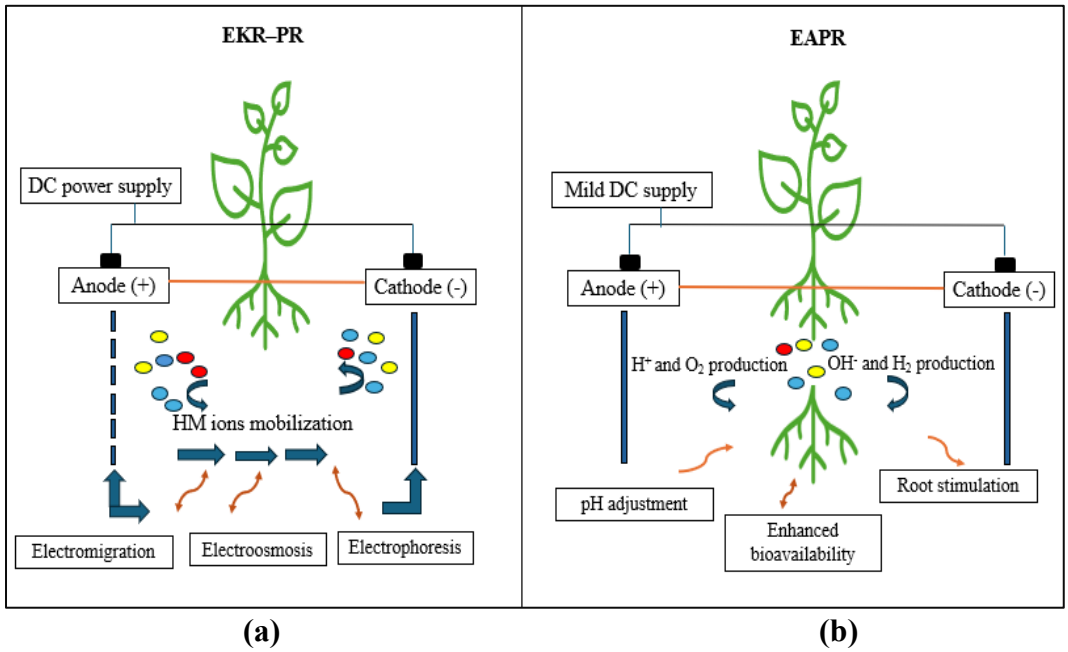

Figure 2.3: Schematic diagram of the comparison between (a) EKR–PR and EAPR (b)

Furthermore, EAPR combines an electrochemical process with phytoremediation [Figure 2.3 (b)] to enhance the effectiveness of phytoremediation. In this system, a direct current electric field of low intensity is applied to the contaminated source (Putra and Hastika, 2018). In the process of water electrolysis, H^+ ions are produced around the anode electrode when a low-intensity electric field is applied. More metalloids and metals are demobilized around the anode electrode under an acidic environment (Thangavel and Subbhuraam, 2004), and eventually, these metals are transferred to the cathode electrode (Dermont, et al., 2008). The mobilization of HM ions increases their uptake by the root zones of the plants via the electromigration process (O'Connor, et al., 2003). Subsequently, the HM ions might be deposited into the shoot system through various transportation pathways (Putra, Ohkawa and Tanaka, 2013; Putra and Hastika, 2018) and then extracted by harvesting the plants (O'Connor, et al., 2003).

EAPR was first introduced to overcome the shortcomings of phytoremediation by Hodko, et al. (2000) and Bedmar, et al. (2009). Since then, numerous studies have been proposed to improve plant HM uptake from soil (Luo, et al., 2018; Chang, Dong and Shen, 2019) and wastewaters (Adams, Raman and Hodgkins, 2012; Akemoto, Putra and Tanaka; 2022). Putra and Hastika (2018) evaluated the efficiency of EAPR in removing HMs from leachate and the uptake of HMs (Cd, Cu, Fe and Pb) by *Eichornia crass*ipes was studied on a laboratory scale. In another study, Putra, et al. (2017) configured a colony system of four EAPR cells connected by a single circulation wastewater treatment using *E.*

*crassipe*s. Their results demonstrated that EAPR could reduce BOD, COD and the HMs (Cu and Pb particularly) in four hours.

Numerous variables demonstrated a significant effect on the EAPR for remediation of polluted soil: (i) Direct Current (DC) or alternate current (AC) current type (ii) continuous or periodical application of voltage (iii) current or voltage level (iv) electrode configuration (v) electrolyte solution (vi) soil pH (vii) facilitating agents (Cameselle, Chirakkara and Reddy, 2013; Akemoto, Putra and Tanaka; 2022). For example, O'Connor, et al. (2003) used a one-dimensional horizontal setup with *Lolium perenne* to treat Cu/Cd/As metal-polluted soils, observing metal redistribution from anode to cathode. Whereas a two-dimensional electrode configuration resulted in elevated Pb and Cu concentrations in the roots of *Pistia stratiotes* (Putra, Cahyana and Novarita, 2015), and Cu was highly absorbed in the roots of water hyacinth (*E. crassipes*) (Putra, Novarita and Cahyana, 2016). The electric current density was unfettered by the position of electrodes in a one-dimensional electrode configuration. In contrast, the electric field's strength and electric current density increased directly with the distance from the anode to the cathode (Kim, et al., 2014).

While these studies demonstrate the efficacy of EAPR, its application to landfill leachate and the underlying molecular responses in plants remain underexplored, particularly for *P. stratiotes*. Due to the complex and dynamic

composition of landfill leachate, an assessment of the viability and efficacy of EAPR in this context is necessary.

2.5 *Pistia stratiotes* Morphology and Its Application in Phytoremediation

Free-floating species, which include *Lemna minor* (duckweed) and *Salvinia* spp. have been reported to effectively decrease the nutrient loads and sequester HMs via bioaccumulation and rhizofiltration processes. Other emergent plants, such as *Centella asiatica and Ipomoea aquatica* demonstrate significant metal uptake and tolerance characteristics in polluted aquatic environments. In addition, aquatic macrophyte species such as *P. stratiotes* and *E. crassipes* are able to effectively remove water contaminants (Mohd Nizam, et al., 2020; Pang, et al., 2023). Both plants possess extensive root systems, rapid biomass growth and great HM accumulation capability (Ergönül, Nassouhi and Atasağun, 2020; Alam, Ahmad and Naaz, 2025).

Despite their physical and physiological similarities, *P. stratiotes* was selected in this study as a potential candidate for EAPR application. Comparative studies reveal varying metal uptake efficiencies, with *E. crassipes* demonstrating higher Cr removal in particular controlled solutions. Whereas, *P. stratiotes* exhibited improved copper uptake and overall HM accumulation in roots, emphasizing species-specific advantages in performance under numerous pollutant

conditions (Tabinda, et al., 2020; Maurya, et al., 2025). Moreover, *P. stratiotes* frequently exhibits greater accumulation of specific HMs, including Cd and Pb (Maurya, et al., 2025), as compared with *E. crassipes*, thereby reinforcing its significant remediation capability in aquatic environments. The compact rosette shape, short root and lower biomass density of *P. stratiotes*, compared to dense mat and strong vegetative reproduction propagation of *E. crassipes* (Eid and Shaltout, 2017; Degaga, 2019), makes *P. stratiotes* easier to handle and allow exposure to low-intensity electric fields evenly. Furthermore, the significant biomass amount and shading effects of *E. crassipes* (Ceschin, et al., 2019) could potentially result in irregular current distribution and experimental variability. Hence, *P. stratiotes* offers a more stable and reproducible experimental model for assessing the effectiveness of EAPR in controlled soil and water environments.

Pistia is a genus of aquatic flora belonging to the Araceae family (Matyas, 1994). It is also known as water lettuce, Nile cabbage, water cabbage, shellflower or jalkhumbhi. It is commonly discovered in ponds, streams and lakes (Quattrocchi, 2017). This plant grows in most tropical regions (Masiyambiri, et al., 2023), spreading rapidly in nutrient-polluted water. The compact arrangement of its succulent leaves, which resemble a lettuce head, makes this plant easy to identify (Figure 2.4). The appearance of water lettuce is characterized by a circular arrangement of leaves with a dense layer of water-repellent hairs that prevent waterlogging and aid in buoyancy. The leaves also have a porous, pale green texture, allowing the plant to stay afloat on the water's surface easily.

At the same time, the roots enable effective nutrient absorption because of their feathery form and capacity to grow up to 20 cm long. Water lettuce can reproduce asexually as well as sexually. It uses stolons, which are horizontal stems that produce new plants at their nodes for asexual reproduction. Water lettuce produces tiny, discrete blossoms when it reproduces. Nevertheless, its sexual reproduction is less common than vegetative proliferation (Ali, et al., 2020).

(a) **(b)**

Figure 2.4: Morphological characterization of *P. stratiotes* (a) leaf and (b) root structures

P. stratiotes has unique characteristics, such as a rapid growth rate within a few months from vegetative to flowering (Greg, 2024), a wide root system and the ability to thrive in nutrient-rich environments, making it an excellent choice for

phytoremediation. One of *P. stratiotes* key advantages is its remarkable rate of growth, which allows the plant to quickly establish itself in polluted environments, spreading over large areas and providing a significant surface area for absorbing contaminants. The biomass's rapid growth increases its capacity to remove pollutants from the environment and permits regular harvesting, which is required to remove accumulated contaminants (Ergönül, Nassouhi and Atasağun, 2020).

The roots provide a significant surface area for absorbing contaminants since they are suspended in the water (Samal and Dash, 2024). This plant's root system is highly effective in absorbing nutrients, organic pollutants, and HMs from water, which makes it a flexible way to treat many types of contamination (Mustafa and Hayder, 2021). According to research by Ergönül, Nassouhi and Atasağun (2020), *P. stratiotes*'s fibrous roots can accumulate significant amounts of HMs. The plant's physiological and biochemical processes, such as storing metals in vacuoles and generating metal-binding proteins, are linked to its ability to withstand and accumulate these metals.

According to Nahar and Hoque (2021), this plant can tolerate a wide range of water pH levels and thrive in environments with high nutritional content (Henry-Silva, Camargo and Pezzato, 2008). It thrives in neither basic nor acidic water, and is commonly found in areas with high nutrient levels, typically due to wastewater discharge or agricultural runoff. Its efficient antioxidant system and the production

of phytochelatins, which bind to HMs, are the reasons it may flourish in contaminated environments (Ergönül, Nassouhi and Atasağun, 2020). *P. stratiotes* is a noteworthy asset for extensive phytoremediation endeavors because it is exceptionally adaptable to cultivation and management. It may produce new plants rapidly by asexual propagation. The simplicity of cultivating *P. stratiotes* ensures the continuous provision of this plant for phytoremediation endeavors.

P. stratiotes is widely used in treating industrial, household and agricultural wastewater due to its availability, bioaccumulation capability, resilience in toxic environments and invasive characteristics (Table 2.3) (Mustafa and Hayder, 2021). *P. stratiotes* is well known for its capacity to absorb and retain large concentrations of HMs (Ali, et al., 2020). Due to these characteristics, it is a suitable option for the EAPR system. In earlier research, this plant effectively eliminated HMs from contaminated water sources. However, the combined benefits of water lettuce and electrical enhancement in landfill leachate remediation have not been well investigated.

Table 2.3: HM removal of *P. stratiotes* from different wastewater sources

Type of wastewater	pH range	Removal performance	Key remarks
Industrial effluent (dyeing wastewater) (Ahila et al., 2021)	~6–8	86% colour removal; 77% COD; 66% TDS; 61.33% chloride	High tolerance to complex industrial contaminants; strong biomass growth
Sugar mill effluent (Kumar, Singh and Chopra, 2018)	Neutral to slightly alkaline	Up to 75% HM (Cd, Cu, Pb, Zn) removal	Roots act as primary HM accumulation site
Industrial wastewater (Mustafa and Hayder, 2021)	Not specified	Significant reduction of colour, BOD and COD.	Effective bioagent for phytoremediation of domestic wastewater, particularly at 12 and 24-hour retention times
Synthetic HM-contaminated water (Putra, Cahyana and Novarita, 2015)	~6–7	Enhanced HM (Pb, Cu) uptake	Electro-assisted phytoremediation improved removal efficiency

2.6 Defense Strategies by Plants to Overcome HM Stress

The increasing generation of waste and associated leachate poses significant environmental risks due to the release of toxic pollutants, including HMs, into ecosystems (Kumar, et al., 2022). Phytoremediation, a cost-effective and sustainable plant-based method, has unfolded as a promising alternative for leachate remediation by employing plants to uptake, contain and detoxify pollutants (Yan, et al., 2020). HM stress, however, can impair plant growth (Ubando, et al.,

2020) and remediation efficiency (Li, et al., 2019c), necessitating strategies to enhance metal tolerance and accumulation.

Two major groups of HMs are characterized based on physicochemical properties and interference with biological activities: redox-active and non-redox-active HMs. Redox-active HMs, such as Cu, Mn and Fe can cause oxidative injuries, leading to further DNA damage, degradation of protein and even cell death in plants. Whereas Ni, Cd, Hg and Zn, which are examples of non-redox-active HMs, notoriously result in oxidative stress via depletion of glutathione, binding to sulfhydryl, inactivation of antioxidants or activation of ROS enzymes (Singh, et al., 2016b; Yap, et al., 2021). HMs can influence chlorosis and cause inhibition of growth, seedling germination and root (Basu, et al., 2018). Plants have developed specific transport channels to absorb essential metals for normal cell functions. Nevertheless, no special channels are available for nonessential and toxic metals uptake into the plant system (Tyagi, et al., 2024). Plants adopt morphological or physiological changes, plant biochemical response and changes at the genomic level defense strategies to mitigate the adverse effects of HMs (Srivastava, et al., 2017).

Freshwater and marine plants, including Canadian waterweed (*Elodea canadensis*), *Posidonia oceanica*, Eelgrass (*Zostera marina*) and duckweed have been studied for their species-specific and shared tolerance mechanism (Wang,

2024). Some of their adapted key strategies in mitigating HM toxicity include chelation, sequestration, antioxidant enzymes, phytochelatins and metallothioneins. Understanding these mechanisms is vital for improving phytoremediation methods, which might then be used in environmental management.

2.6.1 Morphological and Physiological Changes

In plants, physical barriers, such as cell walls, trichomes and cuticles are the first line of defence that alleviate the deleterious effects of HMs via the storage of HMs or the secretion of secondary metabolites (Emamverdian, et al., 2015). It has been observed that plant roots mitigate the passage of HMs into the aerial sections by adsorbing, absorbing and trapping them in the root tissues. In plant roots, the effects of HM stress include decreased root length, browning of the root, enlarged root diameter and enlargement of the parenchymatic as well as cortical tissues (Singh, et al., 2022). For instance, nitric oxide treatment under Cd-stressed circumstances in *Arabidopsis thaliana* reduced the auxin level in primary roots, significantly impacting the root meristem (Yuan and Huang, 2016). Alterations in root system architecture in response to metal stress are directly linked to a plant's capacity to build tolerance to HM stress (Khan, Gemenet and Villordon, 2016).

Besides, hyperaccumulation (accumulation of 0.1 to 1% of HMs in plant dry weight) is a strategy employed by certain plants to tolerate elevated levels of

toxic metals. The tolerance of plants is contingent upon the species, the type of soil and the defence mechanisms they employ. Hyperaccumulators can sequester metal ions via phytochelatins and metallothioneins under low HMs exposure (Tyagi, et al., 2024). Plant metal sequestration involves transportation across the plasma membrane, translocation, xylem loading and detoxification (Rascio and Navari-Izzo, 2011).

Examples of hyperaccumulators include *Biscutella laevigata*, which hyperaccumulates more than 1% thallium (Babst-Kostecka, et al., 2016), *Psychotria gabriellae* which can accumulate over 4% Ni (Reeves, et al., 2021) and 8.5–75.5% of Cd accumulation in the cell wall of soybean (Wang, et al., 2018a). Nonetheless, the reaction of hyperaccumulators differs markedly from that of non-hyperaccumulators. However, once the first line of defense is breached with HMs being absorbed/entered into the plant cell/tissue, a complex cascade will be activated via biochemical and genomic defense strategies to overcome the negative impacts of HMs (Tyagi et al., 2024).

2.6.2 Biochemical Defense System of Plants against HM

Plants have well-developed mechanisms of protection and adaptation systems to various environmental stress factors (Dumanović, et al., 2021). Cellular redox reactions are employed as the first biochemical alterations by plants to

counter imbalanced physiological challenges caused by HMs (Nagajyoti, Lee and Sreekanth, 2010; Munir, et al., 2022). HMs, such as Fe and Cu at +1, +2 or +3 oxidation states affect Fenton/Haber−Weiss reactions in a redox-active reaction that generates OH radicals at neutral pH from hydrogen peroxide. Other metals (such as As, Cd, Hg, Pb, Zn and Ni) utilise redox inactive reaction to inactivate enzyme activity via reacting with -SH groups of enzymes in a single covalent bond, sharing electrons between HMs and -SH groups (Riyazuddin, et al., 2022).

Sies and Jones (2020) define ROS as a cluster of derivatives from molecular oxygen that occur due to typical signs of aerobic life. The generation of ROS includes singlet oxygen ($^1O_2$), hydroxyl radicals ($OH^\bullet$), superoxide anion free radical ($O_2^{\bullet-}$), H_2O_2 and reactive nitrogen species. Intracellular ROS is produced as metabolic by-products of plants in numerous cellular compartments, such as chloroplasts, mitochondria (Waszczak, Carmody and Kangasjärvi, 2018) and peroxisomes (Sandalio and Romero-Puertas, 2015). The increased accumulation of HM ions in plants' cytoplasm triggers ROS production, which may result in oxidative stress (DalCorso, et al., 2019). This occurs as ROS reacts with other biomolecules (e.g. DNA, protein and lipids) to stabilize itself (Singh, et al., 2016b; Mittler, 2017).

The balancing mechanisms and generation of ROS in mitochondria through the reduction of the electron transport chain will determine ROS accumulation

(Tyagi, et al., 2024). Thus, all living organisms must balance ROS generation and ROS quenching. Plants employ ROS as signalling molecules in various biological processes, which include abiotic and biotic stress reactions (Dietz, Turkan and Krieger-Liszkay, 2016; Huang, et al., 2019), which depend on the involvement of the plant's antioxidant system (Singh, et al., 2016b). The plant's antioxidant defense system, which prevents ROS buildup, determines whether ROS functions as a stressor or signalling molecule (Figure 2.5) (Tyagi, et al., 2024).

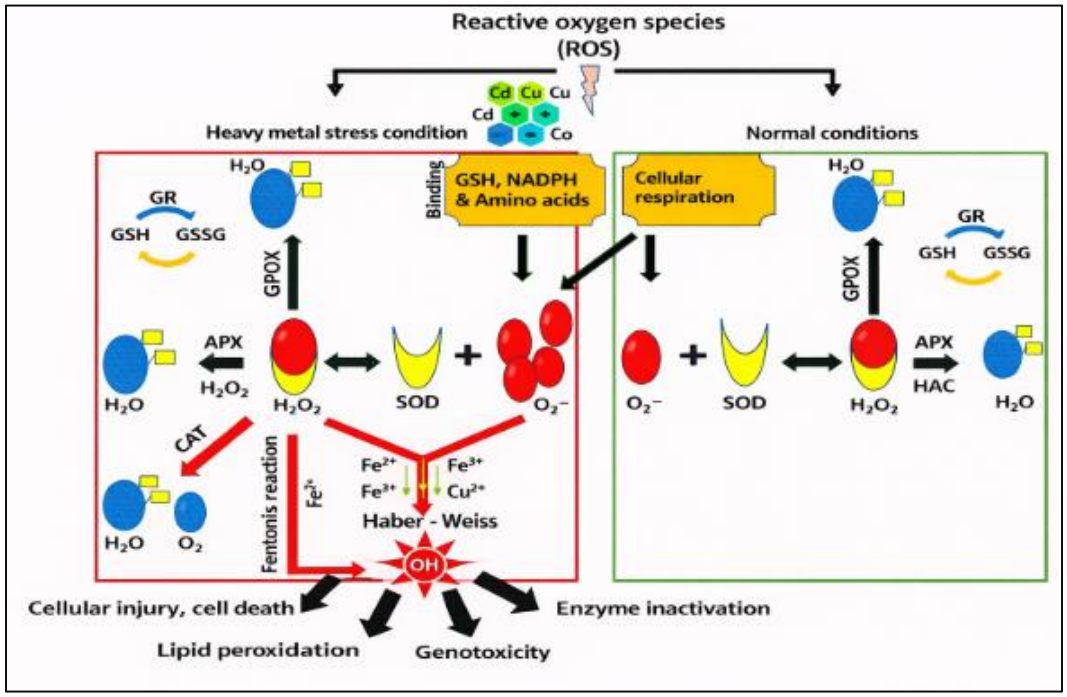

Figure 2.5: ROS's destiny in oxidative bursts caused by HM stress and natural [Hydrogen peroxide (H_2O_2), glutathione reductase (GR), reduced glutathione (GSH), glutathione disulfide (GSSG) and glutathione peroxidase (GPOX), ascorbate peroxidase (APX), hydrogen ascorbate, catalase (HAC), oxygen (O_2), superoxide dismutase enzyme (SOD), ferrous (Fe^{2+}) and cupric (Cu^{2+})] (adopted from Tyagi, et al., 2024)

This system consists of two components: the first utilizes numerous antioxidant enzymes, such as superoxide dismutase, peroxidase, ascorbate peroxidase and catalase. Antioxidant enzymes are found in multiple forms of isoenzymes in different cell organelles, primarily in their aqueous phases (Asada, 1999). The second component utilizes nonenzymatic substances, such as glutathione, flavonoids, carotenoids, ascorbate and tocopherols (Rudenko, et al., 2023; Tyagi, et al., 2024). Non-enzymatic antioxidants, like antioxidant enzymes, work in various cell compartments, including the membrane phases (isoprenoids and flavonoids) and the aqueous phase (ascorbic acid, flavonoids and glutathione). In contrast to antioxidant enzymes, low-molecular-weight antioxidants can interact with multiple forms of ROS. Besides, tocopherols and isoprenoids are crucial for the protection of vital electron transport chains (Rudenko, et al., 2023).

2.6.2.1 Superoxide Dismutase (SOD, EC 1.15.1.1)

SOD are metalloenzymes that catalyse the conversion of superoxide anion free radical ($^{\bullet}O_2^-$) to oxygen (O_2) and H_2O_2 (Rosa, et al., 2021). Based on the metal binding in the catalytic active site in plants, three SOD classes were recognized: manganese SOD (Mn-SOD), iron SOD (Fe-SOD) and copper/zinc SOD (Cu/Zn-SOD) (Abreu and Cabelli, 2010; Miller, 2012). Cu/Zn-SOD is the most abundant SOD form found in numerous plant cell compartments (Leonowicz, et al., 2018), while FeSOD is most found active in the chloroplastic enzyme (Asada, 2006; Pilon,

Ravet and Tapken, 2011). Lastly, MnSOD is found in the matrix of the plant's mitochondria (Candas and Li, 2018).

The primary function of SOD is to shield plant cells from the effects of oxidative damage and transform superoxide radicals into H_2O_2 and O_2 (Su, et al., 2021). This occurs via transition metal ions at the enzyme's active site (Zelko, Mariani and Folz, 2002). SOD needs cofactors (such as Fe, Mn, Cu and Zn) for maximum catalytic activity as it metabolizes toxic intermediates in the elimination of free radicals. The metal binding site is present between two SOD domains, with side chains such as histamine, aspartate and histidine (Paksi, et al., 2008). These cofactors tend to give away electrons to superoxide and then regenerate via a catalytic mechanism (Zheng, et al., 2023). After transformation, the resulting H_2O_2 acts as a second messenger for signal transduction in various physiological processes, influencing the expression of multiple genes. In addition, H_2O_2 diffuses across the cell membrane through aquaporin aqueous channels and transposes redox signals to the target site (Bienert, et al., 2007).

The induction of SOD activity has been observed in HMs-treated plants, reflecting the involvement of the cellular antioxidant system as a response to HMs (Ahmad, et al., 2010). Kisa's (2018) study showed an increase in leaves of *Solanum lycopersicum* treated with Cd, Cu and Pb (10, 20 and 50 ppm). However, in roots, Cd enhanced SOD activity, while increasing Cu concentrations reduced it. Pb

decreased SOD activity at 10 ppm but increased it at 20 and 50 ppm. Hence, this shows metal-specific and concentration-dependent effects on SOD enzyme activity in roots. Meanwhile, Hg exposure in *Clitoria ternatea* L increased the activities of SOD, indicating the plant's antioxidant defence system was activated to mitigate oxidative stress caused by Hg (Priya, et al., 2014). Kebert, et al. (2022) reported that at a Cd concentration of nine ppm, the activities of SOD in *Populus deltoides* were significantly higher in leaves than in the roots.

2.6.2.2 Peroxidase (POX, EC 1.11.1.7)

POX can be classified as haem or non-haem enzymes. They are widely distributed in both lower and higher plants. Their fundamental function is to promote the detoxification of ROS, particularly H_2O_2 and O_2 (Freitas, et al., 2024). This process that involves intermediates and multiple reactions is known as Poulos–Kraut mechanism (Derat and Shaik, 2006). It involves three distinct steps and is a common reaction of two-electron oxidation-reduction. Plant POXs are reported in the plasmalemma and tonoplast, the interior and exterior of the cellular wall as soluble and ionically bound forms (Chen, Shin and Liu, 2002). They can mediate the synthesis and decomposition of hormones, cell wall maintenance and synthesis, fruit growth and defence due to their common catalytic reaction (Pandey, et al., 2017; Kidwai, Ahmad, and Chakrabarty, 2020).

In the presence of H_2O_2, POX catalyses the oxidation of various organic and inorganic substrates. In higher plants, class III peroxidases are classical peroxidases or defined as secretory peroxidases that act as a biomarker of metal stress (Jouili, Bouazizi and Ferjani, 2011; Freitas, et al., 2024). Plants subjected to abiotic stressors, such as HMs, may experience altered ROS metabolism and cell oxidative burst induction (Mittler, et al., 2022), which may increase peroxidase expression levels. Based on this basis, POX expression levels may be enhanced to remove such toxic substances and avoid the inhibition of protein synthesis, degradation of DNA and membrane disruption (Rajput, et al., 2021). POX was significantly upregulated in *Gossypium hirsutum* L. seedlings after co-exposure of zinc oxide nanoparticles with Cd and Pb treatments (Priyanka, et al., 2021), while *Clitoria ternatea* L. treated with mercuric chloride showed an increase in H_2O_2 level and POX activity (Priya, et al., 2014). Exposure of *Solanum lycopersicum* to Cd, Cu and Pb showed increased POX activity in leaves and decreased roots across all doses of the HMs (Kisa, 2018).

2.6.2.3 Ascorbate Peroxidases (APX, EC 1.11.1.11)

APX belongs to the class I haem peroxidase superfamily and is a haem-containing enzyme (Jouili, Bouazizi and El Ferjani, 2011). APX eliminates ROS by converting H_2O_2 into water (Rajput, et al., 2021). The reduction of H_2O_2 is carried out via the ascorbate-glutathione pathway, where ascorbate acts as an electron

donor (Shigeoka, et al., 2002). In plant stroma, monodehydroascorbate (MDAsA) may either spontaneously change into dehydroascorbate (DAsA) or be reduced back to ascorbate by MDAsA reductase, whereas DAsA will also be reduced to ascorbate utilizing DAsA reductase with glutathione as a substrate (Smirnoff, 2018; Dell'Aglio and Mhamdi, 2020).

APX works effectively with Fe-SOD and Cu/Zn-SOD to eliminate ROS (Chagas, et al. 2008). The duration of exposure, treatment option, species and organs involved will affect the antioxidant enzyme activity (del Carmen, et al., 2002). According to a study by Kisa (2018), APX activity in tomato leaves was induced by Pb, Cd and Cu treatments. The same study found that Cd boosted APX activity in the roots while Cu decreased it. Yilmaz, et al. (2017) revealed that APX enzymes showed varying activity levels in response to HMs. It fluctuated between two to 32 ppm for Al, then peaked at 16 ppm, while the highest activities were observed for Cr and Pb at eight ppm and four ppm, respectively. As for the root, Al exposure caused APX activity to increase continuously up to 16 ppm before decreasing at higher concentrations. Both Cromium (Cr) and Pb treatments resulted in the highest activity at 16 ppm. APX activity was generally higher in roots than leaves, indicating a stronger antioxidative response in roots to eliminate ROS.

2.6.2.4 Glutathione reductase (GR, EC 1.8.1.7)

GR is present in both prokaryotic and eukaryotic organisms, belonging to the family of NADPH-dependent oxidoreductases. Besides being found in the cytosol, chloroplasts, and mitochondria of photosynthetic tissues, 80% of GR activity was revealed to be of the chloroplast isoform (Edwards, et al., 1990; Ashraf, 2009). It is essential in regulating cellular redox homeostasis and maintaining supply of reduced glutathione (Couto, Wood and Barber, 2016). Glutathione disulfide (GSSG) is rapidly converted to reduced glutathione (GSH) by GR to maintain the correct ratio of GSH/GSSG (Kumar, Prasad and Sytar, 2012).

Singh, et al. (2015) investigated the roles of the ascorbate-glutathione (AsA-GSH) cycle and thiol metabolism in regulating arsenate [As(V)]-induced oxidative stress and tolerance in *Luffa* seedlings. As the ascorbate concentration increased, the AsA-GSH cycle was discovered to have a minor role as compared to thiol metabolism. The activity of GR and GSH was upregulated, while APX, monodehydroascorbate reductase (MDHAR), dehydroascorbate reductase (DHAR) and reduced ascorbate (AsA) activities were downregulated. Thus, GR plays an essential function in cell defence against notorious reactive oxygen metabolites (Upadhyay and Panda, 2009).

2.6.3 Genomic Level Defense Systems of Plants against HMs

Plants have developed complicated defense strategies to create either resistance or tolerance towards HMs (Figure 2.6). Biosynthesis of biomolecules, such as chelators, metallothioneins and proton ion pumps occurs to nullify HM toxicity (Singh, et al., 2016b). Nevertheless, excessive HM concentration and failure of the strategies above may trigger ROS formation, which interferes with the cellular redox system. This leads to activating the antioxidant defense system (antioxidant enzymes and compounds will be produced) to scavenge the ROS. Metal-chelating compounds, such as metallothioneins, phytochelatins, organic acids and amino acids, provide homeostasis balance in cells. They are capable of detoxing, proliferating and regulating their cycle or causing apoptosis in the cells (Clemens, 2019).

Once the first line of defense is breached, plants will activate their defence response to HMs stress, such as MAPK cascades (Tyagi, et al., 2024), RAS-related GTP-binding proteins (Liu, et al., 2014) and Cyclic AMP (cAMP) (Blanco, et al., 2020).

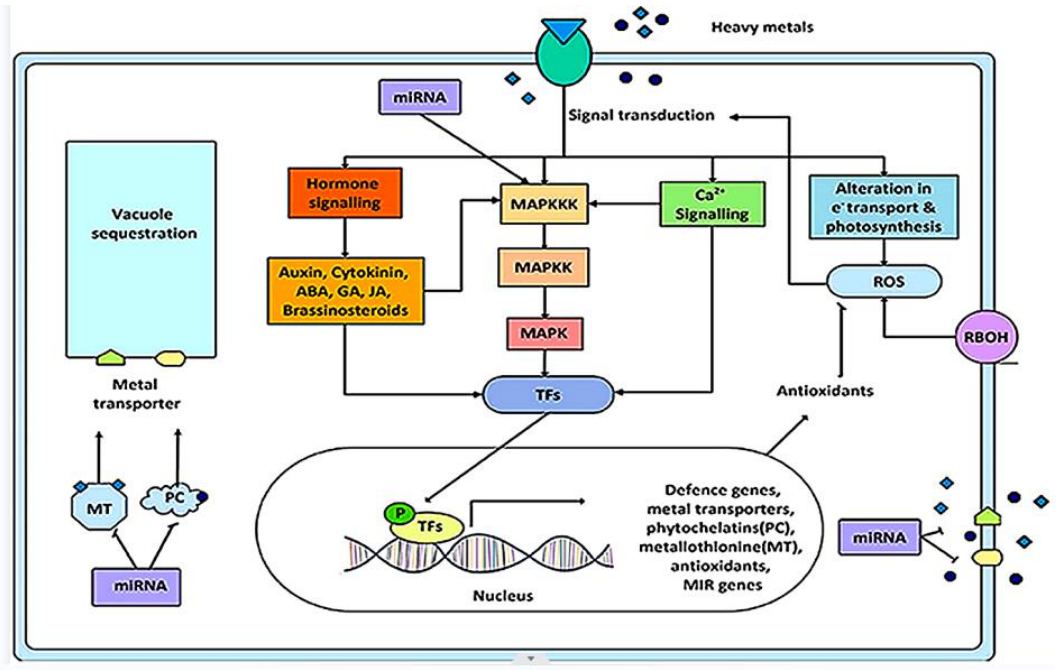

Figure 2.6: Crosstalk across signalling pathways and their ultimate reaction in HM stress [abscisic acid (ABA), gibberellins (GA), jasmonic acid (JA), transcription factors (TFs), metal transporters (MT), phytochellatins (PC), miRNA genes (MIR genes)] (adopted from Jalmi, et al., 2018)

2.6.3.1 Mitogen-Activated Protein Kinase (MAPK) Signalling Pathway

HM stress, among other known abiotic stresses, profoundly affects the MAPK signalling pathways. An essential signalling event linked to almost every aspect of plant growth, yield, development and response to abiotic and biotic stress is the MAPK pathway. It has been documented that MAPK signalling interacts with ROS and abscisic acid (ABA) signalling processes to help plants respond to abiotic stress (Manna, Rengasamy and Sinha, 2023). Although plant MAPKs can occasionally move from the cytoplasm to the nucleus, they are typically found in the cytoplasm and/or nucleus. MAPK cascade is made of three-tier components,

namely Mitogen-Activated Protein Kinase Kinase Kinase (MAPKKK), Mitogen-Activated Protein Kinase Kinase (MAPKK) and MAPK that mediate phosphorylation responses from the upstream receptor to the downstream target (Bigeard and Hirt, 2018).

In the final step of the three-tier cascade, MAPK signalling mediates the direct transmission of HM stress signals to the nucleus via transcription factors (TFs) (Keyster, et al., 2020). TFs are crucial in controlling how plants react to HMs and enhancing their ability to withstand and accumulate them. TFs, such as WRKY, myeloblastosis protein, heat shock TF, ethylene-responsive TF and basic leucine zipper, control the expression of stress-related genes, in particular, genes associated with metal responses (Li, et al., 2022). A transcriptomic study by Karanja, et al. (2017) revealed that 20 RsWRKY transcripts in *Raphanus sativus* L displayed significant increases after Pb treatments. Antioxidant genes, metal transporters, metallothionine phytochellatins and miRNA genes represent most stress-related genes (Jalmi, et al., 2018). The kinetics of MAPK activation vary and rely on upstream signalling events that lead to the activation and deactivation of the MAPKs (Bigeard and Hirt, 2018).

Liu, et al. (2019) explored the relationship between MAPK cascades and ROS in *Zea mays* roots under cadmium chloride stress. The key finding includes that Cd induces ROS production, which activates extracellular signal-regulated kinase (ERK)-like MAPKs, namely ZmMPK3-1 (43 kDa) and ZmMPK6-1 (45

kDa). ROS production occurs before MAPK activation, suggesting ROS acts upstream in the signalling pathway. Li, et al. (2017b) demonstrated that ABA-insensitive protein kinase 1 (AIK1), a MAPKKK, is a key regulator of ABA signalling in *Arabidopsis thaliana*. The AIK1-MKK5-MPK6 cascade is identified as a critical pathway in ABA-regulated root growth and stomatal responses. ABA activates AIK1, which is localized in cytoplasm and phosphorylates MKK5 (MAPK kinase) in an ABA-dependent manner.

2.6.3.2 RAS Signalling Pathway

The RAS pathway, like MAPK, is a signalling pathway that transduces external stimuli into cellular responses. The RAS superfamily of GTPases comprises small (20–40 kDa) monomeric GTPases that are involved in controlling various cellular processes. When attached to a GTP nucleotide, these proteins function as molecular switches that initiate various actions; upon hydrolysis of GTP to GDP, they cease to function. Therefore, the activation and inactivation cycle are completed, and small G proteins act as molecular switches, transducing an upstream signal to a downstream effector(s) (Figure 2.7) (Takai, Sasaki and Matozaki, 2001).

Although the two nucleotide states of RAS superfamily GTPases possess similar conformations, the switch I (Ras residues 30-38) and switch II (59-67) domains exhibit distinct alterations (Wennerberg, Rossman and Der, 2005).

Specific interaction between regulators and effectors is obtained via changes induced by these nucleotides. All eukaryotic creatures have these GTPases (Sørmo, et al., 2006). The five primary functional families of GTPases that comprise the RAS superfamily are Ras, Rab, Ran, Rho and Arf/Sar. However, neither the Ras family nor Rho sub-family members are found in plants. All members of the RAS superfamily share a structurally conserved G domain that interacts with GTPase regulatory proteins to promote nucleotide binding and hydrolysis (Wennerberg, Rossman and Der, 2005).

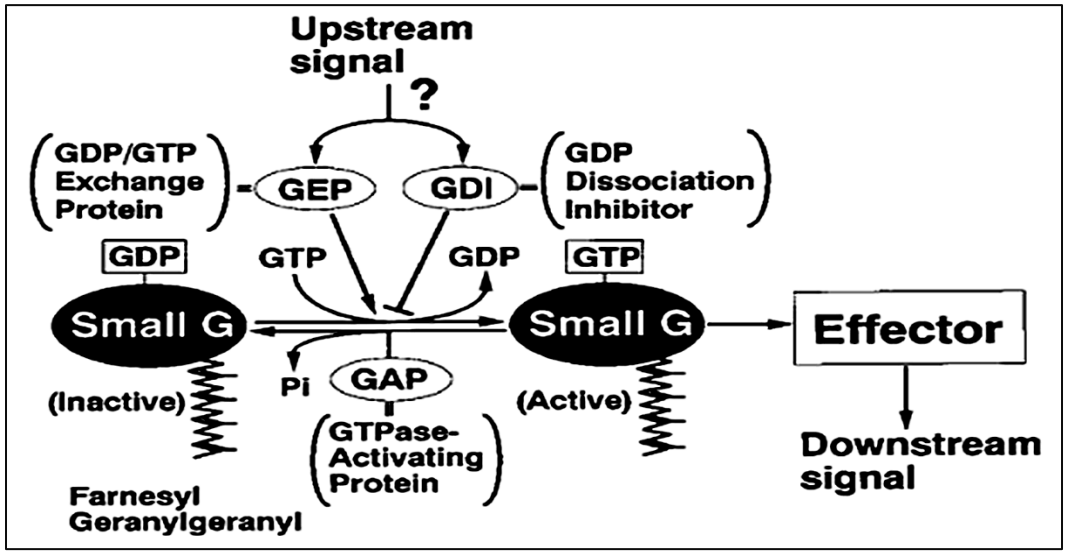

Figure 2.7: Regulation of small G protein activity [Guanine nucleotide exchange factors (GEFs) and Guanine nucleotide dissociation inhibitors (GDIs)] (adopted from Takai, Sasaki and Matozaki, 2001)

It has been demonstrated that the RAS-related small GTP-binding protein, RabE1c can attach to an ABA receptor in the plasma membrane of *Arabidopsis*

thaliana, therefore favorably controlling ABA signalling (Chen, et al., 2021). The primary function of this protein is to regulate cellular processes involving the actin cytoskeleton, including determining cell shape and polarity. While the specific roles of RAS proteins in response to other HMs are less extensively studied, they likely contribute to the broader plant stress response, including ROS management and detoxifications (Niekerk, et al., 2024). HM stress triggers various signalling cascades, including calcium/calmodulin-dependent and ROS-mediated pathways, which activate MAPK. These cascades ultimately lead to the phosphorylation of specific genes. G-proteins, such as Ras, are involved in these signalling pathways, helping plants adapt and cope with HM toxicity (Locato and De Gara, 2018).

2.6.3.3 cAMP Signalling Pathway

Cyclic nucleotide cAMP (3′,5′-cyclic adenosine monophosphate) plays a significant role in various physiological processes in plants (Blanco, et al., 2020), such as ion homeostasis (Trewavas, 1997), cell cycle progression and division (Ehsan, et al., 1999), seed germination, stomatal opening (Jin and Wu, 1999) and heavy metal toxicity tolerance (Ma, et al., 2009). cAMP reactions are complicated, as cAMP signalling pathways are highly compartmentalized in cells. Different stimuli that alter cAMP levels may have distinct physiological effects (Gancedo, 2013; Arora, et al., 2013).

Transmembrane ACs (TmAC) and soluble ACs (sAC) convert ATP to cAMP (Figure 2.8). G proteins activate TmAC upon external signalling. Elevated cAMP levels activate protein kinase A (PKA) through the release of the two catalytic subunits (Cs) from the two regulatory subunits (Rs), leading to phosphorylation of downstream targets like cAMP response element binding protein (CREB). Cyclic nucleotide phosphodiesterases (PDEs) hydrolyze cAMP to AMP, terminating signalling. Balance between ACs and PDEs determines the cAMP level and signalling activity. cAMP can directly activate the cyclic nucleotide-gated channels (CNGCs), exchange protein Epac and Popeye domains (Popdcs). A-kinase anchoring proteins (AKAPs) frequently bind Acs, PKA, PDEs and other downstream effectors at different subcellular sites within a single cAMP cascade (Zhang, et al., 2016).

Zhang, Ryan and Tyerman, (2021) studied Al^{3+}-activated malate efflux and cation channel activity in wheat root apices, comparing between Al^{3+}-tolerant (ET8) and Al^{3+}-sensitive (ES8) genotypes. Al^{3+}-tolerant wheat releases malate from root apices, which chelates toxic Al^{3+} in the rhizosphere, forming non-toxic complexes. Besides, the Al^{3+}-activated anion channel is highly permeable to malate. Al^{3+} inhibits outward K^+ currents in both genotypes, but in ET8 protoplasts, cAMP reactivates outward K^+ currents. cAMP may modulate the activity of outward K^+ channels through direct interaction with channel proteins or via cAMP-dependent protein kinases (Labarca, et al., 1996). Hence, cAMP could act as a secondary

messenger, transducing environmental signals into cellular responses that regulate ion flux (Assmann, 1995).

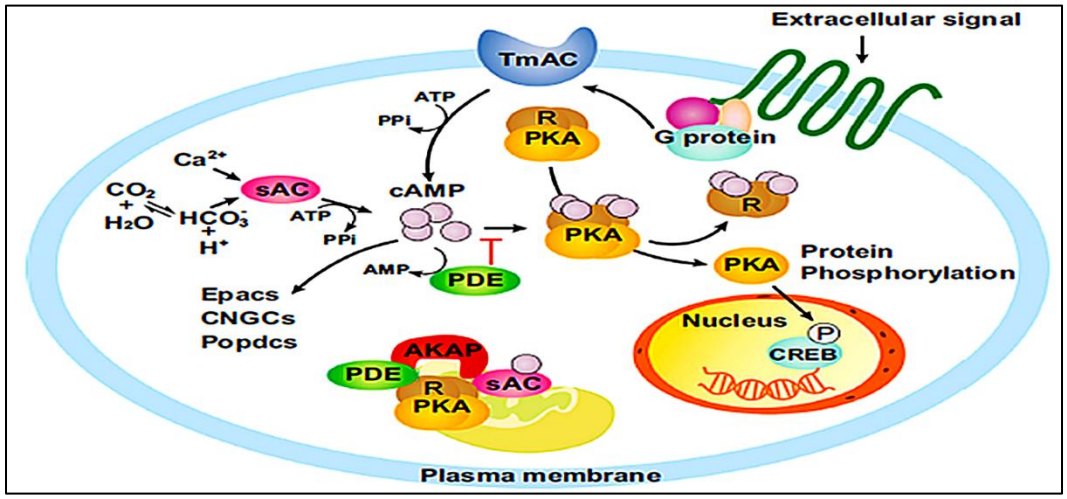

Figure 2.8: Mitochondrial cAMP signalling in general [transmembrane AC (TmAC), soluble AC (sAC), protein kinase A (PKA), catalytic subunits (Cs), regulatory subunits (Rs), cAMP response element binding protein (CREB), phosphodiesterases (PDEs), exchange protein (Epac), cyclic nucleotide-gated channels (CNGCs), Popeye domain-containing proteins (Popdcs), A-kinase anchoring proteins (AKAPs)] (adopted from Zhang, et al., 2016)

2.7 Transcriptomic Study on Plant Defense Systems Towards HM

Development in "omics" approaches, which include transcriptomics, proteomics and metabolomics, has contributed valuable insights into the molecular pathways that underpin a plant's HM stress response. For example, transcriptomic analyses have displayed the genes that regulate metal chelation (e.g. phytochelatins and metallothioneins) and transporters that compartmentalize HMs within a plant

cell. Integration of multiple “omics” has further elucidated the complicated regulatory networks and signalling cascades that govern plant HM stress adaptation (Raza, et al., 2022).

Transcriptome is a comprehensive record of all ribonucleic acid (RNA), which includes messenger RNA, small interfering RNA and long non-coding RNA. Over the decades, this analysis holds the key to unraveling the complexities of gene regulation, cellular function and disease pathogenesis (Wu, et al., 2014). The field of transcriptomics has undergone a remarkable transformation, driven by continuous technological advancements. Two key contemporary techniques in this field are microarrays which measure a collection of predetermined sequences, and RNA sequencing (RNA-Seq) which utilizes high-throughput sequencing to catch all sequences (Lowe, et al., 2017). RNA-Seq can provide an overview of a cell transcriptome. It enables the identification of novel transcripts, discloses gene expression profiles, detects allele-specific expression and identifies unusual, spliced genes (Raghavachari and Garcí‐Reyero, 2018; Peymani, Farzeen and Prokisch, 2022).

Transcriptome analysis has revealed the differentially expressed genes (DEGs) involved in metal chelation, sequestration into vacuoles, antioxidant defense, signal transduction and various metabolic pathways (Chrestensen, Starke and Mieyal, 2000; Shahid, et al., 2015). Hierarchical clustering provides a visual representation of gene expression patterns, enabling the formulation of hypotheses

about gene function and regulation (Smet, Opdebeeck and Vandepoele, 2023). Hierarchical clustering assists in identifying related stress-responsive gene modules and elucidating the signalling pathways that may trigger their activation (Shiri, et al., 2019). This method enables the identification of co-expressed gene clusters involved in the same biological pathways or processes, thereby providing valuable insights into the molecular mechanisms governing plant stress, response development and physiological adaptations (Gasch and Eisen, 2002). Exposure to HMs can trigger a wide range of biochemical and physiological responses in plants, stemming from the transcriptomic regulatory factors and activation of numerous genes. These early signals of metal toxicity often resemble the plant's response to other abiotic stresses, such as osmotic stress, drought and nutrient imbalances, suggesting an interconnected and shared regulatory network (Table 2.4) (Mashabela, Masamba and Kappo, 2023).

Gene expression analysis further suggests that proteins such as metal ion-binding proteins and ATP-binding cassettes play essential functions in the accumulation of CuO-NP by plant leaves (Xiong, et al., 2021). Furthermore, the study of Pb stress response in the roots of *Pogonatherum crinitum* revealed upregulation of key genes related to transportation, antioxidation and transcription functions (Zhu, et al., 2022). In their study, DEGs were significantly enriched in Gene Ontology (GO) related to metabolic processes, catalytic activity and transporter activity. A total of 17 Pb-tolerant genes were identified, involved in antioxidation, Pb transport and stress-response regulation. Key Kyoto

Encyclopedia of Genes and Genomes (KEGG) pathways included the ascorbic acid (ASA)-GSH cycle, heavy metal transporters (ABC transporters, Nramp) and signal transduction (MAPK signalling, plant hormone pathways).

Table 2.4: Gene expression responses involved in plant HM stress tolerance and accumulation

Plant	Stress type	Key DEGs / proteins	Enriched GO terms	Major KEGG pathways	Key remarks
Leaves of lettuce (*Lactuca sativa* L.) (Xiong et al., 2021)	Copper Oxide Nano-particles	Metal ion-binding proteins; ATP-binding cassette (ABC) transporters	Cell wall organization, auxin transport, stress response, hormone levels and metabolic processes related to ROS	Photosynthesis, plant hormone signal transduction, ABC transporters	Various transporters and antioxidant mechanisms that help mitigate the phytotoxic effects of CuO-NPs
Roots of *Pogonatherum crinitum* (Zhu et al., 2022)	Pb stress	17 Pb-tolerant genes (transporters, antioxidation enzymes, and transcription factors)	Metabolic processes, regulation, binding, catalytic activity and transporter activity	Phenylpropanoid biosynthesis, MAPK signaling pathway – plant and Plant hormone signal transduction	Metabolic processes, catalytic activity and transport as key response mechanism of *P. crinitum*'s root

Despite being known as a hyperaccumulator (Rai, et al., 2024), the molecular basis of HMs tolerance in *P. stratiotes* is poorly understood. Identification of the genes involved will provide an insight into the active defense responses which are regulated through a complex and interconnected network of signalling pathways (Di, Gomila and Takken, 2017; Yuan, et al., 2019). Chan, et al., (2022)'s study showed a high accumulation of Pb in the root of *P. stratiotes* grown in EAPR and non-EAPR systems. The study of Pb stress responses at the transcriptional level can be further explored to gain a deeper understanding of the Pb-induced stress response pathways. This may enable better field application of EAPR to maximize HM uptake.

Identifying key genes involved in HMs responses could provide fundamental insights into plant adaptation mechanisms. This knowledge may enhance our ability to address other environmental HM contaminants and pave the way for innovative phytoremediation strategies, enabling more effective waste management in the future. A deeper molecular understanding of these processes could drive the development of bioengineered plants or microbial systems tailored for HM detoxification, offering sustainable solutions for environmental cleanup. This highlights the power of transcriptomics in deciphering plant metal stress responses. However, such comprehensive molecular analyses have not yet been applied to *P. stratiotes* under the combined stress of leachate and an electric field.

CHAPTER 3

METHODOLOGY

3.1 Experimental Set Up

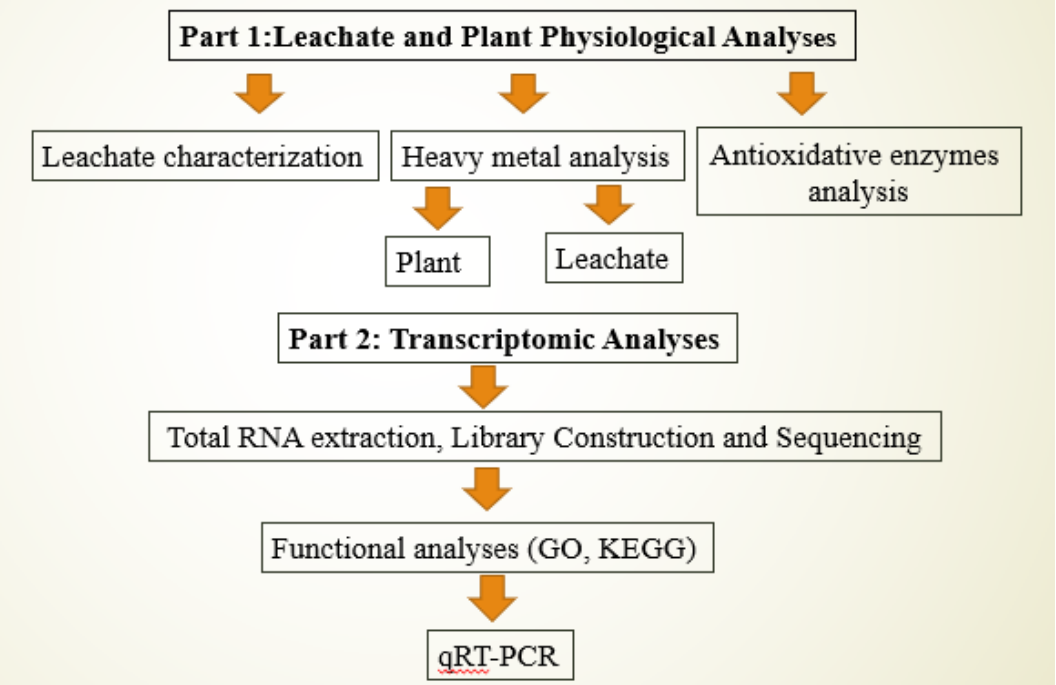

Figure 3.1: Overall research flowchart

3.1.1 Plant Preparation and Growth Conditions

P. stratiotes plants were obtained from Rawang (3°19'02.6"N 101°35'46.9"E) (ambient temperature, natural lightning), Selangor and they were propagated under similar conditions for approximately 3 weeks in Kampar

(4°20'05.5"N 101°09'26.7"E) using tap water (Figure 3.2). The selected plants used in this study had a fresh weight range of 70-80 g, with a well-developed root system and approximately 10 to 15 leaves, indicating a uniform vegetative growth stage. In the absence of chronological age measurements for the plants, morphological criteria were used to ensure consistent growth stages across all experimental units (Tan, et al., 2023; Acharya, et al., 2025). The plants were initially washed with distilled water, subsequently transferred to half-strength Hoagland solution pH 6.5 (one liter of solution containing 0.253 g of KNO_3, 0.0676 g of KH_2PO_4, 0.20 g of $MgCl_2.6H_2O$ and 0.59 g of $Ca(NO_3)_2.4H_2O$) to acclimatize for three days before they were used in the subsequent studies (Putra and Hastika, 2018).

Figure 3.2: Morphological features of water lettuce grown in aquatic medium, displaying buoyant rosettes

3.1.2 Preparation of Synthetic Leachate

Two experimental aquariums were set up, each filled with synthetic leachate: one for the EAPR treatment and one for the non-EAPR treatment. Synthetic leachate with HMs (before treatment) was used as a control. Based on the preparation for a liter of synthetic leachate [0.005 g C_3H_5NaO2 (sodium propionate), 0.1 g $C_2H_3NaO_2$ (sodium acetate), 0.05 g $C_9H_8Na_2O_4$ (disodium salicylate), 0.382 g NH_4Cl (ammonium chloride), 0.084 g $MgCl_2.2H_2O$ (magnesium chloride dihydrate), 0.11 g $CaCl_2.2H_2O$ (calcium chloride dihydrate), 0.012 g $NiCl_2 \cdot 6H_2O$ (nickel(II) chloride hexahydrate), 0.006 g $CdCl_2 \cdot 2.5H_2O$ (cadmium chloride hemipentahydrate), 0.011 g $MnCl_2 \cdot 4H_2O$ (manganese(II) chloride tetrahydrate), 0.013 g $ZnSO_4 \cdot 7H_2O$ (zinc sulfate heptahydrate), 0.007 g $Pb(NO_3)_2$ (lead(II) nitrate) and 0.015 g $FeCl_3 \cdot 6H_2O$ (iron(III) chloride hexahydrate)], 10 L of synthetic wastewater were prepared (Dan, et al., 2017).

The prepared synthetic leachate consisted of low-molecular-weight volatile fatty acids (propionate and acetate), ammonium, humic substances and selected HMs. This simulation resembles the major organic, nitrogenous and metal components commonly found in landfill leachate.

3.1.3 EAPR System Set Up

Ten liters of synthetic leachate were filled into aquariums for EAPR and non-EAPR treatments. The aquariums, with dimensions Length (60 cm), Width (30 cm), and Height (30 cm), were used in this study. Five *P. stratiotes* plants (each with similar fresh weights and growth stage to ensure comparable plant mass–to–leachate ratio across treatments while avoiding overcrowding) were transferred to each aquarium. The effects of the treatments were evaluated for 7 days to balance effective HM uptake and plant survival. Light source was provided by fluorescent tubes (40 W, Philip, positioned approximately 25 cm from the water surface to deliver about 60 – 90 μmol m^{-2} s^{-1} of photosynthetic photon flux density), controlled by a timer to give 12/12 h (light/dark cycle) at a temperature of 26°C. Titanium electrode and stainless steel were applied as anode and cathode, respectively in the EAPR aquarium (Figure 3.3).

The system operated at a constant voltage of 2 V via DC regulated power supply. The non-EAPR aquarium, which without electrodes, was used to compare the effects of electro-assistance on the metal-removal ability and survival of *P. stratiotes.*

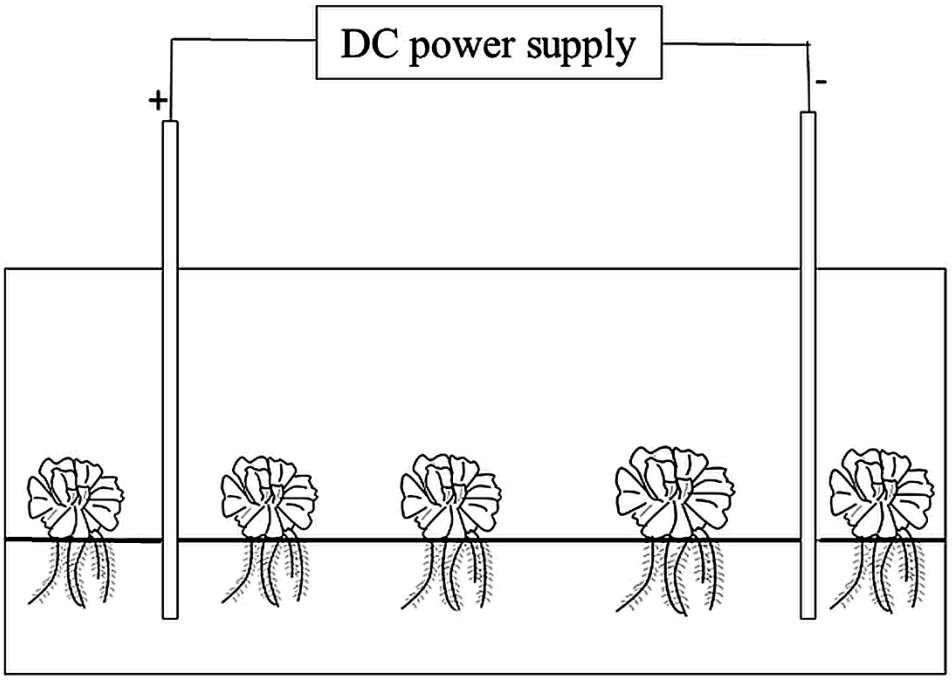

Figure 3.3: The EAPR setup consisted of a titanium electrode (anode) and a stainless steel electrode (cathode)

3.2 Synthetic Leachate Characterization

The leachate analyses, as outlined in Sections 3.2.1 to 3.2.7, were performed according to the Standard Methods for Water and Wastewater Analysis, with modifications (Baird, et al., 2017). All tests under section 3.2. were performed in triplicate.

3.2.1 pH Measurement

The pH meter (Mettler-Toledo) was calibrated with pH 4, pH 7 and pH 10 buffers before use. The probe was immersed in the samples to obtain the pH values.

3.2.2 Colour Determination

One mL of the leachate sample was diluted with 9 mL of distilled water to create a 10-fold dilution. The absorbance of the diluted sample was measured using a DR6000 UV-VIS spectrophotometer at a wavelength of 465 nm. Distilled water was used as a blank (Azmi, et al., 2014).

3.2.3 Conductivity

The conductivity meter (Mettler-Toledo, Five EasyTM30) was calibrated using the standard solution HI 7031L, which yields a conductivity of 1413 μS/cm at 25℃. The leachate sample was transferred into a beaker, and the conductivity meter probe was immersed in it for analysis.

3.2.4 Turbidity

Leachate samples' turbidity was measured at 860 nm using a turbidimeter (HANNA instruments, HI 98703). Two-point calibration was performed with standard cuvettes of less than 0.1 NTU, 15 NTU and 100 NTU. Next, the standard cuvettes containing the sample were placed into the instrument holder to record the turbidity reading.

3.2.5 Measurement of the Oxidation-Reduction Potential (ORP), Dissolved Oxygen (DO) and Total Dissolved Solids (TDS)

ORP, DO, and TDS of the leachate sample were measured using a portable meter that can measure multiple parameters (EUTECH PCD650). ORP calibration was performed using ORP standard solutions (470 mV), DO calibration utilized 100% saturation calibration and TDS calibration was via conductivity standard solution (1413 µS/cm KCl). The samples were poured into a 50 mL beaker, and the reading was taken after the probe was immersed in them.

3.2.6 Biochemical Oxygen Demand (BOD_5)

Leachate samples were sent to MY CO2 (KL) Sdn. Bhd. for BOD analyses using an Eutech DO 2700 BOD meter (15th to 24th May 2019). Three replicates of each sample were collected in 500 mL bottles and sealed in a polystyrene box with ice packs before being sent to the company. Briefly, the procedure involves filling an airtight bottle of the appropriate size with a sample that overflows and then incubating it for five days at the designated temperature. DO measurements are made both before and after incubation, and the difference between the two is used to calculate the BOD, as showin in equation [1] (MRC Laboratory Instruments, n.d.).

$$BOD_5\,(mg/L) = DO_0 - DO_5 \qquad [1]$$

DO_0 = DO on day 0 (initial DO)
DO_5 = DO on day 5 (final DO)

3.2.7 Chemical Oxygen Demand (COD)

The leachate samples were diluted 10 times with deionized water and 200 µL of these samples were transferred into COD vials. A blank was prepared by adding 1 mL of deionized water into an empty COD vial. The sample vials and blank were gently inverted and closed tightly. After preheating to 150℃, the blank and sample vials were placed into the COD digital reactor (HACH, DRB 200) and digested for two hours. After that, the vials were allowed to cool to ambient temperature before absorbance measurements were performed with a DR6000 UV-VIS spectrophotometer at 430 nm.

3.2.8 Total Ammonia Determination

A 50 ppm ammonia stock solution was used to prepare a set of five standard solutions in the range of one ppm, two ppm, three ppm, four ppm and five ppm, each with a volume of 5 mL. Next, each standard solution was added with 100 µL of Rochelle Salt solution and 100 µL of Nessler Reagent. The steps were then repeated by replacing the standard solution with a five mL leachate sample. The absorbances of the standards and the leachate samples were measured at 425 nm with a spectrophotometer (GENESYS 10S UV-Vis). Deionized water was used as a blank. A standard curve was plotted to determine ammonia concentration in the leachate samples (Azmi, et al., 2014).

3.3 Comparative Effects of EAPR and Non-EAPR Treatments on Plant Growth Performance and Heavy Metal (HM) Analyses

3.3.1 Measurement of Plant Total Biomass and Total Chlorophyll Content

The initial biomass of *P. stratiotes* was recorded prior to exposure to synthetic leachate and used as the control reference for calculating biomass reduction after the 7-day treatment period. The plants were rinsed with tap water and patted dry with tissues to ensure accuracy during the weighing process using an electronic analytical balance. By using the equation [2] below, the percentage drop in total biomass was determined:

$$\text{Percentage drop in total biomass} = \frac{B_{D0} - B_{D7}\,(g)}{B_{D0}\,(g)} \times 100\% \qquad [2]$$

B_{D0} is the total biomass (g) at day 0
B_{D7} is the total biomass (g) at day 7

As for the measurement of chlorophyll content, 0.2 g of plant leaves (from the pooling of leaves from five *P. stratiotes* plants within each aquarium to form one replicate per treatment) were cut into 0.5 cm × 0.5 cm segments and subsequently incubated in acetone at 4°C for 24 h in darkness. The absorbance of the solutions was measured using a spectrophotometer (GENESYS 10S UV-Vis) at λ_{645} and λ_{663} nm (Moran and Porath, 1980). Acetone was used as blank. Based on

the equations [3] to [5] below, the chlorophyll concentrations (mg/mL) were determined in triplicate:

$$[\text{Chl } a] = [12.7 \times \text{Absorbance at } \lambda_{663}\,\text{nm}] - [2.69 \times \text{Absorbance at } \lambda_{645}\,\text{nm}] \quad [3]$$
$$[\text{Chl } b] = [22.9 \times \text{Absorbance at } \lambda_{645}\,\text{nm}] - [4.68 \times \text{Absorbance at } \lambda_{663}\,\text{nm}] \quad [4]$$
$$[\text{Total Chl}] = [8.02 \times \text{Absorbance at } \lambda_{663}\,\text{nm}] + [20.2 \times \text{Absorbance at } \lambda_{645}\,\text{nm}] \quad [5]$$

3.4 Comparative Effects of EAPR and Non-EAPR Treatments on Heavy Metals (HMs) Analyses in Synthetic Leachate and Plants

3.4.1 Sample Preparation via Digestion of Synthetic Leachate

In a 250 mL beaker, 5 mL of synthetic leachate sample was digested using 2 mL of 30% (v/v) hydrogen peroxide and 5 mL of nitric acid (70%). All leachate and plant samples were subjected to acid digestion prior to analysis for accurate and reliable quantification of HM by flame atomic adsorption spectrophotometer (FAAS). Leachate contains complex organic matter, colloids and metal–organic complexes. Digestion of leachate eliminates matrix interference and converts metals into measurable ionic forms. In contrast, plant tissues require complete digestion to demolish the solid biological matrix and release intracellular/ cell-wall-bound HMs into solutions. This is a critical step in trace metal analysis, ensuring complete matrix destruction and minimizing FAAS analytical error (Rawat, et al., 2024). The samples were then completely digested on a hot plate. The solutions were allowed to cool down to room temperature and transferred to a calibrated flask before being diluted with deionized water to a final volume of 10 mL. The amounts

of metals in the final solution were measured by FAAS (Figure 3.4) (Bezerra, et al., 2015). Five standard solutions for each HM tested were prepared in different concentrations to calibrate the FAAS (Appendix 1 and 2).

Figure 3.4: Single-beam flame atomic absorption spectrophotometer (FAAS)

3.4.1.1 Evaluation of Heavy Metals Through Removal Efficiency

Results obtained from FAAS were used to calculate the removal efficiency of EAPR and non-EAPR-treated leachate. HM removal efficiency of a treatment was determined using the equation [6] below (Naghipour, et al., 2018):

$$\text{Removal efficiency (\%)} = \frac{C_0 - C_t}{C_0} \times 100\% \qquad [6]$$

C_t = concentration (mg/L) at the end of adsorption
C_0 = initial concentration (mg/L) of heavy metals

3.4.2 Sample Preparation via Digestion of Plant Samples

After seven days of incubation, the plants were harvested from the aquariums (control, EAPR and non-EAPR). Leaves and roots were weighed, separated and washed thoroughly with running tap water. The plant parts were cut separately into small pieces and subsequently dried at 80°C for 2 days. Approximately 0.1 g of each dried part was then digested with 5 mL of 68% HNO_3 overnight. The digested samples were then made up to 50 mL using deionized water (Putra and Hastika, 2018) and analysed using a FAAS.

3.4.2.1 Evaluation of Heavy Metals (HMs) Through Bioconcentration Factor (BCF) and Translocation Factor (TF)

The data obtained from FAAS were then used to get both BCF and TF values. BCF was determined by using the equation [7] of Ndimele, et al. (2014):

$$BCF = \frac{C_{plant}}{C_{solution}} \quad [7]$$

C_{plant} = Metal concentration in plant tissue (mg/kg)
$C_{solution}$ = Initial metal concentration in solution (mg/L)

TF is an indicator of the ability of a plant to translocate a specific heavy metal from its root to shoot. Equation [8] was applied to calculate TF (Das, et al., 2016):

$$TF = \frac{C_{leaf}}{C_{root}} \quad [8]$$

C_{leaf} = Metal in leaf (mg/kg)
C_{root} = Metal in root (mg/kg)

3.5 Comparative Effects of EAPR and Non-EAPR Treatments on Plant Antioxidative Enzyme Assays

3.5.1 Enzyme Extraction Procedures

Three different enzyme extraction buffers were prepared for (a) peroxidase (POX) and Superoxide Dismutase (SOD): 1% (w/v) polyvinylpolypyrrolidone (PVPP), 1 mM phenylmethylsulphonyl fluoride (PMSF), 0.1 mM ethylenediaminetetraacetic acid (EDTA) and 0.1 M of pH 6.8 potassium phosphate buffer, (b) ascorbate peroxidase (APX): 1% (w/v) PVPP, 2 mM dithiothreitol (DTT), 1 mM ascorbic acid, 1 mM PMSF, 1 mM EDTA and 50 mM of pH 7.0 potassium phosphate buffer (Peixoto, et al., 1999) and (c) glutathione reductase (GR): 1% (w/v) PVPP, 1 mM PMSF, 2 mM DTT, 0.02% (w/v) triton X-100, 1 mM EDTA and 0.1 M potassium phosphate buffer (pH 7.0) (Carlberg and Mannervik, 1985).

Enzyme extracts were prepared as follows: one gram of either shoot or root samples was cut into small pieces and ground with liquid nitrogen. The samples were then homogenized in 10 mL of an appropriate enzyme extraction buffer and filtered through two layers of cheesecloth. Subsequently, the filtrate was

centrifuged at 12,000 x *g* for 15 minutes at 4°C. The resulting supernatant, which contained the crude enzyme extract, was collected and stored at -20°C until further analyses (Vestina, et al., 2011).

3.5.2 Enzyme Assays Preparation

Five different enzyme reaction solutions were prepared for each particular assay: (a) POX: 20 mM pyrogallol, 20 mM H_2O_2, and 0.1 M of pH 6.8 potassium phosphate buffer; (b) APX: 1 mM H_2O_2, 0.8 mM ascorbic acid and 50 mM of pH 6.0 potassium phosphate buffer (Cakmak and Horst, 1991); (c) SOD: 60 μM riboflavin, 2.25 mM nitroblue tetrazolium (NBT), 0.1 mM EDTA, 13 mM methionine and 0.1 M potassium phosphate buffer at pH 7.8 (Malar, et al., 2016); (d) GR: 0.1 mM NADPH, 1 mM oxidized glutathione (GSSG) and 50 mM tris-HCl buffer at pH 7.5 (Carlberg and Mannervik, 1985).

3.5.3 Enzyme Assays for POX, APX and GR

The activities of POX and APX were assayed as follows: 0.1 mL of the extracted crude enzyme was mixed with 2.9 mL of the respective POX and APX reaction solution (Section 3.5.2). The mixture was incubated at 30ºC, and the absorbance for the first minute of the reaction was measured at 420 nm and 290 nm

for POX and APX, respectively. Enzyme activities were calculated by applying the following molar extinction coefficients: POX (ε: 2.47 mM^{-1} cm^{-1}) and APX (ε: 2.8 mM^{-1} cm^{-1}). The experiments were conducted in triplicate. GR activity was assayed as follows: 0.1 mL of extracted GR crude enzyme was mixed with 0.9 mL of GR reaction solution (Section 3.5.2) (Carlberg and Mannervik, 1985). This mixture was incubated at 30ºC, and the absorbances for the first minute of the reaction were measured and recorded at 340 nm. Enzyme activity was performed in triplicate and calculated with the molar extinction coefficient, ε = 6.22 mM^{-1} cm^{-1}.

The enzyme activity for POX, APX and GR were calculated using the formula [9] as shown below (Köhler, et al., 2017):

$$\text{Enzyme activity (U/g fw)} = \frac{\Delta A \times V_{total}}{\Delta t \times \varepsilon \times l \times V_{Enzyme}} \quad [9]$$

ΔA = change of absorbance
Δ t = incubation time (minutes)
ε = molar extinction coefficient
l = path length of the cuvette
V_{total} = total assay volume (mL)
V_{Enzyme} = enzyme extract volume (mL)

3.5.4 Enzyme Assay for SOD

SOD enzyme activity was assessed by adding 10 µL of the extracted crude enzyme to 190 µL of the substrate-containing reaction medium (as described in

Section 3.5.2). The resulting mixture was then pipetted into two sets of 96-well microplates. One of the microplates was exposed to a 15 W fluorescent bulb and allowed to react for 5 minutes at 25°C. The other microplate was incubated in darkness. The absorbance of samples in each of the microplates was measured using a microplate reader (560 nm) (Malar, et al., 2016). SOD enzyme activity was performed in triplicates.

The amount of enzyme required for a 50% inhibition of the rate of NBT reduction is defined as one unit of SOD activity (Weydert and Cullen, 2010).

$$\text{Inhibition (\%)} = \frac{(A - B)}{A} \times 100\% \quad [10]$$

$$\text{SOD Unit} = \text{Inhibition (\%)} \times 20 \quad [11]$$

$$\text{SOD activity (U/g fw)} = \frac{\text{SOD Unit}}{100} \quad [12]$$

A = corrected absorbance of the control
B = corrected absorbance of the sample

3.6 Transcriptomic Analyses of *P. stratiotes* Leaves and Roots in Responses to Pb and EAPR

Transcriptomic analysis was performed to further elucidate the molecular mechanism underlying the HM removal efficiency, antioxidant enzyme activities and growth responses in *P. stratiotes* under EAPR treatment. Based on the observed

physiological results that indicated significant Pb accumulation and oxidative stress responses, Pb was selected as the target metal for RNA-seq analysis. This approach aims to identify DEGs associated with *P. stratiotes* stress responses, thereby linking molecular mechanisms to phenotypic and biochemical findings (sections 3.3 – 3.5). Besides, Pb was selected as the target HM for transcriptomic analysis because it is a priority pollutant frequently found in landfill leachate. Besides, it induces strong and well-characterized stress responses in plants (Zhu et al., 2022; Hosseini Beinabaj, et al., 2023). Focusing on Pb enables clear elucidation of EAPR-mediated transcriptional mechanisms while minimizing the complexity of mixed-metal interactions (Zhu et al., 2022).

3.6.1 Preparation of Plant Materials

Aquariums with sizes of Length (30 cm) x Width (30 cm) x Height (30 cm) were filled with 10 L of synthetic leachate as described earlier in Section 3.1.2 [page 74, with only 0.007 g $Pb(NO_3)_2$] added. Other HMs were removed from the synthetic leachate to study the effect of only Pb. Three aquariums, where two were filled with synthetic leachate containing Pb, one equipped with an EAPR system and one for non-EAPR, respectively. At the same time, the third aquarium was filled with synthetic leachate in the absence of both Pb and the EAPR system, which served as a control. Four *P. stratiotes* plants were then transferred to each of the aquariums for 5 days to evaluate the effects of the said treatments. Temperature was regulated at 26°C while other experimental conditions, including temperature,

light source, photoperiod, electrode configuration and voltage, were described earlier on page 75 (Section 3.1.3).

3.6.2 Total RNA Extraction, Library Construction and Sequencing

Total RNA was extracted from the plant leaf and root samples using an RNA extraction kit (EURX, Poland) according to the manufacturer's instructions. The quality and quantity of mRNA were analysed using a NanoDrop 2000 spectrophotometer (NanoDrop, Wilmington, DE) and 1% (w/v) agarose gel electrophoresis. A volume of 0.2 - 0.4 μg of total RNA was applied to prepare a eukaryotic mRNA transcriptome library as per the protocol of NEBNext Ultra RNA Library Prep Kit for Illumina (Cat. No. 7530). Then pair-end sequencing was performed by the service provider on Illumina Novaseq6000 at the NovogeneAIT (Singapore), assigned by Apical Scientific Sdn. Bhd. (Selangor) Malaysia.

3.6.3 Processing and Transcript Assembly

The raw data from RNA-Seq went through three quality control steps (error rate distribution, GC content distribution and data filtering). Raw reads were filtered by removing adapter sequences, reads with more than 10% ambiguous bases (N) and reads where more than 50% of bases had low quality (Q score less

than 5) (Li and Dewey, 2011). The resulting high-quality clean reads were then used for downstream analysis. By using Trinity software, the clean reads were *de novo* assembled into contigs and transcripts. Subsequently, Corset (Davidson and Oshlack, 2014) was employed for clustering contigs based on shared reads. Contigs were separated based on observed differences in expression patterns between samples.

3.6.4 Unigene Functional Annotation and Reference Alignment

Seven databases were used to gain comprehensive gene functional annotation, namely NCBI non-redundant protein sequences (Nr), NCBI nucleotide sequences (Nt), Protein family (PFAM), euKaryotic Orthologous Groups (KOG)/Cluster of Orthologous Groups of proteins (COG), Swiss-Prot, Gene Ontology (GO) and Kyoto Encyclopedia of Genes and Genome (KEGG). Genes were functionally annotated using the following tools and database/-s (e-value threshold value): National Center for Biotechnology Information (NCBI) blast against Nucleotide database (NT) ($1 \text{ X } 10^{-5}$), Diamond for non-redundant (NR), SwissProt and euKaryotic Orthologous Groups (KOG) ($1 \text{ X } 10^{-5}$), HMMER (hmmscan) against Protein Families Database (PFAM) (0.01), Blast2GO (Götz, et al., 2008) for GO annotation (based on NR and PFAM results) ($1 \text{ X } 10^{-6}$) and KAAS (KEGG Automatic Annotation Server) for KEGG pathways ($1 \text{ X } 10^{-5}$) (Dormatey, et al., 2022).

The *de novo* transcriptome, which served as a reference, was filtered by Corset. Reads were mapped back to the transcriptome, and gene expression was quantified using RNA-Seq by Expectation-Maximization (RSEM) (Li and Dewey, 2011). RSEM analyses the mapping results of Bowtie, and the read counts obtained for each gene of each sample were converted into fragments per kilobase of transcript per million mapped reads (FPKM) values to compute the gene expression levels. Differentially expressed genes (DEGs) were recruited according to log2 (fold change) > 1 and corrected $p < 0.005$ by applying edgeR software (Robinson, McCarthy and Smyth, 2010).

3.6.5 Cluster Analysis of DEGs

The DEGs were screened and grouped based on their expression using hierarchical clustering. This was performed using both the built-in R package and a heatmap. The results were shown as a dendrogram, which depicts relationships between the clusters. Additionally, a heatmap was used to visualize gene expression patterns within each cluster. The color gradient of the generated heat map from red to green corresponds to a value range of 2 to -2. This representation is generated by the R package pheatmap, which uses z-score normalization (Andreassen, Ezra and Scheibye-Knudsen, 2019).

3.6.6 Gene Ontology (GO) and Kyoto Encyclopedia of Genes and Genome (KEGG) Pathway Enrichment Analyses

GO enrichment analysis of the DEGs was performed using GOseq package (Young, et al., 2010; Kudapa, et al., 2018) and the topGO package in R software (Li, et al., 2023). The GO term with $p < 0.05$ was deemed significantly enriched. KOBAS software was used to evaluate the statistical enrichment of DEGs in KEGG pathways ($p < 0.05$).

3.6.7 qRT-PCR analyses of DEGs

Quantitative Reverse Transcription-Polymerase Chain Reaction (qRT-PCR) was performed to test the expression of selected genes using HiScript ®II One Step qRT-PCR SYBR Green Kit (Vazyme). β-actin was chosen as the housekeeping gene in this study. It is widely used as an internal control that normalizes gene and protein expression (Zhang, et al., 2019). Six selected candidate unigenes, which were upregulated in the MAPK signalling pathway in plants were selected for a qRT-PCR. These genes may encode important components of the MAPK cascade, such as MAPKKKs, MAPKKs, MAPKs or downstream transcription factors regulating stress responses (Jalmi, et al., 2018). Briefly, 20 μL of the reaction mixture was prepared according to the manufacturer's instructions. The qPCR was performed on the Real-Time PCR Machine Biorad C1000 Touch.

The melting curve for each amplification product was analysed to ensure specificity at the end of the PCR reaction. Primers for the selected genes were designed by Primer-BLAST. Table 3.1 shows the primers used in this study. The experiments were performed in triplicate.

Table 3.1: Primers designed for qRT-PCR

Primer name	Primer sequence (5'->3')
CAForward	GACAACAGCGGAACCATCGAA
CAReverse	TCACCCAAACTGCTCATCATGG
CA5Forward	CGTGCCTTAACTCAGCAGCA
CA5Reverse	GCTGATGGAAATGGGACAATCG
CALForward	CATCAGCATCTGGAGGAGCACT
CALReverse	GCTCTACCCAAGTGGTGACA
GTForward	TGGTGGGTTTGGAAGCGAGA
GTReverse	GGTCGCTTACGAGGAGGGTG
GUAForward	TGGGTCGTCCAATCAAGACCT
GUAReverse	GCATAGGCATCGCAACCACC
RABForward	AGCCTCGGCTGATTCCACTT
RABReverse	TGCAGCAGCCATTGTTGTGT

3.7 Statistical Analyses

Data analysis was carried out using IBM SPSS Version 27.0. The significant difference of leachate parameter analysis between control, non-EAPR and EAPR systems was assessed using one-way ANOVA and Tukey's HSD *post-hoc* test. Similarly, one-way ANOVA and Tukey's HSD were used to evaluate the significant difference in percentage drop in total biomass, total chlorophyll and chlorophyll ratio (a/b) among the control, non-EAPR and EAPR treatments. Two-way ANOVA were applied to determine the significant difference in the BCF of metals in root and leaf, removal efficiency, TF and antioxidative enzyme activities between the EAPR and non-EAPR systems.

Gene expression changes in the qRT-PCR were normalized to a reference gene and quantified using the $2^{-\Delta\Delta CT}$ method (Livak and Schmittgen, 2001). The experiment results were collected in triplicate and presented as mean ± standard error. Statistical differences between the gene expression levels were assessed via one-way ANOVA and HSD *post-hoc* test (Ng and Ngeow, 2022; Wetthasinghe, et al., 2024). The significance level of all statistical tests was set at a p-value < 0.05.

CHAPTER 4

RESULTS

4.1 Synthetic Leachate Characterization

The prepared synthetic leachate consisted of propionate, acetate, ammonium, humate and heavy metals (HMs). It was prepared according to Dan, et al. (2017), and the treated synthetic leachate samples were measured for numerous parameters to evaluate the efficacy of EAPR treatment in removing HMs. The parameters investigated include the potential of hydrogen (pH), biochemical oxygen demand (BOD), chemical oxygen demand (COD), colour, dissolved oxygen (DO), oxidation-reduction potential (ORP), conductivity, turbidity, total dissolved solids and ammonia. Analysis of variance conducted showed the difference in the mean for EAPR and non-EAPR treatments did not reach conventional levels of statistical significance ($p > 0.05$).

However, BOD, colour and turbidity were significantly reduced in the EAPR samples compared to the control ($p < 0.05$) (Table 4.1). For example, the reduction percentage for BOD, colour and turbidity from the EAPR-treated samples were 69.35%, 43.75% and 68.10%, respectively, compared to the control. The synthetic leachate under non-EAPR and EAPR treatments exhibited elevated pH

and DO compared to the control ($p < 0.05$). For both pH and DO, increments of approximately one unit and 10%, respectively, were observed.

Table 4.1: Characteristics of synthetic leachate treated with EAPR and non-EAPR systems as compared to the control

Parameters	Control	EAPR	non-EAPR
pH	5.78 ± 0.16*****[a]	6.75 ± 0.12*[b]	6.74 ± 0.10*****[b,c]
BOD (mg/L)	30.57 ± 2.16*****[a]	9.37 ± 2.36*[b]	11.13 ± 0.98*****[b,c]
Colour (PtCo)	213.33 ± 23.33*****[a]	120.00 ± 5.77*[b]	103.33 ± 12.02*****[b,c]
COD (mg/L)	170.00 ± 25.17[a]	153.33 ± 37.56[a]	216.67 ± 58.40[a]
DO (mg/L)	3.08 ± 0.46*****[a]	3.45 ± 0.19*[b]	3.45 ± 0.19*****[b,c]
ORP (mV)	2.50 ± 0.97[a]	4.13 ± 0.03[a]	4.16 ± 0.03[a]
Conductivity (µS/cm)	1593.67 ± 48.22[a]	1649.33 ± 47.91[a]	1648.33 ± 46.05[a]
Turbidity (NTU)	79.93 ± 0.87*****[a]	25.50 ± 11.96*[b]	30.27 ± 3.07*****[b,c]
TDS (ppt)	1.43 ± 0.01[a]	1.46 ± 0.01[a]	1.45 ± 0.01[a]
Total ammonia (mg/L)	98.73 ± 5.49[a]	98.00 ± 2.56 [a]	95.20 ± 5.10[a]

Data are presented as mean ± standard error of the mean (n=3). Different superscript letters ([a], [b], [c]) and asterisks (*) indicate statistically significant differences ($p < 0.05$) between the control [synthetic leachate with HMs (before treatment], EAPR and non-EAPR treatments as determined by one-way ANOVA with Tukey's HSD post-hoc test.

4.2 Plant Growth and Chlorophyll Contents

In both EAPR and non-EAPR treatments, the plants visibly showed signs of phytotoxicity (such as discoloration, yellowing and withering), as shown in Figure 4.1 after 7 days of incubation. Plants grown in both EAPR (31.85%) and non-EAPR (28.56%) treatments showed a greater reduction in total biomass as compared to the control (4.97%) ($p < 0.05$) (Figure 4.2). Significant differences were observed in the decline of total biomass between EAPR and control, as well as between non-EAPR and control. The percentage drop in total biomass was 6.41-fold for plants incubated with the EAPR system, whereas for plants grown in the non-EAPR system, the reduction was 5.75-fold compared to the control.

Figure 4.1: *P. stratiotes* discoloration and yellowing leaves after the EAPR treatment

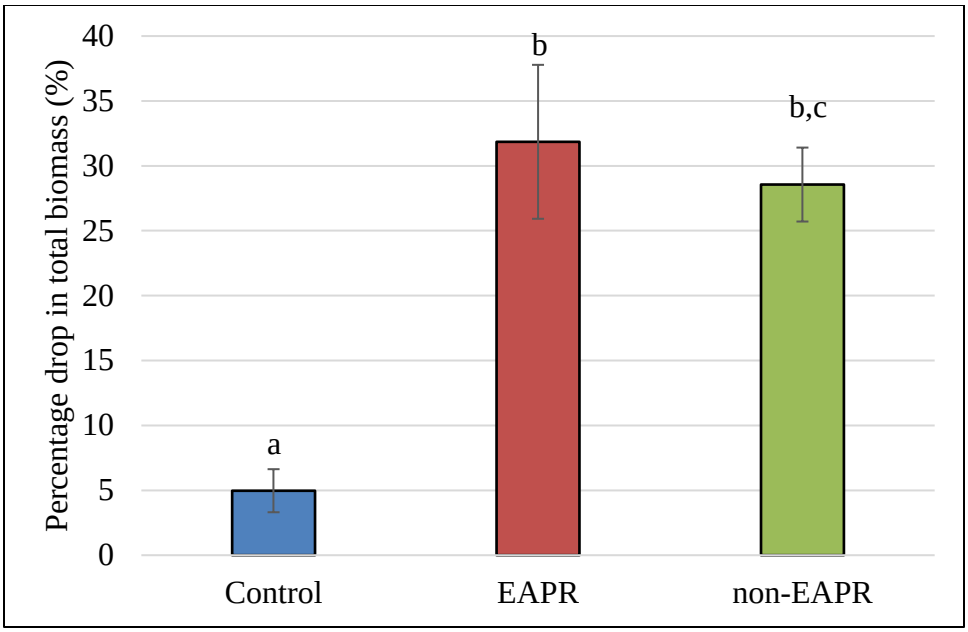

Figure 4.2: Analysis of percentage drop in total biomass (%) of *P. stratiotes* plants after 7 days of treatment relative to the initial biomass (Day 0 control) [Data are presented as mean ± standard error of the mean (n=3). Different superscript letters (^{a}, ^{b}, ^{c}) indicate statistically significant differences ($p < 0.05$) between the control, EAPR and non-EAPR treatments as determined by one-way ANOVA with Tukey's HSD post-hoc test]

Figure 4.3 illustrates a significant decline in total chlorophyll of *P. stratiotes* from the control and non-EAPR treatments. The total chlorophyll content of the plants in the non-EAPR treatment decreased by up to 26.27% compared to the control, whereas the plants placed in the EAPR system showed a decline of 16.21%. However, there was no significant difference in the total chlorophyll between EAPR and non-EAPR. Additionally, a significantly higher chlorophyll a/b ratio was observed in EAPR compared to the control (Figure 4.4), with the chlorophyll a/b ratio increasing by approximately 18.12% to 2.87 (mg/mL). Nevertheless, there was no significant difference in the chlorophyll a/b ratio between EAPR and non-EAPR ($p > 0.05$).

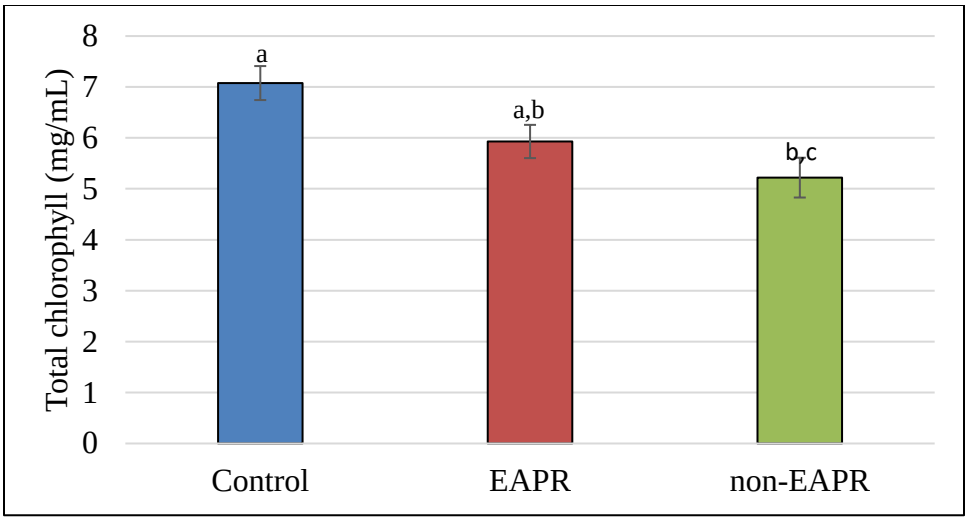

Figure 4.3: Analysis of total chlorophyll of *P. stratiotes* plants after 7 days of treatment relative to the initial total chlorophyll (Day 0 control) [Data are presented as mean ± standard error of the mean (n=3). Different superscript letters (^{a}, ^{b}, ^{c}) indicate statistically significant differences ($p < 0.05$) between the control, EAPR and non-EAPR treatments as determined by one-way ANOVA with Tukey's HSD post-hoc test]

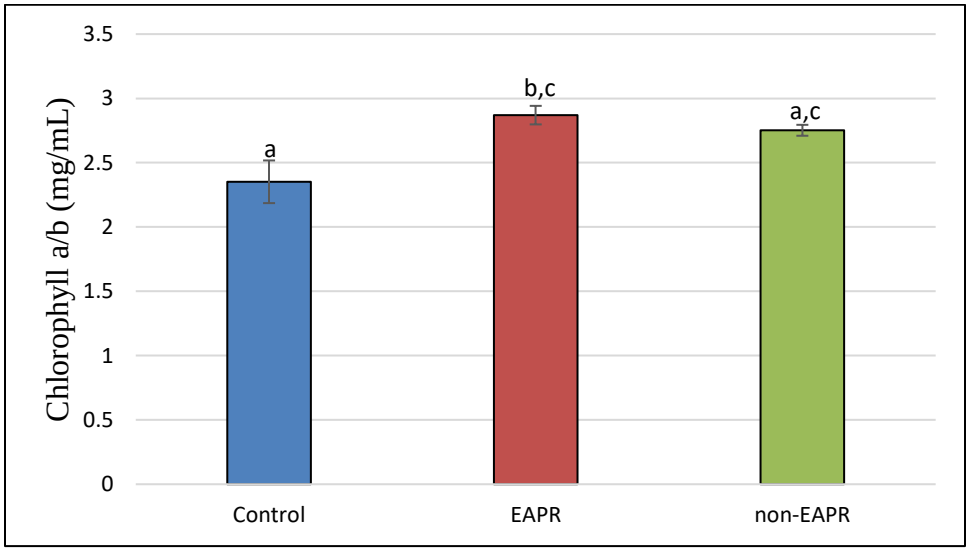

Figure 4.4: Analysis of chlorophyll ratio (a/b) of *P. stratiotes* plants after 7 days of treatment relative to the initial chlorophyll ratio (a/b) (Day 0 control) [Data are presented as mean ± standard error of the mean (n=3). Different superscript letters (^{a}, ^{b}, ^{c}) indicate statistically significant differences ($p < 0.05$) between the control, EAPR and non-EAPR treatments as determined by one-way ANOVA with Tukey's HSD post-hoc test]

4.3 Bioconcentration Factor (BCF) of Leaf and Root

The BCF values were obtained using Equation 7 and measured to study the ability of *P. stratiotes* to accumulate HMs in the leaf and root. Generally, the BCF of the leaf showed a very low value (< 300) as compared to the high value for the root (> 1000) in this study. The BCF values of HMs for the leaf of *P. stratiotes* after EAPR and non-EAPR treatments are shown in Figure 4.5. Results of two-way ANOVA analysis showed that variations in the BCF leaf were primarily driven by metal type. The absence of a significant interaction between treatments and metals suggests that the treatments did not differentially affect BCF leaf values among the tested HMs. Based on BCF leaf values for both treatments, HMs such as Mn, Cd, Ni and Zn displayed higher levels of accumulation in *P. stratiotes* plants under both systems. Mn, Ni, and Zn are micronutrients essential for plant growth and development, while Cd has an unknown biological function (Gaur and Adholeya, 2004).

Similarly, analysis via two-way ANOVA analysis indicated that metals exerted main effect on BCF root, with no interaction between treatments and metals investigated (Figure 4.6). Metal accumulation in the roots in descending order was Pb > Fe > Zn > Ni > Cd > Mn in both the EAPR and non-EAPR systems. The BCF of the root for Pb and Fe in the EAPR was 1.9 and 1.7 times higher than the non-EAPR system, respectively. This showed that both HMs were highly accumulated

in the root of *P. stratiotes* of EAPR treatment. The migration of metal ions is accelerated toward the root area of the plant by the electrode configuration in the EAPR system.

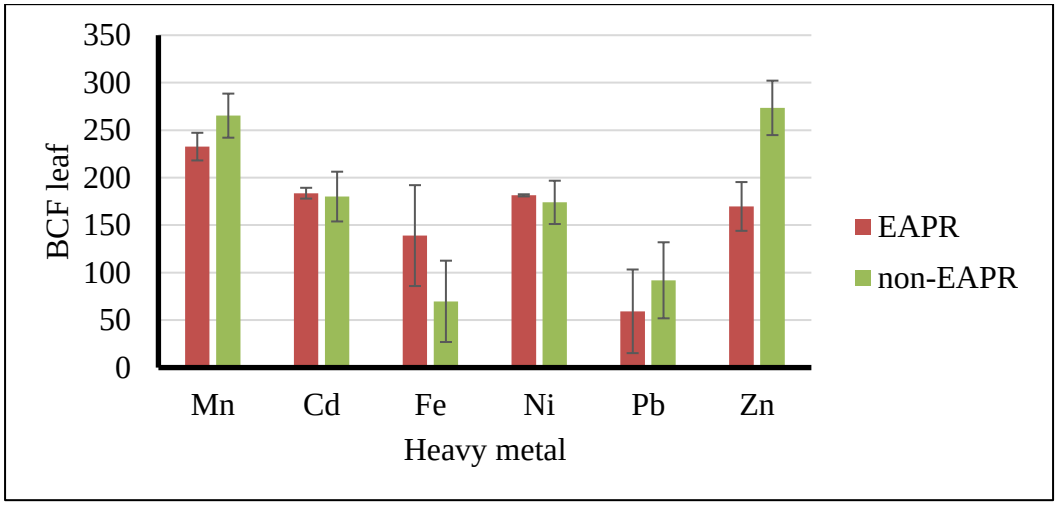

Figure 4.5: BCF of metals *in P. stratiotes's* leaf samples [analysis of between EAPR and non-EAPR treatments via two-way ANOVA; data are presented as mean ± standard error of the mean (n=3)]

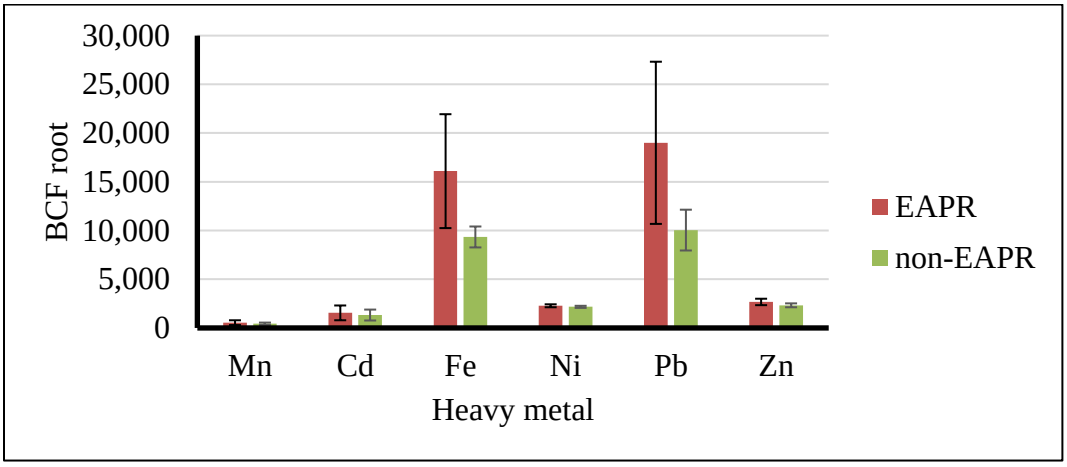

Figure 4.6: BCF of metals *in P. stratiotes's* root samples [analysis of between EAPR and non-EAPR treatments via two-way ANOVA; data are presented as mean ± standard error of the mean (n=3)]

4.4 Translocation Factor (TF)

TF values were used to evaluate the ability of the HM to be translocated in the plants. It was obtained using Equation 8. TF value, which is less than one, indicates the restriction of root-to-shoot transfer (Ahmadpour, et al., 2015). In this study, metal was found as the main effect on TF via two-way ANOVA analysis. However, there was no interaction between treatments and metals, hence the influence of treatments on TF did not vary between metals (Table 4.2). HMs are predominantly absorbed through roots and initially retained in root tissues, with relatively limited transfer to leaves (Yan, et al., 2020), resulting in low and similar TF values irrespective of treatment conditions.

Table 4.2: TF values of HMs for *P. stratiotes*

	Translocation factor	
Metals	**EAPR**	**non-EAPR**
Mn	0.62 ± 0.21	0.73 ± 0.19
Cd	0.18 ± 0.07	0.17 ± 0.04
Fe	0.01 ± 0.00	0.01 ± 0.00
Ni	0.08± 0.01	0.08 ± 0.01
Pb	0.00 ± 0.00	0.01± 0.00
Zn	0.06 ± 0.00	0.12 ± 0.01

[Data are presented as mean ± standard error of the mean (n=3); analysis between EAPR and non-EAPR treatments via two-way ANOVA]

As treatment was not the main effect on TF, hence this indicated that the EAPR did not affect *P. stratiotes* ability to translocate most of the tested HMs. All the HMs measured in this study were primarily stored in the roots (TF < 1), regardless of whether the system was EAPR or non-EAPR. Besides, the results also show that Mn achieved the highest TF value in both the EAPR and non-EAPR systems, indicating Mn was primarily stored in the leaf while Pb and Fe were accumulated mainly in the root for both EAPR and non-EAPR. This result was correlated with the low BCF values in the shoots and high BCF values in the roots of *P. stratiotes*.

4.5 HM Removal Efficiency of EAPR

To evaluate the efficiency of EAPR, the concentration of HMs in synthetic leachate was measured before and after the treatments. Figure 4.7 shows that the HM removal in the EAPR system was higher than in the non-EAPR system, except for Zn. Metals was the main effect on HM removal efficiency using two-way ANOVA analysis, with no interaction detected between treatments and metals. Of all the metals tested, Pb and Fe displayed the highest removal efficiency in both the EAPR (59.86 ± 9.98% for Pb and 56.56 ± 18.08% for Fe) and non-EAPR (53.26 ± 1.84% for Pb and 51.30 ± 12.82% for Fe) systems. In contrast, Mn had the lowest removal efficiency for EAPR (11.92 ± 4.98%) and non-EAPR (9.11 ± 5.35%)

systems. These results correlated with the root BCF values obtained, where the root absorbed more Fe and Pb than Mn.

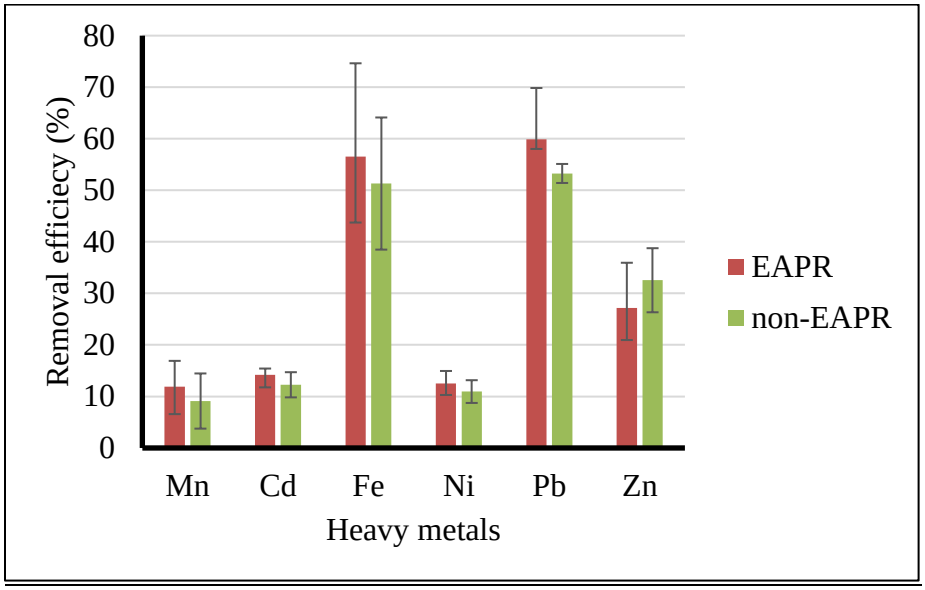

Figure 4.7: HM removal efficiency from the synthetic leachate by *P. stratiotes* [Analysis between EAPR and non-EAPR treatments via two-way ANOVA, data are presented as mean ± standard error of the mean (n=3)]

4.6 Antioxidative Enzyme Activities of *P. stratiotes* Under Different Treatments

Enzymatic activities of superoxide dismutase (SOD), ascorbate peroxidase (APX), peroxidase (POX) and glutathione reductase (GR) were evaluated to compare the antioxidative enzyme responses of *P. stratiotes* under different conditions: EAPR and non-EAPR systems. Although two-way ANOVA analysis showed there was an interaction between treatments and tissue types, neither the

treatments nor the tissue types were the main effects on SOD. This is even though, as shown in Figure 4.8(a), the SOD enzyme activity in the leaf was 37.15% higher in the EAPR treatment (2.74 ± 0.41 U/g fw) than in the non-EAPR treatment (1.72 ± 0.56 U/g fw). Conversely, SOD enzyme activity in the root was 73.75% greater in the non-EAPR (2.71 ± 0.40 U/g fw) compared to the EAPR treatment (0.71 ± 0.68 U/g fw).

The two-way ANOVA analysis revealed that neither treatment nor tissue type had a significant main effect on APX and POX enzyme activities. Furthermore, there was no interaction between treatments and tissue types, indicating that the influence of treatments on both the enzymes was consistent across roots and leaves. The APX activity [Figure 4.8 (b)] follows the trend of SOD activity, exhibiting relatively increase of 12.18% APX activity in the leaves of the EAPR (0.56 ± 0.04 U/g fw) than non-EAPR treatment (0.49 ± 0.08 U/g fw). In the root samples, non-EAPR (0.72 ± 0.16 U/g fw) displayed an increase of 34.16% in its APX activity as compared to EAPR treatment (0.48 ± 0.06 U/g fw). POX activity [Figure 4.8 (c)] showed a different profile from SOD and APX activity for both *P. stratiotes* leaf and root samples. The enzyme activity in the leaf samples was relatively higher (13.44%) in the non-EAPR (10.15 ± 0.34 U/g fw) compared to the EAPR treatment (8.79 ± 2.21 U/g fw). However, in the root samples, POX activity increased 17.25% in the EAPR (11.48 ± 1.41 U/g fw) to the non-EAPR treatment (9.50 ± 0.44 U/g fw). As for GR activity [Figure 4.8 (d)], it was only detected in the leaf samples, with higher activity (22.18%) in leaf samples under EAPR (0.13 U/g fw) than in

non-EAPR treatment (0.10 ± 0.02 U/g fw). GR activity was absent from both EAPR and non-EAPR-treated root samples.

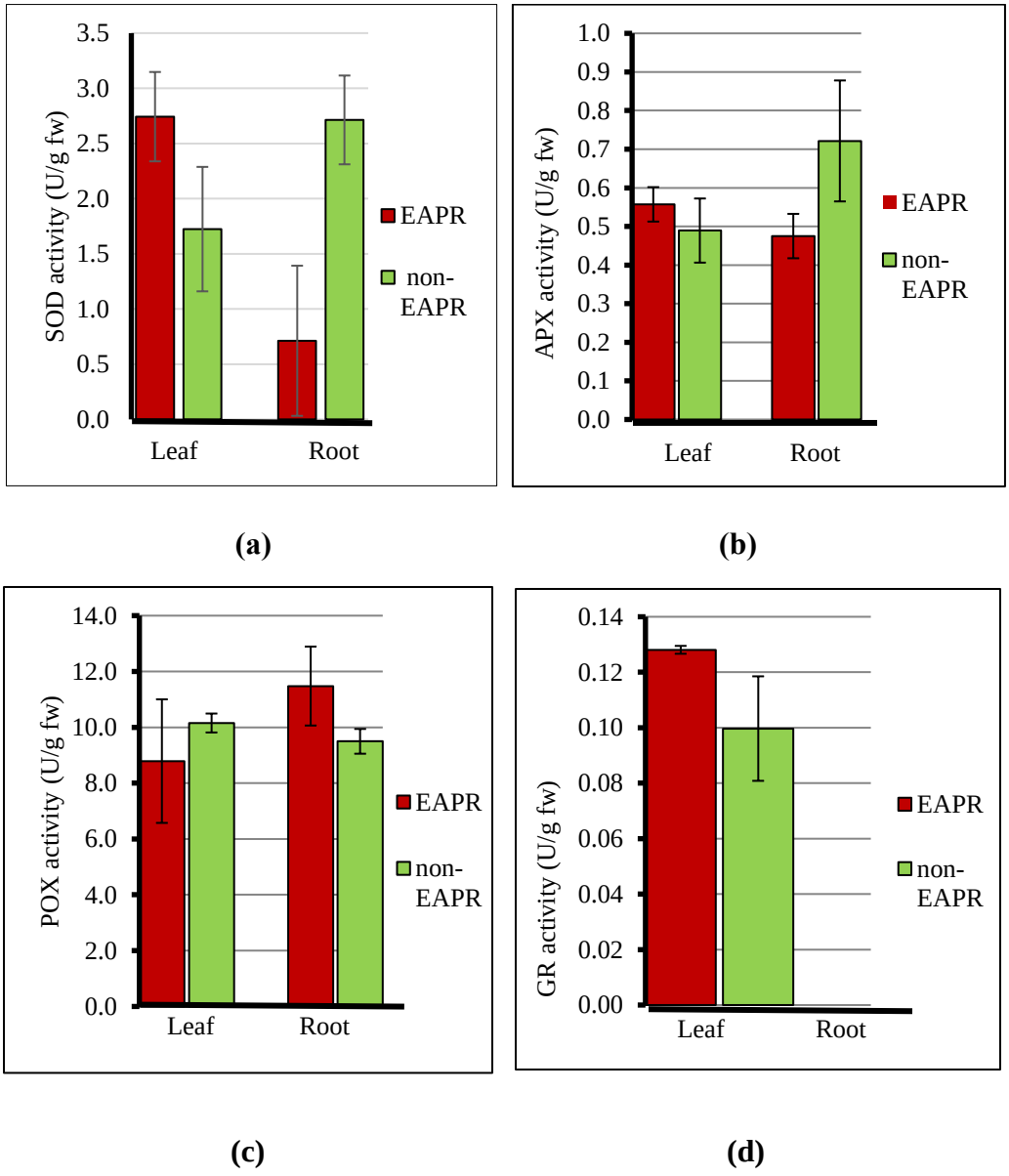

Figure 4.8: Antioxidative enzymes activities of (a) SOD (b) APX (c) POX (d) GR of *P. stratiotes* plants [Analysis of SOD, APX and POX activities between EAPR and non-EAPR treatments via two-way ANOVA; data are presented as mean ± standard error of the mean (n=3)]

4.7 Analyses of RNA-Seq Data

4.7.1 Throughput and Quality of Strand-specific RNA-seq of *P. stratiotes* Libraries

RNA sequencing was conducted to investigate variations in gene expression and regulation in response to Pb and EAPR stresses (Sections 4.2 - 4.6). Total RNA extracted from the leaf and root of the control, EAPR and non-EAPR treatments was used to construct cDNA libraries. The EAPR-treated leaf sample yielded the most raw reads (59,910,117), followed by the non-EAPR sample (51,819,487) and the control sample (51,380,833) (Table 4.3). Similarly, the highest clean reads for the leaf sample were observed to be in the same order: EAPR (59,250,906) > non-EAPR (51,297,444) > control (50,315,699). However, in an opposite trend, the root sample from the control (56,795,785) displayed the highest number of raw reads, followed by the non-EAPR (49,850,872) and EAPR (45,674,321) treatments. The clean reads obtained for root samples of the control were 56,102,540, non-EAPR was 49,327,780 and EAPR was 45,191,136. The average raw reads and clean reads were higher in the leaf than root samples, respectively.

Uniform GC contents were obtained across reads for leaf and root samples from control, EAPR and non-EAPR treatments. The sample GC content for leaves (average 51.95%) and roots (average 51.54%) was within the optimum range for consistent results. Besides, the higher Q20 (98.04% and 97.94% in leaves and roots, respectively) and Q30 values (94.31% and 94.14% for both leaf and root samples)

indicated the high quality of the transcriptome sequencing. In the leaf and root samples, Q20 values were higher than Q30 for control, EAPR and non-EAPR, respectively.

Table 4.3: Summary of the RNA-Seq data from the Trinity *de novo* assembly programme

Sample	Raw reads	Clean_reads	Q20 (%)	Q30 (%)	GC (%)
Leaf (control)	51,380,833	50,315,699	98.16	94.58	51.40
Leaf (EAPR)	59,910,117	59,250,906	97.94	94.02	52.24
Leaf (non-EAPR)	51,819,487	51,297,444	98.01	94.32	52.21
Subtotal average	54,370,146	53,621,350	98.04	94.31	51.95
Root (control)	56,795,785	56,102,540	97.94	94.18	51.92
Root (EAPR)	45,674,321	45,191,136	97.94	94.14	51.96
Root (non-EAPR)	49,850,872	49,327,780	97.93	94.09	50.73
Subtotal average	50,773,659	50,207,152	97.94	94.14	51.54

By using the Trinity assembler, a total of 318,319 transcripts, comprising 386,922,411 nucleotides, were further obtained, with a mean length of 1,159 bp, and N50 and N90 values of 2,136 bp and 426 bp, respectively (Table 4.4). From these transcripts, a total of 204,252 unigenes with 164,929,136 nucleotides were assembled with an average length of 807 bp, N50 of 986 bp and N90 of 377 bp. Both the transcript and unigenes exhibited an identical maximum length of 18,644 bp.

Table 4.4: Overview of the number and length distribution of transcripts and unigenes

Type	Total number	Mean length (bp)	Max length (bp)	N50 (bp)	N90 (bp)	Total nucleotides
Transcript	318,319	1,159	18,644	2,136	426	368,922,411
Unigene	204,252	807	18,644	986	377	164,929,136

4.7.2 Differential Expression Analysis

P. stratiotes had distinct expression patterns for leaf and root samples. This study examined the effect of EAPR and Pb on the gene expression profiles of leaf and root samples. For the root samples under EAPR and Pb stress, a total of 17,531 and 40,101 differentially expressed unigenes (DEGs) were found, as shown in Figure 4.9 and Figure 4.10, respectively. It was interesting to note that under Pb stress, it caused a significantly higher number of upregulated DEGs (29,878) in the root (Figure 4.10), which is 91.58% greater in comparison to the number of upregulated DEGs (2,516) in the root after EAPR treatment (Figure 4.9). In contrast, a different pattern was observed with 31.91% more downregulated DEGs in EAPR-treated root (Figure 4.9) than Pb-treated (Figure 4.10), with the number of DEGs of 15,015 and 10,223, respectively.

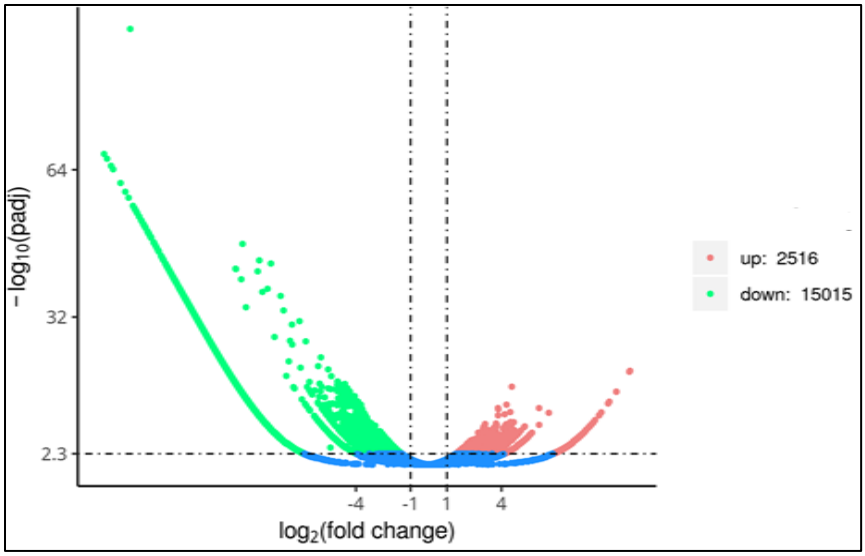

Figure 4.9: Volcano plot of DEGs obtained from the sequenced-transcript samples of *P. stratiotes* root samples (EAPR vs non-EAPR) [The dashed line in each volcano plot indicates an adjusted *padj* < 0.005, log2FoldChange > 1. Red dots indicate upregulated DEGs, green dots indicate downregulated DEGs and blue dots indicate filtered unigenes that are insignificantly regulated. Note: EAPR vs non-EAPR= Effect of EAPR treatment]

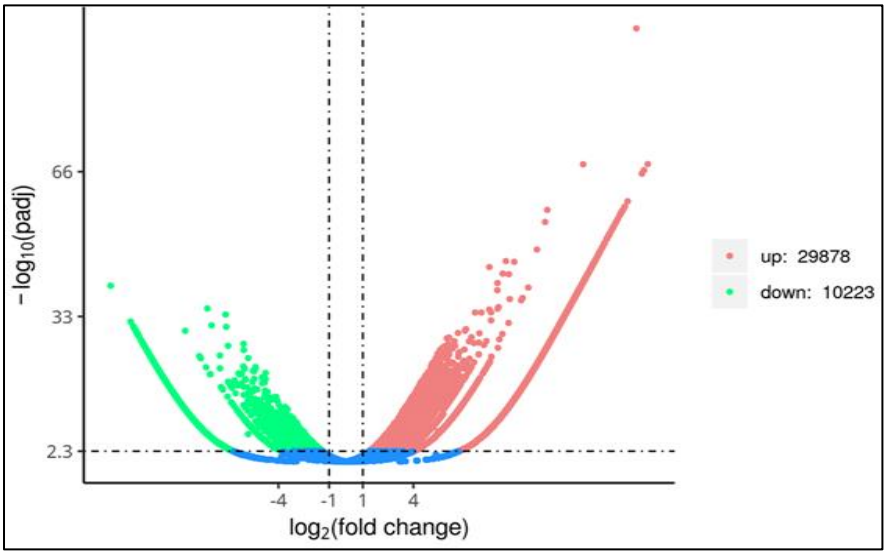

Figure 4.10: Volcano plot of DEGs obtained from the sequenced-transcript samples of *P. stratiotes* root samples (non-EAPR vs control). The dashed line in each volcano plot indicates an adjusted *padj* < 0.005, log2FoldChange > 1. Red dots indicate upregulated DEGs, green dots indicate downregulated DEGs and blue dots indicate filtered unigenes that are insignificantly regulated. Note: non-EAPR vs control= Effect of Pb stress

Meanwhile, a relatively smaller number of unigenes were differentially expressed in the leaf samples of the plants under EAPR (5,258) and Pb (3,441) treatments, as shown in Figure 4.11 and 4.12, respectively. For the leaf samples, EAPR treatment induced a 64.67% higher number of upregulated DEGs (3,433) (Figure 4.11) compared to Pb stress (1,213) (Figure 4.12). In contrast, Pb stress (2,228) caused greater (18.09%) downregulated DEGs (Figure 4.12) than EAPR treatment (1,825) (Fig. 4.11). In general, it was found that distinct expression profiles of DEGs were observed under EAPR treatment and Pb stress, which strongly supports that the different strategies might be triggered in the leaf and root samples to cope with EAPR and Pb stress.

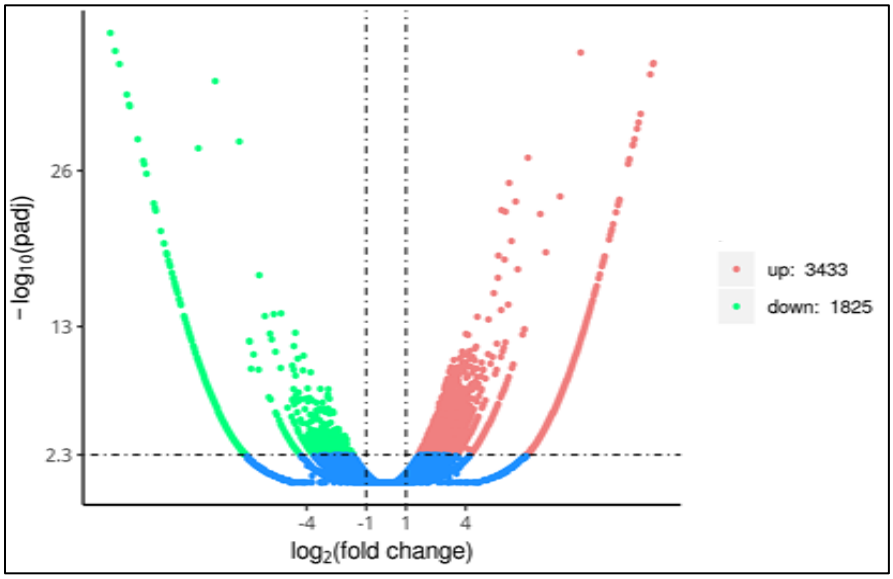

Figure 4.11: Volcano plot of DEGs obtained from the sequenced-transcript samples of *P. stratiotes* leaf samples (EAPR vs non-EAPR) [The dashed line in each volcano plot indicates an adjusted *padj* < 0.005, log2FoldChange > 1. Red dots indicate upregulated DEGs, green dots indicate downregulated DEGs and blue dots indicate filtered unigenes that are insignificantly regulated. Note: EAPR vs non-EAPR= Effect of EAPR treatment]

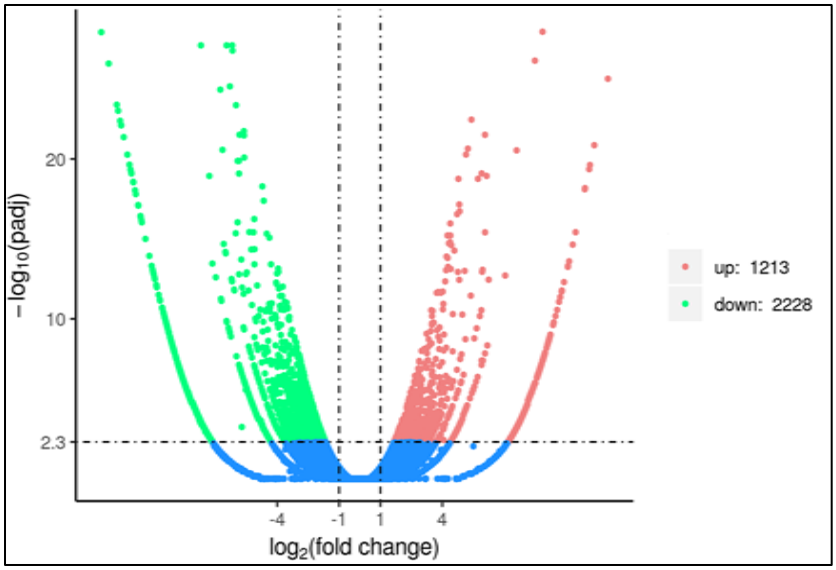

Figure 4.12: Volcano plot of DEGs obtained from the sequenced-transcript samples of *P. stratiotes* leaf samples (non-EAPR vs control) [The dashed line in each volcano plot indicates an adjusted *padj* < 0.005, log2FoldChange > 1. Red dots indicate upregulated DEGs, green dots indicate downregulated DEGs and blue dots indicate filtered unigenes that are insignificantly regulated. Note: non-EAPR vs control= Effect of Pb stress]

4.8 Cluster Analysis of Gene Expression Profiles

4.8.1 Cluster Analysis of DEGs Differences

Normalized FPKM (fragments per kilobase of transcript sequence per million base pairs sequenced) was used to assess each constructed unigenes' abundance and differentiate mRNA levels. The resulting DEGs from various treatments were clustered using the built-in R package, pheatmap. The relationships between Pb and EAPR treatments, which induced changes in gene expression in leaf and root samples, were illustrated using Java Treeview (Figure 4.13). The branch lengths on the tree indicate the degree of similarity among the three

conditions for the leaf and root samples' DEGs. The treatment's gradient sample is presented as Z-scores in the hierarchical heatmaps. The heat-map colours range from red (high gene expression) to green (low gene expression). DEGs obtained from the leaf and root samples of control, EAPR and non-EAPR were clustered and separated based on hierarchical clustering. Each thin column indicates one gene and its expression level in all three treatments (EAPR, non-EAPR and control).

From Figure 4.13, it was evident that the leaf and root groups exhibited contrasting expression patterns by tissue type. All DEGs obtained were clustered into two major groups (leaf and root), suggesting the main source of variation across treatments was organ-specific transcriptional regulation. Most of the DEGs were upregulated in the leaf clusters, with the sample from the EAPR treatment showing a predominance of red signals compared to the non-EAPR and control treatments. In contrast, minimal differences were observed in the gene expression profiles between control and non-EAPR groups. Hence, under the experimental conditions in leaf tissues, Pb exposure alone is indicated to induce limited transcriptional divergence.

Conversely, the root clusters showed evident gene downregulation, with the root sample from non-EAPR (affected by Pb) exhibiting the greatest number of downregulated genes. The expression patterns of the EAPR-treated root sample were more comparable to the control than the non-EAPR treatment. Overall, tissue-

specific expression profiles primarily contributed to the variation in transcriptional patterns, whereas treatment-related differences were secondary. Additionally, in the leaf tissues, EAPR appears to differentially modulate their gene expression.

.

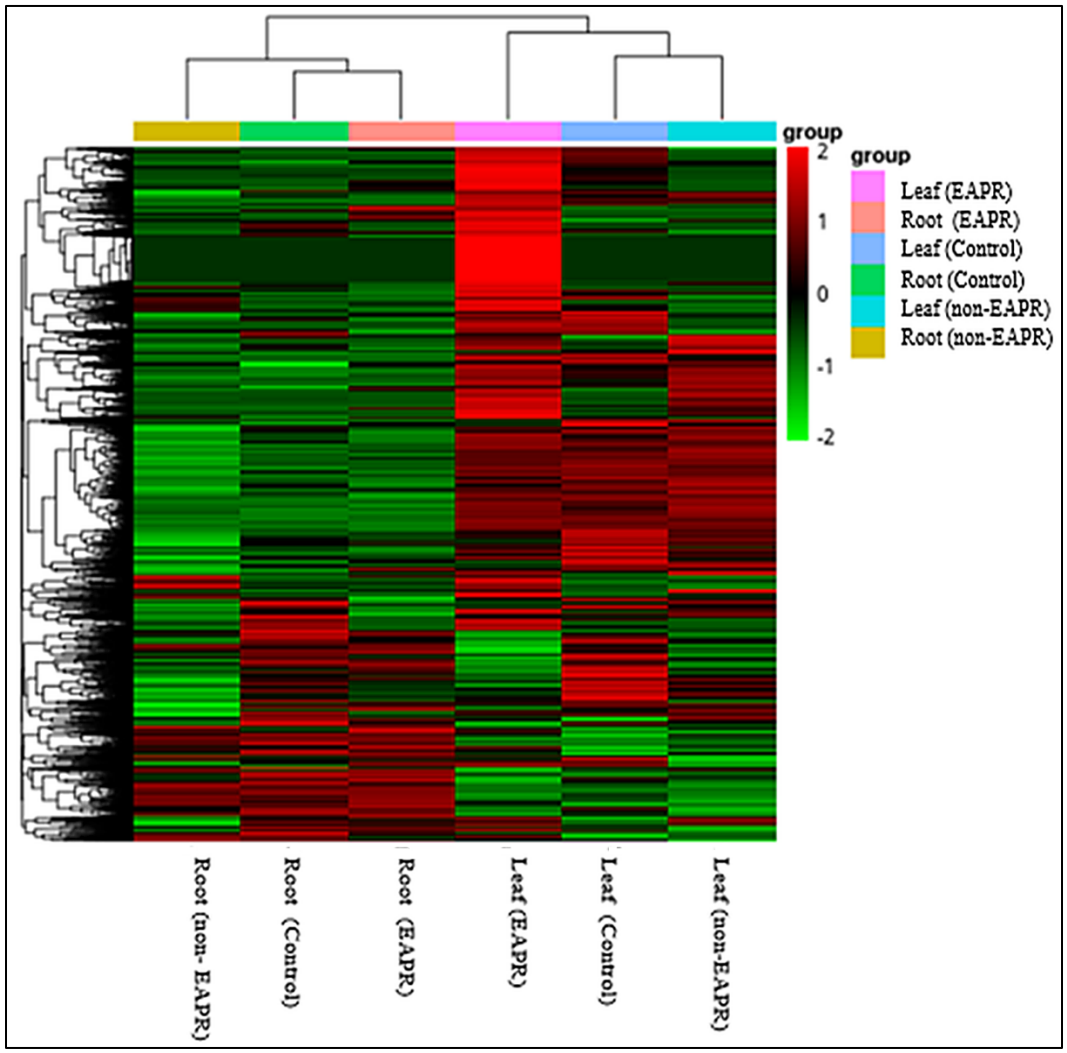

Figure 4:13 The cluster analysis of DEGs of the effect of EAPR and Pb-induced changes in gene expression of *P. stratiotes* leaf and root samples under different conditions (EAPR, non-EAPR and control)

4.9 Gene Ontology (GO) Functional Enrichment

Additional investigations were conducted using GO enrichment analyses to categorize the functions of *P. stratiotes* DEG into the biological process (BP), cellular component (CC), and molecular function (MF) categories. In the threshold range of $padj < 0.05$, the results showed the terms significantly upregulated and downregulated as a result of EAPR and Pb effects.

4.9.1 GO Analysis of Root Samples

4.9.1.1 GO Analyses of Root Samples for EAPR versus non-EAPR (Effects of EAPR)

GO enrichment analysis of the root samples of EAPR versus non-EAPR treatment revealed that most DEGs were upregulated in 12 terms (Figure 4.14) and downregulated in 14 terms (Figure 4.15) differently, probably due to the effects of EAPR. These terms are grouped into three categories: biological process (BP group), cellular component (CC group) and molecular function (MF group). After EAPR treatment, the most upregulated genes [$-log(padj) > 10$] mainly belonged to the five terms, namely ribosome biogenesis and translation from the BP group, ribosome from the CC group, and structural constituents of the ribosome and structural molecule activity from the MF group (Figure 4.14).

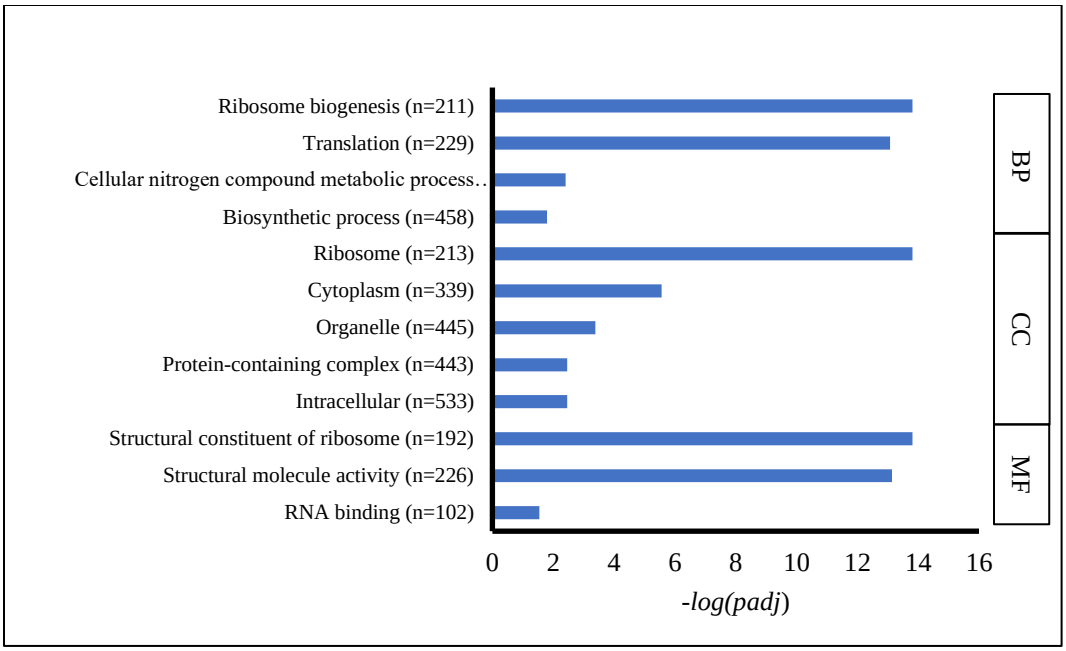

Figure 4.14: GO enrichment analysis of the upregulated DEGs (root) under EAPR versus non-EAPR condition [Category: biological process (BP), cellular component (CC) and molecular function (MF)]

Meanwhile, the most obvious downregulated terms belonged to the cellular protein modification process, which was part of the BP group, for which the *-log(padj)* value was greater than five (Figure 4.15). However, it was also noteworthy that other downregulated genes in different terms, such as nucleocytoplasmic transport, membrane organisation, vesicle-mediated transport, signal transduction and transport from the BP group, might play an essential role in cell functions and diseases. On the other hand, the cytoskeleton term (CC group) and kinase activity and GTPase activity, both terms belonging to the MF group, displayed a *-log(padj)* value of more than two. The upregulated DEG terms (Figure 4.14) achieved higher *-log(padj)* values than the downregulated DEG (Figure 4.15).

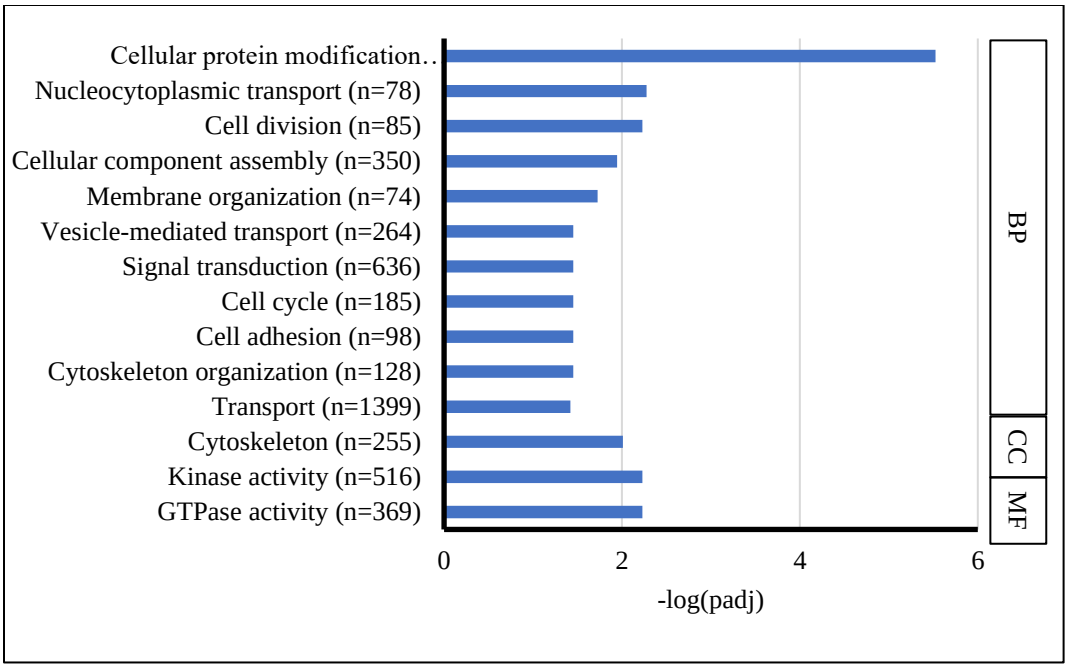

Figure 4.15: GO enrichment analysis of the downregulated DEGs (root) under EAPR versus non-EAPR condition [Category: biological process (BP), cellular component (CC), and molecular function (MF)]

4.9.1.2 GO Analyses of Root Samples for Non-EAPR versus Control (Effects of Pb Stress)

In this study, a total of 19 terms were identified as enriched in both the upregulated (Figure 4.16) and downregulated DEGs (Figure 4.17). All the upregulated genes achieved a lower *-log(padj)* value of less than three, except for GTPase activity (MF group). The terms enriched in the BP group [*-log (padj)* > 2] including cellular protein modification process, transport, vesicle-mediated transport, cellular component assembly, nucleocytoplasmic transport, membrane organization, cellular amino acid metabolic process and signal transduction. Other

enriched terms that were upregulated included endosome and cytoplasmic vesicle (CC group), as well as kinase and phosphatase activity from the MF group.

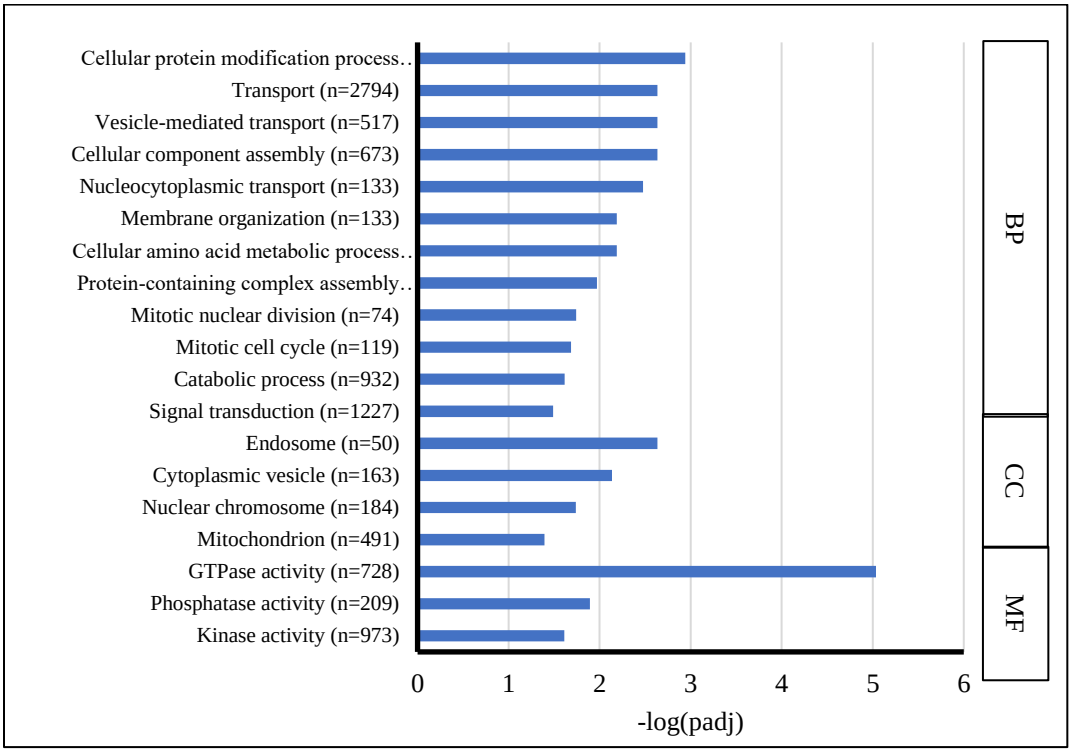

Figure 4.16: GO enrichment analysis of the upregulated DEGs (root) under non-EAPR versus control condition [Category: biological process (BP), cellular component (CC), and molecular function (MF)]

According to Figure 4.17, Pb stress might cause the downregulation of genes enriched in terms such as ribosome biogenesis, translation (BP group), ribosome (CC group), and structural constituents of ribosome and structural molecule activity (MF group). The *-log(padj)* values for downregulated DEGs were observed to be much higher than those for upregulated DEG genes.

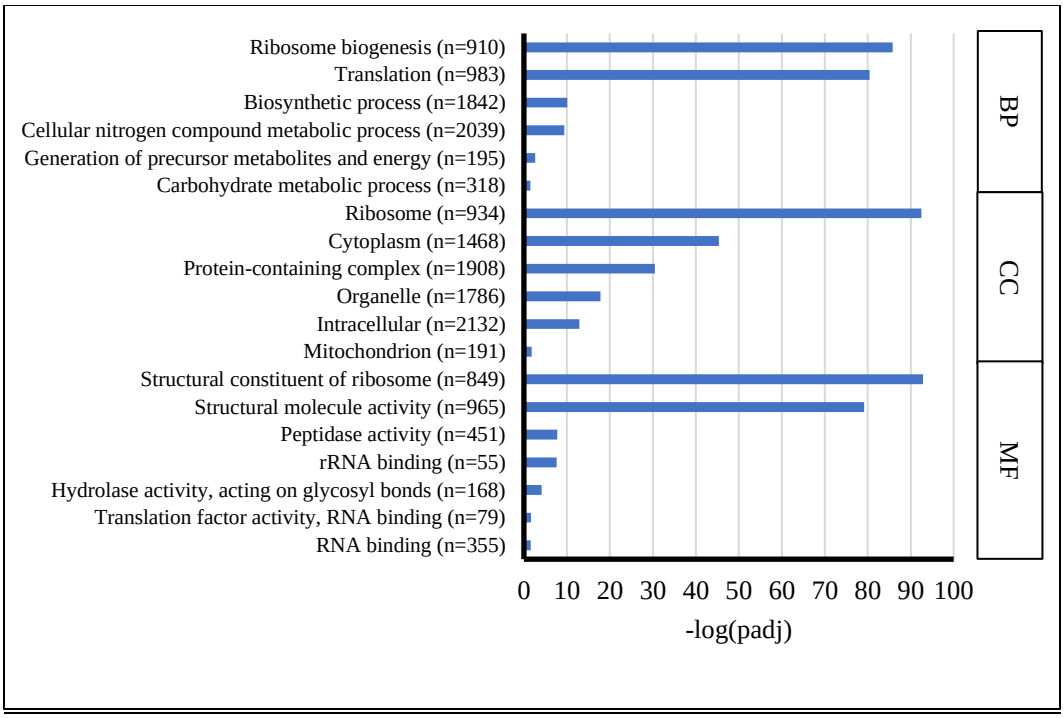

Figure 4.17: GO enrichment analysis of the downregulated DEGs (root) under non-EAPR versus control condition [Category: biological process (BP), cellular component (CC), and molecular function (MF)]

4.9.2 GO Analysis of Leaf Samples

4.9.2.1 GO Analyses of Leaf Samples for EAPR versus non-EAPR (Effects of EAPR)

Via GO analysis, it was observed that EAPR treatment likely caused enrichment of upregulated and downregulated genes in 12 (Figure 4.18) and 10 terms (Figure 4.19), respectively. Some similar terms were observed in both figures due to the introduction of the electric field. These terms include translation, ribosome biogenesis, biosynthetic process (BP group), ribosome, cytoplasm, protein-containing complex, organelle (CC group), structural constituent of

ribosome and structural molecule activity (MF group). Three additional GO terms enriched with the upregulated genes were cellular nitrogen compound metabolic process (BP group), oxidoreductase activity and RNA binding (MF group), as shown in Figure 4.18. In contrast, only additional hydrolase activity, acting on glycosyl bonds term was enriched with downregulated genes, as shown in Figure 4.19.

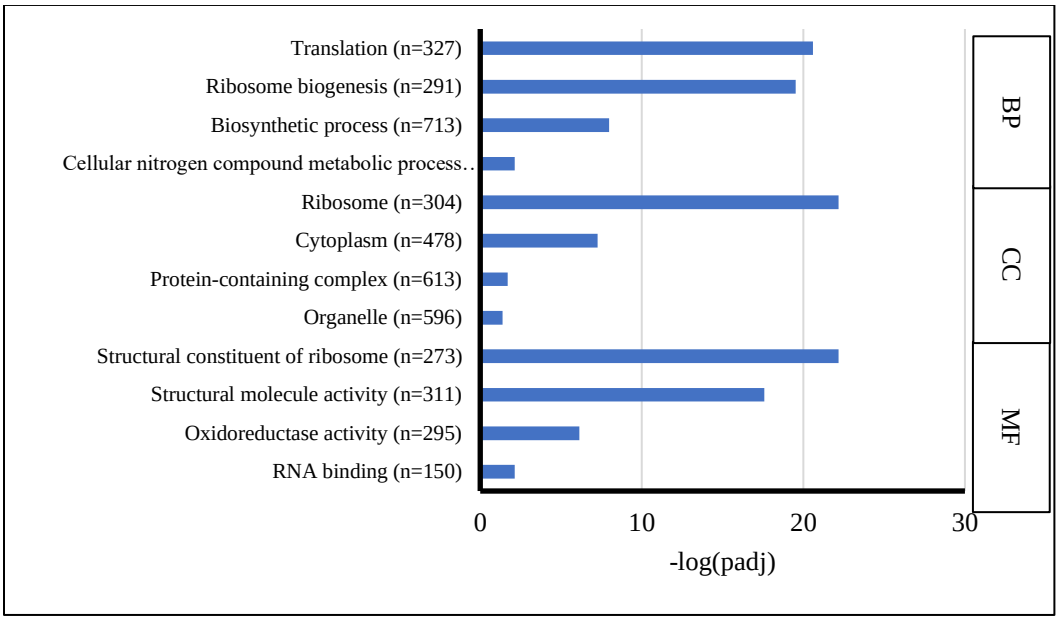

Figure 4.18: GO enrichment analysis of the upregulated DEGs (leaf) under EAPR versus non-EAPR condition [Category: biological process (BP), cellular component (CC), and molecular function (MF)]

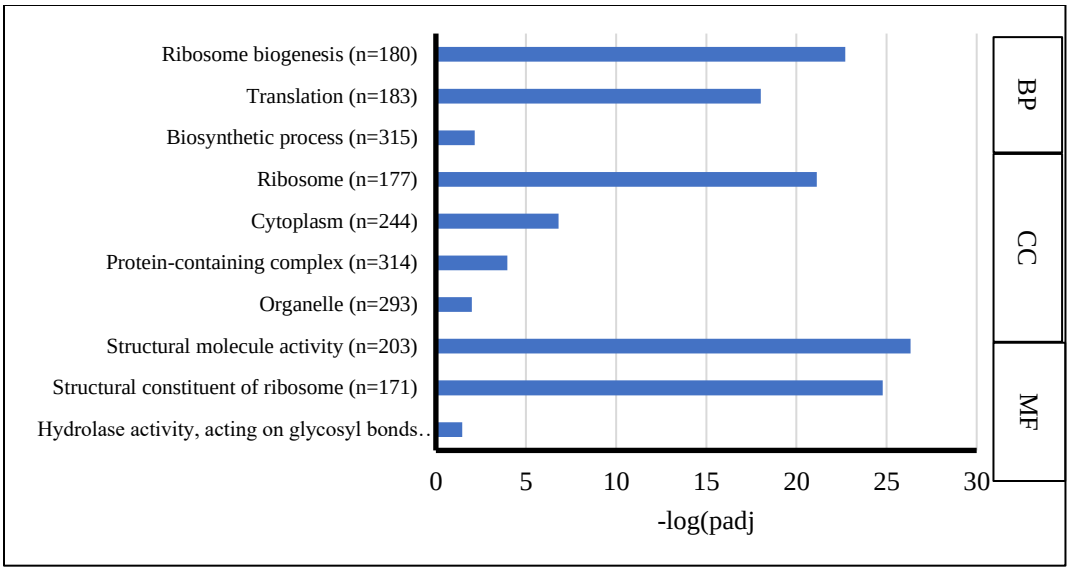

Figure 4.19: GO enrichment analysis of the downregulated DEGs (leaf) under EAPR versus non-EAPR condition [Category: biological process (BP), cellular component (CC), and molecular function (MF)]

4.9.2.2 GO Analyses of Leaf Samples for Non-EAPR versus Control (Effects of Pb Stress)

As shown in Figures 4.20 and 4.21, both upregulated and downregulated DEGs were mainly enriched in the same terms. These terms include translation, ribosome biogenesis, biosynthetic process, cellular nitrogen compound metabolic process from the BP group, ribosome, cytoplasm, protein-containing complex, organelle, intracellular from the CC group, structural constituent of ribosome and structural molecule activity derived from the MF group. In addition, GO enrichment analyses of the downregulated DEGs revealed two additional terms from the MF group: enzyme regulator activity and rRNA binding (Figure 4.21).

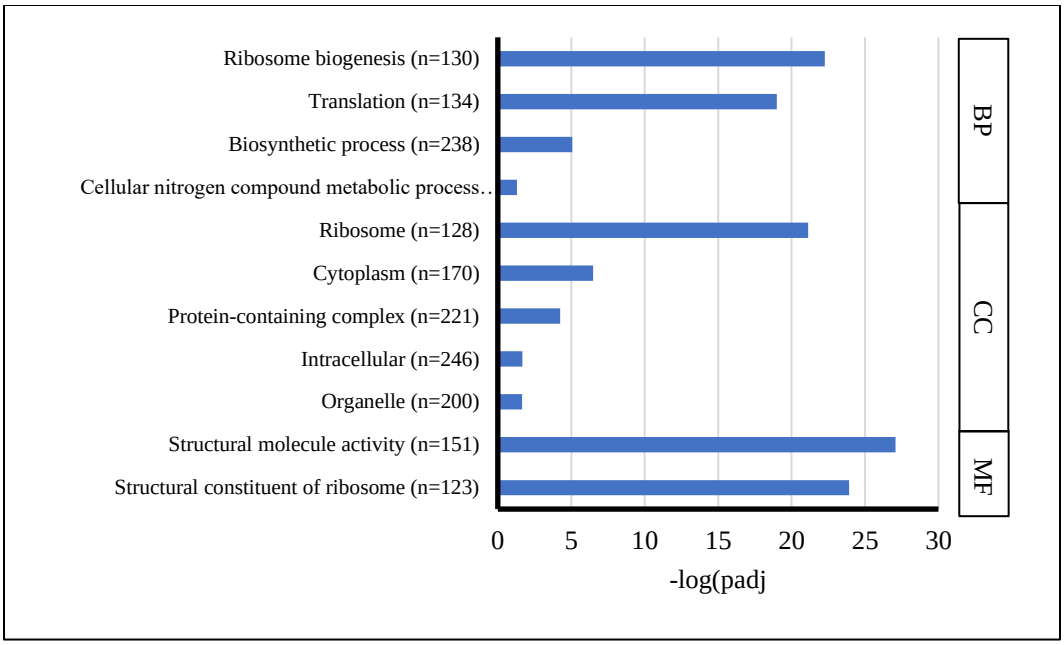

Figure 4.20: GO enrichment analysis of the upregulated DEGs (leaf) under non-EAPR versus control condition [Category: biological process (BP), cellular component (CC), and molecular function (MF)]

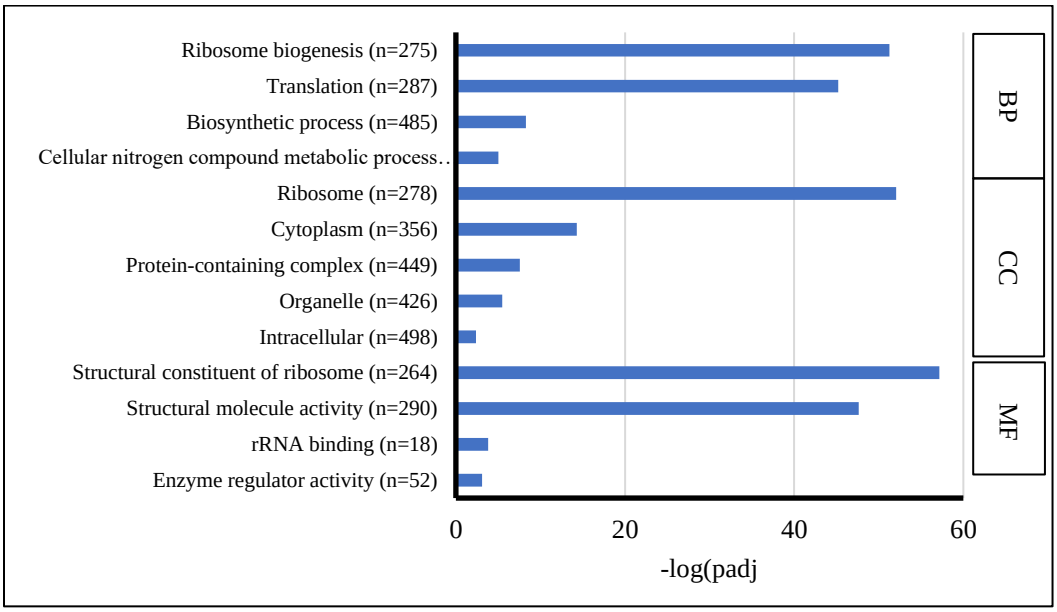

Figure 4.21: GO enrichment analysis of the downregulated DEGs (leaf) under non-EAPR versus control condition [Category: biological process (BP), cellular component (CC), and molecular function (MF)]

4.10 Kyoto Encyclopedia of Genes and Genomes (KEGG) Enrichment Analyses

4.10.1 KEGG Enrichment Analyses of Root Samples for EAPR versus non-EAPR (Effects of EAPR)

The KEGG pathway enrichment was assessed to identify specific biological pathways associated with these DEGs, and the significantly enriched pathways were filtered based on *-log(padj)* < 0.05. As shown in the KEGG enrichment analysis, six KEGG pathways were identified because of EAPR treatment (Table 4.5). Based on the *-log(padj)* values, upregulated DEGs were significantly enriched in ribosome (14.76). In contrast, downregulated DEGs were most significantly enriched in the MAPK signaling pathway-plant (7.00), followed by Ras signaling pathway (2.72), Rap1 signaling pathway (1.88), cAMP signaling pathway (1.77) and the calcium signaling pathway (1.60).

Table 4.5: Comparative KEGG pathway enrichment analysis of root DEGs due to EAPR treatment

EAPR versus non-EAPR	ID	Description	*-log(padj)*
Upregulated	ko03010	Ribosome (n = 242)	14.76
Downregulated	ko04016	MAPK signaling pathway - plant	7.00
	ko04014	Ras signaling pathway	2.72
	ko04015	Rap1 signaling pathway	1.88
	ko04024	cAMP signaling pathway	1.77
	ko04020	Calcium signaling pathway	1.60

4.10.2 KEGG Enrichment Analyses of Root Samples for non-EAPR versus control (Effects of Pb stress)

Additionally, the effects of Pb stress may impact eight KEGG pathways, as determined by KEGG enrichment analysis (Table 4.6). In contrast to the impact of EAPR, MAPK signalling pathway- plant, Ras signalling pathway and cAMP signalling pathway were found to be under the upregulated DEGs group, which could be under the influence of Pb stress. Among all, the MAPK signalling pathway- plant was the most significant upregulated pathway, with a *-log(padj)* score of 3.07 compared to the rest, which are below 2.0. The downregulated DEGs were significantly enriched in the ribosome pathway, with a *-log(padj)* value of 89.80. Other pathways enriched include oxidative phosphorylation (7.96), photosynthesis-antenna proteins (6.33), necroptosis (3.60), apoptosis (3.57), cGMP- PKG signalling pathway (2.15) and mineral absorption (1.68).

Table 4.6: Comparative KEGG pathway enrichment analysis of root DEGs due to Pb stress

Non-EAPR versus control	ID	Description	*-log (padj)*
Upregulated	ko04016	MAPK signaling pathway - plant	3.07
	ko04014	Ras signaling pathway	1.66
	ko04024	cAMP signaling pathway	1.66
Downregulated	ko03010	Ribosome	89.80
	ko00190	Oxidative phosphorylation	7.96
	ko00196	Photosynthesis - antenna proteins	6.33
	ko04217	Necroptosis	3.60
	ko04210	Apoptosis	3.57
	ko04022	cGMP-PKG signaling pathway	2.15
	ko04978	Mineral absorption	1.68

4.11 KEGG Enrichment Analyses of Leaf DEGs

4.11.1 KEGG Enrichment Analyses of Leaf Samples for EAPR versus non-EAPR (Effects of EAPR)

Seven KEGG enrichment pathways were identified as the effect of EAPR treatment (Table 4.7). The ribosome, biosynthesis of secondary metabolite, metabolic pathways, biosynthesis of amino acids, arginine biosynthesis and carbon metabolism pathways were significantly enriched in upregulated DEGs. The *-log(padj)* score by ribosome was the highest (14.80), while the rest of the pathways were in the range of 1.73 to 2.19.

Table 4.7: Comparative KEGG pathway enrichment analysis of leaf DEGs due to EAPR treatment

EAPR versus non-EAPR	ID	Description	*-log (padj)*
Upregulated	ko03010	Ribosome	14.80
	ko01110	Biosynthesis of secondary metabolites	2.19
	ko01100	Metabolic pathways	2.19
	ko01230	Biosynthesis of amino acids	1.93
	ko00220	Arginine biosynthesis	1.73
	ko01200	Carbon metabolism	1.73
Downregulated	ko03010	Ribosome	31.47

4.11.2 KEGG Enrichment Analyses of Leaf Samples for non-EAPR versus control (Effects of Pb stress)

Nine KEGG enrichment pathways were obtained that could be as the result of the influence of Pb stress. Most of the DEGs were downregulated in six pathways, which include ribosome (72.76), flavonoid biosynthesis (4.28), stilbenoid, diarylheptanoid and gingerol biosynthesis (3.82), phenylpropanoid biosynthesis (2.62), alpha-linolenic acid metabolism (1.54) and linoleic acid metabolism (1.37). Upregulated DEGs were significantly enriched in ribosome (31.77), plant hormone signal transduction (5.46) and fatty acid elongation pathways (1.47) as shown in Table 4.8.

Table 4.8: Comparative KEGG pathway enrichment analysis of leaf DEGs due to non-EAPR treatment

Non-EAPR versus negative control.	**ID**	**Description**	***-log (padj)***
Upregulated	ko03010	Ribosome	31.77
	ko04075	Plant hormone signal transduction	5.46
	ko00062	Fatty acid elongation	1.47
Downregulated	ko03010	Ribosome	72.76
	ko00941	Flavonoid biosynthesis	4.28
	ko00945	Stilbenoid, diarylheptanoid and gingerol biosynthesis	3.82
	ko00940	Phenylpropanoid biosynthesis	2.62
	ko00592	alpha-Linolenic acid metabolism	1.54
	ko00591	Linoleic acid metabolism	1.37

4.12 Key Genes in *P. stratiotes* Adaptation under Combined Electrochemical Stress Revealed by EAPR

The discovery that EAPR reverses the gene expression trends induced by Pb stress prompted an investigation of ten key genes that exhibit these trends (Table 4.9). They were key regulators (not effectors) within stress-signaling networks, such as MAPK, hormone signaling and metal homeostasis.

Table 4.9: **Key Pb-Responsive Regulatory Hub Genes Modulated by EAPR Treatment**

Rank	GeneID	Annotation (from NR / KO / GO)	Functional class	Putative regulatory function
1	Cluster-3093.0	Mitogen-Activated Protein Kinase kinase (MAPKK / MAP2K)	MAPK core kinase	Central amplifier of Pb-stress signals that activates WRKY, NAC, ROS genes
2	Cluster-2906.0	NAP1-related protein 2	MAPK scaffold	Organizes MAPK modules; controls intensity & duration of stress signaling
3	Cluster-18206.0	Stress-induced regulatory protein (*Populus* ortholog)	Stress signaling adaptor	Links oxidative & metal stress to transcriptional responses
4	Cluster-18765.0	14-3-3 protein epsilon	Hormone and MAPK integrator	Master switch for ABA, ethylene, ROS and MAPK phosphorylation cascades
5	Cluster-12402.0	Heterotrimeric G-protein α subunit	Hormone / ROS signal transducer	Controls Ca^{2+}, ROS bursts and MAPK activation under heavy metal stress
6	Cluster-32326.0	ABC-F transporter	Metal/oxidative detox regulator	Regulates translation and stress tolerance; induced by Pb and suppressed by EAPR
7	Cluster-11998.0	Glutathione transferase / prostaglandin-H2 isomerase	ROS detox hub	Controls redox balance downstream of MAPK and WRKY
8	Cluster-13607.0	Ribosomal stress-response protein	Stress-activated translational control	Activated by MAPK and Pb-stress to reprogram proteome

Rank	GeneID	Annotation (from NR / KO / GO)	Functional class	Putative regulatory function
9	Cluster-17353.0	Redox-responsive regulatory protein	ROS–signaling node	Couples Pb-induced ROS to transcriptional activation
10	Cluster-15275.0	Stress-induced cell-wall / membrane protein	Stress signaling interface	Controls ion fluxes and Pb sensing at cell surface

4.13. Upregulation of Genes Involved in MAPK Signaling Pathway in Plants (ko04016) due to Pb stress

Three clusters of genes involved in the regulation of the MAPK signalling pathway- plant due to Pb stress were identified (Appendix 15). The first cluster is MKK3-MPK6 with four and eight DEGs (Appendix 16), respectively, triggered by jasmonic acid (JA). The second MEKK1-MKK2-MPK4/6 cluster shows 24, 12, and one/eight DEGs upregulated, respectively due to cold salt stress. The final cluster is the MKK1-MPK6 cluster, actuated by ABA (salt/drought/osmotic stress), with one and eight DEGs upregulated, respectively.

4.14 Gene Expression Analyses by Quantitative Real-time PCR (qRT-PCR)

To analyse the RNA-Seq data (Section 4.7), qRT-PCR was performed on six upregulated genes potentially associated with Pb stress from the root samples

(Appendix 17). These genes were selected from the MAPK signaling pathway (ko04016), a significantly enriched pathway under Pb stress, and were found to be upregulated in both non-EAPR and EAPR treatments (Figure 4.22). Among the tested genes, GTP-binding protein rhoA-like (GT), guanine nucleotide-binding protein subunit beta-like (GUA), and calcium-binding protein NCS-1-like (CAL) showed statistically significant differences ($p < 0.05$). Notably, calmodulin (CA), GT, and GUA exhibited high relative expression levels (> 10) in EAPR treatment. In contrast, calmodulin 5 (CA5), calcium-binding protein NCS-1-like (CAL) and Rab5b rab family GTPase (RAB) displayed lower expression values (< 6).

This qRT-PCR analysis confirmed the RNA-seq findings, highlighting key genes in the MAPK signaling pathway that may play a role in plant responses to Pb stress.

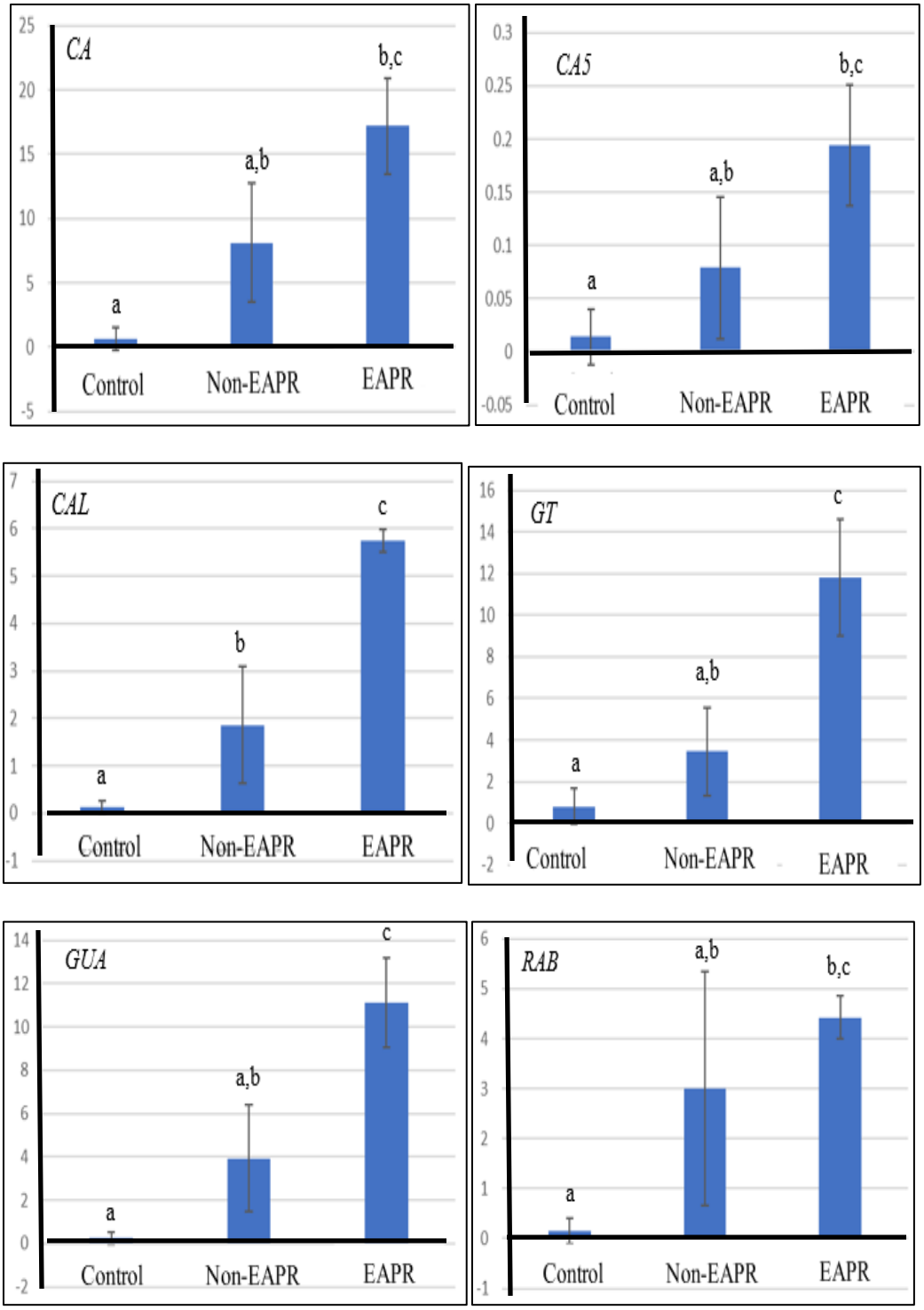

Figure 4.22: Gene expression patterns root samples of *P. stratiotes* [Data are presented as mean ± standard error of the mean (n=3) [y-axis: Relative expression level; different superscript letters letters (^{a}, ^{b}, ^{c}) indicate statistically significant differences ($p < 0.05$) between the control, EAPR and non-EAPR treatments as determined by one-way ANOVA with Tukey's HSD post-hoc test]

CHAPTER 5

DISCUSSIONS

5.1 Leachate Characterization of Synthetic Young Leachate

The pH of both EAPR and non-EAPR leachate samples displayed significant increase compared to the control. However, no significant difference in pH was observed between EAPR and non-EAPR treatments ($p > 0.05$). Although hydroxyl ions are continuously generated at the cathode via water reduction in the EAPR system (Putra and Hastika, 2018), the buffering capacity of the leachate and mass transfer limitations likely mitigated substantial changes in bulk pH (Arhoun, et al., 2023; Zheng, et al., 2024). In a study by Mulati, et al. (2023), the pH values of the treatment groups, which consisted of electro-assisted, wheat and tall fescue varied from 7.45 to 7.71. Similarly, Putra, et al. (2022) observed a pH increase of approximately 6.65- 6.75 in an electro-enhanced phytoremediation system spiked with 500 mg/L of lead (II), which was triggered by the hydrolysis of lead (II) ions in the water.

Some aquatic plants perform photosynthesis during daylight, eradicating carbon dioxide (CO_2) from the medium and causing the pH to rise (Ryplova,

Pokorny and Baxa, 2023). The increased pH in non-EAPR treatment might be, at least in part, due to *P. stratiotes'* absorption of dissolved carbon dioxide (CO_2) from the synthetic leachate for photosynthesis (Jiang, Liao and Li, 2023). This absorption can alter the equilibrium of the CO_2/HCO_3^- buffer system, potentially leading to the exhaustion of protons (H^+), which leads to an increase in the pH (Novita, Moersidik and Priadi, 2019). In this study, the plants were illuminated with a 40 W Philips fluorescent lamp, positioned approximately 20 - 30 cm above the water surface. This corresponds to an estimated photosynthetic photon flux density (PPFD) of approximately 60 - 90 μmol m^{-2} s^{-1}. Although PPFD was not directly measured, the estimated range is consistent with reported values for comparable fluorescent-light environments (Acevedo-Siaca and McAusland, 2025) and is sufficient to trigger net photosynthesis in floating aquatic macrophytes.

Synthetic leachate treated with EAPR showed a significant reduction ($p < 0.05$) in biochemical oxygen demand (BOD), colour and turbidity as compared to the control after 7 days (Table 4.1). An oxidation reaction occurred at the anode, contributing to the increasing DO content (Putra and Hastika, 2018), which may be the reason for the increase in DO value observed in this study. In the EAPR and non-EAPR systems studied, aquatic plants utilize photosynthesis to convert carbon dioxide and water into glucose and oxygen during the day, releasing oxygen into the water. The DO levels in the aquatic environment rise due to this process (Ryplova, Pokorny and Baxa, 2023). In addition, this could be due to the higher oxygen content as aerobic conditions are created within the wastewater that favours

the aerobic bacterial activity to decrease BOD and COD (Mir, et al., 2017). BOD is defined as the amount of dissolved oxygen required by microorganisms to break down organic matter in a solution over a given period and temperature. High BOD can cause oxygen depletion and harm aquatic organisms (Iber and Kasan, 2021). In this study, BOD was reduced significantly more in the EAPR system supplemented with DC than in the control system over the 7-day experiment period. BOD and COD reductions are generally slower and more variable in real landfill leachate applications. This is due to the presence of refractory and humic fractions that are hard to biodegrade. Hence, the combination of electrochemical-biological approaches outperforms a single phytoremediation treatment.

This is supported by Kumar, et al. (2019)'s study, where a significant removal of BOD (83.78%) and COD (93.64%) from sugar mill effluent by *E. crassipes* was obtained by using the Continuous Stirred Tank Reactor (CSTR) assisted with low-level DC. Nevertheless, the higher BOD in the non-EAPR than EAPR system might be resulted from the higher oxygen demand required by microbes to break down organic matter (Dolhan, Arbaan and Bain, 2024).

Similarly, the enhanced reduction in turbidity of synthetic leachate treated with EAPR may be due to the current flow in the system. The synthetic young leachate treated with the EAPR system exhibited a significant reduction in turbidity compared to control. According to Raghab, Abd El Meguid and Hegazi (2013),

turbidity reduction refers to the decrease in suspended solids in leachate. Turbidity reduction suggests removal or aggregation of particulate matter, although suspended solids were not directly measured in this study (Jo, et al., 2024; Behera, Poddar and Byun, 2025). These results are in agreement to those of Foong (2019), which investigated EAPR and non-EAPR (phytoremediation) systems for treating leachate using *E. crassipes*. Their analysis showed that reduced turbidity in the EAPR system (58.13 ± 0.84 NTU) was greater than that in the non-EAPR system (66.20 ± 1.20 NTU). Besides, quantitative UV-VIS analysis at 465 nm showed that the colour intensity of both leachate samples from EAPR (120.00 ± 5.77 PtCo) and non-EAPR (103.33 ± 12.02 PtCo) showed a significant drop compared to the control (213.33 ± 23.33 PtCo). Similarly, Nahar and Hoque (2021) also found that water lettuce effectively treated lake waters, increasing their physical and chemical properties.

Although the EAPR and non-EAPR treatments showed numerical differences in COD, TDS and total ammonia compared with the control, these differences were not statistically significant ($p > 0.05$). Hence, this suggests that electrochemical assistance did not markedly improve the removal of these constituents. Recent research on landfill leachate treatment indicates that refractory organics (COD) and dissolved ions (TDS, ammonia) are more difficult to remove by a sole electrochemical process. The complex composition and high buffering capacity of leachate limit the effectiveness of coagulation and direct oxidation (Rookesh et al., 2022). Factors that enhance the efficiency of electrochemical

processes, such as COD or ammonia removal, include combination with other advanced treatments, sufficient operating time, and current densities (Rookesh, et al., 2022; Kashani et al., 2023).

Despite the applied electric field, the lack of significant differences in ORP among treatments implied that the bulk redox environment remained relatively constant. Competing redox reactions and the buffering effects of complex leachate constituents could contribute to the local anodic and cathodic reactions without significantly altering the ORP of the bulk solution. Recent studies highlight that electrochemical enhancements do not cause quantifiable net ORP changes at the bulk scale in complicated wastewater treatment (Shah, Walia, and Kazemian, 2024).

.

This finding demonstrated that both EAPR and non-EAPR methods can treat leachate. While EAPR displayed greater numerical enhancement in pH, BOD, colour, DO and turbidity compared to non-EAPR treatment, the differences between both treatments were not statistically significant. Additionally, the EAPR system did not significantly enhance the removal of COD, TDS or total ammonia, nor alter ORP as compared to control ($p > 0.05$). The applied electric field had a limited effect on dissolved organics, ionic constituents and bulk redox conditions within the experimental duration. Therefore, the initial hypothesis was not statistically supported under the experimental conditions applied. Enhanced aerobic

bacterial activity and suspended solids removal in EAPR further contributed to more efficient pollutant degradation.

5.1.1 Comparison with Real Landfill Leachate Characteristics and Treatment Responses

Real landfill leachate contains large amounts humic/ fulvic acids, elevated amounts of ammoniacal nitrogen, bicarbonate, organic acids (Lindamulla, et al., 2022; Costa, Pinedo and Riascos, 2025), heavy metals (Al-Yaqout and Hamoda, 2020), diverse cations and TDS. All these characteristics contribute to the strong buffering capability, causing biological and direct electrochemical oxidation reaction less effective than synthetic leachate. Real leachate treatment remains challenging as it contains complex organic fractions and recalcitrant constituents are difficult to biodegrade. Besides, they resist direct electrochemical removal (Sossou, et al., 2024; Xiang, et al., 2025).

Additionally, real landfill leachate exhibits a strong buffering capacity that resists pH shifts, even under electrochemical treatment. In comparison between EAPR and non-EAPR treatment ($p > 0.05$), the observed modest pH changes in synthetic leachate were consistent with real leachate. Even under oxidation or electrochemical forcing, real leachates typically maintain a pH in the range from

near-neutral to slightly alkaline. Thus, it is more difficult to significantly control or change pH and ORP as they resist change (Xiang, et al., 2025).

Furthermore, COD and BOD reductions in real leachate are slower and less substantial due to the presence of refractory organic compounds. The reductions in both parameters in this study might not reflect the high strength of real leachate (Sossou, et al., 2024). It is of crucial importance to consider real leachate components in the interpretation of treatment effectiveness and up scaling of laboratory results.

5.2 Plant Growth and Physiological Parameters

Plant growth is affected by different factors, including nutrients, water, light, temperature (Craker, 2021) and environmental stressors such as HMs (Chaitanya, Pavani and Shasthree, 2023). In addition, electrical stimulation modulates plant cellular behaviors, with effects that highly rely on intensity, frequency and duration applied. While moderate electrical stimulation promotes healing and metabolic activity, excessive intensity can cause tissue damage and dysfunction (Ma, et al., 2024). Plant biomass is a key indicator for assessing the health and productivity (Robertson, Schmid and Lundgren, 2023) of *P. stratiotes*.

The initial biomass of *P. stratiotes* measured before exposure to synthetic leachate (Day 0) serves as the control in this study. Therefore, after seven days of exposure, the biomass values for the EAPR and non-EAPR treatments indicated the percentage decrease in plant biomass relative to the baseline. Based on Figure 4.2, the percentage drop in total plant biomass in the control group (4.97 ± 1.66 %) was significantly lower than that observed under EAPR (31.85 ± 5.93 %) and non-EAPR (28.56 ± 2.85 %) treatments. The greater biomass reduction observed under EAPR and non-EAPR treatments induces physiological stress in *P. stratiotes*. Similarly, Singh, et al. (2023) reported that leachate-induced changes include the reduction in growth and yield of crop-based mustard plants. HM can disrupt membrane permeability, plant metabolic processes and decrease enzymatic activity. Eventually, all these can lower plant growth and biomass output (Soni, et al., 2024; Yadav, et al., 2021).

These results agreed with the observation of *P. stratiotes'* physical appearance, which was grown in synthetic young leachate with HMs under both EAPR and non-EAPR treatments that showed phytotoxic symptoms (discoloration, pigmentation, yellowing and withering) (Agarwal, et al., 2022; Kazmi et al., 2025), which are consistent with HM–induced stress. On the other hand, the control's minimal biomass reduction indicated the plants' initial physiological state before treatment. Incorporating detailed quantitative morphological measurements (e.g. root length analysis or systematic photographic documentation) in future studies would enable further understanding of plant responses to leachate exposure.

Although insignificant, the loss of total biomass was slightly higher in the EAPR system than in the non-EAPR system, indicating stronger physiological interaction between the plants and pollutants during the remediation process. Hence, the electro-assisted system showed a minor effect on the growth of the plants. It was suggested that the plants had lower tolerance to the HMs (Putra, Novarita and Cahyana, 2016; Putra, et al., 2017) present in the leachate. The fresh biomass, growth development and tolerance index of leaves, roots and shoots were adversely affected by increased concentrations of Pb in *Pisum Sativum*, *Zea mays* (Çimrin, Turan, and Kapur, 2007) and tomato seedlings (Nas and Ali, 2018). The extreme level of Pb alters the reaction of the sulphydryl groups with cations, cell membrane permeability, and the possibility of reaction with active groups of ADP/ ATP and phosphate groups (Chugh and Sawhney, 1999). Cd has been reported to cause stunted growth, chlorosis, osmotic stress and water content (Soni, et al., 2024), while plants exhibiting Fe toxicity display leaf bronzing and stunted root systems (Li, Kronzucker, and Shi, 2016). Sturikova, et al. (2018) reported that excessive levels of Zn could inhibit plant growth and cause chlorosis of young leaves. Symptoms of Mn toxicity include chlorosis, brown spots, and leaf necrosis (Faria, et al., 2020; Garcia, et al., 2020). Reduction in biomass production (Yadav, et al., 2021), germination and plant growth (Lešková, et al., 2020) have been associated with excess Ni in plants.

Besides, the growth of a plant can be closely related to the changes in total chlorophyll content in a plant (Li, et al., 2006a; Putra and Hastika, 2018). Total

chlorophyll content has been employed to measure the photosynthetic capacity of a plant. A plant in active growth or a healthy plant will have a high chlorophyll content (Li, et al., 2018). Chlorophyll content in leaves may be a good indicator of environmental stress, pollutant exposure, as well as changes in temperature and humidity because it exhibits a greater sensitivity to changes in external conditions than do other pigments in foliage, such as carotenoids (Talebzadeh and Valeo, 2022).

In this study, *P. stratiotes* showed a lower amount of total chlorophyll content under HM stress in both EAPR (5.93 ± 0.33 mg/mL) and non-EAPR (5.22 ± 0.39 mg/mL) compared to the control (7.08 ± 0.33 mg/mL) (Figure 4.3). This showed that the presence of HMs in synthetic young leachate could have badly affected *P. stratiotes* growth. Although statistically insignificant, the total chlorophyll in the EAPR was higher than in the non-EAPR. Thus, EAPR probably would have less effect on the development of *P. stratiotes*. Nevertheless, the application of an enhanced phytoremediation system caused significantly higher total chlorophyll (60-70 mg/mL) in Kentucky bluegrass (*Poa pratensis* L.) as compared to conventional hydroponic phytoremediation (Putra, et al., 2022). However, *E. crassipes* grown in EAPR cells maintained normal levels of total chlorophyll content compared to the control, without signs of phytotoxicity (Putra, et al., 2017). Hence, plant species may react differently to enhanced phytoremediation systems, with some showing improved physiological traits while others remain unaffected.

EAPR treatment displayed relatively higher total chlorophyll content, while simultaneously caused greater reduction in total biomass, as compared to non-EAPR. The electrical field may induce physiological changes that increase metabolic costs associated with ion balance and repair (Ma, et al., 2025). This shifts stress-induced resources toward defense and maintenance at the expense of growth. Plants commonly redirect carbon and nitrogen away from growth into protective pathways and maintenance of photosynthetic apparatus under abiotic stress (Xu and Fu, 2022). Hence, biomass accumulation is reduced while simultaneously preserving photosynthetic activity, resulting in a growth–defence trade-off (Jiao, et al., 2024).

Transcriptomic results revealed a leaf-specific upregulation pattern, suggesting activation of photosynthesis-related and leaf protection pathways. Despite whole plant stress, such responses may stabilize chloroplast function or increase chlorophyll synthesis. Additionally, leaves often upregulate genes related to antioxidative responses to maintain carbon assimilation under stress (Rosas-Ramírez, et al., 2024; Zhang, et al., 2025). This contributed to the increase in chlorophyll concentration, despite total biomass decline

Conversely, the gene-downregulation pattern was predominantly observed in root tissues, contributing to reduced biomass accumulation and whole-plant growth. These genes (such as Cyclin-dependent kinases, *NRT1* / *NRT2*) are likely

to impair growth, nutrient uptake and root functions. Transcriptional suppression of root tissues under HM or abiotic stress often causes inhibition of root elongation and impaired uptake capability, which leads to a reduction in total biomass (Li, et al., 2025; Mohamed, et al., 2025). These results imply that EAPR shifted energy allocation from growth to stress adaptation by enhancing chlorophyll content while decreasing biomass accumulation.

Like total chlorophyll, chlorophyll a/b has been employed to indicate photosynthetic activity and plant stress. This parameter has been used to detect and assess plants' exposure to environmental contaminants, such as metals, herbicides and organic pollutants (Marwood, Solomon and Greenberg, 2001; Chantachon, et al., 2004). The chlorophyll a/b ratio displayed a significant difference between the control and EAPR (Figure 4.4). In addition, the chlorophyll a/b ratio in EAPR was slightly higher than in plants under non-EAPR treatment, although insignificant ($p > 0.05$). Similar results were reported by Jayanthi-Rao (2019), who found that by using *E. crassipes*, compared to the phytoremediation system (non-EAPR), chlorophyll a/b in EAPR was higher. A high chlorophyll a/b ratio implies that the plants were exposed to stressful toxic chemicals (Huang, et al., 2004; Putra and Hastika, 2018). Thus, EAPR is unlikely to affect the growth of *P. stratiotes* significantly.

Elevated HM concentrations harm plants' photosynthetic pigment content and negatively impact photosynthesis (Ahmad, et al., 2022). This is due to the HMs' replacement of Mg^{2+} in the porphyrin ring in chlorophyll and suppression of the enzymes that produce it (Rastgoo and Alemzadeh, 2011; Sumalan, et al., 2023). Chlorophyll a is the main pigment in Photosystem I (PSI) that is involved in light absorption. In contrast, both chlorophylls a and b are present in Photosystem II (PSII) (Farnese, et. al., 2014). Chlorophyll a is relatively more sensitive to HM stress than chlorophyll b (Zhang, et al., 2020), resulting in a 47.6% increase in the chlorophyll a/b ratio at the highest arsenic concentration (Farnese, et al., 2014). The increased chlorophyll a/b ratio suggests a higher PSI/PSII ratio, likely due to stress adaptation, which may lead to improved cyclic electron transport and mitigate PSII damage (Takabayashi, et al., 2005; Li, et al., 2006b). The concentration of HMs generally has a negative correlation with the chlorophyll a/b ratio (Parić, et al., 2025). A greater chlorophyll a/b ratio in plants exposed to toxic chemical stress typically indicates that the plant has adapted to the stress conditions (Putra, Annisa and Budiarjo, 2020; Uka, Belford and Elebe, 2021).

Results on chlorophyll a/b ratios and growth show no significant difference between EAPR and non-EAPR groups. This suggests that the decline in chl a/b ratios and growth in the HM-stressed plants can be attributed primarily to the presence of HMs themselves, not to EAPR. Importantly, the application of the EAPR electrical field did not further exacerbate plant growth or photosynthetic activity in HM-stressed plants. It is noted that EAPR did not restore these two

parameters to their control levels. However, this observation does not detract from the utility of EAPR technology, as its primary goal is to phytoremediate HM from the environment rather than promote plant growth. By modulating metal mobility and rhizosphere conditions (Kafle, et al., 2022), EAPR may also prolong plant physiological function and survival in toxic environments, thereby supporting sustained remediation activity.

5.3 BCF of Leaf and Root

To determine if the absorbed HMs are accumulated in specific parts of a plant, the BCF is calculated to assess the ability of a plant organ to accumulate HMs from contaminated samples. This study examined Mn, Cd, Fe, Ni, Pb and Zn in *P. stratiotes* as these HMs were present in landfill leachate (Urase, et al., 1997; Dan, et al., 2017). *P. stratiotes* possesses a simplified vascular structure instead of a true shoot system (Dipu, Kumar and Thanga, 2011; Ali, et al., 2020) to assist in direct HM uptake and translocation from root to leaf. Under limited intermediate redistribution, the HM-specific variation in leaf accumulation is reduced under different treatments.

In the EAPR system, higher amounts of Cd (183.64 ± 5.69), Fe (138.99 ± 53.12) and Ni (181.39 ± 1.12) were found accumulated in the leaf, as shown in Figure 4.5. Similarly, Foong (2019) discovered higher BCF values for Cd (2,

718.31 ± 13.17), Fe (2, 070.14 ± 48.66) and Ni (3, 035.12 ± 48.24) in the shoot of *E. crassipes* in the EAPR system. Although Cd is a non-essential metal, it is chemically similar to Zn and could be taken up via Zn transporters (Tavarez, Macri and Sankaran, 2015). Besides, although no BCF value was mentioned, Bi, et al. (2010) observed that transportation or accumulation of Cd to the lettuce *(Lactuca sativa)* plant shoot was increased by about 20% when a 50 Hz AC field was introduced as compared to without an electrical treatment. As for Fe, despite being an essential metal, redox interactions can cause it to accumulate excessively (Wairich, et al., 2024). In a study by Putra and Hastika (2018), Fe uptake was mainly accumulated in the shoot part of water hyacinth in the EAPR system. Conversely, Ni is absorbed and frequently accumulates in the tolerant species through Mg/Fe transporters (Pinto and Ferreira, 2015).

Variations in HM speciation and translocation behavior could have contributed to the increase in BCFs of Zn, Pb, and Mn in leaves treated under non-EAPR conditions. Xylem can carry more easily some of the soluble or organically bound forms to shoots (Alghamdi and El-Zohri, 2024; Ur Rahman, et al., 2024). In contrast, electric field in EAPR can alter pH and drive redox reactions near electrodes. This results in processes of metal desorption, precipitation or electromigration. Consequently, the rhizosphere's metal bioavailability and spatial distribution will be affected (Zheng et al., 2024). Thus, the absorption of other HMs, such as Cd, Fe, and Ni increased. These HMs are generally less stable and

readily migrate toward the roots under electric field influence (Cai, et al., 2022; Zheng, et al., 2024).

Elevated BCF leaf values for Cd, Fe, and Ni in the EAPR treatment could be driven by electroassisted mobilization and plant uptake. Cationic metals, particularly loosely-bound Cd^{2+} and $Ni^{2,+}$ are desorbed by an anodic acid front near the anode generated from the application of a low DC field. Electromigration and electroosmotic flow then move the dissolved cation metals and pore water towards the rhizosphere, increasing the short-term bioavailability (Cai, et al., 2022; Mulati, et al., 2023). Both Cd and Ni maintain their solubility and are ready for uptake, while Fe's movement relies heavily on complexation and redox reactions. Hence, EAPR changes metal speciation via the local pH and redox gradients it creates (Zhang, et al., 2024b; Zheng, et al., 2024). Besides, HM flux into roots and translocation to leaves were increased by altering root membrane permeability and rhizosphere chemistry. Both electrochemical and physiological effects lead to HM-type variability (Priya, et al., 2023).

Regardless of EAPR or non-EAPR treatments, the BCF values for the leaf ranged between 59.26 ± 44.03 to 273.49 ± 28.68, while the BCF for roots ranged from 428.12 ± 120.67 to 18,999.06 ± 8,321.76, as shown in Figure 4.6. Similar to the BCF leaf, metals were found to have the main effect on the BCF root, in the absence of interaction between treatments and metals (two-way ANOVA). Plant

roots can function as a barrier against HM translocation, serving as a potential tolerance mechanism that operates within the root (Ernst, Verkleij and Schat, 1992). In this study, by comparing the BCF values of the leaf and root, it was found that the absorbed HMs were accumulated mainly in the root. The translocation of the absorbed HMs might not occur or be inefficient. Considering that the absorbed HMs were inadequate to be transported to the leaf, the BCF values for the EAPR system in the root indicated that EAPR might enhance the absorption of these HMs by the plants (particularly for Pb and Fe), albeit treatments were not the main effect (two-way ANOVA).

The electric field applied may increase the bioavailability of metal ions through electromigration into roots (Yeung, 2011; Akemoto, Putra and Tanaka, 2022). The BCF values for Pb and Fe were relatively higher in the root samples for both treatments (Chan, et al., 2022), possibly indicating antagonist effects on Mn, Cd, Ni, and Zn. This could be due to metals and metalloids competing for plant uptake, resulting in synergistic or antagonistic interactive effects (Kanu, et al., 2019; Saleem, et al., 2023). Additionally, plant metal transporters exhibit different affinities towards various metal elements (Williams, Pittman and Hall, 2000). This could eventually affect plants' ability to uptake certain elements more effectively, including essential elements (Gautam, et al., 2023). These might explain why the BCFs of Pb and Fe were higher than those of the other HMs. Additionally, the plant species used can affect the types of HM absorbed, which depends on the plant species' preference. For example, *Sedum alfredii* plants were

reported to hyperaccumulate more than two elements, Zn, Pb and Cd (Xv, et al., 2020). Several species of the Brassicaceae family's *Thlaspi* genus are well known for their ability to accumulate numerous HMs, such as Ni and Zn, which can be hyperaccumulated by *T. caerulescens* and *T. ochroleucum* (Prasad and Freitas, 2003).

BCF value of Pb was highest at 18,999.06 ± 8,321.76 (1.9 times) in the root of *P. stratiotes*. Besides possibly due to the supply of low electric current in the EAPR system that enhanced the accumulation of Pb, it could also be a result of most of the absorbed Pb being stored in the roots due to Casparian strips (Kumar, Smita, and Flores, 2017; Usman, et al., 2020). The Casparian strip in the endodermis precipitates Pb, which moves through the symplastic pathway, breaking down as the plant detoxifies. It restricts the transportation of Pb into vascular tissue from endodermis tissues (Usman, et al., 2020), thereby localizing Pb in the roots. Pb binds to the carboxyl group of mucilage uronic acids or directly to the rhizoderm cell surface polysaccharides (Ashraf, et al., 2021). Therefore, the higher BCF value was recorded in the root. In a study, the findings using *E. crassipes* plants grown in EAPR conditions (Putra and Hastika, 2018) showed that Pb was the most accumulated in roots, followed by Cd, Fe and Cu. Similarly, the total deposition of Pb concentration and absorption in the roots of Kentucky bluegrass (*Poa pratensis* L.) was higher in the EAPR system than in the phytoremediation process (Putra, Ohkawa and Tanaka, 2013).

Fe tends to precipitate in the oxidized zone of the root surface, forming iron plaque (IP). According to Zandi, et al. (2023), IP forms on rice roots due to the oxidation of soluble ferrous iron (Fe^{2+}) to ferric iron (Fe^{3+}) in anaerobic conditions, driven by radial oxygen loss from the roots. IP consists of iron oxyhydroxides, such as ferrihydrite and goethite (Hansel, et al., 2001), which may co-precipitate with Mn and other elements. These plaques store Fe on the root surface, making it readily available for plant uptake. Under certain conditions, such as root decay and the decomposition of organic matter, Fe^{2+} stored in IP can be released into the surrounding soil or water, increasing its availability for absorption by rice roots.

The high oxygen content in the water accelerates the breakdown of Fe plaques, thereby improving the HMs uptake process (Suriyagoda, Dittert, and Lambers, 2018). IP can also act as a protective layer, reducing the uptake and translocation of toxic metals, such as Cd, Cr, As and Pb into plant tissues. Hence, their bioavailability and toxicity in plants are further reduced. However, its effectiveness varies based on factors (Zandi, et al., 2023), including soil conditions (Zandi, et al., 2020) and plant genotype (Syu, et al., 2014). Similarly, *E. crassipes* displayed the highest accumulation of Fe when treated with synthetic leachate using the EAPR system, with a BCF value for roots of 56,568.88 ± 2267.13 (Foong, 2019). Fe in plant roots is essential for controlling root development and reducing toxicity during metal stress. Fe affects root architecture, scavenges ROS and limits metal uptake (Li, et al., 2024a).

5.4 Translocation Factor (TF)

In this study, the TF value was less than one for all the HMs measured in EAPR and non-EAPR treatments (Chan, et al., 2022) (Table 4.2), which correlated with the high BCF in roots of *P. stratiotes*. These results showed that *P. stratiotes* plants were unable to translocate the absorbed HMs to their leaves. The TF values in descending order of EAPR treatment are Mn > Cd > Ni > Zn > Fe > Pb (Chan, et al., 2022), which is also consistent with the BCF of root values, which showed that Fe and Pb were highly accumulated in the roots. In a study using *E. crassipes* plants, the descending sequence of TF values (Cu > Fe > Cd > Pb) obtained using EAPR to treat leachate differed, which could be attributed to the varying types of plant species and leachate samples used (Putra and Hastika, 2018).

HMs, particularly Pb and Fe, were accumulated in the roots for both EAPR and non-EAPR, as indicated by BCF > 1 and TF < 1 values. The low TF values suggest restricted translocation from roots to shoots (Aziz, et al., 2023), although microscopic localization analysis (e.g. SEM-EDX) was not conducted. This pattern is consistent with studies on plant protective mechanisms that limit the transfer of HMs to other parts of plants (Yan, et al., 2020). Many studies using other plants have supported these findings. For example, *E. crassipes* accumulates a higher concentration of metal in its roots than in its shoots (Eid, et al., 2021). In addition, Foong's (2019) study using *E. crassipes* also showed that in both EAPR and

phytoremediation treatments, the absorbed HMs were accumulated in the roots as the translocation factor of Pb, Cr, Cd, Fe, Ni, Zn and Mn were less than 1 (TF <1). Direct current increases the metal ion uptake but does not enhance the translocation of metal ions to the aerial parts of the plant. An increase in voltage strengthens the electric field, thus enhancing root accumulation via HM mobilisation (Yuan, et al., 2021; Zeng, et al., 2024). Nevertheless, higher voltages can intensify electrode reactions, formation of insoluble precipitates near electrodes and phytotoxicity that limit translocation to shoots (Cameselle, Gouveia and Urréjola, 2019; Ma, et al., 2024). In contrast, lowering the voltage can prevent electrochemical stress but also reduce electric-field mobilisation, which potentially leads to a drop in absorption (Abou-Shady and Yu, 2023; Bu, et al., 2024).

In this study, treatment did not have a main effect on TF, as revealed by a two-way ANOVA. Hence, EAPR at 2V did not affect *P. stratiotes'* capacity to translocate metals. Previous studies have shown that electric-field parameters (e.g. voltage/field strength and exposure time) can affect electroosmotic and electromigration transport of ions (Abou-Shady and Yu, 2023). These can change metal bioavailability and plant accumulation patterns (Yuan, et al., 2021). Thus TF can be sensitive to the chosen electrical parameters. Regardless of the presence of electrical current, *P. stratiotes* absorbed the HMs from the synthetic young leachate and stored the majority of them in its root system. The highest TF in the EAPR and non-EAPR systems was observed for Mn, while Pb displayed the lowest TF. This indicated that, compared to Mn, there was little transport of Pb to the leaves. The

TF values for Pb in both electro-enhanced phytoremediation and sole phytoremediation systems were low (0.06-0.16) in Kentucky bluegrass (*Poa pratensis* L.) grown in contaminated water, suggesting translocation to shoots was low (Putra, et al., 2022). In *E. crassipes*, TF for Pb was lowest (0.48), as compared to Fe (1.76), Cu (4.79) and Cd (0.92), showing that Pb is primarily retained in the root part of the plant rather than being translocated to the shoot (Putra and Hastika, 2018). Thus, this difference in TF values reflects that different plants employ varying abilities to translocate HMs.

5.5 Removal Efficiency

The ability of the EAPR system to remove heavy metals and the resulting decrease in their concentration in the synthetic young leachate were evaluated using *P. stratiotes*. Based on the calculated removal efficiency, the EAPR system demonstrated a higher ability to remove most of the HMs from the leachate samples compared to the non-EAPR system (Figure 4.7). EAPR system enhanced the strength of phytoremediation in HM uptake by *P. stratiotes* (Chan, et al., 2022). In a study conducted by Putra, Cahyana and Novarita (2015) using *P. stratiotes*, approximately 99% of Pb concentration was removed from contaminated Pb and Cu water by the EAPR system as compared to the sole phytoremediation system. Ferniza-García, et al. (2017) also reported a similar result in a study on the effect of a coupled electrocoagulation-phytoremediation treatment for the reduction of

Cu, Cd, Pb and Zn present in aqueous solution. The results showed that removal efficiencies were up to 98.3% for Cu, 78.7% for Cd, 100% for Zn, and 96.9% for Pb in the electric-assisted system. Nevertheless, *E. crassipes* was least able to remove Pb (19.65 ± 2.17%) but effectively removed Ni (62.52 ± 0.61%) from synthetic leachate via EAPR (Foong, 2019). This showed that the coupled process of EAPR may have different removal efficiency capabilities on different plants or HMs.

In addition, the removal efficiency of Pb in synthetic young leachate samples was the highest in both the EAPR (59.86 ± 9.98%) and non-EAPR (53.26 ± 1.84%) systems in this study, followed by Fe (EAPR: 56.56 ± 18.08%; non-EAPR: 51.30 ± 12.82%). This further supports two-way ANOVA analysis, whereby metal was the main effect on removal efficiency. These results were consistent with the obtained BCF values, in which Pb and Fe also achieved very high BCF root values, reflecting that the removed metals were probably accumulated in the root systems. Pb and Fe seemed to be removed more efficiently than other HMs in this study. Putra and Hastika (2018) study showed that *E. crassipes* was able to remove heavy metals efficiently from leachate via EAPR in the order of Fe (77.8%) > Cd (22%) > Pb (31.6%) > Cu (30.0%). While using Kentucky bluegrass, 98% of Pb^{2+} was removed from contaminated water in electro-enhanced phytoremediation (Akemoto, Putra and Tanaka, 2022).

The observed enhancement in removal efficiency in EAPR treatment can be due to the application of direct current, which causes an electrochemical mechanism. Water electrolysis produces H^+ at the anode and OH^- at the cathode, thereby generating strong pH gradients. These gradients promote either metal dissolution (in acidic regions) or precipitation (in alkaline zones), altering HM speciation (Zheng, et al., 2024). The electric field simultaneously moves the positively charged metal ions (e.g. Pb^{2+}, Cd^{2+}, Zn^{2+}, Ni^{2+}) toward the cathode via electromigration. This enhances ion mobility and redistributes HMs within the rhizosphere. Whereas, electroosmotic flow assists in the transport of dissolved HM species in synthetic leachate, further improving the contact between pollutants and roots (Bai, et al., 2025).

Based on the BCF values for certain HMs, EAPR increased the uptake and accumulation in *P. stratiotes*. Nevertheless, excessive accumulation or pH may reduce uptake and cause phytotoxicity. Hence, the removal efficiency was metal-specific and voltage-dependent (Zheng, et al., 2024; Jiang, et al., 2025). This contributed to a balance between improved metal mobilization and plant uptake (Mulati, et al., 2023), as seen in the EAPR treatment. The unexpectedly higher removal of Zn in non-EAPR could be explained by the presence of electrochemical effects introduced by EAPR treatment. An electric field generated strong electrode reactions and pH gradients, causing Zn precipitation/immobilisation near the electrode (Gidudu and Chirwa, 2022). Subsequently, the electromigration/electroosmotic process moves dissolved Zn away from the root

zone of *P. stratiotes*, reducing plant uptake (Abou-Shady and Yu, 2023). Besides, electric field parameters (e.g. voltages and durations) can cause plant stress that further reduces phytoextraction (Zhang, et al., 2024a; Bu, et al., 2024). Hence, EAPR under the single voltage applied here did not improve Zn removal.

Thus, the different removal efficiency among other types of HMs could depend on the type of plant used, besides other factors such as electrode material, applied voltage/field strength, exposure time and electrolyte composition (Abou-Shady and Yu, 2023; Zhang, et al., 2024a). These influences alter HMs speciation, bioavailability and the subsequent uptake capacity (Zhang, et al., 2024a). The ability of plants to absorb and accumulate HMs could be due to activation of biological feedback mechanisms that could change biotic ligand binding properties in the plants and other factors, such as trace elements competition, might also contribute to it (Fortin, 2024).

5.6 Antioxidative Enzymes

Biotic and abiotic stresses can induce an overproduction of ROS, leading to oxidative stress that damages cellular structures and functions in plants or results in cell (Dannehl, 2018). Dannehl, et al. (2012) reported that the application of direct electric current (DC) can stimulate the production of ROS, which triggers the metabolite synthesis pathway to synthesize proteins, thioglucosides, polyphenols

and carotenoids (Dannehl, et al., 2012; Su, et al., 2024). Furthermore, DC treatments can increase membrane permeability, allowing for a rapid influx of calcium ions (Ca^{2+}) through cation channels (Sanders, et al., 2002; De Vriese, et al., 2018). The Ca^{2+} signals in plants selectively inhibit or activate the activities of downstream targets, such as signal transducers or specific antioxidative enzymes to regulate biochemical reactions (Lenzoni, Liu and Knight, 2018; Liang, Zhang and Ren, 2021). The antioxidant enzymes, including superoxide dismutase (SOD), ascorbate peroxidase (APX), and monodehydroascorbate reductase are synthesized to regulate ROS toxicity during stress situations (Dannehl, 2018).

SOD is regarded as the frontline defence in plants against increased levels of ROS. It catalyses the conversion of oxygen radicals into oxygen and hydrogen peroxide (Bernard, et al., 2014; Wang, et al., 2018b). Depending on factors such as plant tissue, species, stage of development and exposure time to the metal, SOD's response to HM stress varies (Gratão, et al., 2005). Figure 4.8 (a) shows that the calculated SOD enzyme activity in the leaf was relatively 37.15% higher in EAPR than in the non-EAPR treatment. According to He, Xi and Liu, (2017), low-frequency electric fields (e.g. 1–10 V/m) can upregulate SOD expression, as they could generate small amounts of ROS (Wang, et al., 2024a) through electrolysis (Rajagopalan, et al., 2024) and alter membrane electron transport (Onukwufor, Berry and Wojtovich, 2019). ROS act as secondary messengers, upregulating the expression of SOD and other antioxidants to counteract oxidative stress (Wang, et al., 2024a). Additionally, DC alters the membrane potential, activating Ca^{2+}

channels and MAPK pathways, which trigger SOD gene expression (Ikram, et al., 2025). Ewe (2024) study similarly showed that *P. stratiotes*' leaves exposed to Pb and Ni in synthetic leachate exhibited induced SOD activity in the EAPR treatment.

In contrast, non-EAPR treatment for roots exhibited numerically higher SOD enzyme activity (73.75%) compared to EAPR treatment. Upon electrode application, HM accumulation increases, especially in the plant root area. Hence, the plant may not be able to tolerate HM toxicity and the oxidative stress induced (Yan, et al., 2015). The overproduction of ROS derivatives and H_2O_2 serves as inhibitors of SOD (Farnese, et al., 2014). This may explain the lower SOD activity in roots for EAPR treatment compared to non-EAPR, as EAPR tends to accumulate high concentrations of HM ions in plants, which can adversely inhibit SOD activity. In addition, BCF in roots (Figure 4.6) was reported to be higher than in leaves because HMs favour amassing in the roots (Chan, et al., 2022). Lower root BCF and removal efficiency values (Figure 4.7) were observed for most tested metals in non-EAPR compared to EAPR. This reflects a lower amount of HMs present in the non-EAPR, sufficient to induce the expression of SOD enzymes and overcome oxidative stress (Wang, et al., 2024b). Therefore, higher SOD activity was observed in roots harvested from the non-EAPR compared to the EAPR treatment.

The APX enzyme activity [Figure 4.8 (b)] showed a similar trend as the SOD activity, whereby the APX activity was analytically higher (12.18%) in the

EAPR than in the non-EAPR for the leaf samples. The elevated APX activity may indicate enhanced oxidative stress responses under EAPR treatment. Electrochemical processes can change the redox status, pH gradients and ion distribution in the rhizosphere (Gidudu and Chirwa, 2022). The ROS signalling pathways are then stimulated. ROS act as signalling molecules, upregulating APX and detoxifying H_2O_2 using ascorbate (Qin, Hu and Zhu, 2008). However, the observed increase in APX implied an associated physiological response (Hasanuzzaman, et al., 2020) under the EAPR conditions due to the absence of variation in DC intensity. A study by Ali, Şensoy and Bitik (2022) has shown that specific DC applications (e.g. 8V) can increase APX enzyme activities in spinach. The application of electricity can stimulate the production of secondary metabolites, such as phenolic compounds and carotenoids, which contribute to higher antioxidant activity (Dannehl, 2018). The increased antioxidant capacity may be due to higher APX activity, as APX is a key enzyme in the plant's antioxidant defence system (Rao, et al., 2025). Moreover, increased APX activity also further enhanced plant growth and development (as indicated by improved germination rates, fresh weight of leaves and roots) in sunflower and pea (Maffei, 2014).

Meanwhile, in the roots, APX activity was relatively higher (34.16%) in the non-EAPR than in the EAPR treatment. HMs can disrupt plant cell metabolism, leading to the overproduction of ROS. With the increase in the accumulation of HM ions in the EAPR-treated roots of *P. stratiotes* (Figure 4.6), greater ROS

accumulation could overwhelm the plant's natural defence mechanisms, including reducing APX enzyme, which is essential for neutralizing ROS and mitigating oxidative stress (Babli, Singh and Srivastava, 2022). Additionally, the application of DC electric fields may disrupt the APX enzyme's structure and stability through conformational change. This potentially leads to denaturation, where the protein loses its functional shape (Cadena-Ramírez, Alonso-Vargas and Cesar-Ríos-Guzmán, 2024). The conformational changes induced by electric fields could alter APX's ability in its catalysing reactions, binding to its substrates and potentially influence the chaperone activity during its expression (Kaur, et al., 2021), which further reduces its functionality. For instance, tobacco cells exposed to a magnetic field, which shares specific characteristics with DC fields, led to a decrease in APX expression (Sahebjamei, Abdolmaleki and Ghanati, 2007).

On the other hand, POX plays a variety of roles in the growth and development of plants. This family of enzymes is engaged in cell wall loosening, cell wall cross-linking, suberization, lignification and auxin catabolism. By employing H_2O_2 as an electron acceptor to catalyze the oxidation of phenolic substrates, the POX enzyme scavenges the H_2O_2. Figure 4.8 (c) shows that in the leaves of *P. stratiotes*, non-EAPR treatment had relatively higher (13.44%) POX activity than EAPR treatment. However, the POX activity of roots for EAPR was analytically higher (17.25%) than that of non-EAPR. The enzymatic pattern observed here was opposite to the SOD and APX enzyme activities. Regardless of leaves or roots, the POX activity was relatively higher (11.48 ± 1.41 U/g fw), as

compared to SOD (2.74 ± 0.40 U/g fw) and APX (0.72 ± 0.16 U/g fw). POX could function as the central enzyme in eliminating H_2O_2 after SOD. According to Mansoor, et al. (2023), the accumulation of HM ions in plants can increase ROS, which then enhances POX expression and enzyme activity.

The DC electric field can increase POX activity in roots but not in leaves due to various factors, including differential sensitivity to the field. Roots and leaves may exhibit different sensitivities to the applied DC electric field due to the presence of specific ion channels (Karcz and Burdach, 2022), variations in cellular structure (Wawrecki and Zagorska-Marek, 2007) and membrane composition (Kessouri, et al., 2019). Electric current can alter root metabolism (Saktioto, et al., 2023), potentially impacting the production and activity of POX in *P. stratiotes.* This indicates that under certain conditions, POX activity in roots can be enhanced, whereas in leaves, it may not be significantly affected or may even be inhibited. Saktioto, et al. (2023) study on the variation of electric field effects on oil palm seed roots showed that while controlled electric field exposure (e.g. 100 V/m) can enhance root germination and growth, a high intensity of 1000 V/m has inhibitory effects. In addition, POX plays numerous roles in various root processes, including root meristem development and root cap function (Cheniany, et al., 2010). The electric field may influence these processes, leading to changes in POX activity in the roots. Hence, the intensity of the electric field, the duration of exposure (Saktioto, et al., 2023) and the specific plant species (Rajput, et al., 2021), can also influence the POX activity.

Applying a direct electric current (DC) to a plant leaf can stimulate the activity of antioxidant enzymes, including GR, through various mechanisms. This stimulation can enhance plant tolerance to stress and improve overall plant health (Wang, 2022). The GR activity in the leaf samples shown in Figure 4.8 (d) exhibits a similar trend with the SOD [Figure 4.8 (a)] and APX activities [Figure 4.8 (b)], with GR activity relatively higher (22.18%) in EAPR than in non-EAPR. The application of DC increases GR expression and activity, as an electric field can alter plant membrane permeability, potentially enhancing the physiological processes that lead to the accumulation of antioxidants (Dannehl, 2018), such as glutathione (GSH), which GR utilizes to reduce oxidative damage (Espinosa-Diez, et al., 2015). Other antioxidants accumulated include ascorbate and secondary metabolites, such as carotenoids and phenolic compounds (Dannehl, et al., 2012), which further strengthen the plant's antioxidant defences. Under HM stress, the GR enzyme activity can be inhibited or depleted in plant roots. This is because HMs can disrupt the normal function of antioxidant enzymes, including GR, which is crucial for maintaining the balance of reduced glutathione (GSH) and oxidized glutathione (GSSG). The depletion of GSH, a key player in the antioxidant system, can lead to increased oxidative stress, plants' inability to detox ROS and damage to plant cells (Oestreicher and Morgan, 2019).

In this study, differential antioxidant enzyme activities observed between EAPR and non-EAPR treatments suggest a close relationship with plant growth and HM removal efficiency. HM stress increased ROS production, impairing cellular

processes and reducing plant growth. Nevertheless, the enhancement of antioxidant enzyme activities reduces oxidative damage, sustained leaf physiology/growth and continuous HM uptake (Jarin, et al., 2025). Increased SOD, APX, and GR activities in the leaves under EAPR may have contributed to maintaining photosynthetic activity by reducing HM-induced oxidative stress. Although chlorophyll content and biomass were reduced under HM stress, enhancement of antioxidant activity likely preserves redox balance and avoids further damage to photosynthesis capacity (Yan, et al., 2023; Asiminicesei, Fertu and Gavrilescu, 2024) in EAPR treatment. In contrast, the reduction of SOD and APX activities in EAPR-treated roots (despite higher BCF values) may imply overwhelming of the root antioxidant defence system. HM uptake by the root may be limited despite enhanced metal mobilization, thereby influencing overall removal performance (Mahdavian, 2025). The relatively higher root POX activity indicates a compensatory mechanism for H_2O_2 detoxification when SOD and APX activities are reduced. POX enzymes are important for cell wall modification and lignification (Kidwai, Ahmad and Chakrabarty, 2020). Thus, an increase in this enzyme influences structural adaptation that alters HM binding capacity and sequestration in the roots.

In general, under EAPR treatment, the direct current caused an increase and a reduction in the SOD and APX activities of *P. stratiotes* leaf and root, respectively. There was interaction observed between treatments and plant parts for SOD enzyme. Similarly, a higher GR activity was only detected in the leaf part of this plant under EAPR treatment. However, an opposite trend was observed for both

leaf and root samples in terms of POX activity. POX activity in the leaves and roots of both treatments was relatively higher than that of other enzymes. Hence, *P. stratiotes* could adapt to HM stress by activating specific antioxidant defense mechanisms, such as increasing the expression/activity of SOD and POX enzymes. Although antioxidant activation does not necessarily increase biomass under HM stress, it does support the maintenance of physiological activity for HM uptake.

5.7 Transcriptome Analyses of RNA-Seq Data

5.7.1 Illumina Sequencing and de novo Transcriptome Assembly of *P. stratiotes*

RNA-Seq offers a wide range of applications, including gene/transcript quantification, the discovery of novel genes, functional and differential expression analysis (Pereira, Imada and Guedes, 2017). Hence, a transcriptomic study can be carried out to enhance knowledge of gene expression profiles, which can also serve as a tool to investigate the molecular mechanisms involved in *P. stratiotes* in response to stresses, particularly Pb stress and EAPR treatment in this study. To date, there is a lack of information on *P. stratiotes'* molecular response, which hinders a better understanding of stress signals in cellular processes. *de novo* assembly was performed using the Trinity software to construct transcripts from clean reads (RNA-Seq data), as no *P. stratiotes* genomic sequences were available. Total RNA extracted from the leaf and root samples of *P. stratiotes* that underwent EAPR and non-EAPR treatments were used to construct a set of cDNA libraries.

This study aims to investigate the gene expression profiles in response to EAPR treatment and Pb stress. The Illumina HiSeq 2000 platform was used to sequence the libraries. As shown in Table 4.3, the raw reads for the leaf samples fell within a range of 51 to 60 million, while the raw reads for root samples from the range of 45 to 57 million. Raw reads often contain reads with adapters or low-quality sequences that can impact downstream analysis. Thus, to obtain the clean reads, it is imperative to filter the raw reads (Raghavan, et al., 2022).

The average GC content for all samples obtained was approximately 51% (Table 4.3). The coverage of a gene region is affected by its GC content, with regions having 50 - 60% GC content obtaining the highest coverage, while regions with 70 - 80% (high) or 30 - 40% (low) GC content are indicated to have the least coverage (Gnirke, et al., 2009). Sufficient coverage of GC - rich regions is crucial for achieving high analytical sensitivity in a targeted gene panel (Amr and Funke, 2015). These regions usually exist in the first exon and the promoters of many genes (Antequera and Bird, 1993). The coverage bias observed in the GC-rich regions is partly attributed to the suboptimal hybridization of baits in these regions. Other reasons include the PCR amplification steps of the library construction and the introduction of compression artifacts by GC stretches (Amr and Funke, 2015). GC content bias refers to the relationship between GC content and fragment count (read coverage) observed in Illumina sequencing data. This bias can impact the measurement of fragment abundance found within a genome by influencing the targeted signal of interest for analyses, for example, the estimated copy number

(DNA sequencing). Nevertheless, no consensus is available on the best options to eradicate bias in a sample, as there is inconsistency between samples (Benjamini and Speed, 2012).

Q20 is the percentage of the bases with a q-score greater than 20 (an error rate of one in 100), while Q30 is the percentage of the bases with a q-score greater than 30 (an error rate of one in 1000). The average Q20 and Q30 (leaf: approximately 98% and 94%, respectively) of all samples in this study (Table 4.3), which were higher than the average of 70 - 80% Q30 data, indicated high quality of the data obtained from the transcriptome sequencing. The emergence of various computational tools has enabled NGS analyses based on sequence reads alignment to a reference, base calling, de novo assembly of final variant detection and genome annotation. Base calling accuracy is the common standard applied for sequencer precision. This method indicates the probability of the sequencing platform incorrectly calling (Massingham and Goldman, 2012), which can be transformed into a Phred quality score (Q). The Phred score is utilised in DNA sequencing to measure base quality. Greater values of Phred suggest the high consistency of a sequenced base. The accuracy of the base calling is 99% when the probability of locating one error base calling among 100 bases, with a Phred Score of 20 (Goswami and Sanan-Mishra, 2022).

The data highlight differences in sequence redundancy and assembly quality between transcripts (raw or longer sequences) and unigenes (processed,

shorter, non-redundant sequences) (Table 4.4). Transcript length is a key parameter in NGS studies, reflecting transcriptome diversity and complexity, and influencing RNA stability, processing and gene expression levels. It correlates with regulatory process (Veneziano, et al., 2016; Cipriano and Ballarino, 2018), which includes coding capacity, RNA translation, localization and stability (Wang, et al., 2019. Analysing transcript length helps understand genetic variations (Geisert and Williams, 2020) and splicing events, with longer transcripts more prone to alternative splicing. On the other hand, unigene length indicated the efficacy of assembling sequence fragments, such as expressed sequence tags (ESTs) (Bouck and Vision, 2007), into a full-length transcript. The length of a unigene reflects the depth and quality of the transcriptome assembly and sequencing process (Xiao, et al., 2015).

Mean length is defined as the average length of the sequences in nucleotides (Yang, et al., 2023). Transcripts have a higher mean length than unigenes (1,159 bp versus 807 bp), and larger total nucleotides (368,922,411 versus 164,929,136) (Table 4.4), indicating they include more extensive or redundant sequences (Therkildsen and Baumann, 2020). The unigene dataset is smaller in total number (204,252 versus 318,319), likely due to redundancy removal during clustering (Yuan, et al., 2020). Max length is the length of the most extended sequence (in nucleotides) (Novichkov, Gelfand and Mironov, 2001) whereby both transcripts and unigenes have the same maximum length of 18,644 bp, suggesting the most

extended sequence is shared between the two categories that occur possibly due to a highly expressed or conserved gene (Honaas, et al., 2016).

Besides, N50 represents the length associated with the transcript added last when transcripts are arranged in descending order by length, gathering the lengths of transcripts that constitute at least 50% of the overall length (Yang, et al., 2023). Higher N50 indicates better assembly continuity. The higher N50 (2,136 bp) for transcripts obtained in this study suggests they are less fragmented, while unigenes (986 bp) provide a more concise representation of the transcriptome (Mäkinen, Salmela and Ylinen, 2012). Similarly, the N90 (426 bp) for transcripts is higher than that for unigenes (377 bp). N50 and N90 are higher for transcripts, reflecting better assembly continuity compared to unigenes, which are typically clustered or non-redundant versions of transcripts (Yuan, et al., 2020). Transcriptome sequencing is advantageous for acquiring numerous unigenes from species lacking a reference sequence (Guo, et al., 2021). The N50 (986 bp) and mean length (807 bp) of unigenes derived from this investigation indicate that the sequence assembly was precise and efficient (Ge, et al., 2019). The N50 and mean lengths were superior to those recorded for other species, specifically *Bletilla striata* (957 and 612 bp) (Xu, et al., 2018) and sweet potato (765 and 481 bp) (Wang, et al., 2010).

5.7.2 Distribution of Differentially Expressed Genes (DEGs) Visualized by Volcano Plot

Subsequently, volcano plots were used to infer the overall distribution of DEGs obtained. The upregulated DEGs in response to Pb stress (91.58% more than due to EAPR treatment) are likely due to the plant's initial defence mechanisms to mitigate Pb toxicity, which involve activating specific pathways and processes in the roots. This upregulation is primarily driven by the plant's need to activate genes involved in defence mechanisms, including those related to defence against oxidative stress, cell wall modifications (Zheng, et al., 2021), glutathione metabolism (Cui, et al., 2021) and metal transportation (Clemens, 2019) or detoxification (Wang, et al., 2020a). Moreover, increased DEGs may encompass signal transduction, including signalling protein kinases and transcription factors (Wei, et al., 2025), which may play a role in orchestrating the plant's response to Pb stress. In the roots of *Hirschfeldia incana* L. subjected to Pb stress, among the 577 DEGs, 508 transcripts were upregulated and 69 were downregulated (Hasnaoui, et al., 2022).

In plant roots exposed to a DC electric field, the observed predominance of downregulated DEGs (31.91% more than Pb alone) is likely due to a variety of factors, including changes in gene regulatory networks. DC electric fields can directly influence gene expression by affecting DNA replication, transcription factors and other regulatory processes that are dynamically regulated in root tips

(Reynoso, et al., 2022). In addition, DC field can interfere with signalling pathways that regulate root growth, development and stress responses (Rowe, et al., 2016). The electric field can influence intracellular ion fluxes and membrane potential (Karcz and Burdach, 2022), potentially leading to downregulation of genes involved in these pathways. In some cases, DC fields can cause altered cellular damages (Saktioto, et al., 2023), leading to a shift in gene expression towards a stress response, often involving downregulation of genes related to normal cell function. DC electric fields can inhibit root growth and development, potentially leading to the downregulation of genes involved in cell elongation and division (Karcz and Burdach, 2022). Other than that, DC fields can also influence the activity of root apical meristems, the regions responsible for root development, potentially causing downregulation of genes related to meristematic functions (Wawrecki and Zagórska-Marek, 2007).

The dominance of downregulated root genes in the EAPR vs non-EAPR (Figure 4.9) transcriptome reflects a major suppression of Pb-induced stress genes rather than general transcriptional repression. Under non-EAPR vs control (Figure 4.10; Pb-stress), plants typically maintain a critical stress state characterized by sustained activation of MAPK cascades, ROS-amplifying loops, stress-responsive transcription factors (e.g. WRKY and bZIP), metal transporters and defense-related metabolic pathways (Jarin, et al., 2025). Many of the genes repressed under EAPR vs non-EAPR are associated with mitochondrial activity (Mansoor, et al., 2023), protein synthesis, and stress-responsive signaling networks (Niekerk, et al., 2023)

that are normally upregulated during Pb toxicity. Their coordinated downregulation indicates that EAPR does not merely activate protective genes, but actively silences maladaptive Pb-activated regulatory and metabolic networks, thereby restoring cellular homeostasis (Basharat, et al., 2025).

The volcano plot further reveals a transcriptomic shift from a Pb-induced "emergency" state toward a more controlled and efficient physiological mode. As the need for persistent stress compensation was reduced, consequently, thousands of genes previously induced to cope with Pb toxicity became unnecessary and were transcriptionally suppressed. This includes key regulatory hubs such as MAPK cascades (Basharat, et al., 2025) and hormone signaling pathways [e.g. ABA (Niekerk, et al., 2023), ethylene, jasmonate (Sabagh, et al., 2022)], leading to a coordinated shutdown of large downstream gene networks.

The large-scale downregulation may reflect a reallocation of energy away from costly detoxification and damage-response programs, such as ROS scavenging, toward a more balanced metabolic state (Basharat, et al., 2025). EAPR therefore appears to reduce the energetic burden imposed by Pb stress, allowing *P. stratiotes* to suppress energy-intensive stress programs while selectively upregulating a smaller set of high-impact genes related to electro-responsive transport, metal sequestration and compartmentalization. Together, these transcriptional patterns indicate that the overwhelming downregulation observed in

the volcano plot signifies mitigation of Pb-induced stress and establishment of a metabolically optimized phytoremediation phenotype, rather than increased toxicity.

As for the leaf, electro-assisted process that occur in EAPR treatment (Figure 4.11) leads to higher total amount of DEG's than the effect of Pb stress (Figure 4.12). The upregulated DEGs resulting from EAPR were found to be higher (64.67%) than those caused by Pb stress. Exposure of plant leaves to a DC electric field can result in more upregulated DEGs that could be due to the physiological and biochemical responses triggered by the direct current (DC) field. These changes can manifest in various aspects of the plant's response, including stomatal opening, water stress and metabolic adjustments (Zvitov, et al., 2003; Collin, et al., 2025). Transcriptomic study of rapeseed (*Brassica napus*), a member of the Brassicaceae family, indicated that upregulated DEGs were associated with responses to water scarcity, osmotic stress, ABA signalling, fatty acid degradation, cutin, suberin, metabolic pathways and secondary metabolites biosynthesis (Fang, et al., 2022). DC electric fields can modify the equilibrium of numerous metabolites, including those associated with photosynthesis and lipid metabolism (Collin, et al., 2025). This may be linked to modifications in the expression of genes, leading to specific metabolic pathways or defence against various stresses, increasing the quantity of upregulated DEGs. The specific genes and pathways that are upregulated can vary depending on the intensity (Afrasiyab, Zafar and Muhmmad, 2020), duration and

type of DC electric field used (Jovanić, Belča, and Kasalica, 2001), as well as the plant species and developmental stage (Zvitov, et al., 2003).

Contradicting to this, down regulated DEGs owing to the effect of Pb stress was 18.09% more as compared to EAPR. The higher number of downregulated than upregulated DEGs observed was similar to the transcriptomic study of *Fagopyrum tataricum* leaves in response to Pb stress (Wang, et al., 2020b). In plant leaves subjected to HMs, a higher quantity of DEGs are downregulated relative to those that are upregulated, presumably as a result of the plant's early attempts to inhibit or diminish the activity of particular metabolic pathways and stress responses (Seregin and Kozhevnikova, 2025). This downregulation conserves energy and resources as the plant commences detoxifying processes and adjusts to stress (Singroha and Sharma, 2019). Concurrently, the plant activates detoxification processes to eliminate or sequester HMs from its tissues. This entails the upregulation of genes associated with metal transport, detoxifying enzymes (such as metallothioneins and phytochelatins) and antioxidants (Khanam, et al., 2020). HM exposure triggers chemical reactions in plants, leading to differential gene expression in leaves through a complex process initiated by the detection of metal ions. This perception then triggers signalling pathways, which lead to the activation of transcription factors that subsequently bind to the promoter regions of target genes, thereby upregulating their expression (Ovečka and Takáč, 2013). The signal transduction pathways involved are diverse and may include mitogen-activated

protein kinase cascades, calcium and phytohormone signalling (Singh, et al., 2016b).

5.7.3 Cluster Analysis of Gene Expression Differences

Hierarchical clustering of DEGs (Figure 4.13) showed that leaf and root samples formed two distinct clusters, indicating a primary partition by tissue origin. This pattern is consistent with current comparative transcriptome studies in plants under stress, in which leaves and roots often display distinct DEG profiles. The organ-specific transcriptome divergence implied fundamental differences between tissues in the regulation and adaptation responses (Chen, et al., 2025). In particular, the leaf clusters under EAPR treatment showed a larger set of upregulated DEGs, mostly in red, compared to the non-EAPR and control groups. Under abiotic stress or treatment, leaves often exhibited greater diversity and a greater magnitude of DEGs. Factors such as their central role in photosynthesis, signaling, and stress perception may contribute to this observation.

The development of leaves in *P. stratiotes* could possibly result from a complex interplay of regulatory pathways (Kalve, Vos and Beemster, 2014; Chen, et al., 2025). Besides, electrical treatment can induce a cascade of effects within the leaf, initiating alterations in membrane potential and ion channel activity. This subsequently influences downstream signaling pathways and possibly upregulates

gene expression patterns (Adams and Levin, 2012). Duration of the treatments and voltage can differentially modulate the plant's response, leading to distinct clustering patterns (Grzelka, Matkowski and Ślusarczyk, 2023).

However, most of the DEGs in the root cluster, particularly those from the non-EAPR treatment, exhibited predominantly downregulated gene expression patterns, which appeared green. The process of down-regulation via the suppression of particular genes is crucial for the adaptation of root systems to environmental stimuli (Kul, et al., 2021). The decrease in the expression of specific genes that might be involved in processes that worsen the toxic effects of lead makes this a crucial part of the plant's adaptation to HM stress (Zamani, Yaftian and Parizanganeh, 2012; Wang, et al., 2024c). Other plants may evade metal absorption and neutralize metals through unique processes, such as symbiosis with microbes and may reduce gene expression for metal transport (Skuza, et al., 2022). Plants exposed to HMs trigger various mechanisms, which include signal transduction and modulation of molecular, biochemical and physiological processes to overcome stress effects (Singh, et al., 2016b).

It was noticeable that the DEGs in the leaf and root groups under EAPR treatment exhibited contrasting expression profiles. These results strongly affirm that multiple gene modulation strategies, adapted by *P. stratiotes*, enable it to cope with Pb stress and EAPR treatment. Overall, the hierarchical clustering indicates

that tissue type exerts a stronger influence on the transcriptomic profiles than treatment effects. Leaf and root transcriptomes can respond differently to the same stressor, with similar observations documented across numerous plant systems.

5.7.4 Gene Ontology (GO) Analyses

Identifying the enriched GO terms and DEGs linked to a particular biological process is essential to comprehending the molecular mechanisms underlying that process (Yao, et al., 2020; Liu, n.d.).

5.7.4.1 GO Analyses of Root Samples for EAPR versus non-EAPR (Effects of EAPR)

There is a vast difference in terms found in the Biological Process (BP), Cellular Component (CC) and Molecular Function (MF) groups for the root samples. After EAPR treatment, the upregulated genes were mainly enriched in terms such as ribosome biogenesis and translation (BP group), ribosome (CC group), structural constituents of ribosome and structural molecule activity (MF group) (Figure 4.14). This indicated that the *P. stratiotes*' machinery of ribosome synthesis is markedly enhanced for the translation of mRNA into proteins. Ribosomes are composed of ribosomal RNA (rRNA) (Ni and Buszczak, 2023) and

ribosomal proteins (RPs) with rRNA (Fromont-Racine, et al., 2003). Ribosome biogenesis is the cellular process of synthesizing new ribosomes (Ni and Buszczak, 2023). The electric field could have stimulated an enhancement in ribosome synthesis. In addition, the upregulation of translation suggests the plant is actively producing more proteins (Raabe, Honys and Michailidis, 2019) in response to EAPR.

Structural constituent of ribosome and structural molecule activity (MF group) refers to the components that form the ribosome, such as rRNAs and r-proteins (Catalanotto, et al., 2023). Upregulation of these genes ensures that the ribosome is assembled correctly and can function efficiently. Electric fields can be used in plant biology as a stressor, or as a tool to promote specific biological processes (Ma, et al., 2024). The upregulation of ribosome-related genes after an electric field could be a sign that the plant is initiating a response to the stimulus (McIntosh and Bonham-Smith, 2006), such as repairing cellular damage and synthesizing new proteins for defense mechanisms (Fabbrini, et al., 2017) in response to the electric field.

As indicated by the results from GO analysis, the downregulated genes were mainly enriched in terms such as nucleocytoplasmic transport, membrane organisation, vesicle-mediated transport, signal transduction and transport from the BP group, as well as kinase activity and GTPase activity from the MF group (Figure

4.15). Dominant up- or downregulation of genes, which are due to the effect of EAPR, will be influenced by plant species. Different plant species may respond differently to the same electric field, as similar conditions can enhance the growth of certain plants, while inhibiting others (Xu, et al., 2020). Nucleocytoplasmic transport is one of the terms (BF group) that was downregulated under the influence of EAPR. It suggests that electric fields may influence nucleocytoplasmic transport, a process that involves the movement of molecules between the nucleus and cytoplasm through modulation of gene expression (Sukhova and Sukhov, 2021). Nuclear pore complex embedded in the nuclear envelope functions as the gatekeeper for this transport via modulation of the bidirectional flow of macromolecules (Tamura and Hara-Nishimura, 2014; Yang, et al., 2017). The presence of electric field can disrupt. can disrupt the normal function of the nuclear pore complex, leading to the downregulation of nucleocytoplasmic transport (Gul and Mumtaz, 2025). Disruptions of nucleocytoplasmic transport can have a significant impact on gene expression, as the transport of mRNA, transcription factors and other regulatory molecules is crucial for proper gene regulation (Parry, 2015; Bishop, et al., 2021). Thus, the application of electric field in EAPR treatment can downregulate nucleocytoplasmic transport, which may disrupt nuclear pore complex function and impair the bidirectional flow of macromolecules, ultimately affecting gene expression modulation.

In Figure 4.15, the term membrane organization (BP group) was observed to be downregulated. Electric fields have a significant impact on membrane

organization, which is essential for the regulation of numerous cellular processes and maintaining cellular integrity (Ranjha, et al., 2021). Electric fields can change the transmembrane potential, membrane permeability, and the electroactivity of membrane ligands or receptors (Abasi, et al., 2023). The flow of ions via ionic pumping proteins within the cell membrane, which in turn activates specific intracellular signaling pathways, can be stimulated by external electric stimuli (Johns, et al., 2021). Electric fields can destabilize lipid bilayers by altering membrane fluidity and lipid composition, which in turn disrupts membrane organization (Hemmerlé, et al., 2016). Electroporation studies suggest that electric fields can induce the formation and expansion of small pores in the membrane, facilitating the transport of molecules and ions (Kotnik, et al., 2019). Thus, EAPR treatment can disrupt membrane organization by altering transmembrane potential, permeability, and lipid bilayer stability, potentially leading to pore formation and impaired cellular signalling.

Another term from the BP group that was downregulated is vesicle-mediated transport. It is responsible for molecular movement between various membrane-enclosed compartments (Cooper, 2000). EAPR can interfere with the production, trafficking, and fusion of vesicles, resulting in a downregulation of vesicle-mediated transport (Dimova, et al., 2009; Tokarev, Alfonso, and Segev, 2013). Specifically, the application of a strong electric field can modify the characteristics of membranes, encompassing the shape and function of vesicles, which are crucial for the transfer of materials within and between plant cells. This

includes increasing the permeability and formation of pores (electroporation) (Fan, et al., 2015; Delsart, 2016). Changes in vesicle-mediated transport can disrupt the normal flow of proteins, lipids, and other molecules within the cell, affecting various cellular processes (Kumar, et al., 2024). The altered membrane properties and vesicle dysfunction can lead to a reduction or downregulation of vesicle-mediated transport processes (Delsart, 2016). Hence, EAPR can inhibit vesicle-mediated transport by interfering with vesicle production, trafficking, and membrane integrity, further compromising intracellular molecular transport and cellular functions. Factors influencing the effects of electric fields include field strength, exposure duration (Pliquett, et al., 2007) and cell type (Fan, et al., 2015).

Based on Figure 4.15, EAPR affects the downregulation of signal transduction terms from the BP group. Cells can respond to their surrounding environment through ion channels and receptors embedded in their cell membranes. This further transmits mechanical, chemical and electrical signals inside-out and outside-in the cells. Signal transduction pathways, which mediate the cellular response to external stimuli, are also vulnerable to electric field interference (Taghian, Narmoneva and Kogan, 2015). Plant defense responses are triggered as a result of the interaction of many signalling substances at the cellular level. In this way, disrupted or damaged membranes are sensors of environmental changes. In contrast, secondary messengers (e.g. Ca^{2+} and ROS) and phytohormones (e.g. jasmonic acid (JA), ABA and ethylene are transducers of information from membranes to metabolism (Gaspar, et al., 2002). As a result, electric currents could

have indirectly activated protein kinases and phosphatases, thereby disrupting the normal flow of information within the cell (Taghian, Narmoneva and Kogan, 2015; Dannehl, 2018). The interference of electric fields with signal transduction pathways can have a wide range of effects on plant cells, including altered growth, development and stress responses (Dannehl, 2018). In this way, electric fields in EAPR can disrupt plant cell signal transduction pathways by interfering with ion channels, receptors and secondary messengers, ultimately altering cellular responses, growth and stress adaptation.

The transport term from the BP group was observed to be downregulated as electric fields can influence the transport of nutrients, ions and other molecules across cell membranes (Szechyńska-Hebda, Lewandowska and Karpiński, 2017). Electrochemical gradients induce the transport of charged molecules across membranes, influenced by the electrical potential difference across the membrane. Electric fields can alter electrochemical gradients, influencing transport rate and direction. The application of pulsed electric fields can change membrane structure (Dróżdź, et al., 2021). When cells are subjected to an external electric field, charge accumulation on the membrane's surface might cause high transmembrane potential (Ranjha, et al., 2021). This can disrupt cellular uptake of nutrients, ions and other essential chemicals, subsequently affecting plant development and growth (Ladeynova et al., 2023). EAPR-induced electric fields disrupt membrane transport by altering electrochemical gradients and transmembrane potential, resulting in

impaired nutrient and ion uptake, which negatively impacts plant growth and development.

Furthermore, in the GO analysis, terms related to kinase activity and GTP activity were also downregulated due to the influence of EAPR. In plants, kinases catalyse the addition of phosphate groups to target proteins (Cheng, et al., 2011), while GTPases hydrolyse GTP to GDP (Zhou, Herbst-Robinson and Zhang, 2012). Both enzymes are key components of the signalling cascades that control diverse cellular processes and stress responses. Considered as an abiotic stress elicitor, the application of electric fields to plants leads to the activation of numerous defence responses (Szechyńska-Hebda, Lewandowska and Karpińskiet, 2017; Dannehl, 2018). Electric current may trigger a cascade of events in plants that ultimately leads to the downregulation of specific kinases and GTPases. This down-regulation could occur via numerous mechanisms, such as alteration of gene expression, protein degradation or protein activity.

5.7.4.2 GO Analyses of Root Samples for Non-EAPR versus Control (Effects of Pb Stress)

Figure 4.16 shows the influence of Pb stress which might cause the upregulated genes that were enriched in terms including transport, vesicle-mediated transport, nucleocytoplasmic transport, membrane organisation and signal

transduction from the BP group, as well as GTPase and kinase activity from the MF group. Similarly, root DEGs of *Pogonatherum crinitum* under Pb stress were considerably enriched in functional terms related to transport. Due to Pb exposure, plants might adapt to stress via transport of the HM ions to detox Pb (Zhu, et al., 2022). Intracellular vesicle trafficking plays a crucial role in eukaryotic cells, facilitating the transport of membranes and the delivery of substances to their respective destinations. A significant endocytic pathway in plants, involving vesicle transport to the vacuole, has been reported to be crucial for plant salt tolerance (Leshem, et al., 2006). Vesicle-mediated transport was shown to be enriched up to 4-fold in *Arabidopsis thaliana* roots' response towards uranium stress (Przybyla-Toscano, et al., in press). Cytoplasmic vesicle was significantly enriched in *Oryza sativa's* response towards iron and aluminum exposure *(*Azad, et al., 2024).

The role of nuclear pore complex components in plant stress responses is attributed chiefly to various processes, including transcriptional gene regulation and control of mRNA or protein nucleocytoplasmic trafficking (Yang, et al., 2017). Enrichment of DEGs related to nucleocytoplasmic transport was observed in *Gracilariopsis lemaneiformis* as a response to Cu stress (Tang, et al., 2023). Pb stress also caused damage in root membrane lipidation (Zhu, et al., 2022) as membrane organization/integrity was disrupted (Devi and Prasad, 1999). Regulation of genes involved in signal transduction, transporters, antioxidants, and transcription factors is part of a plant’s response to heavy metal exposure (Auguy,

et al., 2013). ROS can directly affect signaling cascades via protein interactions or indirectly by altering the phenolic compounds synthesis, which are crucial phytochemicals in plant defense mechanisms. Plants may produce these chemicals in response to stress as a component of their defense mechanisms (Sankaranarayanan, Ju and Kessler, 2020).

The upregulation of plant GTPase and kinase activity in response to Pb stress is a complex phenomenon that occurs as the plant attempts to mitigate the toxic effects and restore cellular homeostasis (Ovečka and Takáč, 2013). GTPases from the Rho family have been implicated in plant responses to HM stress. These proteins are involved in vesicle trafficking, cytoskeletal rearrangements and other cellular processes that are crucial to combat stress (Nagawa, Xu and Yang, 2010; Manara, 2012). Exposure to heavy metals, such as Pb (Huang and Huang, 2008), Cu and Cd (Jonak, Nakagami and Hirt, 2004) significantly increased MAP kinase activity in plants. The activation of kinases can induce downstream signaling processes, leading to the expression of genes that encode antioxidant enzymes, metal transporters and other stress-related proteins (Jalmi, et al., 2018).

As shown in Figure 4.17, ribosome biogenesis and translation (BP group), ribosome (CC group), structural constitute of ribosome and structural molecule activity (MF group) were significantly downregulated after Pb exposure, with *-log(padj)* values ranging from 70 to 100. Pb stress significantly reduces ribosome

biogenesis and translation (BP group) as the assembly of ribosomes is compromised, resulting in diminished ribosome synthesis. This is mainly attributable to reduced transcription of rRNA genes (Ni and Buszczak, 2023), processing of pre-rRNA (Sáez-Vásquez and Delseny, 2019) and the assembly of ribosomal proteins (RPs) with rRNA (Fromont-Racine, et al., 2003). The downregulation of these processes results in a reduced protein synthesis capacity (Rahman, Shamsuzzaman and Lindahl, 2020) as the translation of mRNA into proteins is affected due to fewer ribosomes being available to bind to mRNA (Norris, Hopes and Aspden, 2021; Fedry, et al., 2024). Furthermore, ribosomes undergo inactivation through a mechanism known as ribosome hibernation that occurs within chloroplasts to diminish protein synthesis under stressful conditions (Trösch and Willmund, 2019).

Downregulated genes were also enriched in the ribosome term (CC group), as well as structural constituents of ribosome and structural molecule activity (MF group) affected by Pb stress. The structure and function of ribosomes are compromised under stress, potentially due to altered interactions between ribosomal proteins and rRNA (Dörner, et al., 2023). The diminished abundance of ribosomal proteins (RPs) was typically associated with the compromised stability of the ribosome and its degraded structural integrity (He, et al., 2018). It fundamentally impairs the intricate mechanisms governing protein synthesis in plants by adversely affecting the rRNA synthesis and ribosome biogenesis in the nucleolus (Jiao, et al., 2023). This may have substantial implications for plant

growth and development, as protein synthesis is crucial for numerous cellular activities (Sugiyama and Machida, 2018). Hence, Pb stress impacts the assembly and activity of these components, disrupting ribosome function (Lafontaine, et al., 2021).

5.7.4.3 GO Analyses of Leaf Samples for EAPR versus non-EAPR (Effects of EAPR)

For EAPR treatment, upregulated (Figure 4.18) and downregulated (Figure 4.19) genes were enriched almost within similar terms, such as translation, ribosome biogenesis, biosynthetic process from the BP group, ribosome, cytoplasm, protein-containing complex and organelle from the CC group as well as structural constituent of ribosome and structural molecule activity from the MF group. However, upregulated genes were enriched in additional terms, such as cellular nitrogen compound metabolic process (BP group), oxidoreductase activity and RNA binding (MF group). HMs disrupt the nitrogen metabolism, which regulates plant growth and development (Singh, et al., 2016b).

The observed upregulation of genes involved in cellular nitrogen compound metabolic processes in this study may reflect an adaptive response aimed at maintaining nitrogen homeostasis (Hossain, et al., 2012) after electric exposure. Nitrogen is a crucial ingredient for the synthesis of several compounds involved in the plant defense responses, such as enzymes, proteins and phytoalexins. The

overexpression of genes associated with cellular nitrogen compound metabolic process in bean (*Phaseolus vulgaris* L) leaf samples indicates a transformation in nitrogen metabolism, potentially linked to increased synthesis of proteins, amino acids and secondary metabolites (Sun, et al., 2020). Hence, this suggests that EAPR might stimulate or enhance the plant's cellular metabolism of nitrogen-containing compounds. The specific mechanism by which the electric field influences nitrogen metabolism is complicated and may involve changes in gene expression, signal transduction pathways or other cellular processes (Osogo, et al., n.d.).

Upregulated genes in the leaves of *P. stratiotes* under the EAPR treatment were also enriched in the oxidoreductase activity term. Exposure to electric fields can affect plant physiology and metabolism, including oxidoreductase activity. The effects range from stimulation to inhibition that depend on the field type, intensity and duration of exposure (Ma, et al., 2024). The enrichment of the oxidoreductase activity term under EAPR treatment correlates with the observed elevated SOD [Figure 4.8(a)] and APX [Figure 4.8(b)] activities, as compared to non-EAPR-treated leaves. The coordinated transcriptomic response and antioxidative enzyme activities enabled *P. stratiotes* to sustain both photosynthesis and growth. Plant exposure to HMs results in the excessive generation of ROS due to alterations in mitochondrial membrane permeability and the inhibition of ROS detoxifying enzymes within the cellular antioxidant system (Mansoor, et al., 2023). Hence, the electric field may enable the plant to enhance its ability to detoxify ROS and mitigate the adverse effects of oxidative stress by

upregulating oxidoreductase enzymes (Osogo, et al., n.d.). Besides, Huang, et al. (2020a) reveal that at lower concentrations of Pb-Zn, activities of CAT, SOD and peroxidase (POD) were increased in *Ligustrum lucidum* and *Melia azedarach* as a stress response.

Similarly, upregulated genes enriched in the RNA binding term within *P. stratiotes* leaves in response to electric fields might imply a role for these genes in influencing RNA metabolism, such as export, stability, splicing and translation (Manavella, et al., 2023). This can impact the cellular environment and indirectly influence RNA-binding protein activity (Yan, et al., 2022), potentially affecting various aspects of plant physiology, including processes related to Pb stress. The electric field can potentially affect membrane permeability and the movement of molecules within the cell (Hart and Palisano, 2018). It can affect plant photosynthesis (Li, et al., 2024b), development, nutrient absorption, and stress responses (Ma, et al., 2024), potentially altering plant management strategies in response to electric field.

Downregulated genes were enriched in hydrolase activity, acting on glycosyl bonds (Figure 4.19). Plant glycosyl hydrolases are crucial for selectively breaking down carbohydrates and glycoconjugates throughout numerous cellular functions, such as reserve mobilization, signalling pathways and cell wall modification/disassembly (Kfoury, et al., 2024). These enzymes are crucial in

breaking down complex carbohydrates into simpler monosaccharides, which serve as vital sources of energy and building blocks for various cellular components (Valliyodan and Nguyen, 2006). Thus, the downregulation of hydrolase activity-related genes after EAPR treatment could be a mechanism by which *P. stratiotes* might adjust its carbohydrate metabolism, cell wall composition, or defense mechanisms in response to numerous developmental cues or stressors.

5.7.4.4 GO Analyses of Leaf Samples for Non-EAPR versus Control (Effects of Pb Stress)

For *P. stratiotes* plants under Pb stress, upregulated (Figure 4.20) and downregulated (Figure 4.21) genes were enriched in 11 similar terms. These include translation, ribosome biogenesis, biosynthetic process, cellular nitrogen compound metabolic process (BP group), ribosome, cytoplasm, protein-containing complex, organelle, intracellular (CC group), structural constituent of ribosome and structural molecule activity (MF group). GO enrichment analyses of the downregulated DEGs revealed an additional two terms, specifically enzyme regulator activity and rRNA binding, from the MF group. The enzyme regulator activity is significantly impacted in plants after Pb exposure, which causes the downregulation of specific DEGs that participate in numerous regulatory functions (Riyazuddin, et al., 2022). This may entail altered control of enzyme activity, affecting multiple pathways, such as phenylpropanoid production. Zinati and

Delavari (2019)'s study on rice aroma demonstrated the downregulation of genes involved in phenylpropanoid biosynthesis, such as phenylalanine ammonia-lyase, 4-coumarate:CoA ligase and laccase. This further suggests alternative pathways for phenylpropanoid production. The electric field could be triggering stress responses or influencing signal transduction, potentially leading to changes in gene expression and enzyme regulation (Bakshi, et al., 2019).

Pb stress might be able to cause the downregulation of rRNA binding term in *P. stratiotes* leaves by many processes, including modifications to the nucleolus, alterations in RNA metabolism (Lee, et al., 2024) and impacting protein synthesis. Pb stress can diminish the quantity of translation-related proteins and impede protein synthesis (Xia, et al., 2019), potentially affecting cell proliferation and cell cycle progression (Lee, et al., 2024). Furthermore, the nucleolus, an essential locus for ribosome biogenesis (Sáez-Vásquez and Delsenymay, 2019), experiences structural modifications and regulates rRNA production and processing in response to Pb stress. Moreover, RNA-binding proteins, integral to RNA metabolism, might be impacted by Pb stress, hence affecting the expression of stress-response genes (Xia, et al., 2019). Pb can disrupt the alteration of rRNAs, such as pseudouridylation, which is essential for chloroplast ribosome functionality and cold tolerance in plants (Wang and Botella, 2022).

5.7.5 Kyoto Encyclopedia of Genes and Genomes (KEGG) Enrichment Analyses

Plants are continuously subjected to multiple biotic and abiotic stresses due to their sessile nature. This can adversely affect their development, growth, and overall productivity. To avoid such challenges, plants have developed intricate mechanisms to overcome these stresses, which involve a complex interplay of transcriptional and post-transcriptional gene regulations (Kumar, 2016).

5.7.5.1 KEGG Enrichment Analyses of Root Samples for EAPR versus non-EAPR (Effects of EAPR)

Based on Table 4.5, the ribosome pathway (n = 242) was significantly enriched with upregulated DEGs affected by EAPR treatment. Similarly, Figure 4.14 reveals that GO enrichment analysis of upregulated DEGs in roots under EAPR treatment highlighted enrichment in terms related to ribosome biogenesis, translation, ribosome assembly and structural constituents of the ribosome. An electric field may augment ribosome activity in plants, potentially alleviating Pb stress by boosting protein synthesis (Mori, et al., 2021) associated with stress response and defense mechanisms (Zhang, Zhao and Zhu, 2020). Under EAPR, ribosomes facilitate protein synthesis and an elevated rate of ribosomal activity may result in enhanced production of proteins that assist plants in managing stress. The recovery sustains cellular metabolism and improves plant physiology. A relatively

higher total chlorophyll (Figure 4.3) under EAPR treatment supports this finding, despite the greater reduction in total biomass (Figure 4.2).

This can be accomplished by altering the expression of stress-related genes (Liu, et al., 2021a) or by affecting the total rate of protein synthesis (Koyama, et al., 2021). In addition, the increased production of antioxidant proteins could help neutralize ROS generated by Pb stress (Mazaheri-Tirani, et al., 2024). Upon exposure to an electrical field in the root, MAPK signalling pathway - plant was the most significantly enriched with downregulated DEGs (Table 4.5). To adapt to HM stresses, plants have developed signalling mechanisms to regulate and respond appropriately (Keyster, et al., 2020). MAPK signalling is the most predominant in plants and exhibits tolerance mechanisms against abiotic and biotic stressors (Mondal, 2023). EAPR might enhance the antioxidant effects and reduce the bioavailability of ROS. Under less stressful conditions, it may lead to the downregulation of MAPK (Shirahata, et al., 1997; Yoshiaka, et al., 2023). The reduction of oxidative stress and DNA damage affects the decrease of cAMP signalling (Das, et al., 2015), Rap1 signalling, calcium signalling (Kosuru and Chrzanowska, 2020) and reduction of Ras/Raf and MPK3/4 expression regulation in MAPK (González Besteiro and Ulm, 2013; Bigeard and Hirt, 2018).

Besides MAPK, Ras signalling pathway, Rap1 signalling pathway, cAMP signalling pathway and calcium signalling pathway were also enriched with

downregulated DEGs. Ras and Rap proteins are closely associated small GTPases. While Ras is recognized for its function in cell proliferation and survival, Rap1 primarily participates in cell adhesion and the development of cell junctions (Raaijmakers and Bos, 2009). In reaction to Pb stress, these pathways may be activated. However, the introduction of electric fields alleviates the stress-induced condition, resulting in a reduction of their activity. On the other hand, cAMP is involved in numerous biological activities, including stress reactions. The activation can initiate downstream signalling cascades, resulting in alterations in gene expression (Blanco, et al., 2020). Electric fields may attenuate cAMP signalling, hence diminishing the total stress response. Furthermore, transcriptomic analyses in this study revealed the downregulation of Ras and cAMP-related proteins, including MPK3/4/6, under EAPR treatment.

Calcium ions are vital for plant growth and stress responses, with their signalling being integral to numerous activities (Ghosh, et al., 2022). Electric fields may affect calcium signalling via altering calcium influx, efflux (Yadav, et al., 2022) and the function of calcium-binding proteins (Negi, et al., 2023). The downregulation may involve modulating the activity of ion channels (Guo, Liu and Chong, 2018) and impacting signalling pathways related to stress responses (Tyagi, et al., 2024). By influencing these signalling pathways, electric fields could help plants mitigate the adverse effects of Pb toxicity.

5.7.5.2 KEGG Enrichment Analyses of Root Samples for non-EAPR versus control (Effects of Pb stress)

In contrast, under Pb stress, upregulated DEGs were mainly enriched in MAPK signalling pathway- plant, Ras signalling pathway and cAMP signalling pathway (Table 4.6). High MAPK expression might be due to exposure to extracellular stimuli, such as Pb, in this study. MAPK signaling pathways are crucial in the defense response of *Cladophora rupestris* to Pb stress (Liu, et al., 2022a). They are essential for regulating crosstalk between various plant signaling systems (Smekalova, et al., 2014). Similar defense mechanisms may occur in *P. stratiotes*, as a higher upregulation, with a -*log(padj*) value of 3.067, was observed in the KEGG analysis under Pb stress. Calmodulin, the principal eukaryotic calcium-binding protein, detects and reacts to variations in intracellular Ca^{2+} concentrations (Bergey, et al., 2014). Calmodulin could modulate the MAPK signaling pathway (Tebar, Lladó and Enrich, 2002) and this defines their interplay probability in regulating heavy metal stress responses (Jalmi, et al., 2018). Calcium/calmodulin is involved in the reaction due to toxicity mediated by heavy metals such as Pb, Ni and Cd (Ahmad, Hadi and Ali, 2015). In this study, calmodulin (*CAL*) expression was upregulated in *P. stratiotes* roots exposed to Pb, which could indicate an increase in binding of Ca^{2+} in roots (Table 4.9).

The upregulated DEGs were also enriched in the Ras signalling pathway. Ras-related proteins play key roles in detoxifying, transporting, and

compartmentalizing heavy metals in vacuoles (Goodwin and Sutter, 2009). Rho-like GTPases from Plants (ROPs) are functional analogs of mammalian Ras GTPases (Vernoud, et al., 2003) and play key roles in stress responses, cytoskeleton organization (Burridge and Wennerberg, 2004) and ROS signalling (Baxter-Burrell, et al., 2002). Ras-related GTP-binding proteins and a small G-protein that were responsive towards copper stress in *Elsholtzia splendens* root cell walls (Liu, et al., 2014). Ras were significantly enriched in seedlings supplemented with plant hormones under Cr(VI) stress (Mumtaz, et al., 2022). Pb stress induces oxidative stress, leading to the activation of ROP GTPases to regulate NADPH oxidase (RBOH)-mediated ROS production (Wong, et al., 2007), actin cytoskeleton reorganization and **c**ell wall remodelling (Feiguelman, Fu and Yalovsky, 2018).

Pb exposure may increase cAMP levels due to disturbances in Ca^{2+} influx, leading to compensatory signalling. Metals begin signalling cascades upon being perceived by receptors via changes in cAMP positioned downstream to ROS signal (Singh, et al., 2016b). A decrease in calcium content in Pb-exposed plants has been documented in various species, including maize, tomato and mustard (White and Broadley, 2003; Sharma and Dubey, 2005). This phenomenon may arise from the inhibition of calcium transporters by Pb ions (Wojas, et al., 2007) and/or the substitution of Ca^{2+} with Pb^{2+} due to Pb's strong affinity for calcium binding sites on biological structures (Habermann, et al., 1983). Besides, the elevation of cAMP levels is predominantly associated with the activation of adenylyl cyclases (ACs), which catalyse the conversion of ATP to cAMP (Yang, et al., 2021)**.** The increase

in cAMP can facilitate numerous downstream effects, including the modulation of ion channels and the activation of protein kinase A (PKA) (Beavo and Brunton, 2002).

Crosstalk among MAPK, Ras-like small GTPases, and cAMP signaling in plants functions distinctly compared to animals. There is a possibility of ROS and MAPK crosstalk, as oxidative stress can modulate cAMP-dependent pathways. cAMP can interact with cyclic nucleotide-gated ion channels (CNGCs), which play a role in the regulation of ion homeostasis during stress responses **(**Ordonez, et al., 2014; Lu, et al., 2016). cAMP targets Ca^{2+} flux, which is crucial for modulating Ca^{2+} signalling in plants (Xu, et al., 2021). Under Pb^{2+} stress, cAMP-dependent protein kinase (complex and regulator) activity was significantly affected in *Cladophora rupestris* (Liu, et al., 2022a). Besides, Pb may indirectly activate ROPs by altering Ca^{2+} signalling or through MAPK cascades, which are known to interact with ROP pathways (Enders, Frick and Strader, 2017). Li, Chen and Li (2023) demonstrate how ROP GTPases like OsRac1 integrate with MAPK signaling pathways to coordinate rice grain development processes. In addition, Pb stress also likely caused crosstalk between Ras and cAMP pathways as cAMP-dependent processes, such as PKA (Beavo and Brunton, 2002) could modulate ROP activity, forming a feedback loop. ROP GTPases may indirectly influence adenylate cyclase activity via regulation of calcium levels (Gu, et al., 2005), increasing cAMP.

In this study, downregulated DEGs under Pb stress were enriched in numerous pathways, including ribosome, oxidative phosphorylation, necroptosis, apoptosis and mineral absorption pathways. Pb stress can impede the normal function of plant root mitochondria and the generation of ATP through oxidative phosphorylation (Ghifari, Saha and Murcha, 2023). Numerous studies indicate that Pb stress can impair plant root oxidative phosphorylation, resulting in the downregulation of associated genes (Zhao, et al., 2024). The downregulation may lead to diminished ATP generation and elevated levels of ROS, thereby causing more damage to root cells and intensifying the stress response (Zhang, et al., 2017). The strong activation of MAPK cascades, calcium signaling and detoxification transporters under Pb stress alone (non-EAPR) indicates that *P. stratiotes* was in a high-stress defense mode. This led to an energy cost, which was supported by the downregulation of pathways for ribosome biogenesis and oxidative phosphorylation. The metabolic repression is consistent with the depletion of plant biomass and phytotoxicity. By disrupting oxidative phosphorylation, plants can alter their energy metabolism and potentially enhance their resistance to Pb stress. Similarly, it was found that Pb exposure in *Solanum lycopersicum* L. caused disordered oxidative phosphorylation and respiration (Irfan, Sermin and Kadir, 2010).

The downregulation of genes associated with necroptosis and apoptosis pathways, as observed in the KEGG analysis of *P. stratiotes* (Table 4.6). This may signify the plant's effort to inhibit unnecessary cell death and conserve energy for

survival, as excessive cell death can be detrimental to the plant (Petrov, et al., 2015). Alternatively, if these genes are repressed, it could imply that Pb toxicity is overwhelming normal programmed cell death pathways, resulting in uncontrolled necrosis instead. Besides, plants may prioritize other defense mechanisms, such as metal detoxification and sequestration over programmed cell death (Manara, 2012). In *Arabidopsis*, the overproduction of ROS triggered by biotic or abiotic stresses is shown to slow down the progression of cell death via the expression of Bax Inhibitor-1 (Watanabe and Lam, 2006).

Pb-induced oxidative stress elevates radical generation, resulting in damage to cell membranes, cellular processes (Ur Rahman, et al., 2024) and DNA (Khaliq, et al., 2021). The initial response to high Pb amount is the overproduction of ROS in the plant that causes the irreversible lipid oxidation (Yang, et al., 2020). Plant cells eventually may not be able to maintain themselves due to disruptions in metabolic pathways that may cause cell death (Sychta, Słomka and Kuta, 2021). Programmed cell death is a fundamental component of plant development and a crucial response to abiotic stressors or pathogens. It allows the exact termination of faulty cells (Chlubek and Baranowska-Bosiacka, 2024). Although ‘apoptosis' is yet to be justified in plants, two distinct classes of programmed cell death can be identified in plants: vacuolar cell death and necrosis (van Doorn, et al., 2011).

Necrosis is a category of rapid cellular death that occurs in response to pathogen invasion or abiotic stress (Minina, et al., 2013). Necrosis is usually caused by the overwhelming impact of external forces (Pb, UV radiation, and extreme temperatures) (Kanduc, et al., 2002; Renu, et al., 2021), which results in mechanical damage to the lipid bilayers of the cell membrane (Vanden Berghe, et al., 2006). On the other hand, apoptosis necessitates active engagement of expression of multiple genes, cellular machinery and expenditure of energy (Chlubek and Baranowska-Bosiacka, 2024). In this study, *P. stratiotes* exposure to HMs in synthetic young leachate under both EAPR and non-EAPR treatments displayed pigmentation, discoloration, yellowing and withering physical appearances. These phytotoxic symptoms suggest the onset of necrosis and apoptosis, triggered by severe oxidative stress and membrane damage from HM toxicity (Sychta, Słomka and Kuta, 2021).

On the other hand, it was observed that the downregulated DEGs under Pb stress were enriched in the mineral absorption pathway. Pb is shown to inhibit plant growth by reducing the uptake and movement of nutrients such as Ca, Mg and Zn. Hence, the entry or binding of the ions to ion-carriers is restricted, rendering them unavailable for transportation from roots to leaves (Munzuroglu and Geckil, 2002). Pb disrupts nutrient uptake via competition with essential minerals (e.g. Ca^{2+}, Fe^{2+}, Mg^{2+}, Zn^{2+}) for transporters (e.g. ZIP, IRT, NRAMP families) (Kim, Yang and Lee, 2002). The downregulation of mineral absorption genes suggests an avoidance strategy by *P. stratiotes* to reduce the non-essential metal uptake to

prevent Pb entry (Mehes-Smith, Nkongolo and Cholew, 2013). Additionally, Pb may directly inhibit transporter expression or function through toxicity-induced repression. The elimination of the analogous *Arabidopsis CNGC1* gene (cyclic nucleotide-gated ion channel) conferred tolerance to lead toxicity. *NtCBP4* and *AtCNGC1* are essential components of a transport pathway that facilitates the entry of Pb^{2+} into plant cells (Sunkar, et al., 2000). Hence, the disruption of these genes may serve as a significant strategy for enhancing HM stress tolerance in plants by restricting the absorption of these heavy metals within the cells. Plants may perform energy reallocation to suspend non-essential processes, such as nutrient absorption, to prioritize detoxifying mechanisms, including phytochelatins and antioxidants (Noor, et al., 2022).

5.7.5.3 KEGG Enrichment Analyses of Leaf Samples for EAPR versus non-EAPR (Effects of EAPR)

Under EAPR treatment, it was found that the upregulated DEGs were significantly enriched ribosome, secondary metabolite biosynthesis, metabolic pathways, amino acid biosynthesis, arginine biosynthesis and carbon metabolism pathways (Table 4.7). Electrical signalling regulates biochemical processes (such as the synthesis of hormones, proteins and secondary metabolites) and gene expression of enzymes (related to ribosome proteins and carbon metabolism) in plants (Li, Gou and Li, 2019). The upregulation of the ribosomal pathway in plant leaves, in response to an electric field, likely indicates an enhanced ability for

protein synthesis to facilitate cellular repair, stress responses and possibly growth stimulation. Electric fields may enhance translational activity to meet the demand for new proteins involved in stress adaptation or signalling.

Upregulation of genes related to secondary metabolite biosynthesis in *P. stratiotes* leaves after EAPR treatment indicates an increased production of these compounds, often in response to environmental stressors or developmental cues (Liu, et al., 2022b). Secondary metabolites, such as phenolics, flavonoids and alkaloids are crucial for stress defense and antioxidant production (Ranner, et al., 2023). An electric field may act as an elicitor, triggering defense mechanisms and boosting the synthesis of protective compounds. Gene regulation of plant secondary metabolism typically involves the assembly of multiprotein complexes through combinatorial interactions between the MYB and bHLH protein families, or among distinct subgroups of bHLH proteins (Chezem and Clay, 2016). In addition, histone modifications, such as acetylation, methylation and phosphorylation, serve as essential components in the epigenetic regulation of secondary metabolite synthesis in plants. Most plants exhibit active transcription by enhancing histone acetylation, decreasing chromatin compactness, and facilitating the binding of transcription factors to regulatory areas of genes essential for secondary metabolite biosynthesis (Peng, et al., 2020; Zhao, et al., 2022).

EAPR might upregulate the genes related to metabolic and carbon metabolism pathways (Table 4.7). The use of electric fields mitigates the Pb stress-induced state, leading to an increase in their activity. The upregulation reflects shifts in energy demand as Pb disrupts mitochondrial function (Chlubek and Baranowska-Bosiacka, 2024), forcing the use of alternative metabolic routes. Electric field may enhance ATP production via stimulation of electron transport (Ahmad, Wolberg and Kahwaji, 2023). Wang, et al. (2022)'s study showed that pulsed electric fields can affect photosynthesis in lettuce leaves, with some evidence suggesting increased ATP generation due to enhanced electron transfer. The cytochrome b6f complex (Simkin, et al., 2017), ferredoxin-$NADP^+$ reductase (Hajirezaei, et al., 2002) and the proton gradient across the thylakoid membrane (Yamori and Shikanai, 2016) are essential elements of photosynthetic electron transport and ATP production that may be influenced by electrical stimulation. The enhanced synthesis of NADPH and ATP during the light reactions provides additional reducing power and energy for the Calvin cycle. Consequently, improved electron transport can result in heightened carbon fixation and total carbon metabolism in the plant (Dusenge, Duarte and Way, 2019), which may further enhance plant tolerance to toxic compounds.

Electric field might potentially enhance the biosynthesis of amino acids, including arginine biosynthesis pathways, in *P. stratiotes* leaves. This is because electric fields can influence various metabolic pathways, including those related to amino acid synthesis (Cadena-Ramírez, Alonso-Vargas, and Cesar-Ríos-Guzmán,

2024). Amino acids are essential building blocks for proteins and play crucial roles in plant growth, development, and responses to stress, such as Pb toxicity (Hildebrandt, et al., 2015). Electric fields can function as an abiotic elicitor, a stress factor that stimulates the synthesis of certain chemicals associated with plant stress response (Jan, et al., 2021). Enrichment of the arginine biosynthesis pathway enables *P. stratiotes* to produce vital signaling chemicals in its defensive responses. This pathway is required for nitrogen metabolism, polyamine synthesis, and the formation of nitric oxide (Winter, et al., 2015). Arginine is a crucial amino acid that participates in numerous metabolic processes, encompassing nitrogen metabolism and stress responses (Cheng, et al., 2023). Abiotic stress, such as Pb exposure, can adversely affect the arginine biosynthesis pathway. The biosynthesis of arginine entails the transformation of ornithine into citrulline and subsequently into arginine, facilitated by specialized enzymes such as ornithine transcarbamoylase, argininosuccinate synthetase and argininosuccinate lyase (Llebrés, et al., 2018).

Hence, electric fields may enhance the activity of these enzymes or alter the availability of precursors, thereby facilitating the production of arginine. EAPR may also affect the activity of enzymes associated with these pathways, either directly or indirectly by altering cellular ion concentrations or membrane potential (Xu, et al., 2016). Electric fields may help plants manage Pb stress by promoting the synthesis of compounds that detoxify Pb or mitigate its detrimental effects (Moradbeygi, et al., 2020).

5.7.5.4 KEGG Enrichment Analyses of Leaf Samples for non-EAPR versus control (Effects of Pb)

Under Pb stress, plant leaves frequently exhibit activation of genes associated with the ribosomal pathway (Meng, et al., 2018), signifying a response to the stress and possible participation in tolerance mechanisms. This increase may entail alterations in ribosomal protein gene expression, influencing ribosome production and perhaps affecting translational efficiency (Stępiński, 2025), to compensate for the adverse effects of Pb. Certain studies indicate that ribosomal proteins may include extra ribosomal roles, including participation in signal transduction pathways under stress conditions (Kwasniak-Owczarek, et al., 2019). The plant nucleolus, responsible for ribosome assembly, may function as a stress sensor, with alterations in ribosome biogenesis potentially contributing to the plant's response to many stresses (Ohbayashi and Sugiyama, 2018), including those associated with Pb.

Upregulation of genes related to plant hormone signal transduction in *P. stratiotes* leaves in this study indicated that Pb might upregulate DEGs involved in plant hormone signal transduction (Table 4.8). In plants, a complex network of signaling pathways is orchestrated by hormones such as auxin, ABA, ethylene and JA, which are crucial for plant stress responses regulation (Gray, 2004). The upregulated DEGs enriched in terms such as plant hormone signal transduction pathways in this study suggested Pb stress might lead to modulation of hormonal

signaling to activate subsequent defensive mechanisms (Auguy, et al., 2016). This indicates that the plant produces a higher quantity of essential hormones and signaling molecules to manage stress (Ang, et al., 2024).

Besides, the upregulation of fatty acid elongation genes under Pb stress in this study indicated that plants might modify their lipid metabolism in response to Pb stress, as an attempt to enhance cell membranes, lipid barriers, or create signaling molecules (Singh, et al., 2016b; Sharma, et al., 2023b). Abiotic stressors, such as cold, salt, hypoxia, and exposure to HMs have been shown to raise the levels of very- long- chain fatty acids in many plant species (De Bigault Du Granrut and Cacas, 2016). The fatty acid elongation process incorporates two-carbon units into a fatty acid chain, hence increasing its length with enzymes such as KAS I and KAS II (Li, et al., 2017c). By enhancing the expression of genes associated with fatty acid elongation, transcription factors, such as PfbZIP85 in tobacco (Huang, et al., 2024), and WRI1 (Liu, et al., 2024) *in Akebia trifoliata*, can elevate the synthesis of longer-chain fatty acids (Ji, et al., 2018). Alterations in fatty acid composition and concentrations can influence the total oil content in plant tissues as an energy reserve for growth (Zhou, et al., 2024).

Under Pb stress, *P. stratiotes* leaves demonstrated greater downregulation (*-log padj* = 72.76) than upregulation (*-log padj* = 31.77) of genes associated with the ribosomal pathway. This indicates that the expression of genes related to

ribosome synthesis and function is diminished relative to normal conditions. This downregulation may serve as a physiological response to Pb stress, presumably aimed at conserving energy or modulating protein production in reaction to the stressor (Horiguchi, et al., 2012; Fakih, Plourde and Germain, 2023). Downregulation may transpire via multiple processes, such as diminished transcription of ribosome-associated genes, mRNA degradation or modified splicing efficiency (Petibon, et al., 2021). The downregulation of ribosomal genes can impact multiple cellular functions, including cell proliferation, division, and overall protein synthesis. This may also be associated with additional stress responses, such as nucleolar stress, which can potentially result in cell cycle arrest or other cellular alterations (Ohbayashi and Sugiyama, 2018). Besides, the genes associated with ribosome biogenesis, including those that encode ribosomal proteins (Moin, et al., 2016) might be downregulated in response to Pb stress.

The phenylpropanoid biosynthesis pathway initiates the production of many secondary metabolites, such as flavonoids, stilbenoids and diarylheptanoids. The downregulation of this biosynthesis pathway in *P. stratiotes* was observed in this study. The downregulation of this pathway markedly affects the synthesis of certain beneficial compounds (Liu, et al., 2021b). Both flavonoids (Wan, et al., 2025) and stilbenoids (Deng, et al., 2017) are significant phenolic antioxidants in plants, aiding in their defense against diverse stressors. Their downregulation during Pb stress signifies a diminished ability of the plant to counteract oxidative stress (Bian, et al., 2020). Diarylheptanoids are a class of secondary metabolites

exhibiting a variety of biological roles, including antibacterial properties (Jahng and Park, 2018). Their reduced output under Pb stress indicates a disturbance in the plant's defence mechanisms. Other than that, alpha-linolenic acid and linoleic acid are fatty acids that are essential constituents of cell membranes and contribute to stress responses (Li, et al., 2016). Their downregulated metabolism under Pb stress may compromise membrane integrity and influence further cellular processes.

5.7.6 Key Genes in *P. stratiotes* Adaptation under Combined Electrochemical Stress Revealed by EAPR

The transcriptomic analysis in this study shows the intersection response mechanisms of *P. stratiotes* within an EAPR system for synthetic leachate treatment. The most significant observation is that EAPR reverses the gene expression trends induced by Pb stress in plant roots, further underscoring the central role of key signaling pathway. This discovery provides fundamental new insights into plants' molecular defence responses under the combined electrochemical stress. Ten genes investigated were those reversed by EAPR, particularly key regulators (not effectors), namely MAPK, hormone signaling, and metal homeostasis within the stress-signaling networks (Table 4.9).

Cluster 3093.0 (a MAPK kinase) is a prominent candidate for EAPR-reversal. MAPK kinases are crucial signaling modules that amplify important abiotic stress signals in plants. They rely on upstream ROS and Ca^{2+} signals to transcription factors, such as WRKY and bZIP (Jarin, et al., 2025). The expression of this gene in response to Pb stress is consistent with prior studies that showed heavy metals activate MAPK cascades to control antioxidant and detoxification mechanisms (Li, et al., 2022; Ur Rahman, et al., 2024). The concurrent downregulation of this MAPKK under EAPR versus non-EAPR treatment suggests that the electric field disrupts the initial phase of Pb detection and signaling. Thus, further hinders the subsequent development of stress responses.

Likewise, NAP1-related protein 2 (Cluster-2906.0), which is involved in chromatin regulation and histone chaperoning to affect gene expression (Wang, et al., 2022), exhibits a comparable reversal pattern. NAP1-like proteins might stabilize MAPK complexes and regulate the duration of signal transduction (Kim, et al., 2022). Hence, their suppression suggests that EAPR may not soley reduces MAPK activation, but also disrupts the structural organization of the MAPK module (Wu and Wang, 2024). This potentially destabilize the the Pb-induced phosphorylation mechanism. Therefore, EAPR is suggested to act as a signal-dampening agent, subsequently inhibiting the stress cascade before the complete establishment of transcriptional reprogramming.

The 14-3-3 protein (Cluster-18765.0) and the heterotrimeric G-protein α subunit (Cluster-12402.0) constitute the second tier of EAPR-reversed hubs. These proteins are vital signal integrators, connecting the MAPK activity (Bhardwaj, et al., 2025) with hormonal and oxidative responses (Sewelam, Kazan and Schenk, 2016). In plant, the 14-3-3 proteins regulate phosphorylation-dependent interactions between MAPKs and transcription factors, further influencing ABA, ethylene and ROS-mediated gene expression (Camoni, et al., 2018). As a result, the downregulation of this 14-3-3 protein following EAPR treatment indicates broader extensive suppression of stress-hormone communication pathways.

The G-protein α subunit also regulates initial oxidative bursts and Ca^{2+} influx when exposed to metal stress (Wang and Botella, 2022). Its reversal under EAPR versus non-EAPR treatment implies that electric field might modulate the signal transduction at plasma membrane, thereby inhibiting the activation of ROS-dependent defense signaling. This discovery indicates that instead of activating detoxification pathways to cope with Pb exposure, EAPR diminishes the need for these responses by inhibiting their upstream initiators.

EAPR treatment partially reverted these Pb-induced transcriptional patterns. The downregulation of MAPKKs, 14-3-3 proteins and G-protein α subunits indicates a reduction of the ROS-dependent signaling. Reduction of these stress-amplifying hubs reduces the need for excessive detoxification mechanisms. This is consistent with observed enhanced HM removal (Figure 4.7) and elevated BCF values (Figure 4.6) for specific metals. Hence, electrochemical reaction in EAPR simultaneously promotes the mobilization of HMs in the rhizosphere and mitigates intracellular stress.

Heavy-metal stress generally triggers the expression of detoxification enzymes and transporters that alleviate metal toxicity (Mohamed, et al., 2025). In this study, ABC-F transporter (Cluster-32326.0) and a glutathione transferase–like protein (Cluster-11998.0) are significantly upregulated by Pb exposure, yet downregulated following EAPR treatment. ABC transporters are knowm to function in HM sequestration and vacuolar compartmentalization (Marques and Mason, 2025). Conversely, glutathione transferases control cellular redox balance via conjugation of the reactive metabolites (Morgenstern, 2024). The observed downregulation of these proteins in response to EAPR suggests that this treatment reduces intracellular Pb accumulation and oxidative damage, hence lessening the requirement for intense detoxification processes.

Besides, the identification of other EAPR-reversed genes, such as redox-responsive regulatory proteins (Cluster-17353.0) and membrane or cell-wall associated stress proteins (Cluster-15275.0), further supports this interpretation. These genes function in mediating ion transport, ROS signaling and structural defense modifications in response to heavy metal stress (Sandalio, et al., 2023). Their suppression implies that EAPR could be restoring cellular homeostasis, in an attempt to shift the root transcriptome away from a defense-dominated state toward a maintenance-dominated state.

Collectively, the transcriptional reversal of these ten regulatory hubs demonstrates that EAPR's protective effect operates at the systems level of stress perception, signal integration and response execution. Pb stress alone initiates a cascade that begins with MAPKK and scaffold proteins, subsequently involving hormone and ROS signaling integrators, eventually resulting in detoxification and metabolic reprogramming. Under EAPR versus non-EAPR treatment, this entire cascade is suppressed, indicating that EAPR acts as a transcriptional and signaling "switch-off" mechanism, rather than a simple detoxification enhancer. The suppression of MAPK, Ras and cAMP signaling pathways in roots under EAPR suggests that the electric field alleviated Pb-induced stress at the signaling level (Bigeard and Hirt, 2018; Keyster, et al., 2020). This molecular dampening corresponds to the observed reduction in oxidative stress burden, as reflected in lower antioxidative enzyme activity (SOD and APX) compared to the non-EAPR system.

This systemic repression is noteworthy because it suggests that EAPR mitigates excessive activation of energy-demanding stress pathways. If unchecked, could hinder root development and metabolic equilibrium. Consequently, even in the presence of Pb, EAPR appears to enable *P. stratiotes* to sustain more stable physiological processes while concurrently increasing HM mobilization via electrochemical processes. The transcriptomic results suggest that EAPR reprogrammes the stress-signalling network to reduce the energetic cost of detoxification, possibly by silencing MAPK-mediated stress signalling, restoring redox and hormonal homeostasis. This integrated physiological–molecular response explains the observed enhancement in phytoremediation performance under the EAPR system.

5.7.7 Upregulation of Genes Involved in MAPK Signaling Pathway in Plants under Pb stress

In this study, there are three cascades in which the upregulation of genes involved in the MAPK signalling pathway (Appendix 15) under Pb stress were identified using RNA-Seq in *P. stratiotes* roots (Appendix 16). The three cascades are MKK3-MPK6, MEKK1-MKK2-MPK4/6 and MKK1-MPK6. According to Kumar, Raina and Sultan (2020), the MAPK signalling pathways' three kinases are activated via sequential phosphorylation. The primary function of the MAPK signalling pathway is to phosphorylate associated transcriptional factors. The subsequent binding of transcriptional factors to cis-regulatory regions can then

trigger the expression of metal response genes. Along the biosynthesis path, a small gene family encodes each tier of the MAPK cascade, and several members of the gene family may perform redundant functions (Zhang and Zhang, 2022).

The activation of such cascades often leads to the phosphorylation of downstream targets, thereby influencing gene expression and various cellular processes associated with stress responses. Numerous studies have documented the symptoms and responses of plants to exposure to toxic metals (Clemens, 2006). The activation or modification of plant metabolism is essential for the effective functioning of metabolic pathways and the rapid repair of damaged cellular structures (Chandra and Kang, 2015).

In the MKK3-MPK6 cascade, 4 DEGs for MKK3 and 8 DEGs for MPK6 were upregulated. MKK3-MPK6, constituents of the MAPK signaling pathway, are essential in plant stress responses. MKK3, a MAPK kinase, phosphorylates and activates MPK6, a MAPK. The activation of MPK6 by MKK3 leads to the phosphorylation of downstream targets. Takahashi, et al. (2007) reported that JA acid activated MPK6, which was primarily dependent on the MKK3 pathway in *Arabidopsis thaliana*. This cascade inhibits root growth and is involved in the negative regulation of ATMYC2/JIN1 expression, which is a central positive regulator of JA-inducible gene expression. Hence, the MKK3–MPK6 cascade is pivotal in the JA signaling pathway of *P. stratiotes* to mediate Pb stress. Identifying

and characterizing stress- responsive genes is essential for enhancing plant tolerance to stress. Recent advancements across multiple fields have enabled the identification of metabolites, transcription factors and stress- inducible proteins associated with HM tolerance (Singh, et al., 2016b). Consequently, this study examines the function of MKK3-MPK6 in lead stress response is crucial for elucidating the molecular processes that govern plant tolerance to Pb.

The second cascade of MAPK signaling pathway, MEKK1-MKK2-MPK4/6 was also upregulated under Pb, in which 24 (MEKK1), 12 (MKK2) and 1 (MPK4)/8 (MPK6) DEGs were identified. The MEKK1-MKK2-MPK6 cascade represents a well- characterized MAPK pathway in *Arabidopsis thaliana*, a model plant extensively employed in plant stress physiology research (Kumar, Raina and Sultan, 2020). The upregulation of MEKK1, MKK2 and MPK6 under lead exposure suggests a critical role for this specific MAPK cascade in mediating Pb stress responses in plants. MEKK1, a MAPKKK, functions as a primary sensor and transducer of stress signals, integrating upstream cues and relaying them to downstream components of the MAPK cascade (Virk, et al., 2015). Upon activation by lead-induced stress signals, MEKK1 phosphorylates and activates MKK2, a MAPKK, which in turn phosphorylates and activates MPK6, a MAPK (He, et al., 2020). The activation of MPK6 triggers a cascade of downstream events, including the phosphorylation of transcription factors involved in stress-responsive gene expression. The induction of stress-responsive genes, such as those encoding detoxification enzymes, metal transporters, and antioxidant proteins, facilitates the

alleviation of lead toxicity and the restoration of cellular homeostasis (Haak, et al., 2017). Thus, this study showed that the upregulation of MEKK1, MKK2 and MPK6 under Pb exposure and it might involve a combination of transcriptional and post-translational regulatory mechanisms. Activation of transcription factors initiates the transcription of defense genes (He, et al., 2023).

Last but not least, MKK1-MPK6 cascade was upregulated by one (MKK1) and eight (MPK6) DEGs, respectively. MKK1-MPK6 modules mediate the ABA signal transduction to mitigate the toxicity and accumulation of metalloids and HMs (Hu, et al., 2020). AtMKK1 and AtMPK6 play crucial roles in regulating seed germination in *Arabidopsis* through ABA- and sugar-related seed signaling pathways. *P. stratiotes* likely employs this pathway, which Pb triggers to mitigate the toxic effects. Under Pb stress, plants perceive the stress and initiate ABA biosynthesis. ABA is perceived by PYR/PYL/RCAR receptors, which then inhibit PP2C phosphatases, leading to the activation of SnRK2 kinases (Fidler, et al., 2022). The SnRK2 kinases can phosphorylate and activate various downstream targets, including transcription factors and other kinases. Ultimately, this leads to the regulation of gene expression and other cellular processes that enable the plant to cope with stress. In the context of Pb stress, the MKK1-MPK6 cascade is activated, possibly through upstream MAPKKKs that are responsive to ABA or oxidative stress signals (Fàbregas, Yoshida and Fernie, 2020). Pb stress may alter cell wall composition (Ronzan, et al., 2018), limiting Pb uptake and the MKK1-MPK6 pathway may be involved in controlling these changes.

The MKK3-MPK6, MEKK1-MKK2-MPK4/6, and MKK1-MPK6 cascades are crucial yet unique in their functions in mediating Pb stress responses in *P. stratiotes*. MKK3-MPK6 is primarily associated with JA signaling, regulating stress-responsive genes, inhibiting root growth, and modulating JA-dependent defense mechanisms. Other than that, MEKK1-MKK2-MPK4/6 functions as a pivotal stress-signaling hub, assimilating Pb-induced signals to activate downstream transcription factors and genes associated with detoxification, hence augmenting metal tolerance. MKK1-MPK6 is associated with ABA signaling, affecting seed germination, cell wall alterations, and oxidative stress reduction in response to Pb exposure. Collectively, these MAPK pathways orchestrate hormonal signaling, transcriptional reprogramming and cellular detoxification, allowing *P. stratiotes* to mitigate Pb toxicity and sustain homeostasis. Comprehending their interaction yields insights into plant adaptation to heavy metal stress, presenting prospective targets for enhancing phytoremediation and stress tolerance.

5.7.8 Expression testing of DEGs by Quantitative Real-time (qRT)-PCR

Plants possess sophisticated defence mechanisms against HMs (Clemens, 2006). The most straightforward tactic is to avoid metal from entering shoots by preventing or excluding metal uptake. Basal HM tolerance in plants consists of uptake/efflux, transport/sequestration and chelation processes. Hence, plants can be divided into (hyper)accumulator and non-accumulator groups (Viehweger, 2014)

when they are used as tools to remove contaminants. Besides, plants have developed signalling systems as an effort to control and react appropriately to full stresses (Keyster, et al., 2020). This includes signal molecules, such as ROS, nitric oxide and plant hormones that can trigger the MAPK cascade via DEGs, antioxidant mechanisms and synergistic crosstalk that occurs between numerous signalling systems.

The activation of the MAPK cascade by these signaling molecules involves a complex interplay of upstream components, ultimately leading to the phosphorylation and activation of downstream transcription factors that modulate gene expression (Ahmad, et al., 2016). Similarly, in this study, MAPK pathway was upregulated in response to Pb. The stress responses, cell cycle, differentiation, growth and death are known to be regulated by conserved MAPK signalling pathways (Li, et al., 2022). Three protein kinases make up the three-phase MAPK cascade: MAPK kinase kinase (MAPKKK), MAPK kinase (MAPKK) and MAPK (Ma, et al., 2022). MAPK in plants under stress circumstances may select and modulate transcription factors (Andreasson and Ellis, 2010) to elicit a multitude of cellular, transcriptomic and physiological responses (Šamajová, et al., 2013).

Thus, six genes were chosen from the most significantly enriched MAPK signaling pathway- plant (ko04016) due to Pb stress to study their expression using qRT-PCR (Figure 4.22). qRT-PCR and RNA-seq results (Appendix 17) showed

that all six selected genes from the MAPK signalling pathway- plant (ko04016) were upregulated in response to both non-EAPR and EAPR treatments. The genes for calcium-binding protein NCS-1-like (CAL), GTP-binding protein rhoA-like (GT) and Guanine nucleotide-binding protein subunit beta-like (GUA) were expressed, with significant differences observed between EAPR and non-EAPR, which implies the effect of EAPR treatment. However, the expression among the genes for Calmodulin (CA), Calmodulin 5 (CA5) and Rab5b rab family GTPase (RAB) was not significantly different.

The plant's adaptive response to Pb may lead to alterations in the expression of calcium-binding proteins such as CAL (Kour, et al., 2023). Under Pb stress, EAPR can increase ion mobility (Cameselle, et al., 2013) and further enhance expression of calcium-dependent signalling pathways and upregulate CAL gene expression. Additionally, EAPR may also reduce Pb-induced oxidative stress, thereby indirectly stabilizing calcium signalling and enhancing CAL expression. The stability of Ca^{2+} channels happens during the exposure to excess HMs, resulting in the flow of calcium into the cell. A temporal increase in the cytosolic calcium level is recognized by sensitive proteins, which cause the alteration of this chemical signal into biological responses. Intracellular free Ca^{2+} serves as a second messenger to convey stress reactions triggered by HMs, which in turn regulate the expression of downstream genes involved in HM metabolism, tolerance and transportation (Hasanzadeh and Hazrati, 2021). Via competing with Ca^{2+} for binding sites or altering calcium channel activity, Pb can disturb calcium

homeostasis. EAPR might mitigates Pb stress by enhancing calcium ion mobility, stabilizing calcium signalling pathways, and upregulating CAL gene expression, thereby counteracting Pb-induced disruptions in calcium homeostasis.

Pb stress can induce oxidative stress and mechanical damage (Gupta, et al., 2024), leading to changes in cytoskeletal dynamics (Horiunova, et al., 2016). It may result in altered expression of GT proteins, helping the plant cope with Pb-induced damage. GT proteins, such as RhoA-like GTPases, regulate cytoskeletal organization, vesicular trafficking and stress signalling in plants (Nagawa, Xu and Yang, 2010). The electric field may induce mechanical stress, leading to the activation of GT genes (Lessey, Guilluy and Burridge, 2012) to maintain cellular structure and function. Proteins implicated in HM responses have been identified in *Camelina sativa* seeds, suggesting a role for the *Gγ* gene (AGG3) in HM tolerance (Wu and Urano, 2018). Thus, the electric field (EAPR) might reduce Pb-induced stress and enhance GTP-binding protein-mediated signalling.

Guanine nucleotide-binding protein (G-protein) plays a crucial role as one of the primary signalling molecules that transmits environmental cues to the interior of the plant. They consist of α-, β-, and γ-subunits, which are modulated by the nucleotide-binding status. Activation or inactivation of the complex happens through the GTP/GDP binding mechanism (Oliveira, et al., 2022). These signalling cascades are activated to trigger appropriate responses to multiple abiotic stresses,

including HM toxicity (Wang and Botella, 2022). G-protein signalling can lead to the activation of pathways, such as ROS burst (Tuteja and Sopory, 2008), stress-responsive kinases (Bhardwaj, et al., 2025) and cell death (Karimian, Trusov and Botella, 2024). EAPR alleviates stress and interfaces with G-proteins via depolarization or hyperpolarization (Hagenfeld, et al., 2010) which triggers the opening of voltage-gated calcium ion (Ca^{2+}) channels in the plasma membrane (Berridge, Bootman and Roderick, 2003). This leads to a rapid, controlled influx of Ca^{2+} into the cytoplasm that modulates G-protein activity or activation of specific proteins like Calcium-Dependent Protein Kinases (CDPKs) (Bredow and Monaghan, 2019).

Although the expression of calmodulin (CA), calmodulin 5 (CA5) and Rab5b rab family GTPase (RAB) genes was insignificant between EAPR and non-EAPR, the expression of these genes was significantly higher in the EAPR than in the control. This implies that EAPR might influence the expression of these genes. Calmodulin is a calcium-binding messenger protein that plays a critical role in calcium signalling pathways (Kasri, et al., 2004). Calmodulin regulates downstream stress-responsive genes (Liu, Qiao and Liao, 2025) and antioxidant enzyme activities (Forman and Zhang, 2021). Pb exposure exacerbates oxidative stress by increasing the formation of ROS in plants (Sinha, Srivastava and Mishra, 1998). This further disrupts calcium homeostasis (Shabbir, et al., 2022), as Pb can mimic Ca^{2+} (Wojas, et al., 2007) and interfere with Ca^{2+}-dependent signalling pathways.

To counteract this, under the influence of an electric field, *P. stratiotes* might upregulate calmodulin and its isoforms, such as CA5, in an attempt to reinstate calcium signalling and sustain cellular functions. The CA gene expression is upregulated to maintain Ca^{2+} buffering and signalling. The electric field amplifies ROS and Ca^{2+} spikes, which activate stress-responsive transcription factors (TFs) (Haberkorn, et al., 2021), subsequently phosphorylated by Ca^{2+}-dependent protein kinases (CDPKs) (Kawamoto, et al., 2015), further possibly increasing CA5 transcription. This study demonstrates that EAPR enhances the expression of Ca^{2+}-binding proteins in response to Pb stress. Pb stress alone elevates CA and CA5, but EAPR amplifies this response by augmenting Ca^{2+} and ROS signalling.

Rab5b is a member of the Rab family of small GTPases, which are involved in vesicle trafficking and endocytosis (Parray, 2025). Rab5b upregulation may subsequently facilitate the sequestration of Pb^{2+} (Keyster, et al., 2020) and mitigate its toxic effects. While there is limited specific research on Pb-induced Rab5b upregulation in plants, studies on vesicle trafficking and HM stress support this mechanism (Singh, et al., 2016b). An external electric field modifies the transmembrane potential of root cells, affecting ion fluxes (e.g. Ca^{2+}, H^{+}, K^{+}) (Zuo, et al., 2025). ROS act as secondary messengers, activating transcription factors, such as WRKY (Wang, et al., 2023), which bind to Rab5 promoters, thereby enhancing their expression (Li, et al., 2021). Electric fields influence auxin (IAA) and JA distribution (Saniewski, Ueda and Miyamoto, 2002; Lee and Oh, 2025), both of which regulate Rab GTPases. Pb stress disrupts auxin transport

(Małkowski, et al., 2020), but an electric field may restore polar IAA (Kral, Hanna Ougolnikova and Sena, 2016) and JA flow indirectly upregulating Rab5 to repair vesicular trafficking (Lu, et al., 2024).

The RNA-seq analysis pointed to the potential involvement of these specific genes. Hence, the high expression levels of these genes, as determined by RNA-seq, strongly supported the qRT-PCR analysis.

5.8 Future studies

The study's results demonstrated that EAPR may improve the ability of *P. stratiotes* to remove HMs, including Pb, from contaminated environments, while also elucidating essential molecular responses, which include MAPK signaling pathways that govern stress responses. The following are research directions that can be prioritized in future:

1. Technological optimization

   Variation in the electrode configuration, intensity and duration of electric current could display different patterns of HM mobilization, providing optimal intensity to balance maximum HM removal and minimum plant damage. This may not have been fully observed with the constant 2 V applied in this 7-day study.

2. Field performance

EAPR can be evaluated in field-scale applications to test for scalability and efficiency. In the real-leachate-contaminated environments, challenges such as fluctuating pH, temperature, competing ions and organic matter may influence the EAPR treatment efficiency.

3. Comparative phytoremediation

To optimize contaminant-specific remediation strategies, comparative studies should evaluate *P. stratiotes* alongside other hyperaccumulator species under EAPR conditions. Such investigations would enable identification of the most effective plant species for various contaminant types and the concurrent assessment of their synergistic interactions with EAPR. Comparing phytoremediation performance with and without EAPR application across different plant species is essential for quantitatively determining the enhancement effects of EAPR on metal uptake and removal efficiency.

4. Molecular Mechanisms

MAPK signaling pathways (MKK3-MPK6, MEKK1-MKK2-MPK4/6, MKK1-MPK6) in Pb stress responses can be validated via functional studies, such as gene knockout or overexpression. Such functional characterization would precisely delineate each cascade's contribution to Pb detoxification mechanisms and the stress signaling networks involved. To elucidate the molecular mechanisms underlying plant stress responses, future studies should investigate the crosstalk between MAPK signaling

pathways and phytohormonal networks, particularly JA and ABA under combined Pb stress and EAPR treatment. This exploration would provide crucial mechanistic insights into how electric field stimulation modulates stress signaling pathways. Furthermore, an integrated multi-omics approach combining RNA-seq with proteomic and metabolomic analyses could systematically identify the key regulatory proteins and metabolic biomarkers associated with Pb detoxification and EAPR-enhanced tolerance.

5. Transporter genes

To enhance the understanding of metal transport and localization, studies on the transporter genes, such as HMAs and NRAMPs that function in root-to-shoot metal translocation and their regulation under EAPR treatment can be done. Such insights might enhance phytoremediation efforts by focusing on specific transport channels to increase metal exclusion or accumulation.

6. Role of root-zone microbes

Furthermore, high-throughput sequencing, such as 6S rRNA should be employed to evaluate microbial-plant interactions under EAPR. This allows the assessment of its impact on rhizosphere microbiome function and composition, particularly concerning metal mobilization or immobilization processes.

The future directions above may enhance EAPR-assisted phytoremediation, elucidate molecular pathways and enable practical implementation for HM remediation.

CHAPTER 6

CONCLUSION

In this study, EAPR was implemented as an additional strategy to enhance phytoremediation performance in synthetic young leachate. Nevertheless, statistical analysis showed that types of treatment setup did not significantly affaect HM removal efficiency. In this study, EAPR was applied to overcome the limitations of the sole phytoremediation method, which is ineffective, particularly in the remediation of synthetic young leachate. The level of BOD, colour and turbidity of synthetic young leachate were significantly reduced in the EAPR system as compared to the control. The percentage reductions in BOD, color and turbidity for the EAPR-treated samples compared to the control were 69.35%, 43.75% and 68.10%, respectively. This suggests that EAPR is effective in treating synthetic leachate.

Plants cultivated under both EAPR (31.85%) and non-EAPR (28.56%) treatments, respectively, exhibited a more significant decrease in total biomass relative to the control (4.97%) ($p < 0.05$). However, a comparison between EAPR and non-EAPR treatments showed that there was no significant difference in the percentage drop in total biomass**,** total chlorophyll and chlorophyll a/b ratio ($p > 0.05$). EAPR appears to support the continued physiological functioning of *P.*

stratiotes under toxic conditions, rather than negatively affecting plant growth. Compared with the non-EAPR treatment, EAPR may extend plant survival and sustain phytoremediation activity.

Based on two-way ANOVA analysis, metals were the main effect on BCF leaf, BCF root, TF and removal efficiencies. An obvious root-mediated accumulation of HMs in *P. stratiotes* by elevated bioconcentration factor (BCF) values in roots (> 1000) relative to leaves (< 300) for Mn, Cd, Fe, Ni, Pb and Zn. This suggests that the root system functions as the main reservoir for HM sequestration, restricting translocation to aerial tissues. Although EAPR treatment marginally increased root BCFs, the treatments were not the primary factor affecting the BCF root, indicating that electro-assisted treatment can enhance the bioavailability of HMs to plant roots. However, the absorption ability of a plant is dependent on the kind of species of aquatic plant that is used in the studies. In leaves, only Mn, Pb and Zn exhibited elevated BCFs in non-EAPR plants, with Zn displaying a notable decrease under EAPR, suggesting that the electric field may modify metal distribution patterns in leaves.

Moreover, TF values for all HMs remained under 1, highlighting that *P. stratiotes* mostly sequesters them in its roots rather than transferring them to its leaves. Pb and Fe exhibited the highest removal efficiency, underscoring the plant's pronounced affinity for these metals in phytoremediation applications. The notably

low TF values, coupled with insignificant differences between EAPR and non-EAPR treatments, indicate that metal immobilization in roots is a critical detoxifying mechanism in *P. stratiotes*. These data underline the plant's potential for rhizofiltration, especially for Pb and Fe.

P. stratiotes adapted to HM stress by relatively upregulated SOD, APX and GR activities in the leaves of EAPR, highlighting its function in ROS scavenging. Besides, POX activity in the leaves and roots of EAPR and non-EAPR, respectively, were relatively higher than SOD, APX and GR. This tissue-specific antioxidant regulation indicates that leaves could be the principal site for electro-stimulated detoxification, whereas roots may depend on different defensive mechanisms. These findings offer essential insights into redox homeostasis during electro-assisted phytoremediation, emphasizing SOD as a pivotal enzymatic factor in alleviating HM-induced oxidative damage.

RNA-Seq demonstrated unique transcriptional responses to non-EAPR (Pb stress) and EAPR treatment in *P. stratiotes*. In this study, high-quality transcriptome sequencing and uniform GC content for the control, non-EAPR and EAPR samples were obtained. Pb stress elevated DEGs in roots but downregulated leaf DEGs, whereas EAPR reversed this pattern. GO enrichment analyses revealed that Pb stress mostly upregulated DEGs associated with transport, signal transduction, membrane dynamics and GTPase/kinase functions terms, while

concurrently downregulating ribosomal genes related to assembly, translation and structural roles, indicating impaired protein synthesis. In contrast, EAPR downregulated the Pb-induced terms, including transport, signal transduction, membrane dynamics, and GTPase/kinase-related functions, suggesting that EAPR mitigates Pb toxicity by restoring cellular homeostasis and reducing stress-responsive signalling. EAPR treatment concurrently upregulated ribosome-related terms—indicating a potential shift towards repair processes.

EAPR-treated leaves exhibited an enhancement in additional terms related to metabolic (cellular nitrogen compounds, oxidoreductase activity) and post-transcriptional (RNA binding) activities, indicating involvement in redox regulation and RNA metabolism. Whereas, only additional hydrolase activity targeting glycosyl bonds was enriched with downregulated genes. Under Pb stress alone, both upregulated and downregulated DEGs were predominantly enriched in identical terms. Downregulated DEGs were particularly enriched in enzyme regulatory activity and rRNA binding terms, indicating specific disturbances to enzymatic and ribosomal activities. These results collectively suggest that EAPR regulates Pb-induced stress by modifying ribosomal function and cellular homeostasis pathways.

KEGG enrichment analyses of leaf samples showed that EAPR treatment significantly upregulated metabolic pathways, including secondary metabolite

biosynthesis, amino acid biosynthesis and carbon metabolism, while downregulating the ribosome pathway, suggesting enhanced detoxification and energy metabolism alongside reduced protein synthesis. Pb stress predominantly downregulated metabolic pathways, including ribosome function, flavonoid/stilbenoid biosynthesis, and lipid metabolism, while upregulated ribosome, plant hormone signalling, and fatty acid elongation, indicating a disruption in secondary metabolism and protein synthesis alongside activation of stress-response signalling.

KEGG pathways of root samples subjected Pb stress revealed that upregulated DEGs were predominantly enriched in MAPK signalling-plant, Ras signalling and cAMP signalling pathways. Notably, DEGs downregulated by EAPR treatment were linked to similar pathways, suggesting regulatory interplay in response to Pb toxicity and its alleviation. The shortlisted ten genes reveal that EAPR suppresses the MAPK signaling core, hormone-ROS integrators and detoxification regulators that are activated by Pb stress, confirming that EAPR reverses Pb-induced transcriptional trends at the level of major signaling hubs. This provides strong molecular evidence that EAPR functions as a stress-network modulator, reshaping root responses to Pb toxicity and promoting physiological stability under adverse conditions. Subsequent RNA-Seq analysis identified three MAPK signalling cascades—MKK3-MPK6, MEKK1-MKK2-MPK4/6 and MKK1-MPK6 that were significantly upregulated in response to Pb stress. These cascades are crucial in regulating hormonal signalling, transcriptional

reprogramming and cellular detoxification, hence improving *P. stratiotes'* ability to mitigate Pb toxicity and maintain cellular homeostasis. qRT-PCR showed the elevation of six chosen MAPK pathway genes in response to both Pb stress and EAPR treatment, hence supporting the RNA-Seq results. The results underscore the essential role of MAPK-mediated signaling in the adaptive defense mechanisms of *P. stratiotes* against heavy metal stress, offering valuable insights for future phytoremediation research.

In conclusion, this study sheds light on potential molecular response mechanisms of *P. stratiotes* under Pb stress and EAPR treatment, contributing to a better understanding of its adaptive strategies at the transcriptomic level. The findings offer insights into HM remediation of synthetic leachate, and may serve as a basis for further research into genetic engineering or bioremediation approaches in aquatic plants. The identification of stress-signaling pathways under combined Pb and EAPR treatments may enable possible Clustered Regularly Interspaced Short Palindromic Repeats (CRISPR)-based genome editing. This further enhances metal hyperaccumulation traits and reduces growth inhibition. Such targeted modification could help develop new phytoremediation platforms for future systems that treat landfill leachate.

REFERENCES

Abasi, S., Jain, A., Cooke, J.P. and Guiseppi-Elie, A., 2023. Electrically stimulated gene expression under exogenously applied electric fields. *Frontiers in Molecular Biosciences*, [e-journal] 10. https://dx.doi.org/10.3389/fmolb.2023.1161191.

Abdulaziz, M., Alshehri, A., Yadav, I.C. and Badri, H., 2022. Pollution level and health risk assessment of heavy metals in ambient air and surface dust from Saudi Arabia: a systematic review and meta-analysis. *Air Quality, Atmosphere and Health*, 15(5), pp.799-810.

Abdullah, Z., Salleh, M.S. and Ismail K.N.I.K., 2017. Survey of household solid waste management and waste minimization in Malaysia: awareness, issues and practices. *International Journal of Environmental and Agriculture Research*, 3(12), pp.38–48.

Abidin, A.U., Maziya, F.B., Susetyo, S.H., Yoneda, M. and Matsui, Y., 2024. Heavy metal air pollution in an Indonesian landfill site: characterization, sources, and health risk assessment for informal workers. *Environmental Advances*, [e-journal] 15. https://dx.doi.org/10.1016/j.envadv.2024.100512.

Abou-Shady, A. and Yu, W., 2023. Recent advances in electrokinetic methods for soil remediation. A critical review of selected data for the period 2021–2022. *International Journal of Electrochemical Science,* [e-journal] 18(8). https://dx.doi.org/10.1016/j.ijoes.2023.100234.

Abreu, I.A. and Cabelli, D.E., 2010. Superoxide dismutases—a review of the metal-associated mechanistic variations. *Biochimica et Biophysica Acta,* [e-journal] 1804, pp.263–274. https://dx.doi.org/10.1016/j.bbapap.2009.11.005.

Abu-Rukah, Y. and Abu-Aljarayesh, I., 2002. Thermodynamic assessment in heavy metal migration at El-Akader landfill site, North Jordan. *Waste Management Journal*, [e-journal] 22(7), pp.727-738. http://dx.doi.org/10.1016/s0956-053x(02)00046-6.

Abuabdou, S.M.A., Ahmad, W., Aun, N.C. and Bashir, M.J.K., 2020. A review of anaerobic membrane bioreactors (AnMBR) for the treatment of highly contaminated landfill leachate and biogas production: effectiveness, limitations and

future perspectives. *Journal of Cleaner Production,* [e-journal] 255. https://dx.doi.org/10. 1016/j.jclepro.2020.120215.

Abubakar, I.R., Maniruzzaman, K.M., Dano, U.L., AlShihri, F.S., AlShammari, M.S., Ahmed, S.M.S., Al-Gehlani, W.A.G. and Alrawaf, T.I., 2022. Environmental sustainability impacts of solid waste management practices in the global south. *International Journal of Environmental Research and Public Health,* [e-journal] 19(19). http://dx.doi.org/10.3390/ijerph191912717.

Abujazar, M.S.S., Karaağaç, S.U., Abu Amr, S.S., Alazaiza, M.Y.D. and Bashir, M.J.K., 2022. Recent advancement in the application of hybrid coagulants in coagulation-flocculation of wastewater: a review. *The Journal of Cleaner Production,* [e-journal] 345. http://dx.doi.org/10.1016/j.jclepro.2022.131133.

Acevedo-Siaca, L.G. and McAusland, L., 2025. A guide to understanding and measuring photosynthetic induction: considerations and recommendations. New Phytologist, [e-journal] 247(2), pp.450-469. http://dx.doi.org/10.1111/nph.70218.

Acharya, A., Bellaloui, N., Pilipovic, A., Perez, E., Maddox-Mandolini, M. and Fuente, H.D.L., 2025. Current assessment and future perspectives on phytoremediation of heavy metals. *Plants*, [e-journal] 14(18), https://dx.doi.org/10.3390/plants14182847

Adamcová, D., Radziemska, M., Ridošková, A., Bartoň, S., Pelcová, P., Elbl, J., Kynický, J., Brtnický, M. and Vaverková, M.D., 2017. Environmental assessment of the effects of a municipal landfill on the content and distribution of heavy metals in *Tanacetum vulgare* L. *Chemosphere*, [e-journal] 185, pp.1011–1018. http://dx.doi.org/10.1016/j.chemosphere.2017.07.060.

Adams, D.S. and Levin, M., 2012. Endogenous voltage gradients as mediators of cell-cell communication: strategies for investigating bioelectrical signals during pattern formation. *Cell and Tissue Research,* [e-journal] 352(1), pp.95-122. https://dx.doi.org/10.1007/s00441-012-1329-4.

Adams, A., Raman, A. and Hodgkins, D., 2012. How do the plants used in phytoremediation in constructed wetlands, a sustainable remediation strategy, perform in heavy-metal-contaminated mine sites? *Water and Environment Journal,* [e-journal] 27, pp.373–386. https://dx.doi.org/10.1111/j.1747-6593.2012.00357.x.

Afrasiyab, A., Zafar, J. and Muhmmad, H., 2020. Effect of electric field on seed germination and growth parameters of chickpea *Cicer arietinum* L. *Ukranian Journal of Ecology*, [e-journal] 10(4), pp.12-16. http://dx.doi.org/10.15421/2020_160.

Agarwal, V.P., Nehra, M.R., Gupta, S. and Nehra, N.G.A., 2022. Heavy metals stress tolerance mechanism in crop plants. *The Pharma Innovation Journal*, 11(11), pp.2716-2726.

Agency for Toxic Substances and Disease Registry, 2024. *Toxicological profile for nickel*. Atlanta: Agency for Toxic Substances and Disease Registry.

Ahila, K.G., Ravindran, B., Muthunarayanan, V., Nguyen, D.D., Nguyen, X.C., Chang, S.W., Nguyen, V.K. and Thamaraiselvi, C., 2021. Phytoremediation potential of freshwater macrophytes for treating dye-containing wastewater. *Sustainability*, [e-journal] 13(1). https://dx.doi.org/10.3390/su13010329.

Ahmad, A., Hadi, F. and Ali, N., 2015. Effective phytoextraction of cadmium (Cd) with increasing concentration of total phenolics and free proline in *Cannabis sativa* (L) plant under various treatments of fertilizers, plant growth regulators and sodium salt. *International Journal of Phytoremediation*, [e-journal] 17, pp.56–65. https://dx.doi.org/10.1080/15226514.2013.828018.

Ahmad, M., Wolberg, A. and Kahwaji, C.I., 2023. *Biochemistry, electron transport chain*. Treasure Island (FL): StatPearls Publishing.

Ahmad, P., Jaleel, C.A., Salem, M.A., Nabi, G. and Sharma, S., 2010. Roles of enzymatic and nonenzymatic antioxidants in plants during abiotic stress. *Critical Reviews in Biotechnology*, [e-journal] 30, pp.161–175. https://dx.doi.org/10.3109/07388550903524243.

Ahmad, P., Rasool, S., Gul, A., Sheikh, S.A., Akram, N.A., Ashraf, M., Kazi, A.M. and Gucel, S., 2016. Jasmonates: multifunctional roles in stress tolerance. *Frontier in Plant Science*, [e-journal] 7. https://dx.doi.org/10.3389/fpls.2016.00813.

Ahmad, R., Hadi, F., Jan, A.U. and Ditta, A., 2022. Straw incorporation in contaminated soil enhances drought tolerance but simultaneously increases the

accumulation of heavy metals in rice. *Sustainability*, [e-journal] 14(17). https://dx.doi.org/10.3390/su141710578.

Ahmadli, N. and Mammadova, A., 2024. The use of cationic polymers in coagulation and flocculation studies of wastewater. *Cit*, 25(9). p.2024.

Ahmadpour, P., Ahmadpour, F., Sadeghi, S.M., Tayefeh, F.H., Soleimani, M. and Abdu, A., 2015. Evaluation of four plant species for phytoremediation of copper contaminated soil. In: K.R. Hakeem, M. Sabir, M. Öztürk and A.R. Mermut, eds. 2015. *Soil remediation and plants*. Cambridge, Massachusetts: Academic Press. pp.147-205.

Akemoto, Y., Putra, R.S. and Tanaka, S., 2022. Electrokinetic remediation. In: D. Barcelo and A.G. Kostianoy, eds. 2022. *The handbook of environmental chemistry*. Berlin: Springer. pp.1-51

Al-Yaqout, A. and HamodaM. F., 2020. Long-term temporal variations in characteristics of leachates from a closed landfill in an arid region. *Water, Air, and Soil Pollution*, [e-journal] 231(319). https://dx.doi.org/10.1007/s11270-020-04688-7.

Alaboudi K.A., Ahmed, B. and Brodie, G., 2018. Phytoremediation of Pb and Cd contaminated soils by using sunflower (*Helianthus annuus*) plant. *Annals of Agricultural Sciences*, [e-journal] 63(1), pp.123–127. https://dx.doi.org/10.1016/j.aoas.2018.05.007.

Alam, M.T., Ahmad, M.M. and Naaz, S., 2025. Water hyacinth is a potential aquatic plant used in water treatment: a short review. *Scholars Academic Journal of Biosciences*, [e-journal] 13(07), pp.898-907. https://dx.doi.org/10.36347/sajb.2025.v13i07.004

Alejandro, S., Holler, S., Meier, B. and Peiter, E., 2020. Manganese in plants: from acquisition to subcellular allocation. *Frontiers in Plant* Science, [e-journal] 11, pp.1–23. http://dx.doi.org/ 10.3389/fpls.2020.00300.

Alghamdi, S.A. and El-Zohri, M., 2024. Phytoremediation characterization of heavy metals by some native plants at anthropogenic polluted sites in Jeddah, Saudi

Arabia. *Resources*, [e-journal] 13(7). https://dx.doi.org/10.3390/resources13070098

Ali, H., Khan, E. and Sajad, M.A., 2013. Phytoremediation of heavy metals - concepts and applications. *Chemosphere*, [e-journal] 91, pp.869–881. http://dx.doi.org/ 10.1016/j.chemosphere.2013.01.075.

Ali, M.L., Şensoy, S. and Bitik, S., 2022. Effects of different electric current (DC) applications on plant development in spinach. *Ereğli Journal of Agricultural Science*, [e-journal] 2(2), pp.48-61. http://dx.doi.org/10.54498/ETBD.2022.11.

Ali, S., Abbas, Z., Rizwan, M., Zaheer, I. E., Tavas, Ilkay, Unay, A., Abdel-DAIM, M., Bin-Jumah, M., Hasanuzzaman, M., and Kalderis, D., 2020. Application of floating aquatic plants in phytoremediation of heavy metals polluted water: A review. *Sustainability (Switzerland)*, [e-journal] 12(5). https://dx.doi.org/10.3390/su12051927.

Alsafran, M., Usman, K., Ahmed, B., Rizwan, M., Saleem, M.H. and Al Jabri, H., 2022. Understanding the phytoremediation mechanisms of potentially toxic elements: a proteomic overview of recent advances. *Frontiers in Plant Science*, [e-journal] 13. http://dx.doi.org/ 10.3389/fpls.2022.881242.

Amr, S.S. and Funke, B., 2015. Targeted hybrid capture for inherited disease panels. In: S. Kulkarni and J. Pfeifer, eds. 2015. *Clinical genomics*. Cambridge, Massachusetts: Academic Press. pp.251-269.

Andreassen, S.N., Ezra, M.B. and Scheibye-Knudsen, M.A., 2019. A defined human aging phenome. *Aging (Albany NY)*, [e-journal] 11(15), pp.5786-5806. https://dx.doi.org/10.18632/aging.102166.

Andreasson, E. and Ellis, B., 2010. Convergence and specificity in the *Arabidopsis* MAPK nexus. *Trends in Plant Science*, 15(2), pp.106-113.

Ang, M.C., Saju, J.M., Porter, T.K., Mohaideen, S., Sarangapani, S., Khong, D.T., Wang, S., Cui, J., Loh, S.I., Singh, G.P., Chua, N.H., Strano, M.S. and Sarojam, R., 2024. Decoding early stress signaling waves in living plants using nanosensor multiplexing. *Nature Communications*, [e-journal] 15(1):2943. https://dx.doi.org/10.1038/s41467-024-47082-1.

Anqi, T., Zhang, Z., Suhua, H. and Xia, L., 2020. Review on landfill leachate treatment methods. *IOP Conference Series: Earth and Environmental Science,* [e-journal] 565. https://dx.doi.org/10.1088/1755-1315/565/1/012038.

Antequera, F. and Bird, A., 1993. CpG islands. In: J.P. Jost, H.P. Saluz, eds. 1993. DNA Methylation: Molecular Biology and Biological Significance. Basel: Birkhauser. pp. 169-185.

Arat, S.A., 2024. Microplastics in landfill leachate: Sources, abundance, characteristics, remediation approaches and future perspective. *Desalination and Water Treatment,* [e-journal] 319. https://dx.doi.org/10.1016/j.dwt.2024.100445.

Aravind P., Subramanyan V., Ferro S. and Gopalakrishnan R., 2016. Eco-friendly and facile integrated biological-cum-photo assisted electrooxidation process for degradation of textile wastewater. *Water Research,* [e-journal] 93, pp.230–241. https://dx.doi.org/10.1016/j.watres.2016.02.041.

Arhoun, B., Villen-Guzman, M., Rodriguez-Maroto, J.M. and Paz-Garcia, J.M., 2023. Electrochemical treatment of landfill leachate. In: V.K. Tyagi, C.S.P., Ojha, eds. 2023. Landfill Leachate Management. London, UK: IWA Publishing. pp.153-194.

Arora, K., Sinha, C., Zhang, W., Ren, A., Moon, C.S., Yarlagadda, S. and Naren, A.P., 2013. Compartmentalization of cyclic nucleotide signaling: A question of when, where, and why? *Pflügers Archiv*, [e-journal] 465, pp.1397–1407. https://dx.doi.org/10.1007/s00424-013-1280-6.

Asada K., 1999. The water-water cycle in chloroplasts: scavenging of active oxygens and dissipation of excess photons. *Annual Review of Plant Physiology and Plant Molecular Biology*, [e-journal] 50, pp.601-639. http://dx.doi.org/10.1146/annurev.arplant.50.1.601.

Asada, K., 2006. Production and scavenging of reactive oxygen species in chloroplasts and their functions. *Plant Physiology*, [e-journal] 141(2), pp.391–396. https://dx.doi.org/10.1104/pp.106.082040.

Ashraf, M., 2009. Biotechnological approach of improving plant salt tolerance using antioxidants as markers. *Biotechnology Advances*, [e-journal] 27, pp.84-93.

http://dx.doi.org/10.1016/j.biotechadv.2008.09.003.

Ashraf, A., Bhardwaj, S., Ishtiaq, H., Devi, Y.K. and Kapoor, D., 2021. Lead uptake, toxicity and mitigation strategies in plants. *Plant Archives,* [e-journal] 21(1), pp.712-721. http://dx.doi.org/10.51470/PLANTARCHIVES.2021.v21.no1.099.

Asif, M.B. and Zhang, Z., 2021. Ceramic membrane technology for water and wastewater treatment: a critical review of performance, full-scale applications, membrane fouling and prospects. *Chemical Engineering Journal*, [e-journal] 418. http://dx.doi.org/10.1016/j.cej.2021.129481.

Asiminicesei, D.M., Fertu, D.I. and Gavrilescu, M., 2024. Impact of heavy metal pollution in the environment on the metabolic profile of medicinal plants and their therapeutic potential. *Plants,* [e-journal] 13(6). https://dx.doi.org/10.3390/plants13060913.

Aslam M., Aslam A., Sheraz M., Ali B., Ulhassan Z., Najeeb U., Zhou W. and Gill R.A., 2021. Lead toxicity in cereals: mechanistic insight into toxicity, mode of action, and management. *Frontiers in Plant Science,* [e-journal] 11. https://dx.doi.org/10.3389/fpls.2020.587785.

Aslam, B., Maqsoom, A., Tahir, M.D., Ullah, F., Ur Rehman, M.S. and Albattah, M., 2022. Identifying and ranking landfill sites for municipal solid waste management: an intemungugrated remote sensing and GIS approach. *Buildings,* [e-journal] 12(605). https://dx.doi.org/10.3390/BUILDINGS12050605.

Assmann, S.M., 1995. Cyclic AMP as a second messenger in higher plants (status and future prospects). *Plant Physiology*, [e-journal] 108(3), pp.885-889. https://dx.doi.org/10.1104/pp.108.3.885.

Auguy, F., Fahr, M., Moulin, P., Brugel, A., Laplaze, L., Mzibri, M.E., Filali-Maltouf, A., Doumas, P. and Smouni, A.., 2013. Lead tolerance and accumulation in *Hirschfeldia incana*, a *Mediterranean brassicaceae* from metalliferous mine spoils. *PloS One*, [e-journal] 8(5): e61932. http://dx.doi.org/10.1371/journal.pone.0061932.

Auguy, F., Fahr, M., Moulin, P., Mzibri, M.E., Smouni, A., Filali-Maltouf, A., Béna, G. and Doumas, P., 2016. Transcriptome changes in *Hirschfeldia incana* in response to lead exposure. *Frontiers in Plant Science*, [e-journal] 6. https://dx.doi.org/10.3389/fpls.2015.01231.

Aweng, E.R., Irfan, A.H.M., Liyana, A.A. and Aisyah, S.O.S., 2018. Potential of phytoremediation using *Scirpus validus* for domestic waste open dumping leachate. *Journal of Applied Sciences and Environmental Management*, [e-journal] 22, pp.74–78. http://dx.doi.org/10.4314/jasem.v22i1.13.

Azad, M., Tohidfar, M., Seraj, R.G.M., Mehralian, M. and Esmaeilzadeh-Salestani, K., 2024. Identification of responsive genes to multiple abiotic stresses in rice (*Oryza sativa*): a meta-analysis of transcriptomics data. *Scientific Reports*, [e-journal] 14(5463). https://dx.doi.org/10.1038/s41598-024-54623-7.

Aziz, M.F.A. and Ariffin, R.N.R., 2024. The implementation of solid waste management policies in Southeast Asia: the present situations and future recommendations. *The Malaysian Journal of Social Administration*, 18, pp.133-179.

Aziz, S.Q., Aziz, H.A., Yusoff, M.S., Mojiri, A. and Abu Amr, S., 2012. Adsorption isotherms in landfill leachate treatment using powdered activated carbon augmented sequencing batch reactor technique: statistical analysis by response surface methodology. *International Journal of Chemical Reactor Engineering*, [e-journal] 10(1), pp.1542–6580. http://dx.doi.org/10.1515/1542-6580.3112.

Aziz, H.A., Zahari, M.S.M., Ahmed, Z., Ismail, S., Jaafar, I., Yusoff, M.S., Wang, L.K. and Wang, M.-H.S., 2022. Landfill leachate treatment. In: L.K. Wang, M.-H. S. Wang, and Y.-T. Hung, eds. 2021. *Solid waste engineering and management*. Cham: Springer International Publishing. pp.435–548.

Aziz, R.A., Yiwen, M., Saleh, M., Salleh, M.N., Gopinath, S.C.B., Giap, S.G.E., Chinni, S.V. and Gobinath, R., 2023. Bioaccumulation and translocation of heavy metals in paddy (*Oryza sativa* L.) and soil in different land use practices. *Sustainability*, [e-journal] 15(18). https://dx.doi.org/10.3390/su151813426.

Azmi, N., Bashir, M., Sethupathi, S. and Ng, C., 2014. Anaerobic stabilized landfill leachate treatment using chemically activated sugarcane bagasse activated carbon: kinetic and equilibrium study. *Desalination and Water Treatment*, [e-journal] 57(9), pp.3916-3927. https://dx.doi.org/10.1080/19443994.2014.988660.

Babli, J.K., Singh V.P and Srivastava, A., 2022. Electric current induced mitigation of lead contamination in *Vetiveria zizanioides*. *Plant Archives*, 22(1), pp.255-260.

Babst-Kostecka, A.A., Waldmann, P., Frérot, H. and Vollenweider, P., 2016. Plant adaptation to metal polluted environments – physiological, morphological, and evolutionary insights from *Biscutella laevigata*. *Environmental and Experimental Botany*, [e-journal] 127, pp.1–13. https://dx.doi.org/10.1016/j.envexpbot.2016.03.001.

Bai, Y., Zhang, Z., Jiang, G., Niu, S., Peng, Z. and Liu, L., 2025. Electrokinetic remediation technology for uranium contaminated soil: from fundamental principles to application challenges and breakthroughs. *Frontiers in Chemical Engineering*, [e-journal] 7. https://dx.doi.org/10.3389/fceng.2025.1687808.

Baird, R.B., Eaton, A.D. and Rice, E.W. eds., 2017. *Standard methods for the examination of water and wastewater*. 23rd Edition. Washington D.C: American Public Health Association, American Water Works Association, Water Environment Federation.

Bakhshoodeh, R., Alavi, N., Oldham, C., Santos, R.M., Babaei, A.A., Vymazal, J. and Paydary, P., 2020. Constructed wetlands for landfill leachate treatment: a review. *Ecological Engineering*, [e-journal] 146. https://dx.doi.org/10.1016/j.ecoleng.2020.105725.

Bakhtiyari-Ramezani, M., Mohammadi, F., Azizi, M., Ziveh, N. and Amani, F., 2025. Comprehensive study of pollution removal from landfill leachate with emphasis on phenolic compounds and heavy metals using non-thermal plasma technology. *Waste Management Bulletin*, [e-journal] 3(3). https://dx.doi.org/10.1016/j.wmb.2025.100233.

Bakshi, P., Handa, N., Gautam, V., Kaur, P., Sareen, S., Mir, B.A. and Bhardwaj, R., 2019. Role and regulation of plant hormones as a signal molecule in response to abiotic stresses. In: M.I.R. Khan, P.S. Reddy, N.A. Khan and A.F. Hernández, eds. 2019. *Plant signaling molecules: role and regulation under stressful*

environments. Sawston, Cambridge: Woodhead Publishing. pp.303–317.

Balachandran, R.C., Mukhopadhyay, S., McBride, D., Veevers, J., Harrison, F.E., Aschner, M., Haynes, E.N. and Bowman A.B., 2020. Brain manganese and the balance between essential roles and neurotoxicity. *Journal of Biological Chemistry,* [e-journal] 295, pp.6312–6329. https://dx.doi.org/10.1074/jbc.REV119.009453.

Basharat, S., Saeed, W., Liu, P. and Waseem, M. 2025. Long-term heat stress induces transcriptomic reprogramming of hormone signaling and metabolic pathways during rapeseed flowering. *Scientific Reports,* [e-journal] 15 (42411). https:// dx.doi.org/10.1038/s41598-025-26508-w.

Bashir, M.J.K., Ibrahim, N., Ismail, M.N. and Jaya, M.A., 2016. Physical treatment technologies for landfill leachate: performance and limitation. In: H. Aziz and S. Amr, eds. 2015. *Control and treatment of landfill leachate for sanitary waste disposal*. Pennsylvania: IGI Global. pp.250–285.

Basu, S., Rabara, R.C., Negi, S. and Shukla, P., 2018. Engineering PGPMOs through gene editing and systems biology: a solution forphytoremediation? *Trends in Biotechnology*, [e-journal] 36(5), pp.499−510. http://dx.doi.org/10.1016/j.tibtech.2018.01.011.

Baxter-Burrell, A., Yang, Z., Springer, P.S. and Bailey-Serres, J., 2002. RopGAP4-dependent Rop GTPase rheostat control of *Arabidopsis* oxygen deprivation tolerance. *Science,* [e-journal] 296(5575), pp.2026-2028. http://dx.doi.org/10.1126/science.1071505.

Bayuo, J., Rwiza, M.J., Choi, J.W., Njau, K.N. and Mtei, K.M., 2024. Recent and sustainable advances in phytoremediation of heavy metals from wastewater using aquatic plant species: Green approach. *Journal of Environmental Management*, 370. http://dx.doi.org/10.1016/j.jenvman.2024.122523.

Beavo, J.A. and Brunton, L.L., 2002. Cyclic nucleotide research—still expanding after half a century. *Nature Reviews Molecular Cell Biology*, [e-journal] 3, pp.710–718. https://dx.doi.org/10.1038/nrm911.

Bedmar, M.C.L., Perez-Sanz, A., Martinez-Inigo, M.J. and Benito, A.P., 2009. Influence of coupled electrokinetic phytoremediation on soil remediation. In: K.R.

Reddy, C. Cameselle, eds. 2009. *Electrochemical remediation technologies for polluted soils, sediments and groundwater*. Hoboken: Wiley. pp.417–437.

Behera, U.S., Poddar, S. and Byun, H.S., 2025. Electrocoagulation treatment of wastewater collected from Haldia industrial region: Performance evaluation and comparison of process optimization. *Water Research*, [e-journal] 268, https://dx.doi.org/10.1016/j.watres.2024.122716.

Beinabaj, S.M.H., Heydariyan, H., Aleii, H.M. and Hosseinzadeh, A., 2023. Concentration of heavy metals in leachate, soil, and plants in Tehran's landfill: investigation of the effect of landfill age on the intensity of pollution. *Heliyon*, [e-journal] 9 (1). https://dx.doi.org/10.1016/j.heliyon.2023.e13017.

Bengtsson, L., Bendz, D., Hogland, W., Rosqvist, H. and Åkesson, M., 1994. Water balance for landfills of different age. *Journal of Hydrology*, [e-journal] 158(3–4), pp.203-217. http://dx.doi.org/10.1016/0022-1694(94)90054-X.

Benjamini, Y. and Speed, T.P., 2012. Summarizing and correcting the GC content bias in high-throughput sequencing. *Nucleic Acids Research*, [e-journal] 40(10), pp.e72. http://dx.doi.org/10.1093/nar/gks001.

Bergey, D.R., Kandel, R., Tyree, B.K., Dutt, M. and Dhekney, S.A., 2014. The role of calmodulin and related proteins in plant cell function: an ever-thickening plot. *Springer Science Reviews*, [e-journal] 2, pp.145–159. https://dx.doi.org/10.1007/s40362-014-0025-z.

Bernama, 2022. Can Malaysia achieve 40 per cent recycling rate by 2025? *News Straits Times*, [online] 3 March. Available at: <https://www.nst.com.my/news/nation/2022/03/778625/can-malaysia-achieve-40-cent-recycling-rate-2025> [Accessed 15 June 2022].

Bernard, F., Brulle, F., Dumez, S., Lemiere, S., Platel, A., Nesslany, F., Cuny, D., Deram, A. and Vandenbulcke, F., 2014. Antioxidant responses of annelids, Brassicaceae and Fabaceae to pollutants: a review. *Ecotoxicology and Environmental Safety*, [e-journal] 114, pp.273-303. https://dx.doi.org/10.1016/j.ecoenv.2014.04.024.

Berridge, M.J., Bootman, M.D. and Roderick, H.L., 2003. Calcium signalling: dynamics, homeostasis and remodelling. *Nature Reviews Molecular Cell Biology*, [e-journal] 4(7), pp.517-529. https://dx.doi.org/10.1038/nrm1155.

Bezerra, M.A., Souza, A.D.S., Oliveira, R.V., Oliveira, D.M., Cardoso, L.A.M. and Sousa Filho, H.R., 2015. Use of doehlert and constrained mixture designs in the development of a photo-oxidation procedure using UV radiation/H_2O_2 for decomposition of landfill leachate samples and determination of metals by flame atomic absorption spectrometry. *Anais da Academia Brasileira de Ciências*, [e-journal] 87(1), pp.3–13. https://dx.doi.org/10.1590/0001-3765201520140258.

Bhagwat R.V., Boralkar D.B. and Chavhan, R.D., 2018. Remediation capabilities of pilot-scale wetlands planted with *Typha aungstifolia* and *Acorus calamus* to treat landfill leachate. *Journal of Ecology and Environment*, [e-journal] 42(1). https://dx.doi.org/10.1186/s41610-018-0085-0.

Bhambore, N. and Suresh Kumar, M., 2022. Municipal solid waste generation, management scenarios, and leachate treatment using sequencing batch biofilter granular reactor. *Process Safety and Environmental Protection*, [e-journal] 167, pp.454–468. http://dx.doi.org/10.1016/j.psep.2022.09.027.

Bhardwaj, D., Sharma, S., Sharma, A., Gill, R., Gill, S.S., Verma, R., Kaul, T. and Tuteja, N., 2025. Decoding the signaling triad: molecular interactions of G-proteins, MAP kinases, and helicases in environmental stress responses. *Plant Science*, [e-journal] 357. https://dx.doi.org/10.1016/j.plantsci.2025.112514.

Bi, R., Schlaak, M., Siefert, E., Lord, R. and Connolly, H., 2010. Alternating current electrical field effects on lettuce (Lactuca sativa) growing in hydroponic culture with and without cadmium contamination. *Journal of Applied Electrochemistry*, [e-journal] 40, pp.1217–1223. https://dx.doi.org/10.1007/s10800-010-0094-x

Bian, X.H., Li, W., Niu, C.F., Wei, W., Hu, Y., Han, J.Q., Lu, X., Tao, J.J., Jin, M., Qin, H., Zhou, B., Zhang, W.K., Ma, B., Wang, G.D., Yu, D.Y., Lai, Y.C., Chen, S.Y. and Zhang, J.S., 2020. A class B heat shock factor selected for during soybean domestication contributes to salt tolerance by promoting flavonoid biosynthesis. *New Phytologist*, [e-journal] 225(1), pp.268-283. http://dx.doi.org/10.1111/nph.16104.

Bibi, A., Rasul, F., Shahzad, S. Sakrabani, R., Din, W., Mckenna, P. and Sajid, M., 2024. Toxicity, bioaccumulation and mitigating strategies of heavy metals stress on morpho-physiology of spinach. *Discover Plants*, [e-journal] 74(1). https://dx.doi.org/10.1007/s44372-024-00083-2.

Bienert, G.P., Møller, A.L., Kristiansen, K.A., Schulz, A., Møller, I.M., Schjoerring, J.K. and Jahn T.P., 2007. Specific aquaporins facilitate the diffusion of hydrogen peroxide across membranes. *Journal of Biological Chemistry,* [e-journal] 282, pp.1183–1192. https://dx.doi.org/10.1074/jbc.M603761200.

Bigeard, J. and Hirt, H., 2018. Nuclear Signaling of plant MAPKs. *Frontiers in Plant Science*, [e-journal] 9. https://dx.doi.org/ 10.3389/fpls.2018.00469.

Bishop, J., Swan, H., Valente, F. and Nützmann, H., 2021. The plant nuclear envelope and its role in gene transcription. *Frontiers in Plant Science*, [e-journal] 12. https://dx.doi.org/10.3389/fpls.2021.674209.

Bisht, R., Chanyal, S. and Srivastava R.K., 2020. A systematic review on phytoremediation technology: removal of pollutants from waste water and soil. *International Journal of Research in Engineering, Science and Management,* 3, pp.54–59.

Blanco, E., Fortunato, S., Viggiano, L., and de Pinto, M.C., 2020. Cyclic AMP: a polyhedral signalling molecule in plants. *International Journal of Molecular Sciences,* [e-journal] 21(14). https://dx.doi.org/10.3390/ijms21144862.

Bouck, A. and Vision, T., 2007. The molecular ecologist's guide to expressed sequence tags. *Molecular Ecology*, [e-journal] 16(5), pp.907-24. https://dx.doi.org/10.1111/j.1365-294X.2006.03195.x.

Bredow, M. and Monaghan, J., 2019. Regulation of plant immune signaling by calcium-dependent protein kinases. *Molecular Plant-Microbe Interactions,* [e-journal] 32(1), pp.6-19. https://dx.doi.org/10.1094/MPMI-09-18-0267-FI.

Briffa, J., Sinagra, E. and Blundell, R., 2020. Heavy metal pollution in the environment and their toxicological effects on humans. *Heliyon,* [e-journal] 6(9). https://dx.doi.org/10.1016/j.envpol.2021.118133.

Bu, A., Yao, G., Zhou, C., Mao, Z., Liu, B., Ma, J., Fang, X., Liu, D. and Ye, Z., 2024. Effect of AC electric field on enhancing phytoremediation of Cd-contaminated soils in different pH soils. *Scientific Reports 14*, [e-journal] 18035. https://dx.doi.org/10.1038/s41598-024-68671-6.

Burridge, K. and Wennerberg, K., 2004. Rho and Rac take center stage. *Cell*, [e-journal] 116(2), pp.167-179. https://dx.doi.org/10.1016/s0092-8674(04)00003-0.

Butti, L., Peres, F. and Lops, C., 2018. Chapter 1.3 - Legal framework of landfilling in different areas of the world. In: R. Cossu, R. Stegmann, eds., 2018. *Solid waste landfilling.* Amsterdam: Elsevier. pp.41-50.

Cadena-Ramírez, A., Alonso-Vargas, M. and Cesar-Ríos-Guzmán, J., 2024. Bridging the world of enzymes with electric fields. In: Khattak, R. ed. 2024. *Chemical kinetics and catalysis - perspectives, developments and applications.* London: IntechOpen. http://dx.doi.org/10.5772/intechopen.1004072.

Cai, K., Yu, Y., Zhang, M. and Kim, K., 2019. Concentration, source, and total health risks of cadmium in multiple media in densely populated areas, China. *International Journal of Environmental Research and Public Health,* [e-journal] 16. https://dx.doi.org/10.3390/ijerph16132269.

Cai, Z., Li, Y., Zhang, H. and Chen, J., 2022. Enhanced electrokinetic remediation of Cadmium (Cd)-contaminated soil with interval power breaking. *International Journal of Environmental Research,* [e-journal] 16(31). https://dx.doi.org/10.1007/s41742-022-00409-6

Cakmak, I. and Horst, W.J., 1991. Effect of aluminium on lipid peroxidation, superoxide dismutase, catalase, and peroxidase activities in root tips of soybean (*Glycine max*). *Physiologia Plantarum*, [e-journal] 83, pp.463-468. https://dx.doi.org/10.1111/j.1399-3054.1991.tb00121.x.

Cameselle, C., Chirakkara, R.A. and Reddy, K.R., 2013. Electrokinetic-enhanced phytoremediation of soils: status and opportunities. *Chemosphere,* [e-journal] 93, pp.626–636. https://dx..doi.org/10.1016/j.chemosphere.2013.06.029.

Cameselle, C., Gouveia, S. and Urréjola, S., 2019. Benefits of phytoremediation amended with DC electric field. Application to soils contaminated with heavy metals. *Chemosphere,* [e-journal] 229, pp.481-488. https://dx..doi.org/10.1016/j.chemosphere.2019.04.222.

Camoni, L., Visconti, S., Aducci, P. and Marra, M., 2018. 14-3-3 Proteins in plant hormone signaling: doing several things at once. *Frontier in Plant Sciences*, [e-journal] 9. https://dx..doi.org/10.3389/fpls.2018.00297.

Candas, D. and Li, J.J., 2018. MnSOD in oxidative stress response-potential regulation via mitochondrial protein influx. *Antioxidants and Redox Signaling*, [e-journal] 20(10), pp.1599-1617. https://dx.doi.org/10.1089/ars.2013.5305.

Carlberg, C. and Mannervik, B., 1985. Glutathione reductase. *Methods in Enzymology*, [e-journal] 113, pp.488-495. https://dx.doi.org/10.1016/s0076-6879(85)13062-4.

Castro, K. and Abejón, R., 2024. Removal of heavy metals from wastewaters and other aqueous streams by pressure-driven membrane technologies: an outlook on reverse osmosis, nanofiltration, ultrafiltration and microfiltration potential from a bibliometric analysis. *Membranes (Basel*), [e-journal] 14(8). http://dx. doi.org/10.3390/membranes14080180.

Catalanotto, C., Barbato, C., Cogoni, C. and Benelli, D., 2023. The RNA-binding function of ribosomal proteins and ribosome biogenesis factors in human health and disease. *Biomedicines*, 11(11). https://dx.doi.org/10.3390/biomedicines11112969.

Ceschin, S., Abati, S., Traversetti, L., Spani, F., Del Grosso, F. and Scalici, M., 2019. Effects of the invasive duckweed *Lemna minuta* on aquatic animals: evidence from an indoor experiment. *Plant Biosystems-An International Journal Dealing with all Aspects of Plant Biology*, 153(6), pp.749-755.

Chafik, Y., Sena-Velez, M., Oujdi, M., Carpin, S., Bourgerie, S. and Morabito, D., 2026. First evaluation of metal contamination and phytoremediation potential in wastes from mine tailings retreatment in touissit, morocco. *International Journal of Environmental Research*, 20(62). https://dx.doi.org/10.1007/s41742-025-01023-y

Chagas, R.M., Silveira, J.A.G., Ribeiro, R.V., Vitorello, V.A. and Carrer, H., 2008. Photochemical damage and comparative performance of superoxide dismutase and ascorbate peroxidase in sugarcane leaves exposed to paraquat-induced oxidative stress. *Pesticide Biochemistry and Physiology*, [e-journal] 90(3), pp.181-188. https://dx.doi.org/10.1016/j.pestbp.2007.11.006.

Chaitanya, G., Pavani, C. and Shasthree, T., 2023. Effect of heavy metals on in vitro growth and development of the *Momordica cymbalaria* Fenzl. *International Journal of Environmental Science and Technology*, [e-journal] 20, pp.8701–8708.

https://dx.doi.org/10.1007/s13762-022-04437-9.

Chan, M.Y., Tee, C.S., Chai, T.T., Sim, Y.L. and Beh, W.L., 2022. Evaluation of electro-assisted phytoremediation (EAPR) system for heavy metal removal from synthetic leachate using *Pistia stratiotes. International Journal of Phytoremediation*, [e-journal] 24(13), pp.1376-1384. https://dx.doi.org/10.1080/15226514.2022.2031863.

Chand, N., Kumar, K. and Suthar, S., 2022. Enhanced wastewater nutrients removal in vertical subsurface flow constructed wetland: effect of biochar addition and tidal flow operation. *Chemosphere*, [e-journal] 286. http://dx.doi.org/10.1016/j.chemosphere.2021.131742.

Chandra, R. and Kang, H.-D., 2015. Mixed heavy metal stress on photosynthesis, transpiration rate, and chlorophyll content in poplar hybrids. *Forest Science and Technology*, [e-journal] 12(2), pp.55-61. https://dx.doi.org/10.1080/21580103.2015.1044024.

Chang, J.H., Dong, C.D. and Shen, S.Y., 2019. The lead contaminated land treated by the circulation-enhanced electrokinetics and phytoremediation in field scale. *Journal of Hazardous Materials*, [e-journal] 368, pp.894–898. https://dx.doi.org/10.1016/j.jhazmat.2018.08.085.

Chantachon, S., Kruatrachue, M., Pokethitiyook, P., Upatham, S., Tantanasarit, S. and Soonthornsarathool, V., 2004. Phytoextraction and accumulation of lead from contaminated soil by Vetiver grass: laboratory and simulated field study. *Water, Air, and Soil Pollution*, [e-journal] 154, pp.37–55. https://dx.doi.org/10.1023/B:WATE.0000022926.05464.74.

Chen, Y.A., Shin, J.W. and Liu, Z.H., 2002. Effect of light on peroxidase and lignin synthesis in mungbean hypocotyls. *Plant Physiology and Biochemistry*, [e-journal] 40(1), pp.33-39. https://dx.doi.org/10.1016/S0981-9428(01)01345-6.

Chen, D., He, L., Lin, M., Jing, Y., Liang, C., Liu, H., Gao, J., Zhang, W. and Wang, M.A., 2021. A ras-related small GTP-binding protein, RabE1c, regulates stomatal movements and drought stress responses by mediating the interaction with ABA receptors. *Plant Science*, [e-journal] 306. https://dx.doi.org/10.1016/j.plantsci.2021.110858.

Chen, H., Xu, H., Zhong, C., Liu, M., Yang, L., He, J., Sun, Y., Zhao, C. and Wang,

D., 2024. Treatment of landfill leachate by coagulation: a review. *Science of the Total Environment*, [e-journal] 912. https://dx.doi.org/10.1016/j.scitotenv.2023.169294.

Chen, Q., Luo, L., Zhou, T., Gan, J., Liu, N., Lu, R., Xu, Q., Hu, L. and Chen, G., 2025. Comparative transcriptome analysis of leaves and roots revealed organ-specific and cross-stress defense strategies of pearl millet under different abiotic stresses. *Agronomy*, [e-journal] 15(12). https://dx.doi.org/10.3390/agronomy15122707

Cheng, H.C., Qi, R.Z., Paudel, H. and Zhu, H.J., 2011. Regulation and function of protein kinases and phosphatases. *Enzyme Research*, [e-journal] 2011. https://dx.doi.org/10.4061/2011/794089.

Cheng, K. M., Tan, J. Y., Wong, S. Y., Koo, A. C. and Sharji, E. A., 2022. A review of future household waste management for sustainable environment in Malaysian cities. *Sustainability (Switzerland)*, [e-journal] 14(11). https://dx.doi.org/10.3390/su14116517.

Cheng, Y., Ban, Q., Mao, J., Lin, M., Zhu, X., Xia, Y., Cao, X., Zhang, X. and Li, Y., 2023. Integrated metabolomic and transcriptomic analysis reveals that amino acid biosynthesis may determine differences in cold-tolerant and cold-sensitive tea cultivars. *International Journal of Molecular Sciences*, [e-journal] 24(3). https://dx.doi.org/10.3390/ijms24031907.

Cheniany, M., ebrahimzadeh, H., Masoudi-Nejad, A., Vahdati, K. and LesliE, C., 2010. Effect of endogenous phenols and some antioxidant enzyme activities on rooting of Persian walnut (*Juglans regia* L.). *African Journal of Plant Science*, 4, pp.479-487.

Chezem, W.R. and Clay, N.K., 2016. Regulation of plant secondary metabolism and associated specialized cell development by MYBs and bHLHs. *Phytochemistry*, [e-journal] 131, pp.26-43. https://dx.doi.org/10.1016/j.phytochem.2016.08.006.

Chin, P.M., Naim, A.N., Suja, F. and Ahmad Usul, M.F., 2020. Impact of effluent from the leachate treatment plant of taman beringin solid waste transfer station on the quality of jinjang river. *Processes*, [e-journal] 8(12). https://dx.doi.org/10.3390/pr8121553.

Chlubek, M. and Baranowska-Bosiacka, I., 2024. Selected functions and disorders of mitochondrial metabolism under lead exposure. *Cells,* [e-journal] 13(14). https://dx.doi.org/10.3390/cells13141182.

Choon, S.W., Tan, S.H. and Chong, LL., 2017. The perception of households about solid waste management issues in Malaysia. *Environment, Development and Sustainability*,19, pp.1685–1700.

Chrestensen, C.A., Starke, D.W. and Mieyal, J.J., 2000. Acute cadmium exposure inactivates thioltransferase (glutaredoxin), inhibits intracellular reduction of protein-glutathionyl-mixed disulfides, and initiates apoptosis. *Journal of Biological Chemistry*, [e-journal] 275(34), pp. 26556-26565. https://dx.doi.org/10.1074/jbc.m004097200.

Chugh, L.K. and Sawhney, S.K., 1999. Photosynthetic activities of *Pisum sativum* seedlings grown in presence of cadmium. *Plant Physiology and Biochemistry*, [e-journal] 37(4), pp.297–303. https://dx.doi.org/10.1016/S0981-9428(99)80028-X.

Çimrin, K.M., Turan, M. and Kapur, B., 2007. Effect of elemental sulphur on heavy metals solubility and remediation by plants in calcareous soils. *Fresenius Environmental Bulletin*, 16(9a), pp.1113-1120.

Cipriano, A. and Ballarino, M., 2018. The ever-evolving concept of the gene: the use of RNA/protein experimental techniques to understand genome functions. *Frontier in Molecular Biosciences,* [e-journal] 5(20). https://dx.doi.org/10.3389/fmolb.2018.00020.

Clemens, S., 2006. Toxic metal accumulation, responses to exposure and mechanisms of tolerance in plants. *Biochimie*, [e-journal] 88(11), pp.1707-1719. https://dx.doi.org/10.1016/j.biochi.2006.07.003.

Clemens, S., 2019. Metal ligands in micronutrient acquisition and homeostasis. *Plant, Cell and Environment*, [e-journal] 42(10), pp.2902–2912. https://dx.doi.org/10.1111/pce.13627.

Collin, A., Pacwa-Plociniczak, M., Plociniczak, T., Novak, Ô., Marzec, M., Guo, W., Simpson, C.G. and Daszkowska-Golec, A., 2025. Hormonal and transcriptomic

regulation of drought adaptation in barley roots and leaves. *Scientific Reports*, 15(1):16368. https://dx.doi.org/10.1038/s41598-025-01590-2.

Cong, W., Miao, Y., Xu, L., Zhang, Y., Yuan, C., Wang, J., Zhuang, T., Lin, X., Jiang, L., Wang, N., Ma, J., Sanguinet, K.A., Liu, B., Rustgi, S. and Ou, X., 2019. Transgenerational memory of gene expression changes induced by heavy metal stress in rice (*Oryza sativa* L.). *BMC Plant Biology*, [e-journal] 19, pp.1–14. https://dx.doi.org/10.1186/s12870-019-1887-7.

Cooper, G.M. 2nd ed., 2000. *The Cell: a molecular approach*. Sunderland (MA): Sinauer Associates.

Costa, C., Pinedo, M.L. and Riascos, B.D., 2025. Presence of humic acids in landfill leachate and treatment by flocculation at low pH to reduce high pollution of this liquid. *Sustainability*, [e-journal] 17(2). https://dx.doi.org/10.3390/su17020481

Couto, N., Wood, J. and Barber, J., 2016. The role of glutathione reductase and related enzymes on cellular redox homoeostasis network. *Free Radical Biology and Medicine*, [e-journal] 95, pp.27-42. http://dx.doi.org/10.1016/j.freeradbiomed.2016.02.028.

Craker, L.E., 2021. 4 Plant Growth Factors That Affect All Plants. *Journal of Soil Science and PlantHealth*, 5:3.

Cui, D., Yin, Y., Li, H., Hu, X., Zhuang, J., Ma, R. and Jiao, Z., 2021. Comparative transcriptome analysis of atmospheric pressure cold plasma enhanced early seedling growth in *Arabidopsis thaliana*. *Plasma Science and Technology*, [e-journal] 23(8). https://dx.doi.org/10.1088/2058-6272/ac0686.

Dagwar, P.P. and Dutta, D., 2024. Landfill leachate a potential challenge towards sustainable environmental management. *Science of The Total Environment*, [e-journal] 926. https://dx.doi.org/10.1016/j.scitotenv.2024.171668.

DalCorso, G., Fasani, E., Manara, A., Visioli, G. and Furini, A., 2019. Heavy metal pollutions: state of the art and innovation in phytoremediation. *International Journal of Molecular Sciences*, [e-journal] 20(14). https://dx.doi.org/10.3390/ijms20143412.

Dan, A., Oka, M., Fujii, Y., Soda, S., Ishigaki, T., Machimura, T. and Ike, M., 2017. Removal of heavy metals from synthetic landfill leachate in lab-scale vertical flow constructed wetlands. *Science of The Total Environment*, [e-journal] 584, pp.742–750. https://dx.doi.org/10.1016/j.scitotenv.2017.01.112.

Dannehl, D., 2018. Effects of electricity on plant responses. *Scientia Horticulturae*, [e-journal] 234, pp.382–392. https://dx.doi.org/10.1016/j.scienta.2018.02.007.

Dannehl, D., Huyskens-Keil, S., Wendorf, D., Ulrichs, C. and Schmidt, U., 2012. Influence of intermittent-direct-electric-current (IDC) on phytochemical compounds in garden cress during growth. *Food Chemistry*, [e-journal] 131(2012), pp.239-246. https://dx.doi.org/10.1016/j.foodchem.2011.08.069.

Das, S., Goswami, S. and Talukdar, A.D., 2016. Physiological responses of water hyacinth, *Eichhornia crassipes* (Mart.) Solms, to cadmium and its phytoremediation potential. *Turkish Journal of Biology*, [e-journal] 40, pp. 84-94. https://dx.doi.org/10.3906/biy-1411-86.

Das, P., Nutan, N., Singla-Pareek, S. and Pareek, A., 2015. Oxidative environment and redox homeostasis in plants: dissecting out significant contribution of major cellular organelles. *Frontiers in Environmental Science*, [e-journal] 2(70), pp.1-11. https://dx.doi.org/10.3389/fenvs.2014.00070.

Das, N., Rajput, H., Aly Hassan, A. and Kumar, S., 2023. Application of different coagulants and cost evaluation for the treatment of oil and gas produced water. *Water*, [e-journal] 15(3). https://dx.doi.org/10.3390/w15030464.

Davidson, N.M. and Oshlack, A., 2014. Corset: enabling differential gene expression analysis for de novoassembled transcriptomes. *Genome Biology*, [e-journal] 15(410). https://dx.doi.org/10.1186/s13059-014-0410-6.

De, S., Hazra, T., and Dutta, A., 2019. Sustainable treatment of municipal landfill leachate by combined association of air stripping, Fenton oxidation, and enhanced coagulation. *Environmental Monitoring and Assessment,* [e-journal] 191:49. http://dx.doi.org/10.1007/s10661-018-7171-8.

De, S., Hazra, T., and Dutta, A., 2022. Application of integrated sequence of air

stripping, coagulation flocculation, electrocoagulation and adsorption for sustainable treatment of municipal landfill leachate. *Cleaner Waste Systems*, [e-journal] 3. http://dx.doi.org/10.1016/j.clwas.2022.100033.

De Bigault Du Granrut, A. and Cacas, J.L., 2016. How very-long-chain fatty acids could signal stressful conditions in plants? *Frontier in Plant Science*, [e-journal] 7. http://dx.doi.org/10.3389/fpls.2016.01490.

De Vriese, K., Costa, A., Beeckman, T. and Vanneste, S., 2018. Pharmacological strategies for manipulating plant Ca^{2+} Signalling. *International Journal of Molecular Sciences*, [e-journal] 19(5). http://dx.doi.org/10.3390/ijms19051506.

Deepika and Haritash, A.K., 2023. Cadmium uptake from soil by ornamental metallophytes: a meta-analytical approach. *Environmental Management*, [e-journal] 71(5), pp.1087-1097. http://dx.doi.org/10.1007/s00267-022-01776-8.

Degaga, A.H., 2019. Water hyacinth (*Eichhornia crassipes*) biology and its impacts on ecosystem, biodiversity, economy and human well-being. *Journal of Natural Sciences Research*, [e-journal] 8(6), pp.94-100. http://dx.doi.org/10.7176/JNSR/9-12-04

del Carmen, E.M., Souza, V., Bucio, L., Hernández, E., Damián-Matsumura, P., Zaga, V. and Gutiérrez-Ruiz, M.C., 2002. Cadmium induces α1collagen (I) and metallothionein II gene and alters the antioxidant system in rat hepatic stellate cells. *Toxicology*, [e-journal] 170, pp.63–73. https://dx.doi.org/10.1016/S0300-483X(01)00531-5.

Dell'Aglio, E. and Mhamdi, A., 2020. What are the roles for dehydroascorbate reductases and glutathione in sustaining ascorbate accumulation? *Plant Physiology*, [e-journal] 183(1), pp.11-12. http://dx.doi.org/10.1104/pp.20.00388.

Delsart, C., 2016. Plant cell wall: description, role in transport, and effect of electroporation. In: D. Miklavcic, eds. 2016. *Handbook of electroporation*. Cham: Springer, pp.1-22.

Deng, N., Liu, C., Chang, E., Ji, J., Yao, X., Yue, J., Bartish, I.V., Chen, L., Jiang, Z. and Shi, S., 2017. High temperature and UV-C treatments affect stilbenoid accumulation and related gene expression levels in *Gnetum parvifolium. Electronic*

Journal of Biotechnology, [e-journal] 25, pp.43-49. https://dx.doi.org/10.1016/j.ejbt.2016.11.001.

Derat, E. and Shaik, S., 2006. The Poulos-kraut mechanism of compound I formation in horseradish peroxidase: a QM/MM study. *The Journal of Physical Chemistry B*, [e-journal] 110, pp.10526-10533. https://dx.doi.org/10.1021/jp055412e.

Dermont, G., Bergeron, M., Mercier, G. and Richer-Lafleche, M., 2008. Soil washing for metal removal: a review of physical/chemical technologies and field applications *Journal of Hazardous Materials*, [e-journal] 152, pp.1-31. https://dx.doi.org/10.1016/j.jhazmat.2007.10.043.

Devi, S.R. and Prasad, M.N.V., 1999. Membrane lipid alterations in heavy metal exposed plants. In: M.N.V. Prasad, J. Hagemeyer, eds. 1999. *Heavy metal stress in plants. From molecules to ecosystems.* Berlin: Springer. pp.99–116.

Di, X., Gomila, J. and Takken, F.L.W., 2017. Involvement of salicylic acid, ethylene and jasmonic acid signalling pathways in the susceptibility of tomato to *Fusarium oxysporum*. *Molecular Plant Pathology*, [e-journal] 18(7), pp.1024-1035. https:/dx.doi.org/10.1111/mpp.12559.

Dietz, K.J., Turkan, I. and Krieger-Liszkay, A., 2016. Redox- and reactive oxygen species-dependent signaling into and out of the photosynthesizing chloroplast. *Plant Physiology*, [e-journal] 171(3), pp.1541-50. https://dx.doi.org/10.1104/pp.16.00375.

Dimova, R., Bezlyepkina, N., Jordö, M.D., Knorr, R.L., Riske, K.A., Staykova, M., Vlahovska, P.M., Yamamoto, T., Yang, P. and Lipowskya, R., 2009. Vesicles in electric fields: some novel aspects of membrane behaviour. *Soft Matter*, [e-journal] 5(17). https://dx.doi.org/10.1039/B901963D.

Dipu, S., Kumar, A.A. and Thanga, V.S.G., 2011. Phytoremediation of dairy effluent by constructed wetland technology. *Environment*, 31, pp. 263–278.

Dolhan, M.M., Arbaan, N.S. and Bain, N.F., 2024. Phytoremediation of POME Using Water Lettuce and Duckweed. *Frontiers in Water and Environment*, [e-journal] 3(1), pp.1–8. https://dx.doi.org/10.37934/fwe.3.1.18.

Dong, C., Taylor, M.P. and Gulson, B., 2020. A 25-year record of childhood blood lead exposure and its relationship to environmental sources. *Environmental Research,* [e-journal] 186. https://dx.doi.org/10.1016/j.envres.2020.109357.

Dormatey, R., Qin, T., Wang, Y., Karikari, B., Dekomah, S.D., Fan, Y., Bi, Z., Yao, P., Ali, K., Sun, C. and Bai, J., 2022. Comparative transcriptome profiling reveals potential candidate genes, transcription factors, and biosynthetic pathways for phosphite response in potato (*Solanum tuberosum* l.). *Genes (Basel),* [e-journal] 13(8). https://dx.doi.org/10.3390/genes13081379.

Dörner, K., Ruggeri, C., Zemp, I. and Kutay, U., 2023. Ribosome biogenesis factors-from names to functions. *EMBO Journal*, [e-journal] 42(7). https://dx.doi.org/10.15252/embj.2022112699.

Dróżdź, T., Kiełbasa, P., Nawara, P. and Miernik, A., 2021. The effect of pulsed electric field on the intercellular structure of biological substances. *Journal of Physics Conference Series*, [e-journal] 1782. https://dx.doi.org/10.1088/1742-6596/1782/1/012004.

Dumanović, J., Nepovimova, E., Natić, M., Kuča, K. and Jaćević, V., 2021. The significance of reactive oxygen species and antioxidant defense system in plants: a concise overview. *Frontiers in Plant Science*, [e-journal] 11. https://dx.doi.org/10.3389/fpls.2020.552969.

Dusenge, M.E., Duarte, A.G. and Way, D.A., 2019. Plant carbon metabolism and climate change: elevated CO_2 and temperature impacts on photosynthesis, photorespiration and respiration. *New Phytologist*, [e-journal] 221(1), pp.32-49. https://dx.doi.org/10.1111/nph.15283.

Edokpayi, J.N., Durowoju, O.S. and Odiyo, J.O., 2018. Assessment of heavy metals in landfill leachate: a case study of Thohoyandou landfill, Limpopo Province, South Africa. In: H.E.M. Saleh and R.F. Aglan, eds. 2018. *Heavy metals*. London: IntechOpen. pp.219–231.

Edwards, E.A., Rawsthorne, S. and Mullineaux, P.M., 1990. Subcellular distribution of multiple forms of glutathione reductase in leaves of pea (*Pisum sativum* L.). *Planta*, [e-journal] 180, pp.278-284. http://dx.doi.org/10.1007/BF00194008.

Ehsan, H., Roef, L., Witters, E., Reichheld, J.P., Van Bockstaele, D., Inze, D. and Van Onckelen, H., 1999. Indomethacin-induced G1/S phase arrest of the plant cell cycle. *FEBS Letters*, [e-journal] 458, pp.349–353. https://dx.doi.org/10.1016/S0014-5793(99)01152-7.

Eid, E.M. and Shaltout, K.H., 2017. Population dynamics of *Eichhornia crassipes* (C. Mart.) Solms in the Nile Delta, Egypt. *Plant Species Biology*, 32, pp.279–291

Eid, E.M., Galal, T.M., Sewelam, N.A., Talha, N.I. and Abdallah, S.M., 2020. Phytoremediation of heavy metals by four aquatic macrophytes and their potential use as contamination indicators: a comparative assessment. *Environmental Science and Pollution Research*, [e-journal] 27(11), pp.12138-12151. http://dx.doi.org/10.1007/s11356-020-07839-9.

Eid, E.M., Shaltout, K.H., Almuqrin, A.H., Aloraini, D.A., Khedher, K.M., Taher, M.A., Alfarhan, A.H., Picó, Y. and Barcelo, D., 2021. Uptake prediction of nine heavy metals by *Eichhornia crassipes* grown in irrigation canals: a biomonitoring approach. *Science of the Total Environment*, [e-journal] 782. http://dx.doi.org/10.1016/j.scitotenv.2021.146887.

El-Amier, Y.A., Bessa, A.Z.E., Elsayed, A., El-Esawi, M.A., AL-Harbi, M.S., Samra, B.N. and Kotb, W.K., 2021. Assessment of the heavy metals pollution and ecological risk in sediments of mediterranean sea drain estuaries in Egypt and phytoremediation potential of two emergent plants. *Sustainability*, [e-journal] 13(21), 12244. http://dx.doi.org/10.3390/su132112244.

El-Saadony, M.T., Saad, A.M., El-Wafai, N.A., Abou-Aly, H.E., Salem, H.M., Soliman, S.M., Abd El-Mageed, T.A., Elrys, A.S., Selim, S., Abd El-Hack, M.E., Kappachery, S., El-Tarabily, K.A., AbuQamar, S.F., 2023. Hazardous wastes and management strategies of landfill leachates: a comprehensive review. *Environmental Technology and Innovation*, [e-journal] 31. http://dx.doi.org/10.1016/j.eti.2023.103150.

El-Sappah, A.H., Zhu, Y., Huang, Q., Chen, B., Soaud, S.A., Abd Elhamid, M.A., Yan, K., Li, J. and El-Tarabily, K.A. 2024. Plants' molecular behavior to heavy metals: from criticality to toxicity. *Frontier in Plant Sciences*, 15. http://dx.doi.org/ 10.3389/fpls.2024.1423625.

Emamverdian, A., Ding, Y., Mokhberdoran, F., and Xie, Y., 2015. Heavy metal stress and some mechanisms of plant defense response. *The Scientific World Journal,* [e-journal] 2015. https://dx.doi.org/10.1155/2015/756120.

Enders, T.A., Frick, E.M. and Strader, L.C., 2017. An *Arabidopsis* kinase cascade influences auxin-responsive cell expansion. *The Plant Journal,* [e-journal] 92, pp.68–81. https://dx.doi.org/10.1111/tpj.13635.

Er, X.Y., Seow, T.W., Lim, C.K., Ibrahim, Z. and Mat Sarip, S.H., 2017. Biological treatment of closed landfill leachate treatment by using *Brevibacillus panacihumi* strain ZB1. *IOP Conference Series: Earth and Environmental Science,* [e-journal] 140. http://dx.doi.org/10.1088/1755-1315/140/1/012012.

Erdogan, R. and Zaimoglu, Z., 2015. The characteristics of phytoremediation of soil and leachate polluted by landfills. In: M. Shiomi, ed. 2014. *Advances in bioremediation of wastewater and polluted soil.* London: IntechOpen. pp.227–246.

Ergönül, M.B., Nassouhi, D. and Atasağun, S., 2020. Modeling of the bioaccumulative efficiency of Pistia stratiotes exposed to Pb, Cd, and Pb + Cd mixtures in nutrient-poor media. *International Journal of Phytoremediation*, [e-journal] 22(2), pp.201-209. https://dx.doi.org/10.1080/15226514.2019.1652566.

Ernst, W.H.O., Verkleij, J.A.C. and Schat, H., 1992. Metal tolerance in plants. *Acta Botanica Neerlandica*, [e-journal] 41, pp.229-248. https://dx.doi.org/10.1111/j.1438-8677.1992.tb01332.x.

Erses, A.S. and Onay, T.T., 2003. In situ heavy metal attenuation in landfills under methanogenic conditions. *Journal of Hazardous Materials,* [e-journal] 99(2), pp.159-175. https://dx.doi.org/10.1016/S0304-3894(02)00354-0.

Espinosa-Diez, C., Miguel, V., Mennerich, D., Kietzmann, T., Sánchez-Pérez, P., Cadenas, S. and Lamas, S., 2015. Antioxidant responses and cellular adjustments to oxidative stress. *Redox Biology,* [e-journal] 6, pp.183–197. https://dx.doi.org/10.1016/j.redox.2015.07.008.

Essien, J.P., Ikpe, D.I., Inam, E.D., Okon, A.O., Ebong, G.A. and Benson, N.U., 2022. Occurrence and spatial distribution of heavy metals in landfill leachates and

impacted freshwater ecosystem: an environmental and human health threat. *PLoS One*, [e-journal] 17(2). http://dx.doi,org/ 10.1371/journal.pone.0263279.

Ewe, H. Y., 2024. *Evaluation of the antioxidant acyivities and chlorophyll content in Pistia stratiotes upon heavy metal exposure*. Bachelor Degree. Universiti Tunku Abdul Rahman

Fabbrini, M.S., Katayama, M., Nakase, I. and Vago, R., 2017. Plant ribosome-inactivating proteins: progesses, challenges and biotechnological applications (and a few Digressions). *Toxins (Basel)*, [e-journal] 9(10). http://dx.doi.org/10.3390/toxins9100314.

Fàbregas, N., Yoshida, T. and Fernie, A.R., 2020. Role of Raf-like kinases in SnRK2 activation and osmotic stress response in plants. *Nature Communications*, [e-journal] 11(6184). https://dx.doi.org/10.1038/s41467-020-19977-2.

Fakih, Z., Plourde, M.B. and Germain, H., 2023. Differential participation of plant ribosomal proteins from the small ribosomal subunit in protein translation under stress. *Biomolecules*, [e-journal] 13(7). https://dx.doi.org/10.3390/biom13071160.

Fan, L., Li, R., Pan, J., Ding, Z. and Lin, J., 2015. Endocytosis and its regulation in plants. *Trends in Plant Science,* [e-journal] 20, pp.388–397. https://dx.doi.org/10.1016/j.tplants.2015.03.014.

Fan, L., Yuan, Q., Lu, Q., Zheng, C., Su, R., Liu, N. and Wu, J., 2024. Remediation of cadmium contaminated soil using electrokinetic-phytoremediation system with rotary switching electrodes. *Environmental Geochemistry and Health*, 46(375). https://dx.doi.org/10.1007/s10653-024-02162-5.

Fang, S., Zhao, P., Tan, Z., Peng, Y., Xu, L., Jin, Y., Wei, F., Guo, L. and Yao, X., 2022. Combining physio-biochemical characterization and transcriptome analysis reveal the responses to varying degrees of drought stress in *Brassica napus* L. *International Journal of Molecular Sciences*, [e-journal] 23. https://dx.doi.org/10.3390/ijms23158555.

Faria, J.M.S., Teixeira, D.M., Pinto, A.P., Brito, I., Barrulas, P., Alho, L. and Carvalho, M., 2020. Toxic levels of manganese in an acidic Cambisol alters antioxidant enzymes activity, element uptake and subcellular distribution in

Triticum aestivum. *Ecotoxicology and Environmental Safety,* [e-journal] 193. https://dx.doi.org/10.1016/j.ecoenv.2020.110355.

Farnese, F.S., Oliveira, J.A., Lima, F.S., Leão, G.A., Gusman, G.S. and Silva, L.C., 2014. Evaluation of the potential of *Pistia stratiotes* L. (water lettuce) for bioindication and phytoremediation of aquatic environments contaminated with arsenic. *Brazilian Journal of Biology,* [e-journal] 74(3 Suppl 1):S108-12. https://dx.doi.org/10.1590/1519-6984.01113.

Fedry, J., Silva, J., Vanevic, M., Fronik, S., Mechulam, Y., Schmitt, E., des Georges, A., Faller, W.J. and Förster, F., 2024. Visualization of translation reorganization upon persistent ribosome collision stress in mammalian cells. *Molecular Cell*, [e-journal] 84(6), pp.1078-1089.e4. https://dx.doi.org/10.1016/j.molcel.2024.01.015.

Feiguelman, G., Fu, Y. and Yalovsky, S., 2018. ROP GTPases structure-function and signaling pathways. *Plant Physiology*, [e-journal] 176(1), pp.57–79. https://dx.doi.org/10.1104/pp.17.01415.

Ferniza-García, F., Amaya-Chávez, A., Roa-Morales, G. and Barrera-Díaz, C.E**.,** 2017**.** Removal of Pb, Cu, Cd and Zn present in aqueous solution using coupled electrocoagulation-phytoremediation treatment**.** *International Journal of Electrochemistry*, [e-journal] 2017(1), pp.1-11. https://dx.doi.org/10.1155/2017/7681451.

Fidler, J., Graska, J., Gietler, M., Nykiel, M., Prabucka, B., Rybarczyk-Płońska, A., Muszyńska, E., Morkunas, I. and Labudda, M., 2022. PYR/PYL/RCAR receptors play a vital role in the abscisic-acid-dependent responses of plants to external or internal stimuli. *Cells*, [e-journal] 11(8). https://dx.doi.org/10.3390/cells11081352.

Foong, W. S., 2019. *Treatment of synthetic leachate via EAPR system and phytoremediation by water hyacinth (Eichhornia crassipes).* Bachelor Degree. Universiti Tunku Abdul Rahman

Forman, H.J. and Zhang, H., 2021. Targeting oxidative stress in disease: promise and limitations of antioxidant therapy. *Nature Reviews Drug Discovery,* [e-journal] 20(9), pp.689–709. https://dx.doi.org/10.1038/s41573-021-00233-1.

Forsyth, J.E., Saiful Islam, M., Parvez, S.M., Raqib, R., Sajjadur Rahman, M.,

Marie Muehe, E., Fendorf, S. and Luby, S.P., 2018. Prevalence of elevated blood lead levels among pregnant women and sources of lead exposure in rural Bangladesh: a case control study. *Environmental Research*, [e-journal] 166, pp.1-9. https://dx.doi.org/10.1016/j.envres.2018.04.019.

Fortin, C., 2024. Metal bioavailability in aquatic systems— beyond complexation and competition. *Frontiers in Environmental Chemistry*, [e-journal] 5. https://dx.doi.org/10.3389/fenvc.2024.1345484.

Freitas, C.D.T., Costa, J.H., Germano, T.A., de O Rocha, R., Ramos, M.V. and Bezerra, L.P., 2024. Class III plant peroxidases: from classification to physiological functions. *International Journal of Biological Macromolecules*, [e-journal] 263(Pt 1). https://dx.doi.org/10.1016/j.ijbiomac.2024.130306.

Fromont-Racine, M., Senger, B., Saveanu, C. and Fasiolo, F., 2003. Ribosome assembly in eukaryotes. *Gene*, [e-journal] 313, pp.17–42. https://dx.doi.org/10.1016/s0378-1119(03)00629-2.

Gancedo, J.M., 2013. Biological roles of cAMP: variations on a theme in the different kingdoms of life. *Biological Reviews*, [e-journal] 88, pp.645–668. https://dx.doi.org/10.1111/brv.12020.

Ganie, S.A., Mazumder, A., Kiran, K., Hossain, F., Sharma, R. and Mondal, T.K., 2020. Transcriptional dynamics of Zn-accumulation in developing kernels of maize reveals important Zn-uptake mechanisms. *Genomics*, [e-journal] 112(5), pp.3435–3447. https://dx.doi.org/10.1016/j.ygeno.2020.06.009.

Garcia, K.G.V., Mendes Filho, P.F., Pinheiro, J.I., do Carmo, J.F., Pereira, A.P.A., Martins, C.M., de Abreu, M.G.P. and Filho, J.S.O., 2020. Attenuation of manganese-induced toxicity in *Leucaena leucocephala* colonized by *Arbuscular Mycorrhizae*. *Water, Air and Soil Pollution*, [e-journal] 231. https://dx.doi.org/10.1007/s11270-019-4381-9.

Gasch, A.P. and Eisen, M.B., 2002. Exploring the conditional coregulation of yeast gene expression through fuzzy k-means clustering. *Genome Biology*, [e-journal] 3(11). https://dx.doi.org/10.1186/gb-2002-3-11-research0059.

Gaspar, T., Franck, T., Bisbis, B., Kevers, C., Jouve, L., Hausman, J.F. and

Dommes, J., 2002. Concepts in plant stress physiology. Application to plant tissue cultures. *Plant Growth Regulation*, [e-journal] 37, pp. 263-285. https://dx.doi.org/10.1023/A:1020835304842.

Gaur, A. and Adholeya, A., 2004. Prospects of arbuscular mycorrhizal fungi in phytoremediation of heavy metal contaminated soils. *Current Science*, [e-journal] 86, pp.528-534.

Gautam, K., Sharma, P., Dwivedi, S., Singh, A., Gaur, V.K., Varjani, S., Srivastava, J.K., Pandey, A., Chang, J.S. and Ngo, H.H., 2023. A review on control and abatement of soil pollution by heavy metals: emphasis on artificial intelligence in recovery of contaminated soil. *Environmental Research*, [e-journal] 225. https://dx.doi.org/10.x1016/j.envres.2023.115592.

Ge, Y., Tan, L., Wu, B., Wang, T., Zhang, T., Chen, H., Zou, M., Ma, F., Xu, Z. and Zhan, R., 2019. Transcriptome sequencing of different avocado ecotypes: *de novo* transcriptome assembly, annotation, identification and validation of EST-SSR markers. *Forests*, [e-journal] 10(5). https://dx.doi.org/10.3390/f10050411.

Ge, J., Tao, J., Zhao, J., Wu, Z., Zhang, H., Gao, Y., Tian, S., Xie, R., Xu, S. and Lu, L., 2022. Transcriptome analysis reveals candidate genes involved in multiple heavy metal tolerance in hyperaccumulator *Sedum alfredii*. *Ecotoxicology and Environmental Safety*, [e-journal] 241. https://dx.doi.org/10.1016/j.ecoenv.2022.113795.

Geisert, E.E. and Williams R.W., 2020. Using BXD mouse strains in vision research: a systems genetics approach. *Molecular Vision*, 26, pp.173–187.

Genchi, G., Sinicropi, M.S., Lauria, G., Carocci, A. and Catalano, A., 2020. The Effects of cadmium toxicity. *International Journal of Environmental Research and Public Health*, [e-journal] 17(11). https://dx.doi.org/10.3390/ijerph17113782.

Gerendas, J. and Sattelmacher, B., 1999. Influence of Ni supply on growth and nitrogen metabolism of *Brassica napus*L. grown with NH_4NO_3 or urea as n source. *Annals of Botany*, 83(1), pp.65-71. https://dx.doi.org/10.1006/anbo.1998.0789.

Ghifari, A.S., Saha, S. and Murcha, M.W., 2023. The biogenesis and regulation of

the plant oxidative phosphorylation system. *Plant Physiology*, [e-journal] 192(2), pp.728-747. https://dx.doi.org/10.1093/plphys/kiad108.

Ghosh, S., Bheri, M., Bisht, D. and Pandey, G.K., 2022. Calcium signaling and transport machinery: potential for development of stress tolerance in plants. *Current Plant Biology*, [e-journal] 29. http://dx.doi.org/10.1016/j.cpb.2022.100235.

Ghosh, B., Padhy, P.K., Niyogi, S., Patra, P.K. and Hecker, M., 2023. A comparative study of heavy metal pollution in ambient air and the health risks assessment in industrial, urban and semi-urban areas of west bengal, india: an evaluation of carcinogenic, non-carcinogenic, and additional lifetime cancer cases. *Environments*, [e-journal] 10(11). https://doi.org/10.3390/environments10110190

Gidudu, B. and Chirwa, E.M.N., 2022. The role of pH, electrodes, surfactants, and electrolytes in electrokinetic remediation of contaminated soil. *Molecules*, [e-journal] 27(21), 7381. https://dx.doi.org/10.3390/molecules27217381.

Gnirke, A., Melnikov, A., Maguire, J., Rogov, P., LeProust, E.M., Brockman, W., Fennell, T., Giannoukos, G., Fisher, S., Russ, C., Gabriel, S., Jaffe, D.B., Lander, E.S. and Nusbaum, C., 2009. Solution hybrid selection with ultra-long oligonucleotides for massively parallel targeted sequencing. *Nature Biotechnology*, [e-journal] 27(2), pp.182-9. http://dx.doi.org/10.1038/nbt.1523.

Gong, Y., Chen, J. and Pu, R., 2019. The enhanced removal and phytodegradation of sodium dodecyl sulfate (SDS) in wastewater using controllable water hyacinth. *International Journal of Phytoremediation*, [e-journal] 21(11), pp.1080–1089. http://dx.doi.org/10.1080/15226514.2019.1606779.

González, H., Fernández-Fuego, D., Bertrand, A. and González, A., 2019. Effect of pH and citric acid on the growth, arsenic accumulation, and phytochelatin synthesis in *Eupatorium cannabinum* L., a promising plant for phytostabilization. *Environmental Science and Pollution Research*, [e-journal] 26(25), pp.26242-26253. http://dx.doi.org/10.1007/s11356-019-05657-2.

González Besteiro, M.A. and Ulm, R., 2013. ATR and MKP1 play distinct roles in response to UV-B stress in *Arabidopsis*. *The Plant Journal*, [e-journal] 73(6), pp.1034-1043. https://dx.doi.org/10.1111/tpj.12095.

Goodwin, S.B. and Sutter, T., 2009. Microarray analysis of *Arabidopsis* genome response to aluminum stress. *Biologia Plantarum*, [e-journal] 53(1), pp.85-99. https://dx.doi.org/10.1007/s10535-009-0012-4

Goswami, K. and Sanan-Mishra, N., 2022. RNA-seq for revealing the function of the transcriptome. In: D.B. Singh and R.K. Pathak, eds. 2021. *Bioinformatics methods and applications*. Cambridge, Massachusetts: Academic Press. pp.105-129.

Götz, S., García-Gómez, J.M., Terol, J., Williams, T.D., Nagaraj, S.H., Nueda, M.J., Robles, M., Talón, M., Dopazo, J. and Conesa, A., 2008. High-throughput functional annotation and data mining with the Blast2GO suite. *Nucleic Acids Research*, [e-journal] 36(10), pp.3420-3435. http://dx.doi.org/10.1093/nar/gkn176.

Gratão, P.L., Polle, A., Lea, P.J. and Azevedo, R.A., 2005. Making the life of heavy metal-stressed plants a little easier. *Functional Plant Biology*, [e-journal] 32, 481-494. http://dx.doi.org/10.1071/FP05016.

Gray, W.M., 2004. Hormonal regulation of plant growth and development. *PLoS Biology*, [e-journal] 2(9). http://dx.doi.org10.1371/journal.pbio.0020311.

Greg, 2024. *Growth Rate of Water Lettuce*. [online] Available at: <https://greg.app/water-lettuce-lifecycle/?utm_source=chatgpt.com> [Accessed: 14 February 2026].

Grossule, V., Fang, D., Yue, D., Lavagnolo, M.C. and Raga, R., 2022. Preparation of artificial MSW leachate for treatment studies: Testing on black soldier fly larvae process. *Waste Management and Research: The Journal for a Sustainable Circular Economy*, [e-journal] 40(8), pp.1231-1241. https://dx.doi.org/10.1177/0734242X211066702

Grzelka, K., Matkowski, A. and Ślusarczyk, S., 2023. Electrostimulation improves plant growth and modulates the flavonoid profile in aeroponic culture of *Scutellaria baicalensis* Georgi. *Frontiers in Plant Science*, [e-journal] 14. https://dx.doi.org/10.3389/fpls.2023.1142624.

Gu, Y., Fu, Y., Dowd, P., Li, S., Vernoud, V., Gilroy, S. and Yang, Z., 2005. A Rho family GTPase controls actin dynamics and tip growth via two counteracting

downstream pathways in pollen tubes. *Journal of Cell Biology*, [e-journal] 169(1), pp.127-138. https://dx.doi.org/10.1083/jcb.200409140.

Guarino, F., Improta, G., Triassi, M., Cicatelli, A. and Castiglione, S., 2020a. Effects of zinc pollution and compost amendment on the root microbiome of a metal tolerant poplar clone. *Frontiers in Microbiology*, [e-journal] 11. https://dx.doi.org/10.3389/fmicb.2020.01677.

Guarino, F., Miranda, A., Castiglione, S. and Cicatelli, A., 2020b. Arsenic phytovolatilization and epigenetic modifications in Arundo donax L. assisted by a PGPR consortium. *Chemosphere*, [e-journal] 251. https://dx.doi.org/10.1016/j.chemosphere.2020.126310.

Gul, K. and Mumtaz, S., 2025. Nanosecond pulsed electric fields (nspefs) for precision intracellular oncotherapy: recent advances and emerging directions. *International Journal of Molecular Sciences*, [e-journal] 26(23). https://dx.doi.org/10.3390/ijms262311268.

Gulli, M., Marchi, L., Fragni, R., Buschini, A. and Visioli, G., 2018. Epigenetic modifications preserve the hyperaccumulator *Noccaea caerulescens* from Ni genotoxicity. *Environmental and Molecular Mutagenesis*, [e-journal] 59, pp.464–475. https://dx.doi.org/1010.1002/em.22191.

Gunarathne, V., Phillips, A.J., Zanoletti, A., Rajapaksha, A.U., Vithanage, M., Di Maria, F., Pivato, A., Korzeniewska, E. and Bontempi, E., 2024. Environmental pitfalls and associated human health risks and ecological impacts from landfill leachate contaminants: Current evidence, recommended interventions and future directions. *Science of the Total Environment*, [e-journal] 912. https://dx.doi.org/10.1016/j.scitotenv.2023.169026.

Guo, X., Liu, D. and Chong, K., 2018. Cold signaling in plants: insights into mechanisms and regulation. *Journal of Integrative Plant Biology*, [e-journal] 60(9), pp.745-756. https://dx.doi.org/10.1111/jipb.12706.

Guo, J., Huang, Z., Sun, J., Cui, X. and Liu, Y., 2021. Research progress and future development trends in medicinal plant transcriptomics. *Frontiers in Plant Science*, [e-journal] 12. https://dx.doi.org/10.3389/fpls.2021.691838.

Gupta, V., Jatav, P.K., Verma, R., Kothari, S.L. and Kachhwaha, S., 2017. Nickel accumulation and its effect on growth, physiological and biochemical parameters in millets and oats. *Environmental Science and Pollution Research*, [e-journal] 24, pp.23915–23925. https://dx.doi.org/10.1007/s11356-017-0057-4.

Gupta, M., Dwivedi, V., Kumar, S., Patel, A., Niazi, P. and Yadav, V.K., 2024. Lead toxicity in plants: mechanistic insights into toxicity, physiological responses of plants and mitigation strategies. *Plant Signaling and Behavior*, [e-journal] 19(1). https://dx.doi.org/10.1080/15592324.2024.2365576.

Güvenç, S.Y. and Güven, E.C., 2019. Pretreatment of food industry wastewater by coagulation: process modeling and optimization. *Celal Bayar University Journal of Science*, [e-journal] 15(3), pp.307–316. https://dx.doi.org/10.18466/cbayarfbe.581611.

Gworek, B., Dmuchowski, W., Koda, E., Marecka, M., Baczewska, A.H., Brągoszewska, P., Sieczka, A. and Osiński, P., 2016. Impact of the municipal solid waste Łubna landfill on environmental pollution by heavy metals. *Water*, [e-journal] 8(10). https://dx.doi.org/10.3390/w8100470.

Haak, D.C., Fukao, T., Grene, R., Hua, Z., Ivanov, R., Perrella, G. and Li, S., 2017. Multilevel regulation of abiotic stress responses in plants. *Frontier in Plant Science*, [e-journal] 8. https://dx.doi.org/10.3389/fpls.2017.01564.

Haberkorn, I., Siegenthaler, L., Buchmann, L., Neutsch, L. and Mathys, A., 2021. Enhancing single-cell bioconversion efficiency by harnessing nanosecond pulsed electric field processing. *Biotechnology Advances*, [e-journal] 53. https://dx.doi.org/10.1016/j.biotechadv.2021.107780.

Habermann, E., Crowell, K. and Janicki, P., 1983. Lead and other metals can substitute for Ca^{2+} in calmodulin. *Archives of Toxicology*, [e-journal] 54, pp.61–70. https://dx.doi.org/10.1007/BF00277816.

Hagenfeld, D., Schulz, T., Ehling, P., Budde, T., Schumacher, U. and Prehm, P., 2010. Depolarization of the membrane potential by hyaluronan. *Journal of Cellular Biochemistry*, [e-journal] 111(4), pp.858–864. https://dx.doi.org/10.1002/jcb.22772.

Haider, F.U., Liqun, C., Coulter, J.A., Cheema, S.A., Wu, J., Zhang, R., Wenjun, M. and Farooq, M. 2021. Cadmium toxicity in plants: impacts and remediation strategies. *Ecotoxicology and Environmental Safety,* [e-journal] 211. https://dx.doi.org/10.1016/j.ecoenv.2020.111887.

Hajirezaei, M., Peisker, M., Tschiersch, H., Palatnik, J.F., Valle, E.M., Carrillo, N. and Sonnewald, U., 2002. Small changes in the activity of chloroplastic $NADP^+$-dependent ferredoxin oxidoreductase lead to impaired plant growth and restrict photosynthetic activity of transgenic tobacco plants. *Plant Journal*, [e-journal] 29, pp.281–293. https://dx.doi.org/10.1046/j.0960-7412.2001.01209.x.

Hansel, C.M., Fendorf, S., Sutton, S. and Newville, M., 2001. Characterization of Fe plaque and associated metals on the roots of mine-waste impacted aquatic plants. *Environmental Science and Technology*, [e-journal] 35, pp.3863–3868. https://dx.doi.org/10.1021/es0105459.

Haque, M.A., 2016. Assessment of nickel leaching phenomena from landfill waste mixed paving block for eco-friendly field ppplication. J*ournal of Cleaner Production*, [e-journal] 139, pp.99-112. https://dx.doi.org/10.1016/j.jclepro.2016.08.028.

Hart, F.X. and Palisano, J.R., 2018. The application of electric fields in biology and medicine. In: M.S. Kandelousi, ed. 2018. *Electric field.* London: IntechOpen. http://dx.doi.org/10.5772/intechopen.71683.

Hasanuzzaman, M., Bhuyan, M.H.M.B., Zulfiqar, F., Raza, A., Mohsin, S.M., Mahmud, J.A., Fujita, M. and Fotopoulos, V., 2020. Reactive oxygen species and antioxidant defense in plants under abiotic stress: revisiting the crucial role of a universal defense regulator. *Antioxidants (Basel),* [e-journal] 9(8). https://dx.doi.org/10.3390/antiox9080681.

Hasanzadeh, M. and Hazrati, N., 2021. Calcium sensing and signaling in plants during metal/metalloid stress. In: A. Roychoudhury, D.K. Tripathi and R. Deshmukh, eds. 2021. *Metal and nutrient transporters in abiotic stress.* Amsterdam: Elsevier. pp.169–197.

Hasnaoui, S.E., Fahr, M., Zouine, M. and Smouni, A., 2022. *De novo* transcriptome assembly, gene annotations, and characterization of functional profiling reveal key genes for lead alleviation in the Pb hyperaccumulator greek mustard (*Hirschfeldia*

incana L.). *Current Issues in Molecular Biology*, [e-journal] 44(10), pp.4658-4675. https://dx.doi.org/10.3390/cimb44100318.

Hassan, M.U., Chattha, M.U., Khan, I., Chattha, M.B., Aamer. M., Nawaz, M., Ali, A., Khan, M.A.U. and Khan, T.A., 2019. Nickel toxicity in plants: reasons, toxic effects, tolerance mechanisms, and remediation possibilities—a review. *Environmental Science and Pollution Research*, [e-journal] 26, pp.12673–12688. https://dx.doi.org/10.1007/s11356-019-04892-x.

Hassan, I., Chowdhury, S.R., Prihartato, P.K., and Razzak, S.A., 2021. Wastewater treatment using constructed wetland: current trends and future potential. *Processes*, [e-journal] 9. https://dx.doi.org/10.3390/pr9111917.

Hazardous Waste Experts, 2019. *A brief primer on hazardous waste landfills*. [online]. Available at: <https://www.hazardouswasteexperts.com/a-brief-primer-on-hazardous-waste-landfills> [Accessed: 1 August 2024).

He, R., Xi, G. and Liu, K., 2017. Alleviating effect of extremely low frequency pulsed electric field on drought damage of maize seedling roots. *Journal of Luminescence*, [e-journal] 188, pp.441–447. https://dx.doi.org/10.1016/j.jlumin.2017.04.042.

He, H., Ma, H. and Liu, L., 2020. Combined photocatalytic preoxidation reactor and sequencing batch bioreactor for advanced treatment of industrial wastewater. *Journal of Water Process Engineering*, [e-journal] 36. https://dx.doi.org/10.1016/j.jwpe.2020. 101259.

He, Y., Langenhoff, A.A.M., Sutton, N.B., Rijnaarts, H.H.M., Blokland, M.H., Chen, F., Huber, C. and Schröder, P., 2017. Metabolism of ibuprofen by *Phragmites australis*: uptake and phytodegradation. *Environmental Science and Technology*, [e-journal] 51(8), pp.4576-4584. http://dx.doi.org/10.1021/acs.est.7b00458.

He, Y., Huang, H., Li, L.H. and Yang, X., 2018. Label-free proteomics of Tilapia fillets and their relationship with meat texture during post-mortem storage. *Food Analytical Methods*, [e-journal] 11(11), pp.3023-3033. http://dx.doi.org/10.1007/s12161-018-1273-3.

He, X., Wang, C., Wang, H., Li, L. and Wang, C., 2020. The Function of MAPK cascades in response to various stresses in horticultural plants. *Frontier in Plant Science*, [e-journal] 11. https://dx.doi.org/10.3389/fpls.2020.00952.

He, H., Yang, M., Li, S., Zhang, G., Ding, Z., Zhang, L., Shi, G. and Li, Y., 2023. Mechanisms and biotechnological applications of transcription factors. *Synthetic and Systems Biotechnology*, [e-journal] 8(4), pp.565-577. https://dx.doi.org/10.1016/j.synbio.2023.08.006.

Hemmerlé, A., Fragneto, G., Daillant, J. and Charitat, T., 2016. Reduction in tension and stiffening of lipid membranes in an electric field revealed by X-Ray scattering. *Physical Review Letters*, [e-journal] 116(22). https://dx.doi.org/10.1103/physrevlett.116.228101.

Henry-Silva, G.G., Camargo, A.F.M. and Pezzato, M.M., 2008. Growth of free-floating aquatic macrophytes in different concentrations of nutrients. *Hydrobiologia*, [e-journal] 610, pp.153–160. https://dx.doi.org/10.1007/s10750-008-9430-0.

Hidayati, N. and Rini, D.S., 2020. Evaluation of wild plants as lead (Pb) and cadmium (Cd) accumulators for phytoremediation of contaminated rice fields. Biodiversitas Journal of Biological Diversity, [e-journal] 21(5), pp.1928-1934. https://doi.org/10.13057/biodiv/d210520

Hildebrandt, T.M., Nunes Nesi, A., Araújo, W.L. and Braun, H.P., 2015. Amino acid catabolism in plants. *Molecular Plant*, [e-journal] 8(11), pp.1563-1579. https://dx.doi.org/10.1016/j.molp.2015.09.005.

Hodko, D., Van Hyfte, J., Denvir, A. and Magnuson, J.W., Lynntech Coatings Ltd., 2000. *Methods for enhancing phytoextraction of contaminants from porous media using electrokinetic phenomena*. U.S. Pat. 6,145,224.

Honaas, L.A., Wafula, E.K., Wickett, N.J., Der, J.P., Zhang, Y., Edger, P.P., Altman, N.S., Pires, J.C., Leebens-Mack, J.H. and dePamphilis, C.W., 2016. Selecting superior *de novo* transcriptome assemblies: lessons learned by leveraging the best plant genome. *PLoS ONE*, [e-journal] 11(1). http://dx.doi.org/10.1371/journal.pone.0146062.

Hori, T., Sasaki, D., Haruta, S., Shigematsu, T., Ueno, Y., Ishii, M. and Igarashi, Y., 2011. Detection of active, potentially acetate-oxidizing syntrophs in an anaerobic digester by flux measurement and formyltetrahydrofolate synthetase (FTHFS) expression profiling. *Microbiology (Reading)*, [e-journal] 157(Pt 7), pp.1980-1989. http://dx.doi.org/10.1099/mic.0.049189-0.

Horiguchi, G., Van Lijsebettens, M., Candela, H., Micol, J.L. and Tsukaya, H., 2012. Ribosomes and translation in plant developmental control. *Plant Science*, [e-journal] 191, pp.192:24-34. http://dx.doi.org/10.1016/j.plantsci.2012.04.008.

Horiunova, I.I., Krasylenko, Y.A., Yemets, A.I. and Blume, Y.B., 2016. Involvement of plant cytoskeleton in cellular mechanisms of metal toxicity. *Cytology and Genetics*, 50(1), pp.57–67.

Horning, K.J., Caito, S.W., Tipps, K.G., Bowman, A.B. and Aschner, M. 2015. Manganese is essential for neuronal health. *Annual Review of Nutrition*, [e-journal] 35, pp.71–108. https://dx.doi.org/10.1146/annurev-nutr-071714-034419.

Hossain, M.A., Pukclai, P., Silva, J.T. and Fujita, M., 2012. Molecular mechanism of heavy metal toxicity and tolerance in plants: central role of glutathione in detoxification of reactive oxygen species and methylglyoxal and in heavy metal chelation. *Journal of Botany*, [e-journal] 2012, pp.1-37. https://dx.doi.org/10.1155/2012/872875.

Hosseini Beinabaj, S.M., Heydariyan, H., Mohammad Aleii, H. and Hosseinzadeh, A., 2023. Concentration of heavy metals in leachate, soil, and plants in Tehran's landfill: Investigation of the effect of landfill age on the intensity of pollution. *Heliyon.* [e-journal] 9(1). https://dx.doi.org/10.1016/j.heliyon.2023.e13017.

Hou, L., Ji, S., Zhang, Y., Wu, X., Zhang, L. and Liu, P., 2023a. The mechanism of silicon on alleviating cadmium toxicity in plants: a review. *Frontiers in Plant Science*, [e-journal] 14. https://dx.doi.org/10.3389/fpls.2023.1141138.

Hou, D., Al-Tabbaa, A., O'Connor, D., Hu, Q., Zhu, Y.-G., Wang, L., Kirkwood, N., Yong, S.O., Tsang, D.C.W., Bolan, N.S. and Rinklebe, J., 2023b. Sustainable remediation and redevelopment of brownfield sites. *Nature Reviews Earth and Environment*, [e-journal] 4, pp.271–286. http://dx.doi.org/10.1038/s43017-023-00404-1.

Hredoy, R.H., Siddique, M.A.B., Akbor, M.A., Shaikh, M.A.A. and Rahman, M.M., 2022. Impacts of landfill leachate on the surrounding environment: a case study on Amin Bazar landfill, Dhaka (Bangladesh). *Soil System*, [e-journal] 6(90). https://dx.doi.org/10.3390/soilsystems6040090.

Hu, B., Deng, F., Chen, G., Chen, X., Gao, W., Long, L., Xia, J. and Chen, Z.H., 2020. Evolution of abscisic acid signaling for stress responses to toxic metals and metalloids. *Frontier in Plant Science*, [e-journal] 11. https://dx.doi.org/10.3389/fpls.2020.00909.

Huang, T.L. and Huang, H.J., 2008. ROS and CDPK-like kinase-mediated activation of MAP kinase in rice roots exposed to lead. *Chemosphere*, [e-journal] 71(7), pp.1377-1385. https://dx.doi.org/10.1016/j.chemosphere.2007.11.031.

Huang, X.D., El-Alawi, Y., Penrose, D.M., Glick, B.R. and Greenberg, B.M., 2004. Responses of three grass species to creosote during phytoremediation. *Environmental Pollution*, [e-journal] 130(3), pp.453–463. https://dx.doi.org/10.1016/j.envpol.2003.12.018.

Huang, H., Ullah, F., Zhou, D.X., Yi, M. and Zhao, Y., 2019. Mechanisms of ROS regulation of plant development and stress responses. *Frontiers in Plant Science*, [e-journal] 10. https://dx.doi.org/10.3389/fpls.2019.00800.

Huang, X., Zhu, F., He, Z., Chen, X., Wang, G., Liu, M., Xu H. 2020a. Photosynthesis performance and antioxidative enzymes response of *Melia azedarach* and *Ligustrum lucidum* plants under Pb-Zn Mine tailing conditions. *Frontiers in Plant Science*, [e-journal] 11. https://dx.doi.org/10.3389/fpls.2020.571157.

Huang, X., Zhou, Y., Shi, X., Wen, J., Sun, Y., Chen, S., Hu, T., Li, R., Wang, J. and Jia, X., 2024. PfbZIP85 transcription factor mediates ω-3 fatty acid-enriched oil biosynthesis by down-regulating *PfLPAT1B* gene expression in plant tissues. *International Journal of Molecular Science*, [e-journal] 25(8). https://dx.doi.org/10.3390/ijms25084375.

Hussain, S., Khan, M., Sheikh, T.M.M., Mumtaz, M.Z., Chohan, T.A., Shamim, S. and Liu, Y., 2022. Zinc essentiality, toxicity, and its bacterial bioremediation: a comprehensive insight. *Frontiers in Microbiology*, [e-journal] 13. https://dx.doi.org/10.3389/fmicb.2022.900740.

Hussein, M., Yoneda, K., Mohd-Zaki, Z., Amir, A. and Othman, N., 2021. Heavy metals in leachate, impacted soils and natural soils of different landfills in Malaysia: an alarming threat. *Chemosphere*, [e-journal] 267. https://dx.doi.org/10.1016/j.chemosphere.2020.128874.

Iber, B.T. and Kasan, N.A., 2021. Recent advances in shrimp aquaculture wastewater management. *Heliyon*, [e-journal] 7(11). https://dx.doi.org/10.1016/j.heliyon.2021.e08283.

Ikram, M., Batool, M., Ullah, M., Khalid, B., El-Badri, A.M., Mohamed, I.A.A., Zhang, L., Kuai, J., Xu, Z., Zhao, J., Wang, J., Wang, B., Zhou, G. and Rehman, H.U., 2025. Molecular alchemy: converting stress into resilience via secondary metabolites and calcium signaling in rice. *Rice*, [e-journal] 18(1):32. https://dx.doi.org/10.1186/s12284-025-00783-7.

International Lead and Zinc Study Group, 2020. *ILZSG Session/Forecasts, 2020 Minerals Yearbook.* [pdf] Lisbon: International Lead and Zinc Study Group. Available at: <http:// https://www.ilzsg.org/> [Accessed 10 October 2023].

Iorhemen, O.T., Hamza, R.A. and Tay, J.H., 2016 Membrane bioreactor (MBR) technology for wastewater treatment and reclamation: membrane fouling. *Membranes*, [e-journal] 6(2). https://dx.doi.org/10.3390/membranes6020033.

Irfan, E.A., Sermin, A. and Kadir, Y., 2010. Response of tomato (*Solanum lycopersicum* L.) to lead toxicity: growth, element uptake, chlorophyll and water content. *African Journal of Agricultural Research,* [e-journal] 5, pp.416-423. https://dx.doi.org/10.5897/AJAR.

Jahng, Y. and Park, J.G., 2018. Recent studies on cyclic 1,7-diarylheptanoids: their isolation, structures, biological activities, and chemical synthesis. *Molecules*, [e-journal] 23. https://dx.doi.org/10.3390/molecules23123107.

Jalmi, S.K., Bhagat, P.K., Verma, D., Noryang, S., Tayyeba, S., Singh, K., Sharma, D. and Sinha, A.K., 2018. Traversing the links between heavy metal stress and plant signaling. *Frontiers in Plant Science,* [e-journal] 9. https://dx.doi.org/10.3389/fpls.2018.00012.

Jamla, M., Khare, T., Joshi, S., Patil, S., Penna, S. and Kumar, V., 2021. Omics approaches for understanding heavy metal responses and tolerance in plants. *Current Plant Biology*, [e-journal] 27. https://dx.doi.org/10.1016/j.cpb.2021.100213

Jan, R., Asaf, S., Numan, M., Lubna and Kim, K.-M., 2021. Plant secondary metabolite biosynthesis and transcriptional regulation in response to biotic and abiotic stress conditions. *Agronomy*, [e-journal] 11(5). https://dx.doi.org/10.3390/agronomy11050968.

Jaradat, A.Q., Telfah, D.B. and Ismail, R., 2024. Heavy metals removal from landfill leachate by coagulation/flocculation process combined with continuous adsorption using eggshell waste materials. *Water, Science and Technology*, [e-journal] 84(12), pp.3817-3832. http://dx.doi.org/10.2166/wst.2021.493.

Jarin, A.S., Khan, M.A.R., Apon, T.A., Islam, M.A., Rahat, A., Akter, M., Anik, T.R., Nguyen, H.M., Nguyen, T.T., Ha, C.V. and Tran, L.P. 2025. Plant responses to heavy metal stresses: mechanisms, defense strategies, and nanoparticle-assisted remediation. *Plants (Basel)*, [e-journal] 14(24):3834. https://dx.doi.org/ 10.3390/plants14243834.

Jayanthi, B., Emenike, C.U., Agamuthu, P., Simarani, K., Mohamad, S. and Fauziah, S.H., 2016. Selected microbial diversity of contaminated landfill soil of Peninsular Malaysia and the behavior towards heavy metal exposure. *Catena*, [e-journal] 147, pp.25-31. https://dx.doi.org/10.1016/j.catena.2016.06.033.
Jayanthi-Rao, D., 2019. *The study of antioxidative enzymes (Ascorbate peroxidase and peroxidase) on Eichhornia crassipes for phytoremediation.* Bachelor Degree. Universiti Tunku Abdul Rahman.

Jayawardhana, Y., Mayakaduwa, S., Kumarathilaka, P., Gamage, S. and Vithanage, M., 2017. Municipal solid waste-derived biochar for the removal of benzene from landfill leachate. *Environmental Geochemistry and Health*, [e-journal] 41, pp.1739–1753. http://dx.doi.org/10.1007/s10653-017-9973-y.

Jeyasundar, P.G.S.A., Ali, A., Azeem, M., Li, Y., Guo, D., Sikdar, A., Abdelrahman, H., Kwon, E., Antoniadis, V., Mani, V.M., Shaheen, S.M., Rinklebe, J. and Zhang, Z., 2021. Green remediation of toxic metals contaminated mining soil using bacterial consortium and *Brassica juncea*. *Environmental Pollution*, [e-journal] 277. http://dx.doi.org/10.1016/j.envpol.2021.116789.

Ji, X.-J., Mao, X., Hao, Q.-T., Liu, B.-L., Xue, J.-A. and Li, R.-Z., 2018. Splice variants of the castor *WRI1* gene upregulate fatty acid and oil biosynthesis when expressed in tobacco leaves. *International Journal of Molecular Sciences*, [e-journal] 19(1). https://dx.doi.org/10.3390/ijms19010146.

Jiang, H.S., Liao, Z.Y. and Li, W., 2023. Photosynthetic inorganic carbon utilization strategies and their ecological adaptability in aquatic plants. *Plant Science*, [e-journal] 41, pp.847–856. https://dx.doi.org/10.11913/PSJ.2095-0837.23171.

Jiang, Y., Wen, M., Sun, Y., Liu, P., Ma, Y., Zhang, C. and Zhang, X., 2025. Effectiveness and remediation mechanisms of geo-electrochemical technology for arsenic removal in paddy soil from northern Guangxi. *Toxics*, [e-journal] 13(9). https://dx.doi.org/10.3390/toxics13090728.

Jiao, L., Liu, Y., Yu, X.Y., Pan, X., Zhang, Y., Tu, J., Song, Y.H. and Li, Y., 2023. Ribosome biogenesis in disease: new players and therapeutic targets. *Signal Transduction and Targeted Therapy*, [e-journal] 8(1):15. https://dx.doi.org/10.1038/s41392-022-01285-4.

Jiao, R., He, P., Bakpa, E.P., Liao, L., Li, Q., Wu, B. and Liu, H., 2024. Different shifts in growth-defense tradeoff for above- and belowground of *Miscanthus floridulus* enhance tolerance to cadmium. *Environmental and Experimental Botany*, [e-journal] 226. https://dx.doi.org/10.1016/j.envexpbot.2024.105951.

Jin, X.C. and Wu, W.H., 1999. Involvement of cyclic AMP in ABA- and Ca^{2+}-mediated signal transduction of stomatal regulation in *Vicia faba*. *Plant and Cell Physiology*, [e-journal] 40, pp.1127–1133. https://dx.doi.org/10.1093/oxfordjournals.pcp.a029497.

Jo, S., Kadam, R., Jang, H., Seo, D. and Park, J., 2024. Recent advances in wastewater electrocoagulation technologies: beyond chemical coagulation. *Energies*, [e-journal] 17(23). https://dx.doi.org/10.3390/en17235863.

Johns, S., Hagihara, T., Toyota, M. and Gilroy, S., 2021. The fast and the furious: Rapid long-range signaling in plants. *Plant Physiology*, 185, pp.694–706.

Johnson F. M., 1998. The genetic effects of environmental lead, *Mutation Research*, [e-journal] 410(2), pp. 123–140. https://dx.doi.org/10.1016/S1383-5742(97)00032-X.

Jonak, C., Nakagami, H. and Hirt, H., 2004. Heavy metal stress. Activation of distinct mitogen-activated protein kinase pathways by copper and cadmium. *Plant Physiology*, [e-journal] 136(2), pp.3276-3283. https://dx.doi.org/10.1104/pp.104.045724.

Jouili, H., Bouazizi, H., and El Ferjani, E., 2011. Plant peroxidases: biomarkers of metallic stress. *Acta Physiologiae Plantarum*, [e-journal] 33, pp.2075-2082. https://dx.doi.org/10.1007/s11738-011-0780-2.

Jovanić, B.R., Belča, I. and Kasalica, B., 2001. Effect of a high DC electric field on plant leaves reflectivity. *International Journal of Environmental Studies*, [e-journal] 58(3), pp.357–363. https://dx.doi.org/10.1080/00207230108711337.

Jyothi, N.R., 2021. Heavy metal sources and their effects on human health. In: M.K. Nazal and H. Zhao, eds. 2020. *Heavy metals - their environmental impacts and mitigation.* London: IntechOpen. http://dx.doi.org/10.5772/intechopen.95370.

Kafle, A., Timilsina, A., Gautam, A., Adhikari, K., Bhattarai, A. and Aryal, N., 2022. Phytoremediation: mechanisms, plant selection and enhancement by natural and synthetic agents. *Environmental Advances*, [e-journal] 8. https://dx.doi.org/10.1016/j.envadv.2022.100203.

Kafle, S., Karki, B. K., Sakhakarmy, M. and Adhikari, S., 2025. A review of global municipal solid waste management and valorization pathways. *Recycling*, [e-journal] 10(3). https://dx.doi.org/10.3390/recycling10030113.
Kalve, S., Vos, D.D. and Beemster, G.T.S., 2014. Leaf development: a cellular perspective. *Frontiers in Plant Science*, [e-journal] 5. https://dx.doi.org/10.3389/fpls.2014.00362.

Kamaruddin, M.A., Yusoff, M.S., Rui, L.M., Isa, A.M., Zawawi, M.H., and Alrozi, R., 2017. An overview of municipal solid waste management and landfill leachate treatment: Malaysia and Asian perspectives. *Environmental Science and Pollution Research*, [e-journal] 24 (5), pp.26988-27020. https://dx.doi.org/10.1007/s11356-017-0303-9.

Kanduc, D., Mittelman, A., Serpico, R., Sinigaglia, E., Sinha, A.A., Natale, C., Santacroce, R., Di Corcia, M.G., Lucchese, A., Dini, L., Pani, P., Santacroce, S., Simone, S., Bucci, R. and Farber, E., 2002. Cell Death: apoptosis versus necrosis (review*).* *International Journal of Oncology,* [e-journal] 21, pp.165–170. https://dx.doi.org/10.3892/ijo.21.1.165.

Kanmani, S. and Gandhimathi, R., 2013. Assessment of heavy metal contamination in soil due to leachate migration from an open dumping site. *Applied Water Science*, [e-journal] 3, pp. 193-205. https://dx.doi.org/10.1007/s13201-012-0072-z.

Kanu, A.S., Ashraf, U., Mo, Z., Sabir, S.U.R., Baggie, I., Charley, C.S. and Tang, X., 2019. Calcium amendment improved the performance of fragrant rice and reduced metal uptake under cadmium toxicity. *Environmental Science and Pollution Research*, [e-journal] 26, pp.24748–24757. https://dx.doi.org/10.1007/s11356-019-05779-7.

Karanja, B.K., Fan, L., Xu, L., Wang, Y., Zhu, X., Tang, M., Wang, R., Zhang, F., Muleke, E.M. and Liu, L., 2017. Genome-wide characterization of the *WRKY* gene family in radish (*Raphanus sativus* L.) reveals its critical functions under different abiotic stresses. *Plant Cell Reports*, [e-journal] 36, pp.1757–1773. https://dx.doi.org/10.1007/s00299-017-2190-4.

Karcz, W. and Burdach, Z., 2022. The effect of DC electric field on the elongation growth, proton extrusion and membrane potential of *Zea mays* L. coleoptile cells; a laboratory study. *BMC Plant Biology,* [e-journal] 22(389). https://dx.doi.org/10.1186/s12870-022-03778-4.

Karimian, P., Trusov, Y. and Botella, J.R., 2024. Conserved role of heterotrimeric G proteins in plant defense and cell death progression. *Genes,* [e-journal] 15. https://dx.doi.org/10.3390/genes15010115.

Kashani, M.R.K., Wang, Q., Khatebasreh, M., Li, X., Sheikh Asadi, A.M., Boczkaj, G. and Ghanbari, F., 2023. Sequential treatment of landfill leachate by electrocoagulation/aeration, PMS/ZVI/UV and electro-Fenton: Performance, biodegradability and toxicity studies. *Journal of Environmental Management*, [e-journal] 338. https://dx.10.1016/j.jenvman.2023.117781.

Kasri, N.N., Parys, J.B., Callewaert, G., Missiaen, L. and De Smedt, H., 2004. Calmodulin and calcium-release channels. *Biological Research*, [e-journal] 37(4), pp.577-582. https://dx.doi.org/10.4067/s0716-97602004000400011.

Kaur, H. and Garg, N., 2021. Zinc toxicity in plants: a review. *Planta*, [e-journal] 253(129). https://dx.doi.org/10.1007/s00425-021-03642-z.

Kaur, S., Prakash, P., Bak, D.H., Hong, S.H., Cho, C., Chung, M.S., Kim, J.H., Lee, S., Bai, H.W., Lee, S.Y., Chung, B.Y. and Lee, S.S., 2021. Regulation of dual activity of ascorbate peroxidase 1 from *Arabidopsis thaliana* by conformational changes and posttranslational modifications. *Frontier in Plant Science*, [e-journal] 12. https://dx.doi.org/10.3389/fpls.2021.678111.

Kawamoto, N., Sasabe, M., Endo, M., Machida, Y. and Araki, T., 2015. Calcium-dependent protein kinases responsible for the phosphorylation of a bZIP transcription factor FD crucial for the florigen complex formation. *Scientific Reports*, [e-journal] 5. https://dx.doi.org/10.1038/srep08341.

Kaza, S., Yao, L., Bhada-Tata, P. and Van Woerden, F., 2018. *What a waste 2.0: a global snapshot of solid waste management to 2050.* Washington, DC: World Bank Publications.

Kazmi, A., Li, G., Yang, J., Zhao, X., Islam, M.F., Li, X., Kimura, S. and Hou, H., 2025. Cadmium stress alters heterophylly, anatomy, and photosynthetic activity of Hygrophila difformis. *Ecotoxicology and Environmental Safety*, [e-journal] 302. https://dx.doi.org/ 10.1016/j.ecoenv.2025.118685.

Kebert, M., Kostić, S., Vuksanović, V., Gavranović Markić, A., Kiprovski, B., Zorić, M. and Orlović, S., 2022. Metal- and organ-specific response to heavy metal-induced stress mediated by antioxidant enzymes' activities, polyamines, and plant hormones levels in *Populus deltoides*. *Plants*, [e-journal] 11(23). https://dx.doi.org/10.3390/plants11233246.

KEGG BRITE Database, 2025. *Functional hierarchies of biological entities*. [online] Available at: <http://www. https://www.genome.jp/kegg/brite.html > [Accessed 10 October 2023].

Kessouri, P., Furman, A., Huisman, J.A., Martin, T., Mellage, A., Ntarlagiannis, D., Bücker, M.B., Ehosioke, S., Fernandez, P., Flores-Orozco, A., Kemna, A.,

Nguyen, F., Pilawski, T., Saneiyan, S., Schmutz, M., Schwartz, N., Weigand, M., Wu, Y., Zhang, C. and Placencia-Gomez, E., 2019. Induced polarization applied to biogeophysics: Recent advances and future prospects. *Near Surface Geophysics,* [e-journal] 17, pp.595–621. https://dx.doi.org/10.1002/nsg.12072.

Keyster, M., Niekerk, L.A., Basson, G., Carelse, M., Bakare, O., Ludidi, N., Klein, A., Mekuto, L. and Gokul, A., 2020. Decoding heavy metal stress signalling in plants: towards improved food security and safety. *Plants*, [e-journal] 9(12). https://dx.doi.org/10.3390/plants9121781.

Kfoury, B., Rodrigues, W.F.C., Kim, S.J., Brandizzi, F. and Del-Bem, L.E., 2024. Multiple horizontal gene transfer events have shaped plant glycosyl hydrolase diversity and function. *New Phytologist*, [e-journal] 242(2), pp.809-824. https://dx.doi.org/10.1111/nph.19595.

Khaliq, S., Iqbal, M., Yaseen, W. and Rasheed, R., 2021. The exogenous menadiol diacetate enhances growth and yield by reducing Pb uptake, translocation and its toxicity through tissue nutrients acquisition in cucumber (*Cucumis sativus* L.). *Environmental Technology and Innovation,* [e-journal] 23. https://dx.doi.org/10.1016/j.eti.2021.101666.

Khan, M.A., Gemenet, D.C. and Villordon, A., 2016. Root system architecture and abiotic stress tolerance: current knowledge in root and tuber crops. *Frontiers in Plant Science,* [e-journal] 7. https://dx.doi.org/10.3389/fpls.2016.01584.

Khanam, R., Kumar, A., Nayak, A.K., Shahid, M., Tripathi, R., Vijayakumar, S., Bhaduri, D., Kumar, U., Mohanty, S., Panneerselvam, P., Chatterjee, D., Satapathy, B.S. and Pathak, H., 2020. Metal(loid)s (As, Hg, Se, Pb and Cd) in paddy soil: bioavailability and potential risk to human health. *Science of the Total Environment*, [e-journal] 699. https://dx.doi.org/10.1016/j.scitotenv.2019.134330

Khoo, K.S., Tan, X., Show, P.L., Pal, P., Juan, J.C., Ling, T.C., Ho, S.H. and Nguyen, T.H.P., 2020. Treatment for landfill leachate via physicochemical approaches: an overview. *Chemical and Biochemical Engineering Quarterly*, [e-journal] 34(1), pp.1-24. https://dx.doi.org/10.15255/CABEQ.2019.1703.

Kidwai, M., Ahmad, I.Z. and Chakrabarty, D., 2020. Class III peroxidase: an indispensable enzyme for biotic/abiotic stress tolerance and a potent candidate for crop improvement. *Plant Cell Reports,* [e-journal] 39, pp.1381-1393.

https://dx.doi.org/10.1007/s00299-020-02588-y.

Kim, Y., Yang Y. and Lee, Y., 2002. Pb and Cd uptake in rice roots. *Physiologia Plantarum*, [e-journal] 116, pp.368–372. https://dx.doi.org/10.1034/j.1399-3054.2002.1160312.x.

Kim, W.S., Jeon, E.K., Jung, J.M., Jung, H.B., Ko, S.H., Seo, C.I. and Baek, K., 2014. Field application of electrokinetic remediation for multi-metal contaminated paddy soil using two-dimensional electrode configuration. *Environmental Science and Pollution Research*, [e-journal] 21, pp.4482–4491. https://dx.doi.org/10.1007/s11356-013-2424-0.

Kim, K., Han, Y., Duan, L. and Chung, K.Y., 2022. Scaffolding of Mitogen-Activated Protein Kinase signaling by β-Arrestins. *International Journal of Molecular Sciences*, [e-journal 23(2). https://dx.doi.org10.3390/ijms23021000.

Kısa, D., 2018. The Responses of antioxidant system against the heavy metal-induced stress in tomato. *Journal of Applied and Natural Science*, [e-journal] 22(1), pp.1-6. https://dx.doi.org/10.19113/sdufbed.52379.

Kochi L.Y., Freitas P.L., Maranho L.T., Juneau P. and Gomes M.P., 2020. Aquatic macrophytes in constructed wetlands: a fight against water pollution. *Sustainability*, [e-journal] 2212. https://dx.doi.org/10.3390/su12219202.

Köhler, H., Contreras, R.A., Pizarro, M., Cortés-Antíquera, R. and Zúñiga, G.E., 2017. Antioxidant responses induced by UVB radiation in *Deschampsia antarctica* Desv. *Frontiers in Plant Science*, [e-journal] 8, pp.12-30. https://dx.doi.org/10.3389/fpls.2017.00921.

Konuk, M., Ciğerci, İ.H. and Korcan, S.E., 2010. ALAD (δ-aminolevulinic Acid Dehydratase) as biosensor for Pb contamination. In: V.S. Somerset, ed. 2010. *Intelligent and Biosensors*. London: InTechOpen. http://dx.doi.org/10.5772/7162.

Kosuru, R. and Chrzanowska, M., 2020. Integration of Rap1 and calcium signaling. *International Journal of Molecular Sciences*, [e-journal] 21(5). http://dx.doi.org/10.3390/ijms21051616.

Kotnik, T., Rems, L., Tarek, M. and Miklavčič, D., 2019. Membrane

electroporation and electropermeabilization: mechanisms and models. *Annual Review of Biophysics*, [e-journal] 6(48), pp.63-91. http://dx.doi.org/10.1146/annurev-biophys-052118-115451.

Kour, J., Khanna, K., Singh, A.D., Dhiman, S., Bhardwaj, T., Devi, K., Sharma, N., Ohri, P. and Bhardwaj, R., 2023. Calcium's multifaceted functions: from nutrient to secondary messenger during stress. *South African Journal of Botany,* [e-journal] 152, pp.247-263. https://dx.doi.org/10.1016/j.sajb.2022.11.048.

Kowalik-Klimczak, A., 2025. Removal of heavy metals from galvanic industry wastewater: a review of different possible methods. *Sustainability*, [e-journal] 17(19). https://doi.org/10.3390/su17198562

Koyama, S., Tamura, Y., Ishikawa, G. and Ishikawa, Y., 2021. Acceleration of germination and early growth of plant seeds by high frequency and low intensity alternating electric fields. *Engineering in Agriculture, Environment and Food*, [e-journal] 2019, pp.95-101. http://dx.doi.org/ 10.37221/eaef.14.3_95.

Kral, N., Hanna Ougolnikova, A. and Sena, G., 2016. Externally imposed electric field enhances plant root tip regeneration. *Regeneration (Oxf),* [e-journal] 3(3), pp.156-67. http://dx.doi.org/ 10.1002/reg2.59.

Krčmar, D., Tenodi, S., Grba, N., Kerkez, D., Watson, M., Rončević, S. and Dalmacija, B., 2018. Preremedial assessment of the municipal landfill pollution impact on soil and shallow groundwater in Subotica, Serbia. *Science of the Total Environment*, [e-journal] 615, pp.1341–1354. http://dx.doi.org/ 10.1016/j.scitotenv.2017.09.283.

Kubier, A., Wilkin, R.T. and Pichler, T., 2019. Cadmium in soils and groundwater: A review. *Applied Geochemistry*, [e-journal] 108, pp.1-16. https://dx.doi.org/10.1016/j.apgeochem.

Kudapa, H., Garg, V., Chitikineni, A. and Varshney, R.K., 2018. The RNA-Seq-based high resolution gene expression atlas of chickpea (*Cicer arietinum* L.) reveals dynamic spatio-temporal changes associated with growth and development. *Plant, Cell and Environment*, [e-journal] 41, pp.2209–2225. https://dx.doi.org/10.1111/pce.13210.

Kul, R., Ekinci, M., Turan, M., Örs, S. and Yıldırım, E., 2021. How abiotic stress conditions affects plant roots. In: E. Yildirim, M. Turan and M. Ekinci, eds. 2021. *Plant roots*. London: IntechOpen. https://doi.org/10.5772/intechopen.95286.

Kumar, S., 2016. Epigenetic regulation of abiotic stress tolerance in plants. In: M. Pessarakli, ed-in-chief, 2016. *Advances in plants and agricultural research*. Oklahoma: MedCrave Group. https://doi.org/10.15406/apar.2016.05.00179.

Kumar A., Prasad M.N.V. and Sytar, O., 2012. Lead toxicity, defense strategies and associated indicative biomarkers in *Talinum triangulare* grown hydroponically. *Chemosphere*, [e-journal] 89, pp.1056–1165. https://dx.doi.org/10.1016/j.chemosphere.2012.05.070.

Kumar, K., Raina, S.K. and Sultan, S.M., 2020. Arabidopsis MAPK signaling pathways and their cross talks in abiotic stress response. *Journal of Plant Biochemistry and Biotechnology*, [e-journal] 29, pp.700–714. https://dx.doi.org/10.1007/s13562-020-00596-3.

Kumar, V., Singh, J. and Chopra, A.K., 2018. Assessment of plant growth attributes, bioaccumulation, enrichment, and translocation of heavy metals in water lettuce (*Pistia stratiotes* L.) grown in sugar mill effluent. *International Journal of Phytoremediation*, [e-journal] 20(5), pp.507–521. https://dx.doi.org/10.1080/15226514.2017.1393391.
Kumar, B., Smita, K. and Flores, L.C., 2017. Plant mediated detoxification of mercury and lead. *Arabian Journal of Chemistry*, [e-journal] 10, pp.S2335-S2342. https://dx.doi.org/10.1016/j.arabjc.2013.08.010.

Kumar, V., Singh, J., Kumar, P. and Kumar, P., 2019. Response surface methodology based electro-kinetic modeling of biological and chemical oxygen demand removal from sugar mill effluent by water hyacinth (*Eichhornia crassipes*) in a continuous stirred tank reactor (CSTR). *Environmental Technology and Innovation*, [e-journal] 14. https://dx.doi.org/10.1016/j.eti.2019.100327

Kumar, A., Kumar, A., Cabral-Pinto, M.M.S., Chaturvedi, A.K., Shabnam, A.A., Subrahmanyam, G., Mondal, R., Gupta, D.K., Malyan, S.K., Kumar, S.S., Khan, S.A. and Yadav, K.K., 2020. Lead toxicity: health hazards, influence on food chain, and sustainable remediation approaches. *International Journal of Environmental Research and Public Health*, [e-journal 17(7). https://dx.doi.org/10.3390/ijerph17072179.

Kumar, V., Ferreira, L.F.R., Sonkar, M. and Singh, J., 2022. Toxicity and environmental impacts approached in the leachate of waste landfill: A case study in Brazil. *Environmental Research,* [e-journal] 204(Pt B). https://dx.doi.org/10.1016/j.envres.2021.112031.

Kumar, A., Singh, E., Mishra, R., Lo, S.L. and Kumar, S., 2023. Global trends in municipal solid waste treatment technologies through the lens of sustainable energy development opportunity. *Energy*, [e-journal] 275. https://dx.doi.org/10.1016/j.energy.2023.127471.

Kumar, M.A., Baba, S.K., Sadida, H.Q., Marzooqi, S.A., Jerobin, J., Altemani, F.H., Algehainy, N., Alanazi, M.A., Abou-Samra, A.B., Kumar, R., Al-Shabeeb Akil, A.S., Macha, M.A., Mir, R. and Bhat, A.A., 2024. Extracellular vesicles as tools and targets in therapy for diseases. *Signal Transduction and Targeted Therapy*, [e-journal] 9(1):27. https://dx.doi.org/10.1038/s41392-024-01735-1.

Kurniawan, T.A., Lo, W., Chan, G. and Sillanpää, M.E.T., 2010. Biological processes for treatment of landfill leachate. *Journal of Environmental Monitoring*, [e-journal] 12, pp.2032–2047. http://dx.doi.org/10.1039/c0em00076k.

Kwasniak-Owczarek, M., Kazmierczak, U., Tomal, A., Mackiewicz, P. and Janska, H., 2019. Deficiency of mitoribosomal S10 protein affects translation and splicing in *Arabidopsis* mitochondria. *Nucleic Acids Research*, [e-journal] 47(22), pp.11790-11806. https://dx.doi.org/10.1093/nar/gkz1069.

Labarca, P., Santio, C., Zapata, O., Morales, E., Beltran, C., Lievano, A. and Darszon, B., 1996. A cAMP regulated K+-selective channel from the sea urchin sperm plasma membrane. *Developmental Biology*, [e-journal] 174(2), pp.271-80. http://dx.doi.org/10.1006/dbio.1996.0072.

Ladeynova, M., Kuznetsova, D., Mudrilov, M. and Vodeneev, V., 2023. Integration of electrical signals and phytohormones in the control of systemic response. *International Journal of Molecular Sciences*, [e-journal] 24(1). https://dx.doi.org/10.3390/ijms24010847.

Lafontaine, D.L.J., Riback, J.A., Bascetin, R. and Brangwynne, C.P., 2021. The nucleolus as a multiphase liquid condensate. *Nature Reviews Molecular Cell Biology*, [e-journal] 22, 165–182. https://dx.doi.org/10.1038/s41580-020-0272-6.

Lee, S. and Oh, M.M., 2025. Electrocultivation of *Arabidopsis thaliana* increases water and mineral absorption, electric charge and auxin accumulation, enhancing growth and development. *Bioelectrochemistry,* [e-journal] 163. https://dx.doi.org/10.1016/j.bioelechem.2024.108893.

Lee, S., Seo, Y.E., Choi, J., Yan, X., Kim, T., Choi, D. and Lee, J.H., 2024. Nucleolar actions in plant development and stress responses. *Plant, Cell and Environment*, [e-journal] 47(12), pp.5189-5204. https://dx.doi.org/10.1111/pce.15099.

Lei, J., Jin, L, Feng, Z., Sima, J., Lou, F., Du, X., Zhu, C., Wang, J. Huang, Q., 2023. Environment-economic-energy (3e) analysis of municipal solid waste landfill mining: a case study in China. *Social Science Research Network*, [online] Available at: < https://papers.ssrn.com/sol3/papers.cfm?abstract_id=4710306> [Accessed 22 July 2025].

Lenzoni, G., Liu, J. and Knight, M.R., 2018. Predicting plant immunity gene expression by identifying the decoding mechanism of calcium signatures. *New Phytologist*, [e-journal] 217, pp.1598–1609. https://dx.doi.org/10.1111/nph.14924.

Leonowicz, G., Trzebuniak, K.F., Zimak-Piekarczyk, P., Ślesak, I. and Mysliwa-Kurdziel, B., 2018. The activity of superoxide dismutases (SODs) at the early stages of wheat deetiolation. *PLoS One*, [e-journal] 13(3). https://dx.doi.org/10.1371/journal.pone.0194678.

Leshem, Y., Melamed-Book, N., Cagnac, O., Ronen, G., Nishri, Y., Solomon, M., Cohen, G. and Levine, A., 2006. Suppression of *Arabidopsis* vesicle-SNARE expression inhibited fusion of H_2O_2-containing vesicles with tonoplast and increased salt tolerance. *Proceedings of the National Academy of Sciences of the United States of America,* [e-journal] 103(47), pp.18008-13. https://dx.doi.org/10.1073/pnas.0604421103.

Leškovï, A., Zvarï, K.M., Araya, T. and Giehl, R.F.H., 2020. Nickel toxicity targets cell wall-related processes and PIN2-mediated auxin transport to inhibit root elongation and gravitropic responses in *Arabidopsi*s. *Plant and Cell Physiology*, [e-journal] 61(3), pp.519-535. https://dx.doi.org/10.1093/pcp/pcz217.

Lessey, E.C., Guilluy, C. and Burridge, K., 2012. From mechanical force to RhoA activation. *Biochemistry*, [e-journal] 51(38), pp.7420-7432.

https://dx.doi.org/10.1021/bi300758e.

Li, B. and Dewey, C.N., 2011. RSEM: accurate transcript quantification from RNA-Seq data with or without a reference genome. *BMC Bioinformatics*, [e-journal] 12. http://dx.doi.org/10.1186/1471-2105-12-323.

Li, G., Kronzucker, H.J, and Shi, W., 2016. Root developmental adaptation to Fe toxicity: mechanisms and management. *Plant Signaling and Behavior*, [e-journal] 11(1). https://dx.doi.org/10.1080/15592324.2015.1117722.

Li, Z., Gou, H.Q. and Li, R., 2019. Electrical stimulation boosts seed germination, seedling growth, and thermotolerance improvement in maize (*Zea mays* L.). *Plant Signaling and Behavior*, [e-journal] 14(12). https://dx.doi.org/10.1080/15592324.2019.1681101.

Li, N., Chen, L. and Li, Y., 2023. Control of grain size and number by MAPK signaling in rice. *Seed Biology*, [e-journal] 2(15). https://dx.doi.org/10.48130/SeedBio-2023-0015.

Li, R., Guo, P., Baum, M., Grando, S. and Ceccarelli, S., 2006a. Evaluation of chlorophyll content and fluorescence parameters as indicators of drought tolerance in barley, *Agricultural Sciences in China*, [e-journal] 5(10), pp.751–757. https://dx.doi.org/10.1016/S1671-2927(06)60120-X.

Li, X.G., Zhao, J.P., Xu, P.L., Meng, J.J. and He, Q.W., 2006b. Effects of cyclic electron flow inhibitor (antimycin a) on photosystem photoinhibition of sweet pepper leaves upon exposure to chilling stess under low irradianc. *Agricultural Sciences in China*, [e-journal] 5(7), pp.506-511. https://dx.doi.org/10.1016/S1671-2927(06)60084-9.

Li, W.B., Yao, J., Xia, F.F., Feng, H.J., Feng, H., Jiang, C.J., Fang, C.R. and Shen, D.S., 2011. Leaching behavior of iron from simulated landfills with different operational modes. *Bioresource Technology*, [e-journal] 102(16), pp.7422-7428. http://dx.doi.org/10.1016/j.biortech.2011.05.024.

Li, Q., Lei, S., Du, K., Li, L., Pang, X., Wang, Z., Wei, M., Fu, S., Hu, L. and Xu, L., 2016. RNA-seq based transcriptomic analysis uncovers α-linolenic acid and jasmonic acid biosynthesis pathways respond to cold acclimation in *Camellia*

japonica. *Scientific Reports*, [e-journal] 6. https://dx.doi.org/10.1038/srep36463.

Li, H., Hu, T., Amombo, E. and Fu, J., 2017a. Transcriptome profilings of two tall fescue (*Festuca arundinacea*) cultivars in response to lead (Pb) stress. *BMC Genomics*, [e-journal] 18(145). https://dx.doi.org/10.1186/s12864-016-3479-3.

Li, K., Yang, F., Zhang, G., Song, S., Li, Y., Ren, D., Miao, Y. and Song, C.P., 2017b. AIK1, a mitogen-activated protein kinase, modulates abscisic acid responses through the MKK5-MPK6 kinase cascade. *Plant Physiology*, [e-journal] 173, pp.1391–1408. https://dx.doi.org/10.1104/pp.16.01386.

Li, Q.T., Lu, X., Song, Q.X., Chen, H.W., Wei, W., Tao, J.J., Bian, X.H., Shen, M., Ma, B., Zhang, W.K., Bi, Y.D., Li, W., Lai, Y.C., Lam, S.M., Shui, G.H., Chen, S.Y. and Zhang, J.S., 2017c. Selection for a zinc-finger protein contributes to seed oil increase during soybean domestication. *Plant Physiology*, [e-journal] 173, pp.2208–2224. https://dx.doi.org/10.1104/pp.16.01610.

Li, Y., He, N., Hou, J., Xu, L., Liu, C., Zhang, J., Wang, Q., Zhang, X. and Wu, X. 2018. Factors influencing leaf chlorophyll content in natural forests at the biome scale. *Frontiers in Ecology and Evolution*, [e-journal] 6. https://dx.doi.org/10.3389/fevo.2018.00064.

Li, J.F., Jia, Y.D., Dong, R.S., Huang, R., Liu, P.D., Li, X.Y., Wang, Z.Y., Liu, G.D. and Chen Z.J., 2019a. Advances in the mechanisms of plant tolerance to Mn toxicity. *International Journal of Molecular Sciences*, [e-journal] 20. http://dx.doi.org/10.3390/ijms20205096.

Li, X., Zhang, X., Wang, X. and Cui, Z., 2019b. Phytoremediation of multi-metal contaminated mine tailings with *Solanum nigrum* L. and biochar/attapulgite amendments. *Ecotoxicology and Environmental Safety*, [e-journal] 180, pp.517-525. http://dx.doi.org/10.1016/j.ecoenv.2019.05.033.

Li, C., Zhou, K., Qin, W., Tian, C., Qi, M., Yan, X. and Han, W., 2019c. A review on heavy metals contamination in soil: effects, sources, and remediation techniques. *Soil and Sediment Contamination: An International Journal*, [e-journal] 28(4), pp.380–394. https://dx.doi.org/10.1080/15320383.2019.1592108.

Li, S., Cerri, M., Strazzer, P., Li, Y., Spelt, C., Bliek, M., Vandenbussche, M.,

Martínez-Calvó, E., Lai, B., Reale, L., Koes, R. and Quattrocchio, F.M., 2021. An ancient RAB5 governs the formation of additional vacuoles and cell shape in petunia petals. *Cell Reports*, [e-journal] 36(13). https://dx.doi.org/10.1016/j.celrep.2021.109749.

Li, S., Han, X., Lu, Z., Qiu, W., Yu, M., Li, H., He, Z. and Zhuo, R., 2022. MAPK cascades and transcriptional factors: regulation of heavy metal tolerance in plants. *International Journal of Molecular Sciences*, [e-journal] 23(8). https://dx.doi.org/10.3390/ijms23084463.

Li, X., Sun, H.F., Fan, J.H., Li, Y.Y., Ma, L.J., Wang, L.L. and Li, X.M., 2023. Transcriptome modulation by endophyte drives rice seedlings response to Pb stress. *Ecotoxicology and Environmental Safety*, [e-journal] 254. https://dx.doi.org/10.1016/j.ecoenv.2023.114740.

Li, G., Wu, J., Kronzucker, H.J., Li, B. and Shi, W., 2024a. Physiological and molecular mechanisms of plant-root responses to iron toxicity. *Journal of Plant Physiology*, [e-journal] 29. https://dx.doi.org/10.1016/j.jplph.2024.154257.

Li, J., Zhao, R., Liu, J., Yao, J., Ma, S., Yin, K., Zhang, Y., Liu, Z., Yan, C. and Zhao, N., 2024b. *Populus euphratica* GRP2 interacts with target mRNAs to negatively regulate salt tolerance by interfering with photosynthesis, Na^+, and ROS homeostasis. *International Journal of Molecular Sciences*, [e-journal] 25. https://dx.doi.org/10.3390/ijms25042046.

Li, J., Nie, M., Wang, C., Zhang, D., Wang, Y., Guo, F., Zhang, C. and Hu, T., 2025. Root morphology and transcriptome analysis reveal key genes responsive to cadmium in wheat (*Triticum aestivum* L.). *Ecotoxicology and Environmental Safety*, [e-journal] 305. https://dx.doi.org/10.1016/j.ecoenv.2025.119263

Liang, C.J., Zhang, Y.Q. and Ren, X.Q., 2021. Calcium regulates antioxidative isozyme activity for enhancing rice adaption to acid rain stress. *Plant Science*, [e-journal] 306. https://dx.doi. org/10.1016/j.plantsci.2021.110876.

Liang, X., Ji, L., Xie, Y. and Huang, G., 2022. Economic-Environment-Energy (3E) objective-driven integrated municipal waste management under deep complexities – a novel multi-objective approach. *Sustainable Cities and Society*, [e-journal] 87. https://dx.doi. org/10.1016/J.SCS.2022.104190.

Lindamulla, L., Nanayakkara, N., Othman, M., Jinadasa, S., Herath, G. and Jegatheesan, V., 2022. Municipal solid waste landfill leachate characteristics and their treatment options in tropical countries. *Current Pollution Reports*, [e-journal] 8, pp.273–287. https://dx.doi.org/10.1007/s40726-022-00222-x.

Liu Y., Li Z.Y. and Xu R.K., 2019. Distribution of Mn (II) chemical forms on soybean roots and Mn (II) toxicity. *Pedosphere*, [e-journal] 29, pp.656–664. http://dx.doi.org/10.1016/S1002-0160(17)60413-2.

Liu, Y., Qiao, Y. and Liao, W., 2025. Calmodulin-binding transcription factors: roles in plant response to abiotic stresses. *Plants*, [e-journal] 14(4). https://dx.doi.org/10.3390/plants14040532.

Liu, T., Shen, C., Wang, Y., Huang, C. and Shi, J., 2014. New insights into regulation of proteome and polysaccharide in cell wall of *Elsholtzia splendens* in response to copper stress. *PLoS ONE*, [e-journal] 9(10). https://dx.doi.org/10.1371/journal.pone.0109573.

Liu, Y., Liu, L., Qi, J., Dang, P. and Xia, T., 2019. Cadmium activates ZmMPK3-1 and ZmMPK6-1 via induction of reactive oxygen species in maize roots. *Biochemical and Biophysical Research Communications*, [e-journal] 516, pp.747–752. https://dx.doi.org/10.1016/j.bbrc.2019.06.116.

Liu, X., Wan, B., Hua, H. and Li, X., 2021a. Electric field generated by high-voltage transmission system is beneficial to cotton growth. *Acta Ecologica Sinica*, [e-journal] 41(6), pp.552-559. https://dx.doi.org/10.1016/j.chnaes.2021.05.002.

Liu, H., Yang, H., Zhao, T., Lin, C., Li, Y., Zhang, X., Ye, Y. and Liao, J., 2021b. Combined metabolome and transcriptome analyses of young, mature, and old rhizome tissues of *Zingiber officinale* Roscoe. *Frontiers in Genetics*, [e-journal] 12. https://dx.doi.org/10.3389/fgene.2021.795201.

Liu, L., Zhang, L., Zhao, L., Chen, Q., Zhang, Q., Cao, D. and Liu, Z., 2022a. Differential gene expression and metabolic pathway analysis of *Cladophora rupestris* under Pb stress conditions. *International Journal of Environmental Research and Public Health*, [e-journal] 19. https://dx.doi.org/10.3390/ijerph192113910.

Liu, H., Huang, C., Li, Q., Wang, M.., Xiao, S., Shi, J., He, Y., Wen, W., Li, L. and Xu, D., 2022b. Genome-wide identification of genes related to biosynthesis of phenolic acid derivatives in *Bletilla striata* at different suspension culture stages. *Frontier in Plant Science*, [e-journal] 17(13). https://dx.doi.org/10.3389/fpls.2022.875404.

Liu, H., Li, J., Xu, C., Liu, H. and Zhao, Z., 2024. Unravelling the molecular regulation network of carbon metabolism and lipid metabolism during seed development in *Akebia trifoliata* via integrated multi-omics analysis. *Scientific Reports*, [e-journal] 14(22893). https://dx.doi.org/10.1038/s41598-024-74075-3.

Liu, K., Cao, N.-J., Zhu, Y. and Wang, W., (in press) Integrate analysis and identification for different expression genes in chondrogenesis. *Research Square (United States).*

Livak, K.J. and Schmittgen, T.D., 2001. Analysis of relative gene expression data using real-time quantitative PCR and the 2(-Delta Delta C(T)) Method. *Methods*, [e-journal] 25, pp.402–408. http://dx.doi.org/10.1006/meth.2001.1262.

Llebrés, M.T., Pascual, M.B., Debille, S., Trontin, J.F., Harvengt, L., Avila, C. and Cánovas, F.M., 2018. The role of arginine metabolic pathway during embryogenesis and germination in maritime pine (*Pinus pinaster* Ait.). *Tree Physiology*, [e-journal] 38(3), pp.471-484. https://dx.doi.org/10.1093/treephys/tpx133.

Locato, V. and De Gara, L., 2018. Programmed cell death in plants: an overview. In: L. De Gara and V. Locato, eds. *Plant programmed cell death. Methods in molecular biology, vol 1743*. New York: Humana Press. pp. 1-8.

Loh, Z.Z., Zaidi, N.S., Syafiuddin, A., Yong, E.L., Boopathy, R., Hong Kueh, A.B. and Prastyo, D.D., 2021. Shifting from conventional to organic filter media in wastewater biofiltration treatment: a review. *Applied Sciences*, [e-journal] 11. http://dx.doi.org/10.3390/app11188650.

Lowe, R., Shirley, N., Bleackley, M., Dolan, S. and Shafee, T., 2017. Transcriptomics technologies. *PLOS Computational Biology*, [e-journal] 13(5). https://dx.doi.org/10.1371/journal.pcbi.1005457.

Lu, M., Zhang, Y., Tang, S., Pan, J., Yu, Y., Han, J., Li, Y., Du, X., Nan, Z. and Sun, Q., 2016. AtCNGC2 is involved in jasmonic acid-induced calcium mobilization. *Journal of Experimental Botany*, [e-journal] 67, pp.809–819. https://dx.doi.org/10.1093/jxb/erv500.

Lu, Y., Cheng, K., Tang, H., Li, J., Zhang, C. and Zhu, H., 2024. The role of Rab GTPase in plant development and stress. *Journal of Plant Physiology*, [e-journal] 296. https://dx.doi.org/10.1016/j.jplph.2024.

Luo, J., Yang, D., Qi, S., Wu, J. and Gu, X.S., 2018. Using solar cell to phytoremediate field-scale metal polluted soil assisted by electric field. *Ecotoxicology and Environmental Safety,* [e-journal] 165, pp.404–410. https://dx.doi.org/10. 1016/j.ecoenv.2018.09.031.

Ma, W., Smigel, A., Verma, R. and Berkowitz, G.A., 2009. Cyclic nucleotide gated channels and related signaling components in plant innate immunity. *Plant Signaling and Behavior,* [e-journal] 4(4), pp.277-82. https://dx.doi.org/10.4161/psb.4.4.8103.

Ma, H., Gao, Y., Wang, Y., Dai, Y. and Ma, H., 2022. Regulatory mechanisms of mitogen-activated protein kinase cascades in plants: more than sequential phosphorylation. *International Journal of Molecular Sciences*, [e-journal] 23. https://dx.doi.org/10.3390/ijms23073572.

Ma, H., Wang, L., Ke, H., Zhou, W., Jiang, C., Jiang, M., Zhan, F. and Li, T., 2024. Effects, physiological response and mechanism of plant under electric field application. *Scientia Horticulturae*, [e-journal] 329(2). http://dx.doi.org/10.1016/j.scienta.2024.112992.

Ma, H., Zhao, M., Yang, N., Feng, L., Wang, L., Jiang, C., Jiang, M., Guo, J. and Li, T., 2025. Regulated the electrokinetic application of different plant growth stages and parameters enhance the economic extraction of soil heavy metals. *Frontier in Plant Science,* [e-journal] 16. http://dx.doi.org/10.3389/fpls.2025.1557261

Maffei, M.E., 2014. Magnetic field effects on plant growth, development, and evolution. *Frontier in Plant Science,* [e-journal] 5. http://dx.doi.org/10.3389/fpls.2014.00445.

Mahajan, P. and Kaushal, J., 2018. Role of phytoremediation in reducing cadmium toxicity in soil and water. *Journal of Toxicology*, [e-journal] 2018, pp.1–16. http://dx.doi.org/ 10.1155/2018/4864365.

Mahdavian, K., 2025. Synergistic modulation of antioxidant enzymes by citric acid and EDTA to enhance lead tolerance and phytoextraction efficiency in harmel. *Scientific Reports*, [e-journal] 15 (37890). https://dx.doi.org/10.1038/s41598-025-21662-7

Mäkinen, V., Salmela, L. and Ylinen, J., 2012. Normalized N50 assembly metric using gap-restricted co-linear chaining. *BMC Bioinformatics*, [e-journal] 13(255). https://dx.doi.org/10.1186/1471-2105-13-255.

Malar, S., Shivendra Vikram, S., Jc Favas, P. and Perumal, V., 2016. Lead heavy metal toxicity induced changes on growth and antioxidative enzymes level in water hyacinths [*Eichhornia crassipes* (Mart.)]. *Botanical Studies*, [e-journal] 55(1):54. https://dx.doi.org/10.1186/s40529-014-0054-6.

Malek, M.I. and Shaaban, M.G., 2008. Landfill common method and practices of solid waste disposal in Malaysia. In: ISWA World Congress (International Solid Waste Association), Don't waste our future. Singapore, 22-23 September 2022. Singapore: ISWA.

Małkowski, E., Sitko, K., Szopiński, M., Gieroń, Ż., Pogrzeba, M., Kalaji, H.M. and Zieleźnik-Rusinowska, P., 2020. Hormesis in plants: the role of oxidative stress, auxins and photosynthesis in corn treated with Cd or Pb. *International Journal of Molecular Sciences*, [e-journal] 21(6). https://dx.doi.org/10.3390/ijms21062099.

Mamun, A.A., Bormon, K.K., Rasu, M.N.S., Talukder, A., Freeman, C., Burch, R. and Chander, H. 2022. An assessment of energy and groundwater consumption of textile dyeing mills in Bangladesh and minimization of environmental impacts via long-term Key Performance Indicators (KPI) baseline. *Textiles*, [e-journal] 2, pp.511-523. https://dx.doi.org/10.3390/textiles2040029.

Manaf, L.A., Samah, M.A.A. and Zukki, N.I.M., 2009. Municipal solid waste management in Malaysia: Practices and Challenges. *Waste Management*, [e-journal] 29(11), pp. 2902–2906. https://dx.doi.org/10.1016/j.wasman.2008.07.015.

Manara, A., 2012. Plant responses to heavy metal toxicity. In: A. Furini, ed. 2012. *Springer briefs in molecular science.* Dordrecht: Springer. pp.27–53.

Manavella, P.A., Godoy Herz, M.A., Kornblihtt, A.R., Sorenson, R., Sieburth, L.E., Nakaminami, K., Seki, M., Ding, Y., Sun, Q., Kang, H., Ariel, F.D., Crespi, M., Giudicatti, A.J., Cai, Q., Jin, H., Feng, X., Qi, Y. and Pikaard, C.S., 2023. Beyond transcription: compelling open questions in plant RNA biology. *Plant Cell*, [e-journal] 35(6), pp.1626-1653. https://dx.doi.org/10.1093/plcell/koac346.

Manna, M., Rengasamy, B. and Sinha, A.K., 2023. Revisiting the role of MAPK signalling pathway in plants and its manipulation for crop improvement. *Plant, Cell and Environment*, [e-journal] 46(8), pp.2277-2295. http://dx.doi.org/10.1111/pce.14606.

Mannaf, M.M., Rahman, M.M., Sabuj, S.T., Talukder, N. and Lee, E.S., 2025. Current progress in advanced functional membranes for water-pollutant removal: a critical review. *Membranes*, [e-journal] 15(10). https://dx.doi.org/10.3390/membranes15100300.

Mansoor, S., Ali, A., Kour, N., Bornhorst, J., AlHarbi, K., Rinklebe, J., Abd El Moneim, D., Ahmad, P. and Chung, Y.S., 2023. Heavy metal induced oxidative stress mitigation and ROS scavenging in plants. *Plants (Basel)*, [e-journal] 12(16). https://dx.doi.org/10.3390/plants12163003.

Mao, X., Han, F.X., Shao, X., Guo, K., McComb, J., Arslan, Z. and Zhang, Z., 2016. Electro-kinetic remediation coupled with phytoremediation to remove lead, arsenic and cesium from contaminated paddy soil. *Ecotoxicology and Environmental Safety*, [e-journal] 125, pp.16-24. https://dx.doi.org/10.1016/j.ecoenv.2015.11.021.

Maphuhla, N.G. and Oyedeji, O.O., 2025. From trash to treasure: systematic evaluation of potential and efficiency of waste-to-energy incineration for electricity generation. *Waste*, [e-journal] 3(4). https:/dx./doi.org/10.3390/waste3040039.

Marques, A.P., Rangel, A.O. and Castro, P.M., 2009. Remediation of heavy metal contaminated soils: phytoremediation as a potentially promising clean-up technology. *Critical Reviews in Environmental Science and Technology*, [e-journal] 39(8), pp.622–654. https://dx.doi.org/ 10.1080/10643380701798272.

Marques, D.N. and Mason, C.M., 2025. Functional genetic frontiers in plant ABC transporters: avenues toward cadmium management. *International Journal of Molecular Sciences,* [e-journal] 26(23). https://dx.doi.org/10.3390/ijms262311662.

Marsidi, N., Hasan, H.A. and Abdullah, S.R.S, 2018. A review of biological aerated filters for iron and manganese ions removal in water treatment. *Journal of Water Process Engineering,* [e-journal] 23. https://dx.doi.org/10.1016/j.jwpe.2018.01.010.

Marwood, C.A., Solomon, K.R. and Greenberg, B.M., 2001. Chlorophyll fluorescence as a bioindicator of effects on growth in aquatic macrophytes from mixtures of polycyclic aromatic hydrocarbons. *Environmental Toxicology and Chemistry*, [e-journal] 20(4), pp.890-898. https://dx.doi.org/10.1897/1551-5028(2001)020<0890:cfaabo>2.0.co;2.

Mashabela, M.D., Masamba, P. and Kappo, A.P., 2023. Applications of metabolomics for the elucidation of abiotic stress tolerance in plants: a special focus on osmotic stress and heavy metal toxicity. *Plants*, [e-journal] 12(2). https://dx.doi.org/10.3390/plants12020269.

Masiyambiri, V., Balarabe, B.Y., Adjama, I., Moussa, H., Oumarou, M.N.I. and Sodo, A.M.I., 2023. A study of the phytoremediation process using water lettuce (*Pistia stratiotes*) in the removal of ciprofloxacin. *American Journal of Life Science and Innovation*, [e-journal] 1, pp.1-8. https://dx.doi.org/10.54536/ajlsi.v1i3.1092.

Massingham, T, and Goldman, N., 2012. All your base: a fast and accurate probabilistic approach to base calling. *Genome Biology*, [e-journal] 13(2):R13. https://dx.doi.org/10.1186/gb-2012-13-2-r13.

Matyas, B., 1994. Inflorescence Development of *Pistia stratiotes* (Araceae). *Botanische Jahrbücher für Systematik,* 115(4), pp.557-570.

Maurya, N.K., Magada, S., Singh, B., Samal, K., Jayaswal, R., Lakshmipathi, M.T., Kumar, V. and Annappaswamy, T.S., 2025. Phytoremediation of metal contamination: evaluating *Pistia stratiotes* and *Eichhornia crassipes* for lead and cadmium removal. *International Journal of Environment and Climate Change*, [e-journal] 15(4), pp.205-221. https://dx.doi.org/10.9734/ijecc/2025/v15i44804.

Mazaheri-Tirani, M., Parsa Motlagh, B., Ahmadzadeh, M. and Seyedi, A., 2024. Mitigating pb toxicity in *Sesbania sesban* L. through activated charcoal supplementation: a hydroponic study on enhanced phytoremediation. *BMC Plant Biology*, [e-journal] 24(744). https://dx.doi.org/10.1186/s12870-024-05478-7.

McIntosh, K.B. and Bonham-Smith, P.C., 2006. Ribosomal protein gene regulation: What about plants? *Canadian Journal of Botany*, [e-journal] 84, pp.342–362. https://dx.doi.org/10.1139/b06-014.

Mehes-Smith, M., Nkongolo, K. and Cholew, E., 2013. Coping mechanisms of plants to metal contaminated soil. In: S. Silvern and S. Young, eds. 2013. *Environmental change and sustainability*. London: IntechOpen. http://dx.doi.org/10.5772/55124.

Mellem, J.J., Baijnath, H. and Odhav, B., 2009. Translocation and accumulation of Cr, Hg, As, Pb, Cu and Ni by *Amaranthus dubius* (Amaranthaceae) from contaminated sites. *Journal of Environmental Science and Health, Part A*, [e-journal] 44(6), pp.568–575. https://dx.doi.org/10.1080/10934520902784583.

Men, J.L., Men, J.Y., Zhang, Y.J., Zhao, L., Zhang, J., Zhang, Z.H., Zhang, D., Shao, H. and Lu, Q.Y., 2021. Investigation on occupational hazards in 20 automobile manufacturing enterprises in Shandong Province. *Chinese Journal of Industrial Hygiene and Occupational Diseases*, [e-journal] 39, pp.198–202. http://dx.doi.org/10.3760/cma.j.cn121094-20200509-00245.

Meng, H., Zhang, W., Zhang, G.H., Wang, J.J., Meng, Z.G., Long, G.Q. and Yang, S.C., 2018. Unigene-based rna-seq provides insights on drought stress responses in *Marsdenia tenacissima*. *PLoS ONE*, [e-journal] 13. http://dx.doi.org/10.1371/journal.pone.0202848.

Meng, Y., Xiang, C., Huo, J., Shen, S., Tang, Y. and Wu, L., 2023. Toxicity effects of zinc supply on growth revealed by physiological and transcriptomic evidences in sweet potato (*Ipomoea batatas* (L.) Lam). *Science Reports*, [e-journal 13(1):19203. https://dx.doi.org/10.1038/s41598-023-46504-2.

Mesjasz-Przybyłowicz, J., Nakonieczny, M., Migula, P., Augustyniak, M., Tarnawska, M., Reimold, U. and Koeberlt, C., 2004. Uptake of cadmium, lead nickel and zinc from soil and water solutions by the nickel hyperaccumulator *Berkheya coddii*. *Acta Biologica Cracoviensia Series Botanica*, 46, pp.75–85.

Michalska, J., Piński, A., Żur, J. and Mrozik, A., 2020. Selecting bacteria candidates for the bioaugmentation of activated sludge to improve the aerobic treatment of landfill leachate. *Water,* [e-journal] 12. https://dx.doi.org/10.3390/w12010140.

Millaleo, R., Reyes-Díaz, M., Ivanov, A.G., Mora, M.L. and Alberdi, M., 2010. Manganese as essential and toxic element for plants: transport, accumulation and resistance mechanisms. *Journal of soil science and plant nutrition*, 10(4), pp.470-481.

Miller, A.F., 2012. Superoxide dismutases: ancient enzymes and new insights. *FEBS* Letters, [e-journal] 586(5), pp.585-95. https://dx.doi.org/10.1016/j.febslet.2011.10.048.

Minina, E.A., Filonova, L.H., Sanchez-Vera, V., Suarez, M.F., Daniel, G. and Bozhkov, P.V., 2013. Detection and measurement of necrosis in plants. In: K. McCall and C. Klein, eds. 2013. *Necrosis. Methods in molecular biology*. Totowa, NJ: Humana Press. pp.229–248.

Mir, S.I., Salah, M.G., Arafat, M., Syukor, A. and Razak, A., 2017. Surface water quality assessment of the Gebeng industrial area using water quality standard and index. *Journal of Engineering and Science Research*, [e-journal] 1(2), pp.118-126. https://dx.doi.org/10.2666/rmp.jesr.2017.2.19.

Mittler R., 2017. ROS Are Good. *Trends in Plant Science,* [e-journal] 22(1), pp.11-19. https://dx.doi.org/10.1016/j.tplants.2016.08.002.

Mittler, R., Zandalinas, S.I., Fichman, Y. and Van Breusegem, F., 2022. Reactive oxygen species signalling in plant stress responses. *Nature Reviews Molecular Cell Biology*, [e-journal] 23, pp.663-679. https://dx.doi.org/10.1038/s41580-022-00499-2.

Mohamed, H.I., Ullah, I., Toor, M.D., Tanveer, N.A., Din, M.M.U., Basit, A., Sultan, Y., Muhammad, M. and Rehman, M.U., 2025. Heavy metals toxicity in plants: understanding mechanisms and developing coping strategies for remediation: a review. *Bioresources and Bioprocessing,* [e-journal] 12(1):95. http://dx.doi.org/10.1186/s40643-025-00930-4.

Mohd Nizam, N.U., Mohd Hanafiah, M., Mohd Noor, I. and Abd Karim, H.I., 2020. Efficiency of five selected aquatic plants in phytoremediation of aquaculture wastewater. *Applied Sciences*, [e-journal] 10(8). https://dx.doi.org/10.3390/app10082712.

Moin, M., Bakshi, A., Saha, A., Dutta, M., Madhav, S.M. and Kirti, P.B., 2016. Rice ribosomal protein large subunit genes and their spatio-temporal and stress regulation. *Frontier in Plant Science*, [e-journal] 7. http://dx.doi.org/10.3389/fpls.2016.01284.

Mojiri, A., Ziyang, L., Tajuddin, R. M., Farraji, H. and Alifar, N., 2016. Co-treatment of landfill leachate and municipal wastewater using the ZELIAC/zeolite constructed wetland system. *Journal of Environmental Management*, [e-journal] 166, pp.124–130. http://dx.doi.org/ 10.1016/j.jenvman.2015.10.020.

Mojiri, A., Zhou, J.L., Ratnaweera, H., Ohashi, A., Ozaki, N., Kindaichi, T. and Asakura, H., 2021. Treatment of landfill leachate with different techniques: an overview. *Water Reuse*, [e-journal] 11(1). http://dx.doi.org/10.2166/wrd.2020.079.

Mondal, S., 2023. Heavy metal stress–induced activation of mitogen-activated protein kinase signalling cascade in plants. *Plant Molecular Biology Reporter*, [e-journal] 41, pp.15–26. https://dx.doi.org/10.1007/s11105-022-01350-w.

Moradbeygi, H., Jamei, R., Heidari, R. and Darvishzadeh, R., 2020. Fe_2O_3 nanoparticles induced biochemical responses and expression of genes involved in rosmarinic acid biosynthesis pathway in Moldavian balm under salinity stress. *Physiologia Plantarum*, [e-journal] 169, pp.555–570. https://dx.doi.org/10.1111/ppl.13077.

Moran, R. and Porath, D., 1980. Chlorophyll determination in intact tissues using N,N-dimethylformamide. *Plant Physiology*, [e-journal] 65(3), pp.478-9. http://dx.doi.org/10.1104/pp.65.3.478.

Morgenstern, R., 2024. Kinetic behavior of Glutathione Transferases: understanding cellular protection from reactive intermediates. *Biomolecules*, [e-journal] 14(6). https://dx.doi.org/10.3390/biom14060641.

Mori, D., Moriyama, A., Kanamaru, H., Aoki, Y., Masumura, Y. and Suzuki, S. 2021. Electrical stimulation enhances plant defense response in grapevine through

salicylic acid-dependent defense pathway. *Plants*, [e-journal] 10(7), pp.1–10. https://dx.doi.org/10.3390/plants10071316.

Moris, S., Garcia-Cabellos, G., Enright, D., Ryan, D. and Enright, A.M., 2018 Bioremediation of landfill leachate using isolated bacterial strains. *International Journal of Environmental Bioremediation and Biodegradation*, [e-journal] 6(1), pp.26–35. https://dx.doi.org/10.12691/ijebb-6-1-4.

MRC Laboratory Instruments, n.d. *How to use Biochemical Oxygen Demand (BOD) effectively*. [online] Available at: <https://www.mrclab.com/how-to-use-biochemical-oxygen-demand-bod-effectively#:~:text=Sample%20upstream%20and%20downstream%20of,Understand%20What%20BOD%20Measures> [Accessed 15 February 2026].

Mulati, H., Mamat, A., Ailijiang, N., Jiang, L., Li, N., Hu, Y. and Su, Y., 2023. Electrokinetic-assisted phytoremediation of Pb-contaminated soil: influences of periodic polarity reversal direct current field. *Sustainability*, [e-journal] 15(11). https://dx.doi.org/10.3390/su15118439.

Mumtaz, M.A., Hao, Y., Mehmood, S., Shu, H., Zhou, Y., Jin, W., Chen, C., Li, L., Altaf, M.A. and Wang, Z., 2022. Physiological and transcriptomic analysis provide molecular insight into 24-epibrassinolide mediated Cr(VI)-toxicity tolerance in pepper plants. *Environmental Pollution*, [e-journal] 306. https://dx.doi.org/10.1016/j.envpol.2022.119375.

Munguía-López, A. del C., Zavala, V. M., Santibañez-Aguilar, J. E. and Ponce-Ortega, J.M., 2020. Optimization of municipal solid waste management using a coordinated framework. *Waste Management*, [e-journal] 115, pp.15-24. https://dx.doi.org/10.1016/j.jksus.2022.101865.

Munir, N., Jahangeer, M., Bouyahya, A., El Omari, N., Ghchime, R., Balahbib, A., Aboulaghras, S., Mahmood, Z., Akram, M., Ali Shah, S.M., Mikolaychik, I.N., Derkho, M., Rebezov, M., Venkidasamy, B., Thiruvengadam, M. and Shariati, M.A., 2022. Heavy metal contamination of natural foods is a serious health issue: a review. *Sustainability*, [e-journal] 14(1). https://dx.doi.org/10.3390/su14010161.

Munzuroglu, O. and Geckil H., 2002. Effects of metals on seed germination, root elongation, and coleoptile and hypocotyl growth in *Triticum aestivum* and *Cucumis sativus*. *Archives of Environmental Contamination and Toxicology*, [e-journal] 43(2), pp.203–213. https://dx.doi.org/10.1007/s00244-002-1116-4.

Mustafa, H.M. and Hayder, G., 2021. Evaluation of water lettuce, giant salvinia and water hyacinth systems in phytoremediation of domestic wastewater. *H2Open Journal*, [e-journal] 4(1), pp.167–181. http://dx.doi.org/10.2166/h2oj.2021.096.

Nadi, A.R., Mohamed, E., Kasem, A.M.M.A., Ghanem, A.E.F.M. and Badry, M.O., 2025. Green solutions for heavy metal pollution in the aquatic environment of the nile islands: cues from some submerged and emergent macrophytes. *Water, Air and Soil Pollution*, [e-journal] 236(410). https://doi.org/10.1007/s11270-025-07966-4

Nagajyoti, P.C., Lee, K.D. and Sreekanth, T., 2010. Heavy metals, occurrence and toxicity for plants: a review. *Environmental Chemistry Letters*, [e-journal] 8(3), pp.199−216. https://dx.doi.org/10.1007/s10311-010-0297-8.

Nagawa, S., Xu, T. and Yang, Z., 2010. RHO GTPase in plants: conservation and invention of regulators and effectors. *Small GTPases*, [e-journal] 1(2), pp.78-88. https://dx.doi.org/10.4161/sgtp.1.2.14544.

Naghipour, D., Ashrafi, S.D., Gholamzadeh, M., Taghavi, K. and Naimi-Joubani, M., 2018. Phytoremediation of heavy metals (Ni, Cd, Pb) by *Azolla filiculoides* from aqueous solution: a dataset. *Data in Brief*, [e-journal] 21, pp.1409–1414. https://dx.doi.org/10.1016/j.dib.2018.10.111.

Nahar, K., and Hoque, S., 2021. Phytoremediation to improve eutrophic ecosystem by the floating aquatic macrophyte, water lettuce (*Pistia stratiotes*) at lab scale. *The Egyptian Journal of Aquatic Research*, [e-journal] 47(2), pp.231–237. https://dx.doi.org/10.1016/j.ejar.2021.05.003.

Nas, F.S. and Ali, M., 2018. The effect of lead on plants in terms of growing and biochemical parameters: a review. *MOJ Ecology and Environmental Sciences*, [e-journal] 3(4), pp.265-268. https://dx.doi.org/10.15406/mojes.2018.03.00098.

Naveen, B.P., Mahapatra , D.M., Sitharam, T.G., Sivapullaiah, P.V. and Ramachandra, T.V., 2017. Physico-chemical and biological characterization of urban municipal landfill leachate. *Environmental Pollution*, [e-journal] 220(Pt A), pp.1-12. https://dx.doi.org/10.1016/j.envpol.2016.09.002.

Ndimele, P.E., Kumolu-Johnson, C.A., Chukwuka, K.S., Ndimele, C.C., Ayorinde, O.A. and Adaramoye, O.R., 2014. Phytoremediation of iron (Fe) and copper (Cu) by water hyacinth (*Eichhornia crassipes* (Mart.) Solms). *Trends in Applied Sciences Research*, [e-journal] 9(9), pp.485–493. https://dx.doi.org/10.3923/tasr.2014.485.493.

Negi, N.P., Prakash, G., Narwal, P., Panwar, R., Kumar, D., Chaudhry, B. and Rustagi, A., 2023. The calcium connection: exploring the intricacies of calcium signaling in plant-microbe interactions. *Frontier in Plant Science*, [e-journal] 14. https://dx.doi.org/10.3389/fpls.2023.1248648.

Ng, H.F. and Ngeow, Y.F., 2022. A simple spreadsheet-based method for relative quantification using quantitative real-time PCR. *Biochemistry and Molecular Biology Education*, [e-journal] 50(1), pp.99-103. https://dx.doi.org/10.1002/bmb.21596.

Ng, K.S., Head, I.M., Premier, G.C., Scott, K., Yu, E., Lloyd, J. and Sadhukhan, J., 2016. A multilevel sustainability analysis of zinc recovery from wastes. *Resources, Conservation and Recycling*, [e-journal] 113, pp. 88–105. https://dx.doi.org/10.1016/j.resconrec.2016.05.013.

Ni, C. and Buszczak, M., 2023. Ribosome biogenesis and function in development and disease. *Development*, [e-journal] 150(5). https://dx.doi.org/10.1242/dev.201187.

Niazi, S., 2018. *Coagulation Effects of biological sludge reject water treatment*. Master. University of South-Eastern Norway.

Nidheesh, P.V., Couras, C., Karim, A.V. and Nadais, H., 2022. A review of integrated advanced oxidation processes and biological processes for organic pollutant removal. *Chemical Engineering Communications*, [e-journal] 209, pp.390–432. http://dx.doi.org/10.1080/00986445.2020.1864626.

Niekerk, L.A., Gokul, A., Basson, G., Badiwe, M., Nkomo, M., Klein, A. and Keyste, M. 2023. Heavy metal stress and mitogen activated kinase trranscription factors in plants: exploring heavy metal-ROS influences on plant signaling pathways. *Authorea*, [e-journal]. https://dx.doi.org/10.22541/au.169998555.59756936/v1

Niekerk, L.A., Gokul, A., Basson, G., Badiwe, M., Nkomo, M., Klein, A. and Keyster, M., 2024. Heavy metal stress and mitogen activated kinase transcription factors in plants: Exploring heavy metal-ROS influences on plant signalling pathways. *Plant, Cell and Environment*, [e-journal] 47(8), pp.2793-2810. https://dx.doi.org/10.1111/pce.14926.

Nik Daud, N.N., Mansor, N.A., Ahsan, A. and Idrus, S., 2015. Leachate treatment using aged refuse (ar) as a biofilter medium. *Polish Journal of Environmental Studies*, 24(2), pp. 605-609.

Ning, Y., Liu, N., Song, Y., Luo, J. and Li, T., 2019. Enhancement of phytoextraction of Pb by compounded activation agent derived from fruit residue. *International Journal of Phytoremediation*, [e-journal] 21(14), pp.1449-1456. http://dx.doi.org/ 10.1080/15226514.2019.1633266.

Noor, I., Sohail, H., Sun, J., Nawaz, M.A., Li, G., Hasanuzzaman, M. and Liu, J., 2022. Heavy metal and metalloid toxicity in horticultural plants: tolerance mechanism and remediation strategies. *Chemosphere*, [e-journal] 303(Pt 3). http://dx.doi.org/ 10.1016/j.chemosphere.2022.135196.

Norris, K., Hopes, T. and Aspden, J.L., 2021. Ribosome heterogeneity and specialization in development. *Wiley Interdisciplinary Reviews: RNA*, [e-journal] 12(4). http://dx.doi.org/10.1002/wrna.1644.

Novichkov, P.S., Gelfand, M.S. and Mironov, A.A., 2001. Gene recognition in eukaryotic DNA by comparison of genomic sequences. *Bioinformatics*, [e-journal] 17(11), pp.1011-1018. http://dx.doi.org/10.1093/bioinformatics/17.11.1011.

Novita, V.Z., Moersidik, S.S. and Priadi, C.R., 2019. Phytoremediation potential of *Pistia stratiotes* to reduce high concentration of copper (cu) in acid mine drainage. *IOP Conference Series: Earth and Environmental Science*, [e-journal] 355, http://dx.doi.org/10.1088/1755-1315/355/1/012063.

Nyabadza, A., Mccarthy, É., Makhesana, M., Heidarinassab, S., Plouze, A., Vazquez, M. and Brabazon D., 2023. A review of physical, chemical and biological synthesis methods of bimetallic nanoparticles and applications in sensing, water treatment, biomedicine, catalysis and hydrogen storage. *Advances in Colloid and Interface Science*, [e-journal] 321. http://dx.doi.org/10.1016/j.cis.2023.103010.

O'Connor, C.S., Leppi, N.W., Edwards, R. and Sunderland, G., 2003. The combined use of electrokinetic remediation and phytoremediation to decontaminate metal–polluted soils: a laboratory-scale feasibility study. *Environmental Monitoring and Assessment,* [e-journal] 84(1–2), pp.141–158. http://dx.doi.org/10.1023/a:1022851501118.

Oestreicher, J. and Morgan, B., 2019. Glutathione: subcellular distribution and membrane transport 1. *Biochemistry and Cell Biology*, [e-journal] 97(3), pp.270-289. http://dx.doi.org/10.1139/bcb-2018-0189.

Ohbayashi, I. and Sugiyama, M., 2018. Plant nucleolar stress response, a new face in the NAC-dependent cellular stress responses. *Frontier in Plant Science*, [e-journal] 8. http://dx.doi.org/10.3389/fpls.2017.02247.

Oladimeji, T.E., Oyedemi, M., Emetere, M.E., Agboola, O., Adeoye, J.B. and Odunlami, O.A., 2024. Review on the impact of heavy metals from industrial wastewater effluent and removal technologies. *Heliyon*, [e-journal] 10(23). http://dx.doi.org/10.1016/j.heliyon.2024.e40370.

Oliveira, C.C., Jones, A.M., Fontes, E.P.B. and Reis, P.A.B.d., 2022. G-protein phosphorylation: aspects of binding specificity and function in the plant kingdom. *International Journal of Molecular Sciences*, [e-journal] 23(12). https://dx.doi.org/10.3390/ijms23126544.

Onukwufor, J.O., Berry, B.J. and Wojtovich, A.P., 2019. Physiologic implications of reactive oxygen species production by mitochondrial complex i reverse electron transport. *Antioxidants (Basel),* [e-journal] 8(8). https://dx.doi.org/10.3390/antiox8080285.

Ordonez, N.M., Marondedze, C., Thomas, L., Pasqualini, S., Shabala, L., Shabala, S. and Gehring, C. 2014. Cyclic mononucleotides modulate potassium and calcium flux responses to H_2O_2 in *Arabidopsis* roots. *FEBS Letters,* [e-journal] 588, pp.1008–1015. https://dx.doi.org/10.1016/j.febslet.2014.01.062.

Osogo, A.K., Shrabana Sarkar, B., Muyekho, F.N., Were, H.K. and Okoth, P., (in press) Genome-wide metatranscriptomics crosswalk of diseased common beans (*Phaseolus vulgaris* L) unravels critical metabolic pathways involved in plant defense mechanisms. *Preprints*.

Othman, N.H., Alias, N.H., Fuzil, N.S., Marpani, F., Shahruddin, M.Z., Chew, C.M., Ng, D.K.M., Lau, W.J. and Ismail, A.F., 2022. A review on the use of membrane technology systems in developing countries. *Membranes,* [e-journal] 12(1). https://dx.doi.org/10.3390/membranes12010030.

Ovečka, M. and Takáč, T., 2013. Managing heavy metal toxicity stress in plants: biological and biotechnological tools. *Biotechnology Advances,* 32(1), pp.73-86. https://dx.doi.org/10.1016/j.biotechadv.2013.11.011.

Özmen, G., and Özsoy, A., 2020. *Waste management optimization by using IoT*. [pdf] Finland: Lappeenranta-Lahti University of Technology. Available at: <https://www.researchgate.net/publication/345941365_Waste_Management_Optimization_by_Using_IoT> [Accessed: 1 June 2024].

Paksi, Z., Jancsó, A., Pacello, F., Nagy, N., Battistoni, A. and Gajda, T., 2008. Copper and zinc binding properties of the N-terminal histidine-rich sequence of *Haemophilus ducreyi* Cu, Zn superoxide dismutase. *Journal of Inorganic Biochemistry,* [e-journal] 102, pp.1700–1710. https://dx.doi.org/10.1016/j.jinorgbio.2008.04.007.

Pan, Z., Song, C., Li, L., Wang, H., Pan, Y., Wang, C., Li, J., Wang, T. and Feng, X., 2019. Membrane technology coupled with electrochemical advanced oxidation processes for organic wastewater treatment: recent advances and future prospects. *Chemical Engineering Journal,* [e-journal] 376. https://dx.doi.org/10.1016/j.cej.2019.01.188.

Pandey, V.P., Awasthi, M., Singh, S., Tiwari, S. and Dwivedi, U.N., 2017. A comprehensive review on function and application of plant peroxidases *Biochemistry and Analytical Biochemistry,* [e-journal] 6. https://dx.doi.org/10.4172/2161-1009.1000308.

Pandis, P.K., Kalogirou, C., Kanellou, E., Vaitsis, C., Savvidou, M.G., Sourkouni, G., Zorpas, A.A. and Argirusis, C., 2022. Key points of advanced oxidation processes (AOPs) for wastewater, organic pollutants and pharmaceutical waste treatment: a mini review. *ChemEngineering,* [e-journal] 6(1):8. http://dx.doi.org/10.3390/chemengineering6010008.

Pang, Y.L., Quek, Y.Y., Lim, S. and Shuit, S.H., 2023. Review on phytoremediation potential of floating aquatic plants for heavy metals: a promising approach. *Sustainabilit*y, [e-journal] 15(2). https://dx.doi.org/10.3390/su15021290.

Parić, A., Muratović, E., Murtić, S., Subašić, M., & Pustahija, F., 2025. Biochemical-physiological responses of *Reseda lutea*, *Epilobium dodonaei*, and *Gentianella ciliata* to stress in an open pit of an abandoned iron mine. *International Journal of Phytoremediation*, [e-journal] 27(8), pp.1110–1118. https://dx.doi.org/10.1080/15226514.2025.2481952.

Park, J.K. and Oh, K., 2023. Advancements in phytoremediation research for soil and water resources: harnessing plant power for environmental cleanup. *Sustainabilit*y, [e-journal] 15(18). http://dx.doi.org/10.3390/su151813901.

Parry, G., 2015. The plant nuclear envelope and regulation of gene expression. *Journal of Experimental Botany*, [e-journal] 66(6), pp.1673-1685. https://dx.doi.org/10.1093/jxb/erv023.

Parray, Z.A., 2025. A review on evolution, structural characteristics, interactions, and regulation of the membrane transport protein: the family of Rab proteins. *International Journal of Biological Macromolecules*, [e-journal] 296. https://dx.doi.org/10.1016/j.ijbiomac.2025.139828

Patra, R.C., Rautray A.K. and Swarup D., 2011. Oxidative stress in lead and cadmium toxicity and its amelioration. *Veterinary Medicine International*, [e-journal] 2011. https://dx.doi.org/10.4061/2011/457327.

Peixoto, P.H.P., Cambraia, J., Sant'Anna, R., Mosquim, P.R. and Moreira, M.A., 1999. Aluminum effects on lipid peroxidation and on the activities of enzymes of oxidative metabolism in sorghum. *Revista Brasileira de Fisiologia Vegetal*, 11, pp.137-143.

Peng, Z., Tian, J., Luo, R., Kang, Y., Lu, Y., Hu, Y., Liu, N., Zhang, J., Cheng, H., Niu, S., Zhang, J. and Yao, Y., 2020. MiR399d and epigenetic modification comodulate anthocyanin accumulation in *Malus* leaves suffering from phosphorus deficiency. *Plant Cell and Environment*, [e-journal] 43(5). https://dx.doi.org/10.1111/pce.13697.

Pereira, M.A., Imada, E.L. and Guedes, R.L.M., 2017. RNA-seq: applications and best practices. In: F.A. Marchi, Cirillo, P.D.R. and E.C. Mateo, eds. 2017. *Applications of RNA-seq and omics strategies - from microorganisms to human health.* London: InTechOpen. http://dx.doi.org/10.5772/intechopen.69250.

Petibon, C., Malik Ghulam, M., Catala, M. and Abou Elela, S., 2021. Regulation of ribosomal protein genes: an ordered anarchy. *Wiley Interdisciplinary Reviews: RNA*, [e-journal] 12(3). https://dx.doi.org/10.1002/wrna.1632.

Petrov, V., Hille, J., Mueller-Roeber, B. and Gechev, T., 2015. ROS-mediated abiotic stress-induced programmed cell death in plants. *Frontiers in Plant Science*, [e-journal] 6. https://dx.doi.org/10.3389/fpls.2015.00069.

Peymani, F., Farzeen, A. and Prokisch, H., 2022. RNA sequencing role and application in clinical diagnostic. *Pediatric Investigation*, [e-journal] 6(1), pp.29-35. https://dx. doi.org/10.1002/ped4.12314.

Pilon, M., Ravet K. and Tapken, W., 2011. The biogenesis and physiological function of chloroplast superoxide dismutases. *Biochimica et Biophysica Acta (BBA) – Bioenergetics*, [e-journal] 1807(8), pp.989–998. https://dx.doi.org/10.1016/j.bbabio.2010.11.002.

Pinho, S. and Ladeiro, B., 2012. Phytotoxicity by lead as heavy metal focus on oxidative stress. *Journal of Botany*, [e-journal] 2012. https://dx.doi.org/10.1155/2012/369572.

Pinto, E. and Ferreira, I.M., 2015. Cation transporters/channels in plants: tools for nutrient biofortification. *Journal of Plant Physiology*, [e-journal] 179, pp.64-82. https://dx.doi.org/10.1016/j.jplph.2015.02.010.

Pliquett, U., Joshi, R.P., Sridhara, V. and Schoenbach, K.H., 2007. High electrical field effects on cell membranes. *Bioelectrochemistry*, [e-journal] 70(2), pp.275-82. https://dx.doi.org/10.1016/j.bioelechem.2006.10.004.

Pohl, A., 2020. Removal of heavy metal ions from water and wastewaters by sulfur-containing precipitation agents. *Water, Air and Soil Pollution*, [e-journal] 231(503). http://dx.doi.org/10.1007/s11270-020-04863-w.

Powrie, W., Velis, C., Cook, E. and Ingham, H., 2021. Open uncontrolled burning of solid waste undermines human health: Time to act. *Waste Management and Research*, [e-journal] 39, pp.1–2. https://dx.doi.org/10.1177/0734242X20981800.

Prasad, M.N.V. and Freitas, H.M.O., 2003. Metal hyperaccumulation in plants: biodiversity prospecting for phytoremediation technology. *Electronic Journal of Biotechnology*, 6(3), pp.285-321.

Priya, M., Balakrishnan, V., Lakshmi, A.K., Aruna, R. and Ravindran, K.C., 2014. Mercury induced oxidative stress of antioxidants in *Clitoria ternatea* L. *International Letters of Natural Sciences*, [e-journal] 23. https://dx.doi.org/10.56431/p-5331fs.

Priya, A.K., Muruganandam, M., Ali, S.S. and Kornaros, M., 2023. Clean-up of heavy metals from contaminated soil by phytoremediation: a multidisciplinary and eco-friendly approach. *Toxics,* [e-journal] 11(5). https://dx.doi.org/10.3390/toxics11050422

Priyanka, N., Geetha, N., Manish, T., Sahi, S.V. and Venkatachalam, P., 2021. Zinc oxide nanocatalyst mediates cadmium and lead toxicity tolerance mechanism by differential regulation of photosynthetic machinery and antioxidant enzymes level in cotton seedlings. *Toxicology Reports*, [e-journal] 8, pp.295-302. https://dx.doi.org/10.1016/j.toxrep.2021.01.016.

Przybyla-Toscano, J., Chetouhi, C., Balliau, T., Alban, C., Bourguignon, J. and Ravanel, S., (in press). Dynamics of the membrane- and cell wall-associated proteome of *Arabidopsis thaliana* roots in response to uranium stress. *New Results.*

Putra, R.S. and Hastika, F.Y., 2018. Removal of heavy metals from leachate using Electro-Assisted Phytoremediation (EAPR) and up-take by water hyacinth (*Eichornia crassipes). Indonesian Journal of Chemistry*, [e-journal] 18(2), pp.306–312. http://dx.doi.org/10.22146/ijc.29713.

Putra, R.S., Ohkawa, Y. and Tanaka, S., 2013. Application of EAPR system on removal of lead from sandy soil and uptake by Kentucky bluegrass (*Poa pratensis* L.). *Separation and Purification Technology,* [e-journal] 102, pp.34–42. http://dx.doi.org/10.1016/j.seppur.2012.09.025.

Putra, R.S., Cahyana, F. and Novarita, D., 2015. Removal of lead and copper from contaminated water using EAPR system and uptake by water lettuce (*Pistia stratiotes* L). *Procedia Chemistry*, [e-journal] 14, pp.381–386. http://dx.doi.org.10.1016/j.proche.2015.03.052.

Putra, R.S., Novarita, D. and Cahyana, F., 2016. Remediation of lead (Pb) and copper (Cu) using water hyacinth [*Eichornia crassipes* (Mart.) Solms] with electro-assisted phytoremediation (EAPR). *AIP Conference Proceedings*, [e-journal] 1744. https://dx.doi.org/10.1063/1.4953526.

Putra, R.S., Annisa, A.D. and Budiarjo, S., 2020. Batik wastewater treatment using simultaneous process of electrocoagulation and electro-assisted phytoremediation (EAPR). *Indonesian Journal of Chemistry*, [e-journal] 20(6), pp.1221-1229. https://dx.doi.org/10.22146/ijc.47898.

Putra, R.S., Trahadinata, G.A., Latif, A. and Solehudin, M., 2017. Wastewater treatment of chemical laboratory using electro assisted-phytoremediation (EAPR). *AIP Conference Proceedings*, [e-journal] 1823. https://dx.doi.org/10.1063/1.4978150.

Putra, R.S., Wicaksono, W.P., Fatimah, I. and Tanaka, S., 2022. Electro-enhanced phytoremediation system on the removal of trace metal concentration from contaminated water. *Heliyon*, [e-journal] 8(11). http://dx.doi.org/1010.1016/j.heliyon.2022.e11451.

Qian, F.Y., Sun X.B. and Liu, Y., 2013. Effect of ozone on removal of dissolved organic matter and its biodegradability and adsorbability in biotreated textile effluents. *Ozone: Science and Engineering*, [e-journal] 35, pp.7–15. http://dx.doi.org/10.1080/01919512.2013.720211.

Qin, Y. M., Hu, C.Y. and Zhu, Y.X., 2008. The ascorbate peroxidase regulated by H_2O_2 and ethylene is involved in cotton fiber cell elongation by modulating ROS homeostasis. *Plant Signaling and Behavior*, [e-journal] 3(3), 194–196. https://dx.doi.org/10.4161/psb.3.3.5208.

Quattrocchi, U. ed., 2017. *CRC World dictionary of plant names: common names, scientific names, eponyms, synonyms, and etymology*. Boca Raton, FL: CRC Press.

Raabe, K., Honys, D. and Michailidis, C., 2019. The role of eukaryotic initiation factor 3 in plant translation regulation. *Plant Physiology and Biochemistry*, [e-journal] 145, pp.75-83. http://dx.doi.org/10.1016/j.plaphy.2019.10.015.

Raaijmakers, J.H. and Bos, J.L., 2009. Specificity in Ras and Rap signaling. *Journal of Biological Chemistry*, [e-journal] 284(17), pp.10995-10999. http://dx.doi.org/10.1074/jbc.R800061200.

Radfard, M., Hashemi, H., Baghapour, M.A., Samaei, M.R., Yunesian, M., Soleimani, H. and Azhdarpoor, A., 2023. Prediction of human health risk and disability-adjusted life years induced by heavy metals exposure through drinking water in Fars Province, Iran. *Scientific Reports*, [e-journal] 13. https://dx.doi.org/10.1038/s41598-023-46262-1.

Radziemska, M., 2018. Study of applying naturally occurring mineral sorbents of Poland (dolomite halloysite, chalcedonite) for aided phytostabilization of soil polluted with heavy metals. *Catena*, [e-journal] 163, pp.123–129. http://dx.doi.org/10.1016/j.catena.2017.12.015.

Raghab, S.M., Abd El Meguid, A.M. and Hegazi, H.A., 2013. Treatment of leachate from municipal solid waste landfill. *HBRC Journal*, [e-journal] 9(2), pp.187–192. http://dx.doi.org/10.1016/j.hbrcj.2013.05.007.

Raghavachari, N. and Garcia-Reyero, N., 2018. Overview of gene expression analysis: transcriptomics. In: N. Raghavachari and N. Garcia-Reyero, eds. 2018. *Gene expression analysis. Methods in molecular biology*. New York: Humana Press. pp.1–6.

Raghavan, V., Kraft, L., Mesny, F. and Rigerte, L., 2022. A simple guide to *de novo* transcriptome assembly and annotation. *Briefings in Bioinformatics*, [e-journal] 23(2). https://dx.doi.org/10.1093/bib/bbab563.

Ragio, R.A., Garcia, J., Subtil, E.L. and Arantes, C., 2022. Assessment of natural tannin-based coagulant for effective ultrafiltration (UF) of UASB effluent: fouling mechanisms, pollutant removal and water reclamation feasibility. *SSRN Electronic Journal*, [e-journal] 2022. http://dx.doi.org/10.2139/ssrn.4303090.

Rahman, Z. and Singh, V.P. 2019. The relative impact of toxic heavy metals (THMs) (arsenic (As), cadmium (Cd), chromium (Cr)(VI), mercury (Hg), and lead (Pb)) on the total environment: an overview. *Environmental Monitoring and Assessment*, [e-journal] 191(7). https://dx.doi.org/10.1007/s10661-019-7528-7.

Rahman, N., Shamsuzzaman, M. and Lindahl, L., 2020. Interaction between the assembly of the ribosomal subunits: disruption of 40S ribosomal assembly causes accumulation of extra-ribosomal 60S ribosomal protein uL18/L5. *PLoS One*, [e-journal] 15(1). https://dx.doi.org/10.1371/journal.pone.0222479.

Rai, B. and Shrivastav, A., 2022. Removal of emerging contaminants in water treatment by nanofiltration and reverse osmosis. In: M. Shah, S. Rodriguez-Couto and J. Biswas, eds. 2022. *Development in wastewater treatment research and processes*. Amsterdam: Elsevier. pp.605–628.

Rai, P.K., Nongtri, E.S., Lalawmpuii and Syngkli, R.B., 2024. *Pistia stratiotes* based heavy metals phytoremediation of a Himalayan river impacted by hydroelectric plant in an Indo Burma hotspot region. *Chemistry and Ecology*, [e-journal] 40(7), pp.796–815. https://dx.doi.org/10.1080/02757540.2024.2350050.

Rajaeifar, M.A., Tabatabaei, M., Ghanavati, H., Khoshnevisan, B. and Rafiee, S., 2015. Comparative life cycle assessment of different municipal solid waste management scenarios in Iran. *Renewable and Sustainable Energy Reviews*, [e-journal] 51, pp.886–898. https://dx.doi.org/10.1016/j.rser.2015.06.037.

Rajagopalan, N.R., Munawar, T., Sheehan, M.C., Fujimori, M., Vista, W.R., Wimmer, T., Gutta, N.B., Solomon, S.B. and Srimathveeravalli, G., 2024. Electrolysis products, reactive oxygen species and ATP loss contribute to cell death following irreversible electroporation with microsecond-long pulsed electric fields. *Bioelectrochemistry*, [e-journal] 155. https://dx.doi.org/10.1016/j.bioelechem.2023.108579

Rajput, V.D., Harish, Singh R.K., Verma, K.K., Sharma, L., Quiroz-Figueroa, F.R., Meena, M., Gour, V.S., Minkina, T., Sushkova, S. and Mandzhieva, S., 2021. Recent developments in enzymatic antioxidant defence mechanism in plants with special reference to abiotic stress. *Biology (Basel)*, [e-journal] 10(4). https://dx.doi.org/10.3390/biology10040267.

Ranjha, M.M.A.N., Kanwal, R., Shafique, B., Arshad, R.N., Irfan, S., Kieliszek, M., Kowalczewski, P.Ł., Irfan, M., Khalid, M.Z., Roobab, U. and Aadil, R.M.,

2021. A critical review on pulsed electric field: a novel technology for the extraction of phytoconstituents. *Molecules*, [e-journal] 26(16). https://dx.doi.org/10.3390/molecules26164893.

Ranner, J.L., Schalk, S., Martyniak, C., Parniske, M., Gutjahr, C., Stark, T.D. and Dawid, C., 2023. Primary and secondary metabolites in *Lotus japonicus*. *Journal of Agricultural and Food Chemistry*, [e-journal] 71, pp.11277–11303. https://dx.doi.org/10.1021/acs.jafc.3c02709.

Rao, M.J., Duan, M., Zhou, C., Jiao, J., Cheng, P., Yang, L., Wei, W., Shen, Q., Ji, P., Yang, Y., Conteh, O., Yan, D., Yuan, H., Rauf, A., Ai, J. and Zheng, B., 2025. Antioxidant defense system in plants: reactive oxygen species production, signaling, and scavenging during abiotic stress-induced oxidative damage. *Horticulturae*, [e-journal] 11(5). https://dx.doi.org/10.3390/horticulturae11050477.

Rascio, N. and Navari-Izzo, F., 2011. Heavy metal hyperaccumulating plants: how and why do they do it? And what makes them so interesting? *Plant Science*, [e-journal] 180(2), pp.169-181. http://dx.doi.org/10.1016/j.plantsci.2010.08.016.

Rastgoo, L. and Alemzadeh, A., 2011. Biochemical responses of Gouan (*Aeluropus littoralis*) to heavy metals stress. *Australian Journal of Crop Science*, [e-journal] 5(4), pp.375–383. https://dx.doi.org/10.3316/informit.281334528451448.

Rawat, H., Bhat, S.A., Dhanjal, D.S., Singh, R., Gandhi, Y., Mishra, S.K., Kumar, V., Shakya, S.K., Narasimhaji, C.V., Singh, A., Singh, R. and Acharya, R., 2024. Emerging techniques for the trace elemental analysis ofplants and food-based extracts: A comprehensive review. *Talanta Open*, [e-journal] 10. https://dx.doi.org/10.1016/j.talo.2024.100341.

Raza, A., Tabassum, J., Zahid, Z., Charagh, S., Bashir, S., Barmukh, R., Khan, R.S.A., Barbosa, F.Jr., Zhang, C., Chen, H., Zhuang, W. and Varshney, R.K., 2022. Advances in "Omics" approaches for improving toxic metals/metalloids tolerance in plants. *Frontier in Plant Science*, [e-journal] 12. https://dx.doi.org/10.3389/fpls.2021.794373.

Razalli, I.I., Abdullah-Zawawi, M.R., Zainal Abidin, R.A., Harun, S., Che Othman, M.H., Ismail, I. and Zainal, Z., 2025. Identification and validation of hub genes associated with biotic and abiotic stresses by modular gene co-expression analysis

in *Oryza sativa* L. Scientific Reports, [e-journal] 5(1). https://dx.doi.org/10.1038/s41598-025-92942-5.

Reeves, R.D., van der Ent, A., Echevarria, G., Isnard, S. and Baker, A.J.M., 2021. Global distribution and ecology of hyperaccumulator plants. In: A. van der Ent, A.J. Baker, G. Echevarria, M.O. Simonnot, J.L. Morel, eds. 2021. *Agromining: Farming for Metals*. Cham: Springer. pp 133–154.

Regmi, C., Kshetri, Y.K. and Wickramasinghe, S.R., 2025. Hybrid combination of advanced oxidation process with membrane technology for wastewater treatment: gains and problems. *Nanotechnology*, [e-journal] 36(13). https://dx.doi.org/10.1088/1361-6528/adb040.

Renou, S., Givaudan, J.G., Poulain, S., Dirassouyan, F. and Moulin, P., 2008. Landfill leachate treatment: review and opportunity. *Journal of Hazardous Materials*, [e-journal] 150, pp.468–493. https://dx.doi.org/10.1016/j.jhazmat.2007.09.077.

Renu, K., Chakraborty, R., Myakala, H., Koti, R., Famurewa, A.C., Madhyastha, H., Vellingiri, B., George, A. and Valsala Gopalakrishnan, A., 2021. Molecular mechanism of heavy metals (lead, chromium, arsenic, mercury, nickel and cadmium) - induced hepatotoxicity - a review. *Chemosphere*, [e-journal] 271. https://dx.doi.org/10.1016/j.chemosphere.2021.129735.

Reyna-Bensusan, N., Wilson, D.C., Davy, P.M., Fuller, G.W., Fowler, G.D. and Smith, S.R., 2019. Experimental measurements of black carbon emission factors to estimate the global impact of uncontrolled burning of waste. *Atmospheric Environment*, [e-journal] 213, pp.629–639. https://dx.doi.org/10.1016/j.atmosenv.2019.06.047.

Reynoso, M.A., Borowsky, A.T., Pauluzzi, G.C., Yeung, E., Zhang, J., Formentin, E., Velasco, J., Cabanlit, S., Duvenjian, C., Prior, M.J., Akmakjian, G.Z., Deal, R.B., Sinha, N.R., Brady, S.M., Girke, T. and Bailey-Serres, J., 2022. Gene regulatory networks shape developmental plasticity of root cell types under water extremes in rice. *Developmental Cell*, [e-journal] 57(9), pp.1177-1192.e6. https://dx.doi.org/10.1016/j.devcel.2022.04.013.

Riyazuddin, R., Nisha, N., Ejaz, B., Khan, M.I.R., Kumar, M., Ramteke, P.W. and Gupta, R.A, 2022. Comprehensive review on the heavy metal toxicity and

sequestration in plants. *Biomolecules,* [e-journal] 12(1). https://dx.doi.org/10.3390/biom12010043.

Robertson, S.M., Schmid, R.B. and Lundgren, J.G., 2023. Estimating plant biomass in agroecosystems using a drop-plate meter. *Peer J,* [e-journal] 11. https://dx.doi.org/10.7717/peerj.15740.

Robinson, M.D., McCarthy, D.J. and Smyth, G.K., 2010. edgeR: a Bioconductor package for differential expression analysis of digital gene expression data. *Bioinformatics*, [e-journal] 26(1), pp.139-40. http://dx.doi.org.10.1093/bioinformatics/btp616.

Ronzan, M., Piacentini, D., Fattorini, L., Della Rovere, F., Eiche, E., Riemann, M., Altamura, M.M. and Falasca, G., 2018. Cadmium and arsenic affect root development in *Oryza sativa* L. negatively interacting with auxin. *Environmental and Experimental Botany*, [e-journal] 151, pp.64–75. https://dx.doi.org/10.1016/j.envexpbot.2018.04.008.

Rookesh, T., Samaei, M. R., Yousefinejad, S., Hashemi, H., Derakhshan, Z., Abbasi, F., Jalili, M., Giannakis, S. and Bilal, M., 2022. Investigating the electrocoagulation treatment of landfill leachate by iron/graphite electrodes: process parameters and efficacy assessment. *Water,* [e-journal] 14(2). https://dx.doi.org/10.3390/w14020205.

Rosa, A.C., Corsi, D., Cavi, N., Bruni, N. and Dosio, F., 2021. Superoxide dismutase administration: a review of proposed human uses. *Molecules*, [e-journal] 26(7). https://dx.doi.org/10.3390/molecules26071844.

Rosas-Ramírez, M., Tovar-Sánchez, E., Rodríguez-Solís, A., Flores-Trujillo, K., Castrejón-Godínez, M.L. and Mussali-Galante, P., 2024. Assisted phytoremediation between biochar and *Crotalaria pumila* to phytostabilize heavy metals in mine tailings. *Plants,* [e-journal] 13(17). https://doi.org/10.3390/plants13172516.

Rosenberg, D. and Hoover, D., 2021. Burned: why waste incineration is harmful. *Natural Resources Defense Council,* [online] Available at: <https://www.nrdc.org/bio/daniel-rosenberg/burned-why-waste-incineration-harmful> [Accessed 22 June 2024].

Rowe, J., Topping, J.F., Liu, J. and Lindsey, K., 2016. Abscisic acid regulates root growth under osmotic stress conditions via an interacting hormonal network with cytokinin, ethylene and auxin. *New Phytologist,* [e-journal] 211, pp.225–239. http://dx.doi.org/10.1111/nph.13882.

Rudenko, N.N., Vetoshkina, D.V., Marenkova, T.V. and Borisova-Mubarakshina, M.M., 2023. Antioxidants of non-enzymatic nature: their function in higher plant cells and the ways of boosting their biosynthesis. *Antioxidants (Basel)*, [e-journal] 12(11). http://dx.doi.org/ 10.3390/antiox12112014.

Ruppert, L., Lin, Z.Q., Dixon, R.P. and Johnson, K.A., 2013. Assessment of solid phase microfiber extraction fibers for the monitoring of volatile organoarsinicals emitted from a plant-soil system. *The Journal of Hazardous Materials*, [e-journal] 262, pp.1230-1236. http://dx.doi.org/ 10.1016/j.jhazmat.2012.06.046.

Ryplova, R., Pokorny, J. and Baxa, M., 2023. Education for sustainability: innovative teaching on photosynthesis of aquatic plants in ecological context. *European Journal of Sustainable Development*, [e-journal] 12(4), pp.69-82. http://dx.doi.org/ 10.14207/ejsd.2023.v12n4p69.

Sabagh, A.E.L., Islam, M.S., Hossain, A., Iqbal, M.A., Mubeen, M., Waleed, M., et al., 2022. Phytohormones as growth regulators during abiotic stress tolerance in plants. *Frontiers in Agronomy*, [e-journal] 4. https:// dx.doi.org/10.3389/fagro.2022.765068

Sáez-Vásquez, J. and Delseny, M., 2019. Ribosome biogenesis in plants: from functional 45S ribosomal DNA organization to ribosome assembly factors. *The Plant Cell*, [e-journal] 31(9), pp.1945–1967. https://dx.doi.org/10.1105/tpc.18.00874.

Saghi, M.H., Nadimi, H., Eslami, A., Bakhtiarvand, S.N.A., Oghazyan, A., Setoudeh, S. and Sargolzaei, M.S., 2024. Characteristics and pollution indices of leachates from municipal solid waste landfills in Iranian metropolises and their implications for MSW management. *Scientific Reports,* [e-journal] 14 (27285). https://dx.doi.org/10.1038/s41598-024-78630-w.

Saha, A., Mukherjee, P., Roy, K., Sen, K. and Sanyal, T., 2022. A review on phyto-remediation by aquatic macrophytes: a natural promising tool for sustainable

management of ecosystem. *International Journal of Experimental Research and Review*, [e-journal] 27, pp.9-31. https://dx.doi.org/10.52756/ijerr.2022.v27.002.

Sahebjamei, H., Abdolmaleki, P. and Ghanati, F., 2007. Effects of magnetic field on the antioxidant enzyme activities of suspension-cultured tobacco cells. *Bioelectromagnetics*, [e-journal] 28(1), pp.42-47. https://dx.doi.org/10.1002/bem.20262.

Saktioto, S., Agustin, D., Zamri, Z., Basdyo, D., Abdullah, H.Y., Hairi, H.M. and Fadhali, M.M., 2023. Effect of direct current electric field on the root growth of oil palm seedlings. *Science, Technology, and Communication Journal,* [e-journal] 3(2), pp.51–56. https://dx.doi.org/10.59190/stc.v3i2.230.

Saleem, K., Zaman, A., Butt, T.A., Mirza, C.R., Iqbal, A., Khan, A.H.A., Yousaf, S. and Iqbal, M., 2023. Uptake and distribution of cadmium and copper by *Solanum lycopersicum* L. and changes in the metabolite production. *Biology Bulletin*, [e-journal] 50, pp.390–399. https://dx.doi.org/10.1134/S1062359022602245.

Saleh, T.A., Mustaqeem, M. and Khaled, M., 2022. Water treatment technologies in removing heavy metal ions from wastewater: a review. *Environmental Nanotechnology, Monitoring and Management*, [e-journal] 17. https://dx.doi.org/10.1016/j.enmm.2021.100617.

Šamajová, O., Plíhal, O., Al-Yousif, M., Hirt, H. and Šamaj, J., 2013. Improvement of stress tolerance in plants by genetic manipulation of mitogen-activated protein kinases. *Biotechnology Advances*, [e-journal] 31(1), pp.118-28. https://dx.doi.org/10.1016/j.biotechadv.2011.12.002.

Samal, K. and Dash, R.R., 2024. Experiments and modeling to develop a *Pistia stratiotes* based Floating Vegetated System (FVS) for the removal of heavy metals (Pb, Zn, Cr, Cu, Ni). *Science of The Total Environment*, [e-journal] 926. https://dx.doi.org/10.1016/j.scitotenv.2024.171981.

Sandalio, L.M. and Romero-Puertas M.C., 2015. Peroxisomes sense and respond to environmental cues by regulating ROS and RNS signalling networks. *Annals of Botany*, [e-journal] 116(4), pp.475-85. https://dx.doi.org/10.1093/aob/mcv074.

Sandalio, L.M., Espinosa, J., Shabala, S., León, J. and Romero-Puertas MC., 2023. Reactive oxygen species- and nitric oxide-dependent regulation of ion and metal homeostasis in plants. Journal of Experimental Botany, 74(19), pp.5970-5988. doi: 10.1093/jxb/erad349.

Sanders, D., Pelloux, J., Brownlee, C. and Harper, J.F., 2002. Calcium at the crossroads of signaling. *Plant Cell*, [e-journal] 14, pp.S401-17. https://dx.doi.org/10.1105/tpc.002899.

Saniewski, M., Ueda, J. and Miyamoto, K., 2002. Relationships between jasmonates and auxin in regulation of some physiological processes in higher plants. *Acta Physiologiae Plantarum,* [e-journal] 24, pp.211–220. https://dx.doi.org/10.1007/s11738-002-0013-9.

Sankaranarayanan, S., Ju, Y. and Kessler, S.A., 2020. Reactive oxygen species as mediators of gametophyte development and double fertilization in flowering plants. *Frontier in Plant Science*, [e-journal] 11. https://dx.doi.org/10.3389/fpls.2020.01199.

Santos, C.S., Roriz, M., Carvalho, S.M. and Vasconcelos, M.W., 2015. Iron partitioning at an early growth stage impacts iron deficiency responses in soybean plants (*Glycine max* L.). *Frontiers in Plant Science*, [e-journal] 6. https://dx.doi.org/10.3389/fpls.2015.00325.

Santoso, N.P., Haumahu, J.P., Maimuna, D. and Habi, L., 2016. Spatial analysis of heavy metals pollution as the impact of waste landfill ambon at Wai Yori watershed in Negeri Passo. *Jurnal Budidaya Pertanian*, 12(2), pp.55-65.

Saravanan, A., Senthil Kumar, P., Jeevanantham, S., Karishma, S., Tajsabreen, B., Yaashikaa, P.R. and Reshma, B., 2021. Effective water/wastewater treatment methodologies for toxic pollutants removal: processes and applications towards sustainable development. *Chemosphere*, [e-journal] 280. http://dx.doi.org/10.1016/j.chemosphere.2021.130595.

Schmidt, W., Thomine, S. and Buckhout, T.J., 2020. Editorial: iron nutrition and interactions in plants. *Frontiers in Plant Science*, [e-journal] 10. https://dx.doi.org/10.3389/fpls.2019.01670.

Schwitzguébel, J.P., 2017. Phytoremediation of soils contaminated by organic compounds: hype, hope and facts. *Journal of Soils and Sediments*, [e-journal] 17(5), pp.1492–1502. http://dx.doi.org/10.1007/s11368-015-1253-9.

Sengupta, S. and Pal, C.K., 2021. Chemistry in wastewater treatment. In: S. Upadhyayula and A. Chaudhary, eds. 2020. *Advanced materials and technologies for wastewater treatment*. Boca Raton, FL: CRC Press. pp.129–152.

Seregin, I.V. and Kozhevnikova, A.D., 2025. Plant responses to heavy metals: from deficiency to excess. *International Journal of Molecular Sciences*, [e-journal] 26(5). http://dx.doi.org/10.3390/ijms26052064.

Sewelam, N., Kazan, K. and Schenk, P.M., 2016. Global plant stress signaling: reactive oxygen species at the cross-road. Frontier in Plant Sciences, [e-journal] 7. https://dx.doi.org/10.3389/fpls.2016.00187.

Shabbir, R., Javed, T., Hussain, S., Ahmar, S., Naz, M., Zafar, H., Pandey, S., Chauhan, J., Siddiqui, M.H. and Chen, P., 2022. Calcium homeostasis and potential roles to combat environmental stresses in plants. *South African Journal of Botany*, [e-journal] 148, pp.683-693. https://dx.doi.org/10.1016/j.sajb.2022.05.038.

Shah, A.A., Walia, S. and Kazemian, H., 2024. Advancements in combined electrocoagulation processes for sustainable wastewater treatment: A comprehensive review of mechanisms, performance, and emerging applications. *Water research*, 252. https://doi.org/10.1016/j.watres.2024.121248

Shahid, M., Khalid, S., Abbas, G., Shahid, N., Nadeem, M., Sabir, M., Aslam, M. and Dumat, C., 2015. Heavy metal stress and crop productivity. In: K. Hakeem, ed. 2015. *Crop production and global environmental issues*. Switzerland: Springer International Publishing. pp.1-25.

Sharma P. and Dubey R., 2005. Lead toxicity in plants. *Brazilian journal of plant physiology*, [e-journal] 17, pp.35–52. http://dx.doi.org/10.1590/S1677-04202005000100004.

Sharma, G., Sharma, S., Kumar, A., Lai, C. W., Naushad, M., Shehnaz, Iqbal, J. and Stadler, F.J., 2022. Activated carbon as superadsorbent and sustainable material for diverse applications. *Adsorption Science and Technology*, [e-journal] 2022. http://dx.doi.org/10.1155/2022/4184809.

Sharma, J.K., Kumar, N., Singh, N.P. and Santal, A.R., 2023a. Phytoremediation technologies and their mechanism for removal of heavy metal from contaminated soil: An approach for a sustainable environment. *Frontier in Plant Sciences*, [e-journal] 14. http://dx.doi.org/10.3389/fpls.2023.1076876.

Sharma, P., Lakra, N., Goyal, A., Ahlawat, Y.K., Zaid, A. and Siddique, K.H.M., 2023b. Drought and heat stress mediated activation of lipid signaling in plants: a critical review. *Frontier in Plant Science*, [e-journal] 14. http://dx.doi.org/10.3389/fpls.2023.1216835.

Sharma, V., Nagpal, G., Naveen, B.P. and Gupta, P., 2026. An updated review on landfill leachate treatment methods. *Discovover Chemistry*, [e-journal] 3**(**34). https://dx.doi.org/10.1007/s44371-026-00473-3.

Shigeoka, S., Ishikawa, T., Tamoi, M., Miyagawa, Y., Takeda, T., Yabuta, Y. and Yoshimura, K., 2002. Regulation and function of ascorbate peroxidase isoenzymes. *Journal of Experimental Botany,* [e-journal] 53, pp.1305–1319. http://dx.doi.org/10.1093/jexbot/53.372.1305.

Shirahata, S., Kabayama, S., Nakano, M., Miura, T., Kusumoto, K., Gotoh, M., Hayashi, H., Otsubo, K., Morisawa, S. and Katakura, Y., 1997. Electrolyzed-reduced water scavenges active oxygen species and protects DNA from oxidative damage. *Biochemical and Biophysical Research Communications*, [e-journal] 234(1), pp.269-74. https://dx.doi.org/10.1006/bbrc.1997.6622.

Shiri, Y., Solouki, M., Ebrahimie, E., Emamjomeh, A. and Zahiri, J., 2019. Gibberellin causes wide transcriptional modifications in the early stage of grape cluster development. *Genomics*, [e-journal] 112(1), pp.820-830. https://dx.doi.org/10.1016/j.ygeno.2019.05.022.

Shofia, S.I., Vickram, A.S. , Saravanan, A. , Deivayanai, V.C. and Yaashikaa, P.R., 2025. Sustainable separation technologies for heavy metal removal from wastewater: An upgraded review of physicochemical methods and its advancements. Sustainable chemistry for the environment, [e-journal] 10. https://dx.oi.org/10.1016/j.scenv.2025.100264.

Shulin, P., Tahri, W., Khaskhoussi, A. and El-Sappah, A.H., 2026. Enhanced water treatment via combined oxidation and adsorption: a synergistic approach. *Frontier in Chemistry,* [e-journal] 13. https://dx.oi.org/10.3389/fchem.2025.1747407.

Siddiqi, S.A., Al-Mamun, A., Sana, A., Baawain, M.S. and Choudhury, M.R., 2022. Characterization and pollution potential of leachate from urban landfills during dry and wet periods in arid regions. *Water Supply*, [e-journal] 22(3), pp.3462–3483. https://dx.doi.org/10.2166/ws.2021.392.

Siddiqua, A., Hahladakis, J.N., Al-Attiya, W.A.K.A., 2022. An overview of the environmental pollution and health effects associated with waste landfilling and open dumping. *Environmental Science and Pollution Research*, [e-journal] 29, pp.58514–58536. https://dx.doi.org/10.1007/s11356-022-21578-z.

Sies, H. and Jones, D.P., 2020. Reactive oxygen species (ROS) as pleiotropic physiological signalling agents. *Nature Reviews Molecular Cell Biology*, [e-journal] 21(7), pp.363-383. https://dx.doi.org/10.1038/s41580-020-0230-3.

Simkin, A.J., McAusland, L., Lawson, T. and Raines, C.A., 2017. Overexpression of the RieskeFeS protein increases electron transport rates and biomass yield. *Plant Physiology*, [e-journal] 175, pp.134–145. https://dx.doi.org/10.1104/pp.17.00622.

Singh, V., Pandey, B. and Suthar, S., 2019. Phytotoxicity and degradation of antibiotic ofloxacin in duckweed (*Spirodela polyrhiza*) system. *Ecotoxicology and Environmental Safety*, [e-journal] 79, pp.88-95. http://dx.doi.org/10.1016/j.ecoenv.2019.04.018.

Singh, B.J., Chakraborty, A. and Sehgal, R., 2023. A systematic review of industrial wastewater management: Evaluating challenges and enablers. *Journal of Environmental Management*, [e-journal] 348. http://dx.doi.org/10.1016/j.jenvman.2023.119230.

Singh V.P., Singh S., Kumar J., Prasad S.M., 2015. Investigating the roles of ascorbate-glutathione cycle and thiol metabolism in arsenate tolerance in ridged *Luffa* seedlings. *Protoplasma*, [e-journal] 252, pp.1217–1229. https://dx.doi.org/10.1007/s00709-014-0753-6.

Singh, S., Raju, N.J., Gossel, W. and Wycisk, P., 2016a. Assessment of pollution potential of leachate from the municipal solid waste disposal site and its impact on groundwater quality, Varanasi environs, India. *Arabian Journal of Geosciences*, [e-journal] 9(131). https://dx.doi.org/10.1007/s12517-015-2131-x.

Singh, S., Parihar, P., Singh, R., Singh, V.P. and Prasad, S.M., 2016b. Heavy metal tolerance in plants: role of transcriptomics, proteomics, metabolomics, and ionomics. *Frontiers in Plant Science,* [e-journal] 6. https://dx.doi.org/10.3389/fpls.2015.01143.

Singh, D., Pandey, H., Dhiman, V.K., Bang, N.T.H., Dhiman, V.K., Singh, V. and Pandey, D., 2022. Secondary metabolite engineering for plant immunity against various pathogens. In: T. Aftab and K.R., Hakeem, eds. 2022. *Metabolic engineering in Plants.* Singapore: Springer Nature Singapore. pp.123−143.

Singh, R., Kumar, V., Tiwari, R.K., Pratap, S.G. and Singh, P., 2023. Hazardous waste leachates induced changes in plant water relation, photosynthetic pigments, heavy metal accumulation and yield of mustard (*Brassica juncea* L.) plant. *Journal of Hazardous Materials Advances,* [e-journal] 10. http://dx.doi.org/10.1016/j.hazadv.2023.100306.

Singroha, G. and Sharma, P., 2019. Epigenetic modifications in plants under abiotic stress. In: R. Meccariello, ed. 2019. *Epigenetics*. London: IntechOpen. http://dx.doi.org/10.5772/intechopen.84455.

Sinha, S.K., Srivastava, H.S. and Mishra, S.N., 1998. Nitrate assimilation in intact and excised maize leaves in the presence of lead. *Bulletin of Environmental Contamination and Toxicology*, [e-journal] 41, pp.419–426. https://dx.doi.org/10.1007/BF01688888.

Skuza, L., Szućko, I., Filip, E. and Bożek, I., 2022. Natural molecular mechanisms of plant hyperaccumulation and hypertolerance towards heavy metals. *International Journal of Molecular Sciences,* [e-journal] 23(16). https://dx.doi.org/10.3390/ijms23169335.

Smekalova, V., Doskocilova, A., Komis, G. and Šamaj, J., 2014. Crosstalk between secondary messengers, hormones and MAPK modules during abiotic stress signalling in plants. *Biotechnology Advances*, [e-journal] 32, pp.2–11. https://dx.doi.org/10.1016/j.biotechadv.2013.07.009.

Smet, D., Opdebeeck, H. and Vandepoele, K., 2023. Predicting transcriptional responses to heat and drought stress from genomic features using a machine learning approach in rice. *Frontiers in Plant Science*, [e-journal] 14. https://dx.doi.org/10.3389/fpls.2023.1212073.

Smirnoff, N., 2018. Ascorbic acid metabolism and functions: a comparison of plants and mammals. *Free Radical Biology and Medicine*, [e-journal] 122, pp.116–129. https://dx.doi.org/ 10.1016/j.freeradbiomed.2018.03.033.

Song, U., Waldman Park, J.S., Lee, K., Park, S.J. and Lee, E.J., 2018. Improving the remediation capacity of a landfill leachate channel by selecting suitable macrophytes. *Journal of Hydro-environment Research,* [e-journal] 20, pp.31–37. https://dx.doi.org/10.1016/j.jher.2018. 04.005.

Soni, S., Jha, A.B., Dubey, R.S. and Sharma, P., 2024. Mitigating cadmium accumulation and toxicity in plants: the promising role of nanoparticles. *Science of The Total Environment*, [e-journal] 912. https://dx.doi.org/10.1016/j.scitotenv.2023.168826.

Sørmo, C.G., Leiros, I., Brembu, T., Winge, P., Os, V. and Bones, A.M., 2006. The crystal structure of *Arabidopsis thaliana* RAC7/ROP9: the first RAS superfamily GTPase from the plant kingdom. *Phytochemistry*, [e-journal] 67(21), pp.2332-2340. https://dx.doi.org/10.1016/j.phytochem.2006.08.011.

Sossou, K., Bala Prasad, S., Agbotsou, K.E., Saidou Souley, H. and Mudigandla, R., 2024. Characteristics of landfill leachate and leachate treatment by biological and advanced coagulation process: feasibility and effectiveness—an overview. *Waste Management Bulletin*, 2, pp.181–198.

Spina, F., Tigini, V., Romagnolo, A. and Varese, G.C., 2018. Bioremediation of landfill leachate with fungi: autochthonous vs. allochthonous strains. *Life (Basel)*, [e-journal] 8(3). http://dx.doi.org/ 10.3390/life8030027.

Sreekanth, T.V.M., Nagajyothi, P.C., Lee, K.D. and Prasad T.N.V.K.V., 2013. Occurrence, physiological responses and toxicity of nickel in plants. *International Journal of Environmental Science and Technology*, [e-journal] 10, pp.1129–1140. https://dx.doi.org/10.1007/s13762-013-0245-9.

Srivastava, V., Sarkar, A., Singh, S., Singh, P., De Araujo, A.S. and Singh, R.P., 2017. Agroecological responses of heavy metal pollution with special emphasis on soil health and plant performances. *Frontiers in Environmental Science*, [e-journal] 5. https://dx.doi.org/10.3389/fenvs.2017.00064.

Stępiński, D., 2025. Decoding plant ribosomal proteins: multitasking players in cellular games. *Cells*, [e-journal] 14(7). https://dx.doi.org/10.3390/cells14070473.

Sturikova, H., Krystofova, O., Huska, D. and Adam, V., 2018. Zinc, zinc nanoparticles and plants. *Journal of Hazardous Materials*, [e-journal] 349, pp.101–110. https://dx.doi.org/10.1016/j.jhazmat.2018.01.040.

Su, W., Raza, A., Gao, A., Jia, Z., Zhang, Y., Hussain, M.A., Mehmood, S.S., Cheng, Y., Lv, Y. and Zou, X., 2021. Genome-wide analysis and expression profile of Superoxide Dismutase (SOD) gene family in rapeseed (*Brassica napus* L.) under different hormones and abiotic stress conditions. *Antioxidants (Basel, Switzerland)*, [e-journal] 10(8). https://dx.doi.org/10.3390/antiox10081182.

Su, W., Wang, Q., Li, J., Qiu, Z. and Qiu, Y., 2024. Effects of pulsed electricfield technology on the nutritional value and biological function of plant food. *Frontiers in Sustainable Food Systems*, [e-journal] 8. https://dx.doi.org/10.3389/fsufs.2024.1385533.

Sugiyama, M. and Machida, Y., 2018. Editorial: novel aspects of nucleolar functions in plant growth and development. *Frontiers in Plant Science*, [e-journal] 9(814). https://dx.doi.org/ 10.3389/fpls.2018.00814.

Sukhova, E. and Sukhov, V., 2021. Electrical signals, plant tolerance to actions of stressors, and programmed cell death: is interaction possible? *Plants (Basel)*, [e-journal] 10(8). https://dx.doi.org/ 10.3390/plants10081704.

Sumalan, R.L., Nescu, V., Berbecea, A., Sumalan, R.M., Crisan, M., Negrea, P. and Ciulca, S., 2023. The impact of heavy metal accumulation on some physiological parameters in *Silphium perfoliatum* L. plants grown in hydroponic systems. *Plants*, [e-journal] 12(8). https://dx.doi.org/10.3390/plants12081718.

Sun, Y., Wang, M., Mur, L.A.J., Shen, Q. and Guo, S., 2020. Unravelling the roles of nitrogen nutrition in plant disease defences. *International Journal of Molecular Sciences*, [e-journal] 21(2). https://dx.doi.org/10.3390/ijms21020572.

Sunkar, R., Kaplan, B., Bouché, N., Arazi, T., Dolev, D., Talke, I.N., Maathuis, F.J.M., Sanders, D., Bouchez, D. and Fromm, H.,2000. Expression of a truncated tobacco NtCBP4 channel in transgenic plants and disruption of the homologous

Arabidopsis CNGC1 gene confer Pb^{2+} tolerance. *Plant Journal*, [e-journal] 24, 533–542. https://dx.doi.org/10.1046/j.1365-313x.2000.00901.x.

Surriya, O., Saleem, S.S., Waqar, K. and Kazi, A.G., 2015. Phytoremediation of soils: prospects and challenges. In: K.R. Hakeem, M. Sabir, M. Öztürk and A..R. Mermut, eds. 2015. *Soil remediation and plants.* Cambridge, Massachusetts: Academic press. pp.1-36.

Suriyagoda, L.D., Dittert, K. and Lambers, H., 2018. Mechanism of arsenic uptake, translocation and plant resistance to accumulate arsenic in rice grains. *Agriculture, Ecosystems and Environment*, [e-journal] 253, pp.23–37. https://dx.doi.org/10.1016/j.agee.2017.10.017.

Sychta, K., Słomka, A. and Kuta, E., 2021. Insights into plant programmed cell death induced by heavy metals—discovering a *Terra Incognita*. *Cells*, [e-journal] 10(1). https://dx.doi.org/10.3390/cells10010065.

Syu, C.H., Lee, C.H., Jiang, P.Y., Chen, M.K. and Lee, D.Y., 2014. Comparison of As sequestration in iron plaque and uptake by different genotypes of rice plants grown in As-contaminated paddy soils. *Plant and Soil*, [e-journal] 374(1/2), pp.411–422. https://dx.doi. org/ 10. 1007/ s11104- 013- 1893-8.

Szechyńska-Hebda, M., Lewandowska, M. and Karpiński, S., 2017. Electrical signaling, photosynthesis and systemic acquired acclimation. *Frontiers in Physiology*, [e-journal] 8. https://dx.doi.org/10.3389/fphys.2017.00684.

Tabinda, A.B., Irfan, R., Yasar, A., Iqbal, A. and Mahmood, A., 2020. Phytoremediation potential of *Pistia stratiotes* and *Eichhornia crassipes* to remove chromium and copper. *Environmental Technology*, [e-journal] 41(12), pp.1514-1519. https://dx.doi.org10.1080/09593330.2018.1540662.

Taghian, T., Narmoneva, D.A. and Kogan, A., 2015. Modulation of cell function by electric field: a high-resolution analysis. *Journal of The Royal Society Interface*, [e-journal] 12(107). https://dx.doi.org/10.1098/rsif.2015.0153.

Taib, M.R., Mook, B.N., Tahir, M.I.H.M. and Aziz, M.A.A., 2021. Electrocoagulation treatment of sanitary landfill leachate in Malaysia. *IOP*

Conference Series: Materials Science and Engineering, [e-journal] 1051. https://dx.doi.org/10.1088/1757-899x/1051/1/012074.

Takabayashi, A., Kishine, M., Asada, K., Endo, T. and Sato, F., 2005. Differential use of two cyclic electron flows around photosystem I for driving CO_2-concentration mechanism in C4 photosynthesis. *Proceedings of the National Academy of Sciences of the United States of America*, [e-journal] 102(46), pp.16898-16903. http://dx.doi.org/10.1073/pnas.0507095102.

Takahashi, F., Yoshida, R., Ichimura, K., Mizoguchi, T., Seo, S., Yonezawa, M., Maruyama, K., Yamaguchi-Shinozaki, K. and Shinozaki, K., 2007. The mitogen-activated protein kinase cascade MKK3-MPK6 is an important part of the jasmonate signal transduction pathway in *Arabidopsis. Plant Cell*, [e-journal] 19(3), pp.805-818. http://dx.doi.org/10.1105/tpc.106.046581.

Takai, Y., Sasaki, T. and Matozaki, T., 2001. Small GTP-binding proteins. *Physiological Reviews*, [e-journal] 81(1), pp.153-208. https://dx.doi.org/10.1152/physrev.2001.81.1.153.

Talebzadeh, F. and Valeo, C., 2022. Evaluating the effects of environmental stress on leaf chlorophyll content as an index for tree health. *IOP Conference Series: Earth and Environmental Science*, [e-journal] 1006. https://dx.doi.org/10.1088/1755-1315/1006/1/012007.

Tamura, K. and Hara-Nishimura, I., 2014. Functional insights of nucleocytoplasmic transport in plants. *Frontiers in Plant Science*, [e-journal] 5. https://dx.doi.org/10.3389/fpls.2014.00118.

Tan, H.W., Pang, Y.L., Lim, S. and Chong, W.C., 2023. A state-of-the-art of phytoremediation approach for sustainable management of heavy metals recovery. *Environmental Technology and Innovation*, [e-journal] 30. https://dx.doi.org/10.1016/j.eti.2023.103043

Tang, Y., Chen, X., Zhang, H., Sun, X. and Xu, N., 2023. 1-Aminocyclopropane-1-carboxylic acid mitigates copper stress by decreasing copper transport and inducing jasmonic acid synthesis in *Gracilariopsis lemaneiformis*. *Environmental and Experimental Botany*, [e-journal] 208. https://dx.doi.org/10.1016/j.envexpbot.2023.105237.

Tangahu, B.V., Abdullah, S.R.S., Basri, H., Idris, M., Anuar, N. and Mukhlisin, M., 2011. A review on heavy metals (As, Pb, and Hg) uptake by plants through phytoremediation. *International Journal of Chemical Engineering*, [e-journal] 2011(1687-806X). https://dx.doi.org/10.1155/2011/939161.

Tavarez, M., Macri, A. and Sankaran, R.P., 2015. Cadmium and zinc partitioning and accumulation during grain filling in two near isogenic lines of durum wheat. *Plant Physiology and Biochemistry*, [e-journal] 97, pp.461-469. https://dx.doi.org/10.1016/j.plaphy.2015.10.024.

Tebar, F., Lladó, A. and Enrich, C., 2002. Role of calmodulin in the modulation of the MAPK signalling pathway and the transactivation of epidermal growth factor receptor mediated by PKC. *FEBS Letters*, [e-journal] 517, pp.206–210. https://dx.doi.org 10.1016/S0014-5793(02)02624-8.

Tejeda, L. and Mallarino, L.P., 2022. Phytoremediation to remove pollutants from water, leachates and soils. *Chemical Engineering Transactions*, 92, pp.553-558.

Tejera, J., Miranda, R., Hermosilla, D., Urra, I., Negro, C. and Blanco, Á., 2019. Treatment of a mature landfill leachate: comparison between homogeneous and heterogeneous photo-fenton with different pretreatments. *Water*, [e-journal] 11(9). https://dx.doi.org/10.3390/w11091849.

Teng, C., Zhou, K., Peng, C. and Chen, W., 2021. Characterization and treatment of landfill leachate: A review. *Water research*, [e-journal] 203. https://doi.org/10.1016/j.watres.2021.117525.

Thangavel, P. and Subbhuraam, C., 2004. Phytoextraction: role of hyperaccumulators in metal contaminated soils. *Proceedings of the Indian National Science Academy*, 70(1), pp.109–130.

The Malaysian Reserve, 2024. *Has Malaysia become a dumping ground?* [online] Available at: <https://themalaysianreserve.com/2024/08/29/has-malaysia-become-a-dumping-ground/> [Accessed 12 February 2026].

Therkildsen, N.O. and Baumann, H.A., 2020. A comprehensive non-redundant reference transcriptome for the Atlantic silverside *Menidia menidia*. *Marine Genomics*, [e-journal] 53. https://dx.doi.org/10.1016/j.margen.2019.100738.

Tokarev, A.A., Alfonso, A. and Segev, N., 2013. Overview of intracellular compartments and trafficking pathways. In: N. Segev, ed. 2013. *Trafficking inside cells*. New York: Springer. pp.3-14.

Traven, L., 2023. Sustainable energy generation from municipal solid waste: A brief overview of existing technologies. *Case Studies in Chemical and Environmental Engineering*, [e-journal] 8. https://dx.doi.org/10.1016/j.cscee.2023.100491.

Trewavas, A.J., 1997. Plant cyclic AMP comes in from the cold. *Nature*, [e-journal] 390, pp.657–658. https://dx.doi.org/10.1038/37720.

Tripathi, S., Singh, V.K., Srivastava, P., Singh, R., Devi, R.S., Kumar, A. and Bhadouria, R., 2020. Phytoremediation of organic pollutants: current status and future directions. In: P. Singh, A. Kumar, A. Borthakur, eds. 2020. *Abatement of environmental pollutants*. Amsterdam: Elsevier. pp.81-105.

Trösch, R. and Willmund, F., 2019. The conserved theme of ribosome hibernation: from bacteria to chloroplasts of plants. *Biological Chemistry*, [e-journal] 400(7), pp.879-893. https://dx.doi.org/10.1515/hsz-2018-0436.

Tsoutsa, E.K., Tolkou, A.K., Kyzas, G.Z. and Katsoyiannis, I.A., 2024. New trends in composite coagulants for water and wastewater treatment. *Macromol*, [e-journal] 4(3), pp.509-532. https://dx.doi.org/10.3390/macromol4030030

Tuteja, N. and Sopory, S.K., 2008. Plant signaling in stress: G-protein coupled receptors, heterotrimeric G-proteins and signal coupling via phospholipases. *Plant Signaling and Behaviour*, [e-journal] 3(2), pp.79-86. https://dx.doi.org/10.4161/psb.3.2.5303.

Tyagi, S., Dhiman, V.K., Dhiman, V.K., Pandey, H., Singh, D., Sharma, A., Sharma, P., Kumar, R., Lee, K.J. and Saharan, B.S., 2024. Plant defense strategies and biomarkers against heavy metal-induced stress: a comprehensive review. *ACS Agricultural Science and Technology*, [e-journal] 4(2), pp.129-143. https://dx.doi.org/10.1021/acsagscitech.3c00271.

Ubando, A.T., Africa, A.D.M., Maniquiz-Redillas, M.C., Culaba, A.B., Chen, W.-H. and Chang, J,-S., 2020. Microalgal biosorption of heavy metals: a

comprehensive bibliometric review. *Journal of Hazardous Materials*, [e-journal] 402. http://dx.doi.org/10.1016/j.jhazmat.2020.123431.

Uka, U.N., Belford, E.J.D. and Elebe, F.A., 2021. Effects of road traffic on photosynthetic pigments and heavy metal accumulation in tree species of Kumasi Metropolis, Ghana. *SN Applied Sciences*, [e-journal] 3(131): 2021. https://dx.doi.org/10.1007/s42452-020-04027-9.

United States Environmental Protection Agency, 2011. *Industrial waste landfills*. [pdf] Washington, D.C.: United States Environmental Protection Agency. Available at: <https://www.epa.gov/sites/default/files/2018-03/documents/ttinformation.pdf> [Accessed 5 February 2024).

United States Environmental Protection Agency, 2022. *Basic information about landfills*. [pdf] Washington, D.C.: United States Environmental Protection Agency. Available at: <https://www.epa.gov/landfills/basic-information-about-landfills> [Accessed 7 February 2024).

Upadhyay, R.K. and Panda, S.K., 2009. Copper-induced growth inhibition, oxidative stress and ultrastructural alterations in freshly grown water lettuce (*Pistia stratiotes* L.). *Comptes Rendus Biologies*, [e-journal] 332(7), pp.623-32. https://dx.doi.org/10.1016/j.crvi.2009.03.001.

Ur Rahman, S., Qin, A., Zain, M., Mushtaq, Z., Mehmood, F., Riaz, L., Naveed, S., Ansari, M.J., Saeed, M., Ahmad, I. and Shehzad, M., 2024. Pb uptake, accumulation, and translocation in plants: Plant physiological, biochemical, and molecular response: A review. *Heliyon*, [e-journal] 10(6). https://dx.doi.org/10.1016/j.heliyon.2024.e27724.

Urase, T., Salequzzaman, M., Kobayashi, S., Matsuo, T., Yamamoto, K. and Suzuki, N., 1997. Effect of high concentration of organic and inorganic matters in landfill leachate on the treatment of heavy metals in very low concentration level. *Water Science and Technology*, [e-journal] 36, pp.349-356. https://dx.doi.org/10.1016/S0273-1223(97)00723-3.

Usman, K., Abu-Dieyeh, M.H., Zouari, N. and Al-Ghouti, M.A., 2020. Lead (Pb) bioaccumulation and antioxidative responses in *Tetraena qataranse*. *Scientific Reports*, [e-journal] 10(17070). https://dx.doi.org/10.1038/s41598-020-73621-z.

Vaccari, M., Vinti, G. and Tudor, T., 2018. An Analysis of the risk posed by leachate from dumpsites in developing countries. *Environments,* [e-journal] 5(9). https://dx.doi.org/10.3390/environments5090099.

Valliyodan, B. and Nguyen, H.T., 2006. Understanding regulatory networks and engineering for enhanced drought tolerance in plants. *Current Opinion in Plant Biology*, [e-journal] 9(2), pp.189-195. http://dx.doi.org/10.1016/j.pbi.2006.01.019.

van Doorn, W.G., Beers, E.P., Dangl, J.L., Franklin-Tong, V.E., Gallois, P., Hara-Nishimura, I., Jones, A.M., Kawai-Yamada, M., Lam, E., Mundy, J., Mur, L.A., Petersen, M., Smertenko, A., Taliansky, M., Van Breusegem, F., Wolpert, T., Woltering, E., Zhivotovsky, B. and Bozhkov, P.V., 2011. Morphological classification of plant cell deaths. *Cell Death and Differentiation*, [e-journal] 18(8), pp.1241-1246. http://dx.doi.org/10.1038/cdd.2011.36.

Vanden Berghe, T., Kalai, M., Denecker, G., Meeus, A., Saelens, X. and Vandenabeele, P., 2006. Necrosis is associated with IL-6 production but apoptosis is not. *Cellular Signalling*, [e-journal] 18(3), pp.328-335. http://dx.doi.org/10.1016/j.cellsig.2005.05.003.

Veneziano, D., Di Bella, S., Nigita, G., Laganà, A., Ferro, A. and Croce, C.M., 2016. Noncoding RNA: current deep sequencing data analysis approaches and challenges. *Human Mutation*, [e-journal] 37(12), pp.1283-1298. http://dx.doi.org/10.1002/humu.23066.

Verma, S. and Kuila, A., 2019. Bioremediation of heavy metals by microbial process. *Environmental Technology and Innovation*, [e-journal] 14. https://doi.org/10.1016/j.eti.2019.100369

Vernoud, V., Horton, A.C., Yang, Z. and Nielsen, E., 2003. Analysis of the small GTPase gene superfamily of *Arabidopsis*. *Plant Physiology*, [e-journal] 131(3), pp.1191-1208. http://dx.doi.org/10.1104/pp.013052.

Vestina, S., Cambraia, J., Ribeiro, C., Oliveira, J. A., Oliva, M. A., 2011. Cadmium-induced oxidative stress and antioxidative enzyme response in water hyacinth and salvinia. *Brazilian Society of Plant Physiology*, 23(2), pp.131-139.

Viehweger, K., 2014. How plants cope with heavy metals. *Botanical Studies*, [e-journal] 55(35). https://dx.doi.org/10.1186/1999-3110-55-35.

Vinti, G., Bauza, V., Clasen, T., Medlicott, K., Tudor, T., Zurbrügg, C. and Vaccari, M., 2021. Municipal solid waste management and adverse health outcomes: a systematic review. *International Journal of Environmental Research and Public Health*, [e-journal] 18(8). https://dx.doi.org/10.3390/ijerph18084331.

Virdi, N., Sharma, M. and Devi, D., 2023. Rising concerns on municipal solid waste - an evaluation of emerging waste generation and lacunae in management. *Journal of Chemical Health Risks*, 13(4), pp.2128-2137.

Virk, N., Li, D., Tian, L., Huang, L., Hong, Y., Li, X., Zhang, Y., Liu, B., Zhang, H. and Song, F, 2015. *Arabidopsis* Raf-like mitogen-activated protein kinase kinase kinase gene *Raf43* is required for tolerance to multiple abiotic stresses. *PLoS One*, [e-journal] 10(7). http://dx.doi.org/10.1371/journal.pone.0133975.

Wairich, A., Aung, M.S., Ricachenevsky, F.K. and Masuda. H., 2024. You can't always get as much iron as you want: how rice plants deal with excess of an essential nutrient. *Frontiers in Plant Science,* [e-journal] 15. http://dx.doi.org/10.3389/fpls.2024.1381856.

Wan, K., Yang, F., Nan, Y., Zhang, S., Huang, Z., Chen, Y., Zhang, Z., Lai, Z. and Lin, Y., 2025. Transcription factor PcERF114 is involved in the regulation of flavonoid accumulation of *Polygonatum cyrtonema* Hua. *Industrial Crops and Products*, [e-journal] 230. https://dx.doi.org/10.1016/j.indcrop.2025.121082

Wang, D., 2022. Improvement of plant growth and control of cultivation environment using electrical stimuli. In: S. Horikoshi, G. Brodie, K. Takaki and N. Serpone, eds. 2022. *Agritech: innovative agriculture using microwaves and plasmas.* Singapore: Springer. pp.227-246.

Wang L.T., 2024, Heavy metal tolerance in aquatic plants: physiological adaptations and detoxification strategies. *International Journal of Aquaculture*, [e-journal] 14(3), pp.165-173. http://dx.doi.org/10.5376/ija.2024.14.0017.

Wang, J., and Chen, H., 2020. Catalytic ozonation for water and wastewater treatment: recent advances and perspective. *Science of the Total Environment*, [e-journal] 704. http://dx.doi.org/10.1016/j.scitotenv.2019.135249.

Wang, Y., and Botella, J.R., 2022. Heterotrimeric G protein signaling in abiotic stress. *Plants*, [e-journal] 11(7). https://dx.doi.org/10.3390/plants11070876.

Wang, J. and Qiao, Z., 2024. A comprehensive review of landfill leachate treatment technologies. *Frontiers in Environmental Science*, [e-journal] 12. https://dx.doi.org/10.3389/fenvs.2024.1439128.

Wang, Z.Y., Fang, B.P., Chen, J.Y., Zhang, X.J., Luo, Z.X., Huang, L.F., Chen, X.L. and Li, Y.L., 2010. *De novo* assembly and characterization of root transcriptome using Illumina paired-end sequencing and development of cSSR markers in sweetpotato (*Ipomoea batatas*). *BMC Genomics*, [e-journal] 11(726). https://dx.doi.org/10.1186/1471-2164-11-726.

Wang, P., Yang, B., Wan, H., Fang, X. and Yang, C., 2018a. The differences of cell wall in roots between two contrasting soybean cultivars exposed to cadmium at young seedlings. *Environmental Science and Pollution Research*, [e-journal] 25, pp.29705–29714. http://dx.doi.org/10.1007/s11356-018-2956-4.

Wang, Y., Branicky, R., Noë, A. and Hekimi, S., 2018b. Superoxide dismutases: dual roles in controlling ROS damage and regulating ROS signaling. *Journal of Cell Biology*, [e-journal] 217(6), pp.1915-1928. http://dx.doi.org/10.1083/jcb.201708007.

Wang, X., You, X., Langer, J.D., Hou, J., Rupprecht, F., Vlatkovic, I., Quedenau, C., Tushev, G., Epstein, I., Schaefke, B., Sun, W., Fang, L., Li, G., Hu, Y., Schuman, E.M. and Chen, W., 2019. Full-length transcriptome reconstruction reveals a large diversity of RNA and protein isoforms in rat hippocampus. *Nature Communications*, [e-journal] 10(1):5009. http://dx.doi.org/10.1038/s41467-019-13037-0.

Wang, Y., Zhong, Z., Zhang, Y., Xu, L., Feng, S., Rayatpisheh, S., Wohlschlegel, J.A., Wang, Z., Jacobsen, S.E. and Ausin, I. 2020a. NAP1-RELATED PROTEIN1 and 2 negatively regulate H2A.Z abundance in chromatin in *Arabidopsis*. Nature Communications. [e-journal] 11(1):2887. https://dx.doi.org10.1038/s41467-020-16691-x.

Wang, L., Zheng, B., Yuan, Y., Xu, Q. and Chen, P., 2020b. Transcriptome profiling of *Fagopyrum tataricum* leaves in response to lead stress. *BMC Plant Biology*, [e-journal] 20(54). http://dx.doi.org/10.1186/s12870-020-2265-1.

Wang, L.K., Wang, M.-H.S., Shammas, N.K. and Hahn, H.H., 2021. Physicochemical treatment consisting of chemical coagulation, precipitation, sedimentation, and flotation. In: L.K. Wang, M.-H.S. Wang, and Y.-T. Hung, eds. 2021. *Integrated natural resources research.* Cham: Springer International Publishing. pp.265–397.

Wang, D., Hayashi, Y., Enoki, T., Nakahara, K., Arita, T., Higashi, Y., Kuno, Y., Terazawa, T., and Namihira, T., 2022. Influence of pulsed electric fields on photosynthesis in light/dark-acclimated lettuce. *Agronomy*, [e-journal] 12(1). https://dx.doi.org/10.3390/agronomy12010173.

Wang, H., Cheng, X., Yin, D., Chen, D., Luo, C., Liu, H. and Huang, C., 2023. Advances in the research on plant WRKY transcription factors responsive to external stresses. *Current Issues in Molecular Biology*, [e-journal] 45(4), pp.2861-2880. https://dx.doi.org/10.3390/cimb45040187.

Wang, P., Liu, W.C., Han, C., Wang, S., Bai, M.Y and Song, C.P., 2024a. Reactive oxygen species: multidimensional regulators of plant adaptation to abiotic stress and development. *Journal of Integrative Plant Biology*, [e-journal] 66(3), pp.330–367. https://dx.doi.org/10.1111/jipb.13601.

Wang, X., Yu, Q., Gong, Y. and Zhang, Y., 2024b. Enhancing the production of reactive oxygen species in the rhizosphere to promote contaminants degradation in sediments by electrically strengthening microbial extracellular electron transfer. *Journal of Hazardous Materials*, [e-journal] 479. https://dx.doi.org/10.1016/j.jhazmat.2024.135644.

Wang. J., Chen, X., Chu, S., Hayat, K., Chi, Y., Liao, X., Zhang, H., Xie, Y., Zhou, P. and Zhang, D., 2024c. Conjoint analysis of physio-biochemical, transcriptomic, and metabolomic reveals the response characteristics of *Solanum nigrum* L. to cadmium stress. *BMC Plant Biology*, [e-journal] 24(567). https://dx.doi.org/10.1186/s12870-024-05278-z.

Waszczak, C., Carmody, M. and Kangasjärvi, J., 2018. Reactive oxygen species in plant signaling. *Annual Review of Plant Biology*, [e-journal] 69, pp.209-236. https://dx.doi.org/10.1146/annurev-arplant-042817-040322.

Watanabe, N. and Lam, E., 2006. *Arabidopsis* Bax inhibitor-1 functions as an attenuator of biotic and abiotic types of cell death. *Plant Journal*, [e-journal] 45(6), pp.884-94. https://dx.doi.org/10.1111/j.1365-313X.2006.02654.x.

Wawrecki, W and Zagórska-Marek, B., 2007. Influence of a weak DC electric field on root meristem architecture. *Annals of Botany*, [e-journal] 100(4), pp.791-796. http://dx.doi.org/10.1093/aob/mcm164.

Wei, Z., Van Le, Q., Peng, W., Yang, Y., Yang, H., Gu, H., Lam, S.S. and Sonne, C., 2021. A review on phytoremediation of contaminants in air, water and soil. *Journal of Hazardous Materials*, [e-journal] 403. http://dx.doi.org/10.1016/j.jhazmat.2020.123658.

Wei, S., Moriuchi, R., Wiyono, C.D.A.P, Inoue, C. and Chien, M.F., 2025. Unraveling tissue-specific molecular mechanisms orchestrating arsenic response processes in *Pteris vittata* through transcriptomic analysis. *Ecotoxicology and Environmental Safety*, [e-journal] 294 http://dx.doi.org/10.1016/j.ecoenv.2025.118059.

Wennerberg, K., Rossman, K.L. and Der, C.J., 2005. The Ras superfamily at a glance. *Journal of Cell Science*, [e-journal] 118(Pt 5), pp.843-846. https://dx.doi.org/10.1242/jcs.01660.

Wetthasinghe, L., Ng, H.F., Ngeow, Y.F., Chew, K.S. and Lee, W.S., 2024. Navigating the intricacies of RT-qPCR data analysis in gene expression studies. *Functional and Integrative Genomics*, [e-journal] 24(115). https://dx.doi.org/10.1007/s10142-024-01393-0.

Weydert, C.J. and Cullen, J.J., 2010. Measurement of superoxide dismutase, catalase and glutathione peroxidase in cultured cells and tissue. *Nature Protocols*, [e-journal] 5(1), pp.51-66. https://dx.doi.org/10.1038/nprot.2009.197.

White, P.J. and Broadley, M.R., 2003. Calcium in plants. *Annals of Botany*, [e-journal] 92(4), pp.487-511. https://dx.doi.org/10.1093/aob/mcg164.

Wibowo, Y.G., Nugraha, A.T. and Rohman, A., 2023. Phytoremediation of several wastewater sources using *Pistia stratiotes* and *Eichhornia crassipes* in Indonesia.

Environmental Nanotechnology, Monitoring and Management, [e-journal] 20. https://dx.doi.org/10.1016/j.enmm.2023.100781.

Wiessner, A., Kappelmeyer, U., Kaestner, M., Schultze-Nobre, L. and Kuschk, P., 2013. Response of ammonium removal to growth and transpiration of *Juncus effusus* during the treatment of artificial sewage in laboratory-scale wetlands. *Water Research*, [e-journal] 47(13), pp.4265-4273. http://dx.doi.org/10.1016/j.watres.2013.04.045.

Williams, L.E., Pittman, J.K. and Hall, J.L., 2000. Emerging mechanisms for heavy metal transport in plants. *Biochim Biophys Acta*, [e-journal] 1465(1-2), pp.104-26. http://dx.doi.org/10.1016/s0005-2736(00)00133-4.

Winter, G., Todd, C. D., Trovato, M., Forlani, G. and Funck, D., 2015. Physiological implications of arginine metabolism in plants. *Frontiers in Plant Science*, [e-journal] 6. https://dx.doi.org/10.3389/fpls.2015.00534.

Wojas, S., Ruszczyńska, A., Bulska, E., Wojciechowski, M. and Antosiewicz, D.M., 2007. Ca^{2+} -dependent plant response to Pb^{2+} is regulated by LCT1. *Environmental Pollution*, [e-journal] 147(3), pp.584-92. https://dx.doi.org/10.1016/j.envpol.2006.10.012.

Wong, H.L., Pinontoan, R., Hayashi, K., Tabata, R., Yaeno, T., Hasegawa, K., Kojima, C., Yoshioka, H., Iba, K., Kawasaki, T. and Shimamoto, K., 2007. Regulation of rice NADPH oxidase by binding of Rac GTPase to its N-terminal extension. *Plant Cell*, [e-journal] 19(12), pp.4022-4034. https://dx.doi.org/10.1105/tpc.107.055624.

World Health Organization, 2022. *Treatment methods and performance.* [online] Available at: <https://www.who.int/publications/m/item/treatment-methods-and-performance> [Accessed 13 February 2026].

Worldwide Environment, n.d. *Solid waste management*. [online] Available at: <https://worldwideenvironment.com.my/solid-waste-management/?utm_source=chatgpt.com#> [Accessed 12 February 2026].

Wu, T.Y. and Urano, D., 2018. Genetic and systematic approaches toward G protein-coupled abiotic stress signaling in plants. *Frontier in Plant Science*, [e-journal] 9. http://dx.doi.org/ 10.3389/fpls.2018.01378.

Wu, G. and Wang, W., 2024 Recent advances in understanding the role of two mitogen-activated protein kinase cascades in plant immunity. *Journal of Experimental Botany*, [e-journal] 75(8), pp. 2256-2265. http://dx.doi.org/10.1093/jxb/erae020.

Wu, B., An, Y., Li, Y. and Wong, F.S., 2009. Effect of adsorption/coagulation on membrane fouling in microfiltration process post-treating anaerobic digestion effluent. *Desalination*, [e-journal] 242, pp.183-192. https://dx.doi.org/10.1016/j.desal.2008.04.005.

Wu, Y., Zhou, S., Qin, F., Ye, X. and Zheng, K., 2010. Modeling physical and oxidative removal properties of Fenton process for treatment of landfill leachate using response surface methodology (RSM). *Journal of Hazardous Materials*, [e-journal] 180 (1–3), pp.456–465. https://dx.doi.org/10.1016/j.jhazmat.2010.04.052.

Wu, J., Xiao, J., Zhang, Z., Wang, X., Hu, S. and Yu, J., 2014. Ribogenomics: the science and knowledge of RNA. *Genomics Proteomics Bioinformatics*, [e-journal] 12(2), pp.57-63. https://dx.doi.org/ 10.1016/j.gpb.2014.04.002.

Wu, D., Wang, T., Huang, X., Dolfing, J., and Xie, B., 2015. Perspective of harnessing energy from landfill leachate via microbial fuel cells: novel biofuels and electrogenic physiologies. *Applied Microbiology and Biotechnology*, [e-journal] 99, pp.7827–7836. http://dx.doi.org/10.1007/s00253-015-6857-.

Xaypanya, P., Takemura, J., Chiemchaisri, C., Seingheng, H. and Tanchuling, M.A.N., 2018. Characterization of landfill leachates and sediments in major cities of Indochina peninsular countries – heavy metal partitioning in municipal solid waste leachate. *Environments*, [e-journal] 5. https://dx.doi.org/10.3390/environments5060065.

Xia, C., Hong, L., Yang, Y., Yanping, X., Xing, H. and Gang, D., 2019. Protein changes in response to lead stress of lead-tolerant and lead-sensitive industrial hemp using SWATH technology. *Genes (Basel)*, [e-journal] 10(5). https://dx.doi.org/10.3390/genes10050396.

Xiang, Q., Nomura, Y., Fukahori, S., Mizuno, T., Tanaka, H. and Fujiwara, T., 2019. Innovative treatment of organic contaminants in reverse osmosis concentrate

from water reuse: a mini review. *Current Pollution Reports*, [e-journal] 5, pp.294–307. https://dx.doi.org/10.1007/s40726-019-00119-2.

Xiang, R., Wei, W., Mei, T., Wei, Z., Yang, X., Liang, J. and Zhu, J., 2025. A review on landfill leachate treatment technologies: comparative analysis of methods and process innovation. *Applied Sciences*, [e-journal] 15(7). https://dx.doi.org/10.3390/app15073878.

Xiao, X., Ma, J., Sun, Y. and Yao, Y., 2015. A method for the further assembly of targeted unigenes in a transcriptome after assembly by Trinity. *Frontier in Plant Science*, [e-journal] 6. https://dx.doi.org/10.3389/fpls.2015.00843.

Xiong, T., Zhang, T., Xian, Y., Kang, Z., Zhang, S., Dumat, C., Shahid, M. and Li, S., 2021. Foliar uptake, biotransformation, and impact of CuO nanoparticles in *Lactuca sativa* L. var. *ramosa* Hort. *Environmental Geochemistry and Health*, [e-journal] 43, pp.423–439. https://dx.doi.org/10.1007/s10653-020-00734-9.

Xu, Y. and Fu, X., 2022. Reprogramming of plant central metabolism in response to abiotic stresses: a metabolomics view. *International Journal of Molecular Sciences*, [e-journal] 23(10). https://dx.doi.org/10.3390/ijms23105716

Xu, C., Tang, X., Shao, H. and Wang, H., 2016. Salinity tolerance mechanism of economic halophytes from physiological to molecular hierarchy for improving food quality. *Current Genomics*, [e-journal] 17, 207–214. https://dx.doi.org/10.2174/1389202917666160202215548.

Xu, D., Chen, H., Aci, M., Pan, Y., Shangguan, Y., Ma, J., Li, L., Qian, G. and Wang, Q.X., 2018. *De Novo* assembly, characterization and development of EST-SSRs from *Bletilla striata* transcriptomes profiled throughout the whole growing period. *PLoS ONE*, [e-journal] 13. https://dx.doi.org/10.1371/journal.pone.0205954.

Xu, L., Dai, H., Skuza, L. and Wei, S., 2020. The effects of different electric fields and electrodes on *Solanum nigrum* L. Cd hyperaccumulation in soil. *Chemosphere*, [e-journal] 246. https://dx.doi.org/10.1016/j.chemosphere.2019.125666.

Xu, R., Guo, Y., Peng, S., Liu, J., Li, P., Jia, W. and Zhao, J., 2021. Molecular targets and biological functions of cAMP signaling in *Arabidopsis. Biomolecules*, [e-journal] 11(5). https://dx.doi.org/10.3390/biom11050688.

Xv, L., Ge, J., Tian, S., Wang, H., Yu, H., Zhao, J. and Lu, L., 2020. A Cd/Zn co-hyperaccumulator and Pb accumulator, *Sedum alfredii*, is of high Cu tolerance. *Environmental Pollution*, [e-journal] 263(Pt B). https://dx.doi.org/10.1016/j.envpol.2020.114401.

Yaashikaa, P.R., Kumar, P.S., Nhung, T.C., Hemavathy, R.V., Jawahar, M.J., Neshaanthini, J.P. and Rangasamy, G., 2022. A review on landfill system for municipal solid wastes: insight into leachate, gas emissions, environmental and economic analysis. *Chemosphere*, [e-journal] 309(1). https://dx.doi.org/10.1016/j.chemosphere.2022.136627.

Yadav, J.S. and Dikshit, A.K., 2017. Stabilized old landfill leachate treatment using electrocoagulation. *Environment Asia*, [e-journal] 10(1), pp.25-33. http://dx.doi.org/ 10.14456/ea.2017.4.

Yadav, B.K., Siebel, M.A. and van Bruggen, J.J., 2011. Rhizofiltration of a heavy metal (lead) containing wastewater using the wetland plant *Carex pendula*. *CLEAN–Soil, Air, Water*, [e-journal] 39, pp.467–474. https://dx.doi.org/10.1002/clen.201000385.

Yadav, V., Arif, N., Kováč, J., Singh, V.P., Tripathi, D.K., Chauhan, D.K. and Vaculík, M., 2021. Structural modifications of plant organs and tissues by metals and metalloids in the environment: a review. *Plant Physiology and Biochemistry*, [e-journal] 159, pp.100-112. http://dx.doi.org/ 10.1016/j.plaphy.2020.11.047.

Yadav, M., Pandey, J., Chakraborty, A., Hassan, M.I., Kundu, J.K., Roy, A., Singh, I.K. and Singh, A., 2022. A comprehensive analysis of calmodulin-like proteins of glycine max indicates their role in calcium signaling and plant defense against insect attack. *Frontier in Plant Science*, [e-journal] 13. http://dx.doi.org/10.3389/fpls.2022.817950.

Yamori, W. and Shikanai, T., 2016. Physiological functions of cyclic electron transport around photosystem I in sustaining photosynthesis and plant growth. *Annual Review of Plant Biology*, [e-journal] 67, pp.81–106. http://dx.doi.org/10.1146/annurev-arplant-043015-112002.

Yan, H., Filardo, F., Hu, X., Zhao, X. and Fu, D., 2015. Cadmium stress alters the redox reaction and hormone balance in oilseed rape (*Brassica napus* L.) leaves. *Environmental Science and Pollution Research,* [e-journal] 23(4), pp.3758-3769. https://dx.doi.org/10.1007/s11356-015-5640-y.

Yan, A., Wang, Y., Tan, S.N., Mohd Yusof, M.L., Ghosh, S. and Chen, Z., 2020. Phytoremediation: a promising approach for revegetation of heavy metal-polluted land. *Frontiers in Plant Science,* [e-journal] 11. https://dx.doi.org/10.3389/fpls.2020.00359.

Yan, Y., Gan, J., Tao, Y., Okita, T.W. and Tian, L., 2022. RNA-binding proteins: the key modulator in stress granule formation and abiotic stress response. *Frontiers in Plant Science,* [e-journal] 13. https://dx.doi.org/10.3389/fpls.2022.882596.

Yan, D., Xue, S., Zhang, Z., Xu, G., Zhang, Y., Shi, Y., Xing, M. and Zhang, W., 2023. Physiological changes and antioxidative mechanisms of Alternanthera philoxeroides in phytoremediation of cadmium. *Environment and Health*, 1(2), pp.90-101.

Yang, Y., Wang, W., Chu, Z., Zhu, J. and Zhang, H., 2017. Roles of nuclear pores and nucleo-cytoplasmic trafficking in plant stress responses. *Frontiers in Plant Science*, [e-journal] 8. https://dx.doi.org/10.3389/fpls.2017.00574.

Yang, W.D., Yang, Y., Ding, Z.L., Yang, X.E., Zhao, F.L. and Zhu, Z.Q., 2019. Uptake and accumulation of cadmium in flooded versus non-flooded Salix genotypes: Implications for phytoremediation. *Ecological Engineering*, [e-journal] 136, pp.79–88. http://dx.doi.org/10.1016/j.ecoleng.2019.06.001

Yang, Y., Li, W., He, X., Hu, D. and Fei, Y., 2020. Effects of lead on growth, osmotic adjustment, antioxidant activity and photosynthetic responses in *Phoebe chekiangensis* seedlings. *Notulae Botanicae Horti Agrobotanici Cluj-Napoca*, [e-journal] 48(3), pp.1637–1648. https://dx.doi.org/10.15835/nbha48311933.

Yang, H.., Zhao, Y., Chen, N., Liu, Y., Yang, S., Du, H., Wang, W., Wu, J., Tai, F., Chen, F. and Hu X., 2021. A new adenylyl cyclase, putative disease resistance RPP13-like protein 3, participates in abscisic acid-mediated heat stress resistance

in maize. *Journal of Experimental Botany*, [e-journal] 72(2), pp.283–301. https://dx.doi.org/10.1093/jxb/eraa431.

Yang, W., Chen, X., Liu, Z., Zhao, Y., Chen, Y. and Geng, Z., 2023. Integrated transcriptome and proteome revealed that the declined expression of cell cycle-related genes associated with follicular atresia in geese. *BMC Genomics*, [online] 24. https://dx.doi.org/10.1186/s12864-022-09088-1.

Yao, X., Nie, J., Bai, R. and Sui, X., 2020. Amino acid transporters in plants: identification and function. *Plants (Basel)*, [e-journal] 9(8). https://dx.doi.org/10.3390/plants9080972.

Yap, C.K., Tan, W.S., Wong, K.W., Ong, G.H., Cheng, W.H., Nulit, R., Ibrahim, M.H., Chew, W., Berandah Edward, F., Okamura, H., Al-Mutairi, K.A., Al-Shami, S.A., Sharifinia, M., Mustafa, M., Leong, W.J. and You, C.F., 2021. Antioxidant enzyme activities as biomarkers of Cu and Pb stress in *Centella asiatica. Stresses*, [e-journal] 1(4), pp.253−265. https://dx.doi.org/10.3390/stresses1040018.

Yeung, A.T., 2011. Milestone developments, myths, and future directions of electrokinetic remediation. *Separation and Purification Technology*, [e-journal] 79, pp.124–132. https://dx.doi.org/10.1016/j.seppur.2011.01.022.

Yilmaz, S.H., Kaplan., M., Temizgul, R. and Yilmaz, S., 2017. Antioxidant enzyme response of sorghum plant upon exposure to aluminum, chromium and lead heavy metals. *Turkish Journal of Biochemistry*, [e-journal] 42, pp.503-512. https://dx.doi.org/10.1515/tjb-2016-0112.

Yoshioka, H., Hino, Y., Iwata, K., Ogawa, T., Yoshioka, M., Ishihama, N. and Adachi, H., 2023. Dynamics of plant immune MAPK activity and ROS signaling in response to invaders. *Physiological and Molecular Plant Pathology*, [e-journal] 125. https://dx.doi.org/10.1016/j.pmpp.2023.102000.

Younas, F., Mustafa, A., Farooqi, Z. U.R., Wang, X., Younas, S., Mohy-Ud-Din, W., Ashir Hameed, M., Mohsin Abrar, M., Maitlo, A.A., Noreen, S. and Hussain, M.M., 2021. Current and emerging adsorbent technologies for wastewater treatment: trends, limitations, and environmental implications. *Water*, [e-journal] 13(2). https://dx.doi.org/10.3390/w13020215.

Young, M.D., Wakefield, M.J., Smyth, G.K. and Oshlack, A., 2010. Gene ontology analysis for RNA-seq: accounting for selection bias. *Genome Biology*, [e-journal] 11(2): R14. https://dx.doi.org/10.1186/gb-2010-11-2-r14.

Yuan, H.M. and Huang, X., 2016. Inhibition of root meristem growth by cadmium involves nitric oxide-mediated repression of auxin accumulation and signalling in *Arabidopsis*. *Plant, Cell and Environment*, [e-journal] 39(1), pp.120-35. https://dx.doi.org/10.1111/pce.12597.

Yuan, M., Huang, Y., Ge, W., Jia, Z., Song, S., Zhang, L. and Huang, Y., 2019. Involvement of jasmonic acid, ethylene and salicylic acid signaling pathways behind the systemic resistance induced by *Trichoderma longibrachiatum* H9 in cucumber. *BMC Genomics*, [e-journal] 20(1), pp.144. https://dx.doi.org/10.1186/s12864-019-5513-8.

Yuan J., Zhang X., Gao Y., Liu C., Xiang J. and Li, F., 2020. Adaptation and molecular evidence for convergence in decapod crustaceans from deep-sea hydrothermal vent environments. *Molecular Ecolology*, [e-journal] 29, pp.3954–3969. https://dx.doi.org/10.1111/mec.15610.

Yuan, L., Guo, P., Guo, S., Wang, J. and Huang, Y., 2021. Influence of electrical fields enhanced phytoremediation of multi-metal contaminated soil on soil parameters and plants uptake in different soil sections. *Environmental Research*, [e-journal] 198. https://dx.doi.org/10.1016/j.envres.2021.111290.

Yukalang, N., Clarke, B. and Ross, K., 2017. Barriers to effective municipal solid waste management in a rapidly urbanizing area in Thailand. *International Journal of Environmental Research and Public Health*, [e-journal] 14(9). https://dx.doi.org/10.3390/ijerph14091013.

Yusof, T.A., 2024. 18 possible sites for waste-to-energy plants identified. *The Star*, [online] 2 July 2024. Available at: <https://www.thestar.com.my/news/nation/2024/07/02/18-possible-sites-for-waste-to-energy-plants-identified?utm_source=chatgpt.com>[Accessed 12 February 2026].

Yusof, N, Haraguchi, A., Hassan, M A., Othman, M.R., Wakisaka, and Shirai, Y., 2009. Measuring organic carbon, nutrients and heavy metals in rivers receiving leachate from controlled and uncontrolled municipal solid waste (MSW) landfills.

Waste Management, [e-journal] 29(10). https://dx.doi.org/10.1016/j.wasman.2009.05.022.

Zakaria, S.N.F., Aziz, H.A., Hung, Y.-T., Wang, M.-H. S., and Wang, L.K., 2023. Treatment of hazardous sludge from water and wastewater treatment plants. In: L.K. Wang, M.-H. S. Wang, and Y.-T. Hung, eds. 2023. *Industrial waste engineering.* Cham: Springer International Publishing. pp.1–41.

Zamani, A., Yaftian, M.R. and Parizanganeh, A., 2012. Multivariate statistical assessment of heavy metal pollution sources of groundwater around a lead and zinc plant. *Iranian Journal of Environmental Health Science and Engineering*, [e-journal] 9(1). https://dx.doi.org/10.1186/1735-2746-9-29.

Zamri, M.F.M.A., Hasmady, S., Akhiar, A., Ideris, F., Shamsuddin, A.H., Mofijur, M., Rizwanul Fattah, I.M. and Mahlia, T.M.I., 2021. A comprehensive review on anaerobic digestion of organic fraction of municipal solid waste. *Renewable and Sustainable Energy Reviews*, [e-journal] 137. http://dx.doi.org/110637.

Zandi, P., Yang, J., Xing Xia, Y., Tian, Q. L., Możdżeń, K., Barabasz-Krasny, B., and Wang, Y., 2020. Do sulfur addition and rhizoplane iron plaque affect chromium uptake by rice (*Oryza sativa* L.) seedlings in culture solution? *Journal of Hazardous Materials*, [e-journal] 388. https://dx.doi. org/10. 1016/j. jhazm at. 2019. 121803.

Zandi, P., Yang, J., Darma, A., Bloem, E., Xia, X., Wang, Y., Li, Q. and Schnug, E., 2023. Iron plaque formation, characteristics, and its role as a barrier and/or facilitator to heavy metal uptake in hydrophyte rice (*Oryza sativa* L.). *Environmental Geochemistry and Health*, [e-journal] 45(3), pp.525-559. https://dx.doi. org/10.1007/s10653-022-01246-4.

Zazouli, M.A., Yousefi, Z., Babanezhad, E., Mohammadpour, R.A. and Ala, A., 2024. Landfill leachate treatment using a combined method of coagulation, flocculation, advanced oxidation, and extended aeration. *Environmental Health Engineering And Management Journal*, [e-journal] 11(2), pp.177-190. https://dx.doi.org/10.34172/EHEM.2024.18

Zelko, I.N., Mariani, T.J. and Folz R.J., 2002. Superoxide dismutase multigene family: A comparison of the CuZn-SOD (SOD1), Mn-SOD (SOD2), and EC-SOD (SOD3) gene structures, evolution, and expression. *Free Radical Biology and*

Medicine, [e-journal] 33, pp.337–349. https://dx.doi.org/10.1016/S0891-5849(02)00905-X.

Zeng, J., Liu, X., Chen, Q. and Hu, D., 2024. A chemical coating strategy for assembling a boron-doped diamond anode towards electrocatalytic degradation of late landfill leachate. RSC Advances, [e-journal] 14(26), pp.18355-18366. https://dx.doi.org/10.1039/d4ra03107e.

Zhang, M.M. and Zhang, S.Q., 2022. Mitogen-activated protein kinase cascades in plant signaling. *Journal of Integrative Plant Biology*, [e-journal] 64(2), pp.301-341. https://dx.doi.org/10.1111/jipb.13215.

Zhang, H., Zhao, Y. and Zhu, J.K., 2020. Thriving under stress: how plants balance growth and the stress response. *Developmental Cell*, [e-journal] 55(5), pp.529-543. https://dx.doi.org/10.1016/j.devcel.2020.10.012.

Zhang, W.H., Ryan, P.R. and Tyerman, S.D., 2021. Malate-permeable channels and cation channels activated by aluminum in the apical cells of wheat roots. Plant Physiology, [e-journal] 125, pp.1459–1472. https://dx.doi.org/10.1104/pp.125.3.1459.

Zhang, F., Zhang, L., Qi, Y. and Xu, H., 2016. Mitochondrial cAMP signaling. *Cellular and Molecular Life Sciences*, [e-journal] 73(24), pp.4577-4590. https://dx.doi.org/10.1007/s00018-016-2282-2.

Zhang, H., Liu, X.L., Zhang, R.X., Yuan, H.Y., Wang, M.M., Yang, H.Y., Ma, H.Y., Liu, D., Jiang, C.J and Liang, Z.W., 2017. Root damage under alkaline stress is associated with reactive oxygen species accumulation in rice (*Oryza sativa* L.). *Frontier in Plant Science*, [e-journal] 8. https://dx.doi.org/10.3389/fpls.2017.01580.

Zhang P., Zhong K., Zhong Z., Tong H., 2019. Mining candidate gene for rice aluminum tolerance through genome wide association study and transcriptomic analysis. *BMC Plant Biology*, [e-journal] 19(490). https://dx.doi.org/10.1186/s12870-019-2036-z.

Zhang, H., Li, X., Xu, Z., Wang, Y., Teng Z., An, M., Zhang Y., Zhu W., Xu, N. and Sun G., 2020. Toxic effects of heavy metals Pb and Cd on mulberry (*Morus alba* L.) seedling leaves: photosynthetic function and reactive oxygen species

(ROS) metabolism responses. *Ecotoxicology and Environmental Safety*, [e-journal] 195. https://dx.doi.org/10.1016/j.ecoenv.2020.110469.

Zhang, Z., Zhou, D., He, J., He, Y., Yu, C., Long, Y., Shen, D., Yao, J. and Chen, H., 2023. Insight into the impact of industrial waste co-disposal with MSW on groundwater contamination at the open solid waste dumping sites. *Chemosphere*, [e-journal] 344. http://dx.doi.org/ 10.1016/j.chemosphere.2023.140429.

Zhang, X., Yang, J., Qi, L., Zhou, W., Zhu, Y., Li, Z., Chen, F. and Guan, C., 2024a. Evaluation of electrokinetic-assisted phytoremediation efficiency of dibutyl phthalate contaminated soil by maize (*Zea mays* L.) under different electric field intensities. Science of The Total Environment, [e-journal] 944. http://dx.doi.org/ 10.1016/j.scitotenv.2024.173838.

Zhang, X., Yang, M., Yang, H., Pian, R., Wang, J. and Wu, A.M., 2024b. The uptake, transfer, and detoxification of cadmium in plants and its exogenous effects. *Cells*, [e-journal] 13(11). https://dx.doi.org/10.3390/cells13110907

Zhang, C., Li, W., Wu, Y., Li, S., Hua, B. and Sun, H., 2025. Chloroplast functionality at the interface of growth, defense, and genetic innovation: a multi-omics and technological perspective. *Plants*, [e-journal] 14(6). https://dx.doi.org/10.3390/plants14060978.

Zhao, S., 2021. Thermochemical processes for biohydrogen production. In: Q. Zhang, C. He, J. Ren and M. Goodsite, eds. 2021. *Waste to Renewable Biohydrogen.* Cambridge, Massachusetts: Academic Press. pp.139-177.

Zhao, Y., Zhang, G., Tang, Q., Song, W., Gao, Q., Xiang, G., Li, X., Liu, G., Fan, W., Li, X., Yang, S. and Zhai, C., 2022. *EbMYBP1*, a R2R3-MYB transcription factor, promotes flavonoid biosynthesis in *Erigeron Breviscapus. Frontier in Plant Science*, [e-journal] 13. https://dx.doi.org/10.3389/fpls.2022.946827.

Zhao, Q., Feng, Y., Shao, Y., Huang, J. and Chen, Z., 2024. Response mechanism of *Cynodon dactylon* to flooding stress based on integrating metabonomics and transcriptomics analysis. *Environmental and Experimental Botany*, [e-journal] 225. https://dx.doi.org/10.1016/j.envexpbot.2024.105846.

Zheng, S., Ren, P., Zhai, M., Li., C. and Chen, Q., 2021. Identification of genes involved in root growth inhibition under lead stress by transcriptome profiling in

Arabidopsis. *Plant Molecular Biology Reporter*, [e-journal] 39, pp.50–59. https://dx.doi.org/10.1007/s11105-020-01233-y.

Zheng, M., Liu, Y., Zhang, G., Yang, Z., Xu, W. and Chen, Q., 2023. The applications and mechanisms of superoxide dismutase in medicine, food, and cosmetics. *Antioxidants (Basel, Switzerland)*, [e-journal] 12(9). https://dx.doi.org/10.3390/antiox12091675.

Zheng, X., Li, Q., Wang, Z. and Chen, M., 2024. Remediation of heavy metal contaminated soil by enhanced electrokinetic technology: A review. *Arabian Journal of Chemistry*, [e-journal] 17(6). http://dx.doi.org/10.1016/j.arabjc.2024.105773.

Zhou, X., Herbst-Robinson, K.J. and Zhang, J., 2012. Visualizing dynamic activities of signaling enzymes using genetically encodable FRET-based biosensors from designs to applications. *Methods in Enzymology*, [e-journal] 504, pp.317-340. https://dx.doi.org/10.1016/B978-0-12-391857-4.00016-1.

Zhou, L., Wu, Q., Yang, Y., Li, Q., Li, R. and Ye, J., 2024. Regulation of oil biosynthesis and genetic improvement in plants: advances and prospects. *Genes*, [e-journal] 15(9). https://dx.doi.org/10.3390/genes15091125

Zhu, C., Yu, J., Cao, S., Wu, X., Meng, W. and Hou, X., 2022. Transcriptomics-based analysis of genes related to lead stress and their expression in the roots of *Pogonatherum crinitum*. *Frontiers in Plant Science*, [e-journal] 13. https://dx.doi.org/10.3389/fpls.2022.1066329.

Zinati, Z. and Delavari, A., 2019. Identification of candidate genes related to aroma in rice by analyzing the microarray data of highly aromatic and nonaromatic recombinant inbred line bulks. *BioTechnologia*, [e-journal] 100(3), pp.227-240. https://dx.doi.org/10.5114/bta.2019.87582.

Zulkipli, F., Jamian, N.H. and Zulkifli, I.Z., 2020. Forecasting model for organic waste generation at administration cafe in UiTM Tapah Campus. *International Journal of Academic Research in Business and Social Sciences*, [e-journal] 10(9), pp.1023-1032.

Zuo, Y., Abbas, A., Dauda, S.O., Chen, C., Bose, J., Donovan-Mak, M., Wang, Y., He, J., Zhang, P., Yan, Z. and Chen, Z.H., 2025. Function of key ion channels in abiotic stresses and stomatal dynamics. *Plant Physiology and Biochemistry*, [e-journal] 220. https://dx.doi.org/10.1016/j.plaphy.2025.109574.

Zvitov, R., Schwartz, A., Zamski, E. and Nussinovitch, A., 2003. Direct current electrical field effects on intact plant organs. *Biotechnology Progress*, [e-journal] 19(3), pp.965-971. http://dx.doi.org/10.1021/bp034022b.

APPENDICES

APPENDIX 1

Standard solution for Flame Atomic Absorption Spectrometer (FAAS)

Preparation of standard solution of Manganese

Standard (mg/L)	1.0	1.5	2.0	2.5	3.0
Volume of 10 mg/L metal stock solution (mL)	10	15	20	25	30
Volume of 0.5M HNO_3 (mL)	90	85	80	75	70

Preparation of standard solution of Cadmium

Standard (mg/L)	0.4	0.6	0.8	1.0	1.2
Volume of 2 mg/L metal stock solution (mL)	20	30	40	50	60
Volume of 0.5M HNO_3 (mL)	80	70	60	50	40

Preparation of standard solution of Ferum

Standard (mg/L)	2	3	4	5	6
Volume of 10 mg/L metal stock solution (mL)	20	30	40	50	60
Volume of 0.5M HNO_3 (mL)	80	70	60	50	40

Preparation of standard solution of Nickel

Standard (mg/L)	2	3	4	5	6
Volume of 10 mg/L metal stock solution (mL)	20	30	40	50	60
Volume of 0.5M HNO_3 (mL)	80	70	60	50	40

Preparation of standard solution of Lead

Standard (mg/L)	4	8	12	16	20
Volume of 20 mg/L metal stock solution (mL)	20	40	60	80	100
Volume of 0.5M HNO_3 (mL)	80	60	40	20	0

Preparation of standard solution of Zinc

Standard (mg/L)	0.2	0.4	0.6	0.8	1.0
Volume of 2 mg/L metal stock solution (mL)	10	20	30	40	50
Volume of 0.5M HNO_3 (mL)	90	80	70	60	50

APPENDIX 2

Agilent Flame Atomic Absorption Spectrometer 280FSAA Cookbook

Summary of recommended setting

Element	Wavelength (nm)	Slit (nm)	Conc (mg/L) for 0.2 Abs	Lamp Intensity	Effetive Conc Range (mg/L)		Type of Gas	Remarks
					0.1ABS	0.8ABS		
Al	**309.3**	**0.5**	**40**	**100**	**20**	**160**	N2O/C2H2	Default Setting
	396.2	0.5	80	100	40	320	N2O/C2H2	
Cd	**228.8**	**0.5**	**0.6**	**40**	**0.3**	**2.4**	Air/C2H2	Default Setting
	326.1	0.5	240	100	120	960	Air/C2H2	
Ca	**422.7**	**0.5**	**0.8**	**100**	**0.4**	**3.2**	N2O/C2H2	Default Setting
Co	**240.7**	**0.2**	**2.5**	**20**	**1.25**	**10**	Air/C2H2	Default Setting
	304.4	0.5	40	40	20	160	Air/C2H2	
	346.6	0.2	90	100	45	360	Air/C2H2	
Cu	**324.8**	**0.5**	**1.5**	**100**	**0.75**	**6**	Air/C2H2	Default Setting
	327.4	0.5	3	87	1.5	12	Air/C2H2	
Cr	**357.9**	**0.2**	**2.5**	**40**	**1.25**	**10**	Air/C2H2	Default Setting
	429	0.5	20	100	10	80	Air/C2H2	
	425.4	0.2	12	85	6	48	Air/C2H2	
Fe	**248.3**	**0.2**	**2.5**	**15**	**1.25**	**10**	Air/C2H2	Default Setting
	372	0.2	25	100	12.5	100	Air/C2H2	
Pb	**217**	**1**	**5**	**20**	**2.5**	**20**	Air/C2H2	Default Setting
	283.3	0.5	10	100	5	40	Air/C2H2	
Mg	**285.2**	**0.5**	**0.15**	**100**	**0.075**	**0.6**	Air/C2H2	Default Setting
Mn	**279.5**	**0.2**	**1**	**90**	**0.5**	**4**	Air/C2H2	Default Setting
	403.1	0.2	12	100	6	48	Air/C2H2	
Ni	**232**	**0.2**	**2**	**5**	**1**	**8**	Air/C2H2	Default Setting
	352.5	0.2	10	100	5	40	Air/C2H2	
K	**766.5**	**1**	**0.4**	**100**	**0.2**	**1.6**	Air/C2H2	Default Setting
Ag	**328.1**	**0.5**	**1.5**	**100**	**0.75**	**6**	Air/C2H2	Default Setting
Na	**589**	**0.5**	**0.3**	**100**	**0.15**	**1.2**	Air/C2H2	Default Setting
Sn	**235.5**	**0.5**	**50**	**60**	**25**	**200**	N2O/C2H2	Default Setting
	286.3	0.5	100	100	50	400	N2O/C2H2	
Zn	**213.9**	**1**	**0.3**	**100**	**0.15**	**1.2**	Air/C2H2	Default Setting
As	**193.7**	**0.5**	**40**	**50**	**20**	**160**		Default Setting
	197.2	1	60	100	30	240		
Hg	**253.7**	**0.5**	**70**	**100**	**35**	**280**		Default Setting

APPENDIX 3

AAS results

SpectrAA Report 1:27 PM 1/8/2019 Page 1 of 4

Analyst	GMY
Date Started	12:22 PM 1/8/2019 GMT: 4:22 AM 1/8/2019
Worksheet	GMY_01082019_Mn
Comment	
Methods	Mn
Computer name	DESKTOP-ISKDK3R
Serial Number:	

Method: Mn 0.5M HNO3 (Flame)

Sample ID	Conc mg/L	%RSD	Mean Abs
CAL ZERO	0.000	>100	0.0000
	Readings:		
	-0.0003 0.0004		-0.0002
STANDARD 1	1.000	0.7	0.2075
	Readings:		
	0.2061 0.2072		0.2091
STANDARD 2	1.500	0.5	0.3151
	Readings:		
	0.3132 0.3156		0.3164
STANDARD 3	2.000	2.4	0.4112
	Readings:		
	0.4211 0.4017		0.4108
STANDARD 4	2.500	1.4	0.4956
	Readings:		
	0.4915 0.4916		0.5037
STANDARD 5	3.000	1.8	0.5919
	Readings:		
	0.6027 0.5921		0.5810

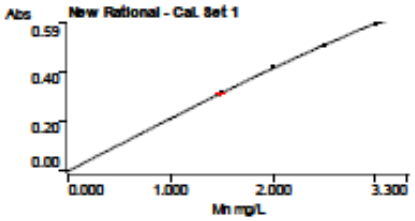

Curve Fit = New Rational
Characteristic Conc = 0.021 mg/L
r = 1.0000
Calculated Conc = 0.000 0.992 1.518 2.008 2.462 3.019
Residuals = 0.000 0.008 -0.018 -0.008 0.038 -0.019

$$Conc = \frac{A}{(-0.07156 \times A \times A + 0.02331 \times A + 0.20733)}$$

Leachate 15.5	1.478	1.6	0.3070

	Readings		
	0.3074	0.3118	0.3019
Leachate 16.5	1.500	0.9	0.3115
	Readings		
	0.3131	0.3082	0.3131
Leachate 17.5	1.955	0.9	0.4011
	Readings		
	0.4041	0.4021	0.3972
Leachate 22.5 E	1.459	0.6	0.3032
	Readings		
	0.3032	0.3052	0.3014
Leachate 22.5 P	1.630	0.2	0.3374
	Readings		
	0.3369	0.3373	0.3380
Leachate 23.5 E	1.373	2.0	0.2857
	Readings		
	0.2802	0.2857	0.2913
Leachate 23.5 P	1.526	1.1	0.3168
	Readings		
	0.3205	0.3139	0.3159
Leachate 24.5 E	1.530	1.4	0.3175
	Readings		
	0.3220	0.3171	0.3133
Leachate 24.5 P	1.568	1.0	0.3251
	Readings		
	0.3230	0.3290	0.3233
MN	0.410	0.4	0.0856
	Readings		
	0.0853	0.0854	0.0859
TP1	0.119	2.6	0.0246
	Readings		
	0.0249	0.0251	0.0239
HLeaf 15.5	0.227	0.8	0.0472
	Readings		
	0.0473	0.0468	0.0476
HRoot 15.5	0.141	0.6	0.0294
	Readings		
	0.0293	0.0296	0.0293
HLeaf 16.5	0.332	2.9	0.0693
	Readings		
	0.0670	0.0702	0.0708
HRoot 16.5	0.195	1.3	0.0405
	Readings		
	0.0400	0.0410	0.0405
Hleaf 17.5	0.336	0.6	0.0701

	Readings		
	0.0697	0.0700	0.0705
H Root 17.5	0.194	1.1	0.0404
	Readings		
	0.0401	0.0402	0.0409
H Leaf 22.5	0.341	1.2	0.0712
	Readings		
	0.0717	0.0702	0.0716
H Root 22.5	0.657	2.0	0.1374
	Readings		
	0.1405	0.1353	0.1365
E Leaf 22.5	0.863	0.5	0.1805
	Readings		
	0.1794	0.1806	0.1813
E Root 22.5	3.142	0.8	0.6120
	Readings		
	0.6126	0.6166	0.6067
P Leaf 22.5	0.906	2.3	0.1896
	Readings		
	0.1923	0.1845	0.1919
H Leaf 23.5	0.358	0.9	0.0747
	Readings		
	0.0751	0.0751	0.0739
H Root 23.5	0.241	1.2	0.0502
	Readings		
	0.0498	0.0499	0.0509
E leaf 23.5	1.051	1.3	0.2196
	Readings		
	0.2162	0.2210	0.2214
P leaf 23.5	1.229	1.0	0.2564
	Readings		
	0.2542	0.2593	0.2558
H leaf 24.5	0.506	1.4	0.1058
	Readings		
	0.1054	0.1074	0.1045
H root 24.5	0.456	1.1	0.0952
	Readings		
	0.0956	0.0959	0.0940
E leaf 24.5	1.004	6.4	0.2099
	Readings		
	0.2156	0.2195	0.1947
E root 24.5	0.916	4.2	0.1916
	Readings		
	0.1999	0.1910	0.1839
P leaf 24.5	0.215	3.0	0.0448

	Readings		
	0.0458	0.0433	0.0455
P root 24.5	1.015	3.6	0.2122
	Readings		
	0.2138	0.2037	0.2189
TF2	1.107m	1.5	0.2312
	Readings		
	0.2353	0.2296	0.2288
P Root 22.5	0.210m	1.4	0.0437
	Readings		
	0.0436	0.0443	0.0431
E Root 23.5	0.118m	5.2	0.0245
	Readings		
	0.0260	0.0236	0.0239
P root 23.5	0.124m	1.1	0.0259
	Readings		
	0.0260	0.0261	0.0256

Analyst
Date Started 12:23 PM 12/6/2019 GMT: 4:23 AM 12/6/2019
Worksheet CMY_12062019_Cd
Comment
Methods Cd
Computer name DESKTOP-ISKDK3R
Serial Number:

Method: Cd 0.5M HNO3 (Flame)

Sample ID	Conc mg/L		%RSD	Mean Abs
CAL ZERO	0.000		>100	0.0001
	Readings			
	-0.0001	0.0002		0.0001
STANDARD 1	0.400		0.4	0.1690
	Readings			
	0.1692	0.1682		0.1695
STANDARD 2	0.600		0.4	0.2420
	Readings			
	0.2414	0.2431		0.2414
STANDARD 3	0.800		0.4	0.3140
	Readings			
	0.3142	0.3151		0.3126
STANDARD 4	1.000		1.1	0.3850
	Readings			
	0.3803	0.3876		0.3873
STANDARD 5	1.200		0.5	0.4421
	Readings			
	0.4422	0.4400		0.4441

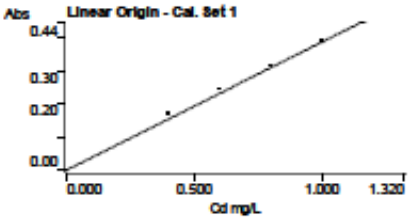

Curve Fit = Linear Origin
Characteristic Conc = 0.011 mg/L
r = 0.9970
Calculated Conc = 0.000 0.441 0.631 0.819 1.005 1.154
Residuals = 0.000 -0.041 -0.031 -0.019 -0.005 0.046

Abs = 0.38320 x C

LEACHATE 15/5	1.248		0.7	0.4781
	Readings			
	0.4794	0.4742		0.4807

LEACHATE 16/5	1.202	0.6	0.4607
	Readings		
	0.4580	0.4611	0.4630
LEACHATE 17/5	1.155	0.6	0.4426
	Readings		
	0.4398	0.4435	0.4445
LEACHATE 22/5 E	1.018	0.6	0.3901
	Readings		
	0.3875	0.3911	0.3916
LEACHATE 22/5 P	1.043	0.4	0.3996
	Readings		
	0.3988	0.4013	0.3987
LEACHATE 23/5 E	1.007	0.4	0.3859
	Readings		
	0.3872	0.3863	0.3842
LEACHATE 23/5 P	1.053	0.3	0.4034
	Readings		
	0.4023	0.4049	0.4029
LEACHATE 24/5 E	1.063	0.5	0.4073
	Readings		
	0.4088	0.4049	0.4080
LEACHATE 24/5 P	1.063	0.6	0.4075
	Readings		
	0.4045	0.4085	0.4094
15/5 LEAF	0.023	1.7	0.0088
	Readings		
	0.0089	0.0086	0.0088
15/5 ROOT	0.023	2.6	0.0087
	Readings		
	0.0088	0.0085	0.0089
16/5 LEAF	0.021	1.0	0.0081
	Readings		
	0.0082	0.0081	0.0081
16/5 ROOT	0.044	1.0	0.0168
	Readings		
	0.0169	0.0166	0.0169
17/5 LEAF	0.014	0.6	0.0054
	Readings		
	0.0054	0.0054	0.0054
17/5 ROOT	0.029	1.2	0.0112
	Readings		
	0.0111	0.0113	0.0111
22/5 HL	0.022	2.7	0.0083
	Readings		
	0.0085	0.0081	0.0081

22/5 HR	0.050	0.4	0.0193
	Readings		
	0.0194	0.0192	0.0193
22/5 EL	0.407	0.4	0.1560
	Readings		
	0.1555	0.1566	0.1558
22/5 FL	0.493	1.7	0.1887
	Readings		
	0.1924	0.1870	0.1868
23/5 HL	0.023	5.7	0.0089
	Readings		
	0.0095	0.0089	0.0085
23/5 HR	0.037	0.2	0.0142
	Readings		
	0.0142	0.0141	0.0142
23/5 EL	0.368	0.2	0.1411
	Readings		
	0.1408	0.1414	0.1410
23/5 FL	0.401	2.4	0.1537
	Readings		
	0.1575	0.1535	0.1502
24/5 HL	0.040	18.2	0.0154
	Readings		
	0.0185	0.0149	0.0129
24/5 HR	0.036	2.8	0.0138
	Readings		
	0.0142	0.0138	0.0135
24/5 EL	0.418	0.7	0.1602
	Readings		
	0.1605	0.1611	0.1591
24/5 FL	0.300	0.4	0.1149
	Readings		
	0.1152	0.1152	0.1144
Mn	0.070	2.1	0.0269
	Readings		
	0.0269	0.0275	0.0264
Transform 1	0.089	2.3	0.0341
	Readings		
	0.0349	0.0343	0.0333
Transform 2	0.037	1.3	0.0141
	Readings		
	0.0139	0.0142	0.0143
22/5 ER	0.625m	0.7	0.2396
	Readings		
	0.2382	0.2414	0.2390

22/5 PR	0.512m	9.9	0.1964
	Readings		
	0.2094	0.2056	0.1741
23/5 ER	0.186m	2.9	0.0712
	Readings		
	0.0688	0.0720	0.0727
23/5 PR	0.176m	1.2	0.0673
	Readings		
	0.0663	0.0677	0.0679
24/5 ER	0.149m	3.2	0.0571
	Readings		
	0.0550	0.0581	0.0581
24/5 PR	0.156m	1.4	0.0598
	Readings		
	0.0597	0.0607	0.0590

Analyst CMY
Date Started 11:05 AM 18/6/2019 GMT: 3:05 AM 18/6/2019
Worksheet CMY_180619_Fe 01
Comment
Methods Fe
Computer name DESKTOP-ISKDK3R
Serial Number:

Method: Fe 0.5M HNO3 (Flame)

Sample ID	Conc mg/L		%RSD	Mean Abs
CAL ZERO	0.000		75.6	0.0006
	Readings			
	0.0010	0.0001		0.0006
STANDARD 1	2.000		2.7	0.1401
	Readings			
	0.1407	0.1434		0.1360
STANDARD 2	3.000		1.4	0.2051
	Readings			
	0.2080	0.2050		0.2022
STANDARD 3	4.000		1.9	0.2607
	Readings			
	0.2634	0.2636		0.2550
STANDARD 4	5.000		1.5	0.3156
	Readings			
	0.3192	0.3104		0.3171
STANDARD 5	6.000		1.2	0.3763
	Readings			
	0.3790	0.3786		0.3712

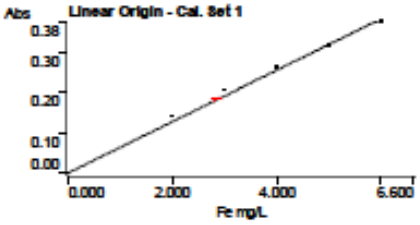

Curve Fit = Linear Origin
Characteristic Conc = 0.069 mg/L
r = 0.9977
Calculated Conc = 0.009 2.183 3.197 4.063 4.919 5.866
Residuals = -0.009 -0.183 -0.197 -0.063 0.081 0.134

Abs = 0.06415 x C

Pre leachate 15.5	2.812		0.2	0.1804
	Readings			
	0.1801	0.1804		0.1806

Pre leachate 16.5	2.037	0.4	0.1307
	Readings		
	0.1303	0.1305	0.1312
Pre leachate 17.5	2.093	1.9	0.1343
	Readings		
	0.1313	0.1353	0.1361
P leachate 22.5	0.826	1.2	0.0530
	Readings		
	0.0534	0.0533	0.0523
E leachate 23.5	0.514	1.4	0.0330
	Readings		
	0.0325	0.0335	0.0330
P leachate 23.5	1.486	2.3	0.0953
	Readings		
	0.0945	0.0936	0.0978
E leachate 24.5	1.666	0.2	0.1069
	Readings		
	0.1072	0.1068	0.1067
P leachate 24.5	0.916	0.7	0.0588
	Readings		
	0.0590	0.0583	0.0590
Plant L 15.5	0.183	1.9	0.0117
	Readings		
	0.0119	0.0115	0.0118
Plant R 15.5	0.733	2.7	0.0470
	Readings		
	0.0485	0.0464	0.0462
Plant L 16.5	0.177	4.1	0.0113
	Readings		
	0.0115	0.0108	0.0117
Plant R 16.5	0.640	0.9	0.0411
	Readings		
	0.0406	0.0412	0.0414
Plant L 17.5	0.194	3.6	0.0125
	Readings		
	0.0130	0.0122	0.0122
Plant R 17.5	0.805	0.9	0.0517
	Readings		
	0.0511	0.0520	0.0519
HL 22.5	0.208	4.9	0.0133
	Readings		
	0.0140	0.0127	0.0134
HR 22.5	0.720	2.2	0.0462
	Readings		
	0.0463	0.0471	0.0451

EL 22.5	0.520	0.9	0.0334
	Readings		
	0.0336	0.0330	0.0335
PL 22.5	0.435	0.5	0.0279
	Readings		
	0.0281	0.0279	0.0278
HL 23.5	0.251	2.5	0.0161
	Readings		
	0.0156	0.0162	0.0164
HR 23.5	0.900	0.6	0.0577
	Readings		
	0.0581	0.0575	0.0576
EL 23.5	0.311	2.7	0.0199
	Readings		
	0.0206	0.0196	0.0196
PL 23.5	0.318	1.7	0.0204
	Readings		
	0.0207	0.0206	0.0200
HL 24.5	0.228	2.3	0.0146
	Readings		
	0.0150	0.0145	0.0143
HR 24.5	1.005	2.9	0.0645
	Readings		
	0.0623	0.0658	0.0653
EL 24.5	0.349	3.4	0.0224
	Readings		
	0.0229	0.0215	0.0227
PL 24.5	0.182	4.7	0.0117
	Readings		
	0.0122	0.0117	0.0111
MN	0.467	1.4	0.0299
	Readings		
	0.0294	0.0301	0.0303
TF 1	0.628	2.9	0.0403
	Readings		
	0.0415	0.0392	0.0401
ER 22.5	3.536m	0.5	0.2268
	Readings		
	0.2260	0.2264	0.2280
PR 22.5	1.916m	1.8	0.1229
	Readings		
	0.1231	0.1207	0.1249
ER 23.5	2.058m	2.3	0.1320
	Readings		
	0.1352	0.1293	0.1316

P R 23.5	2.274m	0.6	0.1459
	Readings		
	0.1459	0.1460	0.1458
E R 24.5	1.656m	1.3	0.1062
	Readings		
	0.1047	0.1066	0.1074
P R 24.5	1.807m	1.2	0.1159
	Readings		
	0.1151	0.1175	0.1151
E leachate 22.5	0.717m	2.3	0.0460
	Readings		
	0.0453	0.0472	0.0456
TF 2	0.746m	3.3	0.0479
	Readings		
	0.0463	0.0480	0.0494

Analyst CMY
Date Started 9:20 AM 18/6/2019 GMT: 1:20 AM 18/6/2019
Worksheet CMY_180619_Ni 01
Comment
Methods Ni
Computer name DESKTOP-ISKDK3R
Serial Number:

Method: Ni 0.5M HNO3 (Flame)

Sample ID	Conc mg/L		%RSD	Mean Abs
CAL ZERO	0.000		>100	0.0007
	Readings			
	0.0008	-0.0004		0.0015
STANDARD 1	2.000		21.7	0.1435
	Readings			
	0.1620	0.1610		0.1075
STANDARD 2	3.000		0.1	0.2316
	Readings			
	0.2314	0.2318		0.2316
STANDARD 3	4.000		0.6	0.3063
	Readings			
	0.3043	0.3063		0.3082
STANDARD 4	5.000		0.6	0.3755
	Readings			
	0.3780	0.3742		0.3744
STANDARD 5	6.000		1.1	0.4368
	Readings			
	0.4362	0.4420		0.4323

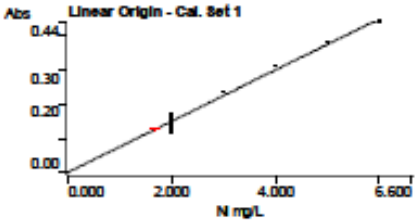

Curve Fit = Linear Origin
Characteristic Conc = 0.059 mg/L
r = 0.9989
Calculated Conc = 0.009 1.926 3.109 4.111 5.040 5.863
Residuals = -0.009 0.074 -0.109 -0.111 -0.040 0.137

Abs = 0.07451 x C

Pre leachate 16.5	1.681		0.7	0.1252
	Readings			
	0.1250	0.1245		0.1262

Pre leachate 17.5	1.644	1.1	0.1225
	Readings		
	0.1237	0.1209	0.1228
Leachate EAPR 22.5	1.435	3.2	0.1069
	Readings		
	0.1102	0.1033	0.1073
Leachate Plant 22.5	1.439	1.5	0.1072
	Readings		
	0.1055	0.1087	0.1075
Leachate EAPR 23.5	1.435	0.8	0.1069
	Readings		
	0.1059	0.1073	0.1076
Leachate Plant 23.5	1.506	0.9	0.1122
	Readings		
	0.1124	0.1110	0.1131
Leachate EAPR 24.5	1.519	0.6	0.1131
	Readings		
	0.1131	0.1125	0.1138
Leachate Plant 24.5	1.522	1.5	0.1134
	Readings		
	0.1116	0.1147	0.1140
Plant L 15.5	0.040	16.2	0.0030
	Readings		
	0.0033	0.0024	0.0031
Plant R 15.5	0.080	31.0	0.0060
	Readings		
	0.0049	0.0049	0.0081
Plant L 16.5	0.032	21.7	0.0024
	Readings		
	0.0019	0.0024	0.0029
Plant R 16.5	0.072	17.1	0.0054
	Readings		
	0.0059	0.0043	0.0060
Plant L 17.5	0.048	12.2	0.0036
	Readings		
	0.0034	0.0041	0.0033
Plant R 17.5	0.077	15.0	0.0058
	Readings		
	0.0065	0.0060	0.0048
H L 22.5	0.039	14.5	0.0029
	Readings		
	0.0027	0.0033	0.0025
H R 22.5	0.096	6.4	0.0072
	Readings		
	0.0075	0.0066	0.0074

EL 22.5	0.558	2.1	0.0416
	Readings		
	0.0409	0.0426	0.0412
PL 22.5	0.651	1.3	0.0485
	Readings		
	0.0480	0.0484	0.0492
HL 23.5	0.058	9.4	0.0043
	Readings		
	0.0048	0.0041	0.0041
HR 23.5	0.102	2.8	0.0076
	Readings		
	0.0074	0.0077	0.0078
EL 23.5	0.559	2.4	0.0416
	Readings		
	0.0406	0.0425	0.0419
PL 23.5	0.563	3.4	0.0420
	Readings		
	0.0413	0.0410	0.0436
HL 24.5	0.043	11.4	0.0032
	Readings		
	0.0030	0.0030	0.0036
HR 24.5	0.089	11.9	0.0066
	Readings		
	0.0057	0.0072	0.0069
EL 24.5	0.595	1.5	0.0443
	Readings		
	0.0436	0.0447	0.0448
ER 24.5	6.079	0.6	0.4529
	Readings		
	0.4546	0.4545	0.4496
PL 24.5	0.454	0.5	0.0338
	Readings		
	0.0339	0.0336	0.0338
PR 24.5	6.550	0.0	0.4880
	Readings		
	0.4880		
MN	0.251	0.8	0.0187
	Readings		
	0.0188	0.0188	0.0185
TP1	0.318	2.8	0.0237
	Readings		
	0.0231	0.0244	0.0236
TP2	0.957	2.3	0.0713
	Readings		
	0.0704	0.0732	0.0703

Pre leachate 15.5	1.693m		1.6	0.1262
	Readings			
	0.1280	0.1240		0.1264
ER22.5	0.695m		1.0	0.0518
	Readings			
	0.0522	0.0520		0.0512
PR22.5	0.669m		0.6	0.0498
	Readings			
	0.0500	0.0495		0.0500
ER23.5	0.713m		0.4	0.0531
	Readings			
	0.0529	0.0534		0.0530
PR23.5	0.685m		1.0	0.0510
	Readings			
	0.0515	0.0505		0.0511

Analyst CMY
Date Started 9:35 AM 6/8/2019 GMT: 1:35 AM 6/8/2019
Worksheet CMY_06082019_Pb 01
Comment
Methods Pb
Computer name DESKTOP-ISKDK3R
Serial Number:

Method: Pb 0.6M HNO3 (Flame)

Sample ID	Conc mg/L		%RSD	Mean Abs
CAL ZERO	0.000		>100	-0.0002
	Readings			
	0.0002	0.0004		-0.0014
STANDARD 1	4.000		1.1	0.1488
	Readings			
	0.1486	0.1505		0.1473
STANDARD 2	8.000		1.5	0.2576
	Readings			
	0.2615	0.2540		0.2573
STANDARD 3	12.000		0.4	0.4088
	Readings			
	0.4102	0.4072		0.4090
STANDARD 4	16.000		2.5	0.5064
	Readings			
	0.5132	0.4918		0.5141
STANDARD 5	20.000		1.0	0.5841
	Readings			
	0.5903	0.5790		0.5831

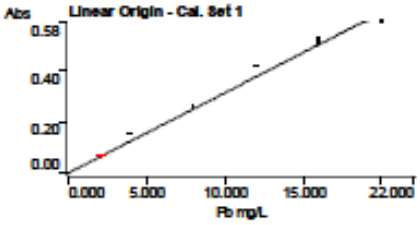

Curve Fit = Linear Origin
Characteristic Conc = 0.142 mg/L
r = 0.9930
Calculated Conc = -0.007 4.788 8.289 13.155 16.295 18.798
Residuals = 0.007 -0.788 -0.289 -1.155 -0.295 1.202

Abs = 0.03108 x C

Leachate 15.5	2.075		0.5	0.0645
	Readings			
	0.0641	0.0646		0.0648

Leachate 16.5	2.758	1.2	0.0857
	Readings		
	0.0847	0.0867	0.0858
Leachate 17.5	3.095	2.0	0.0962
	Readings		
	0.0979	0.0941	0.0966
Leachate E 22.5	0.560	7.9	0.0174
	Readings		
	0.0174	0.0188	0.0160
Leachate P 22.5	1.044	0.3	0.0325
	Readings		
	0.0326	0.0324	0.0324
Leachate E 23.5	0.930	11.1	0.0289
	Readings		
	0.0318	0.0254	0.0295
Leachate P 23.5	1.218	3.9	0.0379
	Readings		
	0.0392	0.0362	0.0382
Leachate E 24.5	1.848	1.4	0.0574
	Readings		
	0.0575	0.0565	0.0582
Leachate P 24.5	1.416	2.2	0.0440
	Readings		
	0.0446	0.0446	0.0429
MN	1.165	4.4	0.0362
	Readings		
	0.0345	0.0364	0.0377
TF 1	1.671	2.4	0.0519
	Readings		
	0.0524	0.0505	0.0528
TF 2	0.539	3.0	0.0167
	Readings		
	0.0173	0.0162	0.0167
Root 15.5	0.212	19.0	0.0066
	Readings		
	0.0052	0.0073	0.0074
Leaf 16.5	0.220	16.0	0.0068
	Readings		
	0.0063	0.0081	0.0061
Root 16.5	0.239	23.9	0.0074
	Readings		
	0.0079	0.0090	0.0055
Leaf 17.5	0.189	12.4	0.0059
	Readings		
	0.0063	0.0063	0.0050

Root 17.5	0.277	19.1	0.0086
	Readings		
	0.0094	0.0067	0.0097
Leaf H 22.5	0.278	16.2	0.0086
	Readings		
	0.0073	0.0101	0.0085
Root H 22.5	0.230	12.3	0.0072
	Readings		
	0.0082	0.0065	0.0068
Leaf E 22.5	0.382	7.8	0.0119
	Readings		
	0.0121	0.0109	0.0127
Leaf P 22.5	0.568	4.7	0.0176
	Readings		
	0.0171	0.0186	0.0173
Root P 22.5	18.879	0.9	0.5867
	Readings		
	0.5928	0.5847	0.5825
Leaf H 23.5	0.207	15.2	0.0064
	Readings		
	0.0075	0.0057	0.0060
Root H 23.5	0.260	21.1	0.0081
	Readings		
	0.0061	0.0091	0.0091
Leaf E 23.5	0.250	10.0	0.0078
	Readings		
	0.0081	0.0069	0.0083
Leaf P 23.5	0.403	10.9	0.0125
	Readings		
	0.0140	0.0121	0.0114
Leaf H 24.5	0.247	12.6	0.0077
	Readings		
	0.0081	0.0084	0.0066
Root H 24.5	0.259	10.1	0.0080
	Readings		
	0.0079	0.0089	0.0073
Leaf E 24.5	0.242	31.5	0.0075
	Readings		
	0.0097	0.0078	0.0050
Root E 24.5	19.353	0.3	0.6014
	Readings		
	0.6025	0.5996	0.6020
Leaf P 24.5	0.281	18.8	0.0087
	Readings		
	0.0092	0.0069	0.0101

Root P 24.5	20.372	0.4	0.6331
	Readings		
	0.6347	0.6298	0.6347
Leaf 15.5	0.217m	18.2	0.0067
	Readings		
	0.0081	0.0061	0.0059
Root E 22.5	3.821m	1.4	0.1187
	Readings		
	0.1171	0.1187	0.1204
Root P 23.5	3.457m	2.7	0.1074
	Readings		
	0.1078	0.1043	0.1102
Root E 23.5	3.355m	0.8	0.1043
	Readings		
	0.1033	0.1050	0.1045

Analyst CMY
Date Started 1:30 PM 1/8/2019 GMT: 5:30 AM 1/8/2019
Worksheet CMY_01082019_Zn(2)
Comment
Methods Zn
Computer name DESKTOP-ISKDK3R
Serial Number:

Method: Zn 0.6M HNO3 (Flame)

Sample ID	Conc mg/L		%RSD	Mean Abs
CAL ZERO	0.000		29.3	0.0020
	Readings			
	0.0026	0.0015		0.0019
STANDARD 1	0.200		0.8	0.1123
	Readings			
	0.1128	0.1129		0.1112
STANDARD 2	0.400		1.2	0.2011
	Readings			
	0.2033	0.1986		0.2015
STANDARD 3	0.600		2.5	0.2978
	Readings			
	0.2892	0.3018		0.3025
STANDARD 4	0.800		1.2	0.3692
	Readings			
	0.3651	0.3684		0.3741
STANDARD 5	1.000		0.5	0.4597
	Readings			
	0.4572	0.4612		0.4606

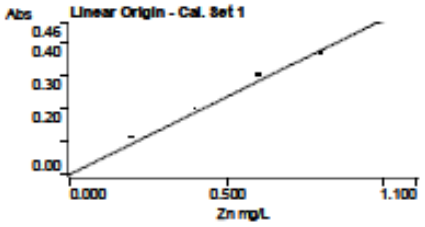

Curve Fit = Linear Origin
Characteristic Conc = 0.009 mg/L
r = 0.9968
Calculated Conc = 0.004 0.238 0.427 0.632 0.784 0.976
Residuals = -0.004 -0.038 -0.027 -0.032 0.016 0.024

Abs = 0.47121 x C

Leachate 22.5 P	1.072		0.4	0.5052
	Readings			
	0.5056	0.5071		0.5029

Leachate 23.5 E	0.995	0.6	0.4689
	Readings		
	0.4693	0.4716	0.4659
MN	0.495	0.7	0.2332
	Readings		
	0.2315	0.2345	0.2337
Hoagland 15.5 leaf	0.387	0.9	0.1824
	Readings		
	0.1833	0.1805	0.1835
Hoagland 16.5 leaf	0.330	2.5	0.1556
	Readings		
	0.1540	0.1600	0.1528
Hoagland 17.5 leaf	0.397	0.6	0.1873
	Readings		
	0.1883	0.1862	0.1873
Hoagland 22.5 leaf	0.383	1.3	0.1807
	Readings		
	0.1827	0.1812	0.1781
EAPR 22.5 leaf	0.855	0.7	0.4028
	Readings		
	0.4023	0.4002	0.4060
Plant 22.5 leaf	0.929	0.5	0.4377
	Readings		
	0.4403	0.4369	0.4358
Hoagland 23.5 leaf	0.436	1.0	0.2057
	Readings		
	0.2066	0.2033	0.2071
EAPR 23.5 leaf	0.766	1.0	0.3611
	Readings		
	0.3650	0.3698	0.3585
Plant 23.5 leaf	0.832	0.2	0.3918
	Readings		
	0.3912	0.3929	0.3914
Hoagland 24.5 leaf	0.384	0.5	0.1811
	Readings		
	0.1820	0.1803	0.1811
EAPR 24.5 leaf	0.793	0.4	0.3735
	Readings		
	0.3737	0.3717	0.3751
Plant 24.5 leaf	0.627	0.2	0.2954
	Readings		
	0.2950	0.2953	0.2960
Leachate 15.5	0.165m	2.8	0.0777
	Readings		
	0.0777	0.0800	0.0756

Leachate 16.5	0.159m	4.5	0.0748
	Readings		
	0.0716	0.0783	0.0744
Leachate 17.5	0.227m	0.9	0.1071
	Readings		
	0.1078	0.1060	0.1076
Leachate 22.5 E	0.149m	0.6	0.0704
	Readings		
	0.0706	0.0698	0.0706
Leachate 24.5 E	0.149m	1.1	0.0704
	Readings		
	0.0705	0.0696	0.0711
Leachate 24.5 P	0.132m	1.4	0.0624
	Readings		
	0.0620	0.0618	0.0634
TF1	OVERm	0.0	1.5550
	Readings		
	1.5550		
TF2	OVERm	0.0	0.9694
	Readings		
	0.9694		
Hoagland 15.5 root	0.365m	0.5	0.1719
	Readings		
	0.1717	0.1728	0.1712
Hoagland 16.5 root	0.351m	0.9	0.1653
	Readings		
	0.1659	0.1663	0.1637
Hoagland 17.5 root	0.213m	2.3	0.1002
	Readings		
	0.0990	0.1029	0.0988
Hoagland 22.5 root	0.509m	4.4	0.2398
	Readings		
	0.2446	0.2470	0.2277
Hoagland 23.5 root	0.424m	0.3	0.1997
	Readings		
	0.2003	0.1998	0.1992
Hoagland 24.5 root	0.322m	1.0	0.1519
	Readings		
	0.1519	0.1533	0.1504
Plant 22.5 root	0.915m	0.5	0.4312
	Readings		
	0.4290	0.4330	0.4316
EAPR 23.5 root	0.985m	0.3	0.4639
	Readings		
	0.4633	0.4656	0.4629

Plant 23.5 root	0.976m	0.7	0.4600
	Readings		
	0.4638	0.4577	0.4585
EAPR 24.5 root	0.826m	2.6	0.3891
	Readings		
	0.3906	0.3982	0.3784
Plant 24.5 root	0.722m	0.4	0.3402
	Readings		
	0.3388	0.3408	0.3409
EAPR 22.5 root	0.119m	1.7	0.0560
	Readings		
	0.0558	0.0552	0.0570
Leachate 23.5 P	0.126m	2.2	0.0593
	Readings		
	0.0607	0.0586	0.0585

APPENDIX 4

BOD analyses

MY CO2 SDN BHD (744438-M) | GST No. 000 462 401 536
MY CO2 (PG) SDN BHD (1256244-P) | GST No. 000 456 159 232 | SAMM No. 384
16, LENGKOK KIKIK 1, TAMAN INDERAWASIH, 13600 PERAI, PENANG, MALAYSIA.
Tel: +604 - 380 8282 Fax: +604 - 380 8280
MY CO2 (KL) SDN BHD (1155142-M) | GST No. 000 685 047 040 | SAMM No. 564
40, JALAN SEPADU B25/B, 40400 SHAH ALAM, SELANGOR, MALAYSIA.
Tel: +603 - 5122 3366 Fax: +603 - 5122 3386
MY CO2 (JB) SDN BHD (1155302-A) | GST No. 000 252 465 152 | SAMM No. 752
15, JALAN MOLEK 1/8, TAMAN MOLEK, 81100 JOHOR BAHRU, JOHOR.
Tel: +607 - 355 8811 Fax: +607 - 355 9808
enquiry@myco2.com.my www.myco2.com.my

myCO2 The Compliance Catalyst

Certificate of Analysis

Lab Ref No.: **AL1905-B20074** SN: **RS8301938839086320** Page 1 / 1

Siti Zaleha Ahmad
Chemist
IKM No.: M/4250/7117/15
AN1: RA1735006573711250

UNIVERSITI TUNKU ABDUL RAHMAN
FACULTY OF SCIENCE
DEPARTMENT OF CHEMICAL SCIENCE
JALAN UNIVERSITY BANDAR BARAT,
KAMPAR PERAK
MALAYSIA

Date of Issue: 2019-05-23
Date of Received: 2019-05-16
Date of Completion: 2019-05-23

Sample Description: CMY 15.5.19 Pre-1

Test Description	Unit	Result(s)	Method or Equipment Used
BOD-5 days @ 20°C	mg/L	32.1	APHA 5210 B & APHA 4500 - O G (2005)

– END OF REPORT –

MY CO2 SDN BHD (744438-M) | GST No. 000 462 401 536
MY CO2 (PG) SDN BHD (1256244-P) | GST No. 000 456 150 232 | SAMM No. 384
16, LENGKOK KIKIK 1, TAMAN INDERAWASIH, 13600 PERAI, PENANG, MALAYSIA.
Tel: +604 - 380 8282 Fax: +604 - 380 8280
MY CO2 (KL) SDN BHD (1155142-M) | GST No. 000 665 047 040 | SAMM No. 564
40, JALAN SEPADU 925/B, 40400 SHAH ALAM, SELANGOR, MALAYSIA.
Tel: +603 - 5122 3366 Fax: +603 - 5122 3386
MY CO2 (JB) SDN BHD (1155302-A) | GST No. 000 252 465 152 | SAMM No. 752
15, JALAN MOLEK 1/8, TAMAN MOLEK, 81100 JOHOR BAHRU, JOHOR.
Tel: +607 - 355 8811 Fax: +607 - 355 9808
enquiry@myco2.com.my www.myco2.com.my

The Compliance Catalyst

Certificate of Analysis

Lab Ref No.: AL1905-B20359 SN: RS1081049886757305 Page 1 / 1

Siti Zaleha Ahmad
Chemist
IKM No.: M/4250/7117/15
AN1: RA68214210372149O8

UNIVERSITI TUNKU ABDUL RAHMAN
FACULTY OF SCIENCE
DEPARTMENT OF CHEMICAL SCIENCE
JALAN UNIVERSITY BANDAR BARAT,
KAMPAR PERAK
MALAYSIA

Date of Issue:	2019-05-27
Date of Received:	2019-05-17
Date of Completion:	2019-05-27

Sample Description: CMY Pre-Synthetic 2 16/5/19

Remark: ND = Not Detected

Test Description	Unit	Result(s)	Method or Equipment Used
BOD-5 days @ 20°C	mg/L	33.3	APHA 5210 B & APHA 4500 - O G (2005)

– END OF REPORT –

MY CO2 SDN BHD (744438-M) | GST No. 000 462 401 536
MY CO2 (PG) SDN BHD (1256244-P) | GST No. 000 466 150 232 | SAMM No. 384
16, LENGKOK KIKIK 1, TAMAN INDERAWASIH, 13600 PERAI, PENANG, MALAYSIA.
Tel: +604 - 380 8282 Fax: +604 - 380 8280
MY CO2 (KL) SDN BHD (1155142-M) | GST No. 000 685 047 040 | SAMM No. 564
40, JALAN SEPADU 926/B, 40400 SHAH ALAM, SELANGOR, MALAYSIA.
Tel: +603 - 5122 3366 Fax: +603 - 5122 3386
MY CO2 (JB) SDN BHD (1155302-A) | GST No. 000 252 465 152 | SAMM No. 752
15, JALAN MOLEK 1/8, TAMAN MOLEK, 81100 JOHOR BAHRU, JOHOR.
Tel: +607 - 355 8811 Fax: +607 - 355 9808
enquiry@myco2.com.my www.myco2.com.my

myCO2 The Compliance Catalyst

Certificate of Analysis

Lab Ref No.: AL1905-B20471 SN: RS1789778007260969

Siti Zaleha Ahmad
Chemist
IKM No.: M/4250/7117/15
AN1: RA1561274604694859

UNIVERSITI TUNKU ABDUL RAHMAN
FACULTY OF SCIENCE
DEPARTMENT OF CHEMICAL SCIENCE
JALAN UNIVERSITY BANDAR BARAT,
KAMPAR PERAK
MALAYSIA

Date of Issue: 2019-05-28
Date of Received: 2019-05-21
Date of Completion: 2019-05-28

Sample Description: CMY Pre-Synthetic 3 17/5/19

Test Description	Unit	Result(s)	Method or Equipment Used
BOD-5 days @ 20°C	mg/L	26.3	APHA 5210 B & APHA 4500 - O G (2005)

– END OF REPORT –

MY CO2 SDN BHD (744438-M) | GST No. 000 462 401 536
MY CO2 (PG) SDN BHD (1256244-P) | GST No. 000 456 159 232 | SAMM No. 384
16, LENGKOK KIKIK 1, TAMAN INDERAWASIH, 13600 PERAI, PENANG, MALAYSIA.
Tel: +604 - 380 8282 Fax: +604 - 380 8280
MY CO2 (KL) SDN BHD (1155142-M) | GST No. 000 885 047 040 | SAMM No. 564
40, JALAN SEPADU B25/B, 40400 SHAH ALAM, SELANGOR, MALAYSIA.
Tel: +603 - 5122 3366 Fax: +603 - 5122 3386
MY CO2 (JB) SDN BHD (1155302-A) | GST No. 000 252 465 152 | SAMM No. 752
15, JALAN MOLEK 1/8, TAMAN MOLEK, 81100 JOHOR BAHRU, JOHOR.
Tel: +607 - 355 8811 Fax: +607 - 355 9808
enquiry@myco2.com.my www.myco2.com.my

myCO2 The Compliance Catalyst

Certificate of Analysis

Lab Ref No.: AL1905-B20751 SN: RS1567467260443771 Page 1 / 1

Siti Zaleha Ahmad
Chemist
IKM No.: M/4250/7117/15
AN1: RA1035044725438347

UNIVERSITI TUNKU ABDUL RAHMAN
FACULTY OF SCIENCE
DEPARTMENT OF CHEMICAL SCIENCE
JALAN UNIVERSITY BANDAR BARAT,
KAMPAR PERAK
MALAYSIA

Date of Issue: 2019-05-31
Date of Received: 2019-05-23
Date of Completion: 2019-05-31

Sample Description: EAPR 15/5/19 CMY

Remark: ND = Not Detected

Test Description	Unit	Result(s)	Method or Equipment Used
BOD-5 days @ 20°C	mg/L	4.8	APHA 5210 B & APHA 4500 - O G (2005)

– END OF REPORT –

MY CO2 SDN BHD (744438-M) | GST No. 000 462 401 536
MY CO2 (PG) SDN BHD (1256244-P) | GST No. 000 456 150 232 | SAMM No. 384
16, LENGKOK KIKIK 1, TAMAN INDERAWASIH, 13600 PERAI, PENANG, MALAYSIA.
Tel: +604 - 380 8282 Fax: +604 - 380 8280
MY CO2 (KL) SDN BHD (1155142-M) | GST No. 000 665 047 040 | SAMM No. 564
40, JALAN SEPADU B26/B, 40400 SHAH ALAM, SELANGOR, MALAYSIA.
Tel: +603 - 5122 3366 Fax: +603 - 5122 3386
MY CO2 (JB) SDN BHD (1155302-A) | GST No. 000 252 465 152 | SAMM No. 752
15, JALAN MOLEK 1/8, TAMAN MOLEK, 81100 JOHOR BAHRU, JOHOR.
Tel: +607 - 355 8811 Fax: +607 - 355 9808
enquiry@myco2.com.my www.myco2.com.my

myCO2 The Compliance Catalyst

Certificate of Analysis

Lab Ref No.: AL1905-B20971 SN: RS1893441841687776 Page 1 / 1

Siti Zaleha Ahmad
Chemist
IKM No.: M/4250/7117/15
AN1: RA1254840455423214

UNIVERSITI TUNKU ABDUL RAHMAN
FACULTY OF SCIENCE
DEPARTMENT OF CHEMICAL SCIENCE
JALAN UNIVERSITY BANDAR BARAT,
KAMPAR PERAK
MALAYSIA

Date of Issue: 2019-06-07
Date of Received: 2019-05-25
Date of Completion: 2019-06-07

Sample Description: CMY EAPR 23/5/19

Remark: ND = Not Detected
BOD analyzed on sample receiving date and incubated for 5 days @ 20 Deg C.

Test Description	Unit	Result(s)	Method or Equipment Used
BOD-5 days @ 20°C	mg/L	10.6	APHA 5210 B & APHA 4500 - O G (2005)

– END OF REPORT –

MY CO2 SDN BHD (744438-M) | GST No. 000 462 401 536
MY CO2 (PG) SDN BHD (1256244-P) | GST No. 000 466 150 232 | SAMM No. 384
16, LENGKOK KIKIK 1, TAMAN INDERAWASIH, 13600 PERAI, PENANG, MALAYSIA.
Tel: +604 - 380 8282 Fax: +604 - 380 8280

MY CO2 (KL) SDN BHD (1155142-M) | GST No. 000 685 047 040 | SAMM No. 564
40, JALAN SERADU 9/5/B, 40400 SHAH ALAM, SELANGOR, MALAYSIA.
Tel: +603 - 5122 3366 Fax: +603 - 5122 3386

MY CO2 (JB) SDN BHD (1155302-A) | GST No. 000 252 465 152 | SAMM No. 752
15, JALAN MOLEK 1/8, TAMAN MOLEK, 81100 JOHOR BAHRU, JOHOR.
Tel: +607 - 355 8811 Fax: +607 - 355 9808

enquiry@myco2.com.my www.myco2.com.my

myCO2 The Compliance Catalyst

Certificate of Analysis

Lab Ref No.: AL1905-B21000 SN: RS2097317339847937 Page 1 / 1

Siti Zaleha Ahmad
Chemist
IKM No.: M/4250/7117/15
AN1: RA1846341324791171

UNIVERSITI TUNKU ABDUL RAHMAN
FACULTY OF SCIENCE
DEPARTMENT OF CHEMICAL SCIENCE
JALAN UNIVERSITY BANDAR BARAT,
KAMPAR PERAK
MALAYSIA

Date of Issue:	2019-06-07
Date of Received:	2019-05-27
Date of Completion:	2019-06-07

Sample Description: CMY EAPR 24/5/19

BOD analyzed on sample receiving date and incubated for 5 days @ 20 Deg C

Test Description	Unit	Result(s)	Method or Equipment Used
BOD-5 days @ 20°C	mg/L	12.7	APHA 5210 B & APHA 4500 - O G (2005)

– END OF REPORT –

MY CO2 SDN BHD (744438-M) | GST No. 000 462 401 536
MY CO2 (PG) SDN BHD (1256244-P) | GST No. 000 456 150 232 | SAMM No. 384
16, LENGKOK KIKIK 1, TAMAN INDERAWASIH, 13600 PERAI, PENANG, MALAYSIA.
Tel: +604 - 380 8282 Fax: +604 - 380 8280
MY CO2 (KL) SDN BHD (1155142-M) | GST No. 000 665 047 040 | SAMM No. 564
40, JALAN SEPADU B25/B, 40400 SHAH ALAM, SELANGOR, MALAYSIA.
Tel: +603 - 5122 3366 Fax: +603 - 5122 3386
MY CO2 (JB) SDN BHD (1155302-A) | GST No. 000 252 465 152 | SAMM No. 752
15, JALAN MOLEK 1/8, TAMAN MOLEK, 81100 JOHOR BAHRU, JOHOR.
Tel: +607 - 355 8811 Fax: +607 - 355 9808
enquiry@myco2.com.my www.myco2.com.my

myCO2 The Compliance Catalyst

Certificate of Analysis

Lab Ref No.: AL1905-B20750 SN: RS6755086756957801 Page 1 / 1

Siti Zaleha Ahmad
Chemist
IKM No.: M/4250/7117/15
AN1: RA1454971007305130

UNIVERSITI TUNKU ABDUL RAHMAN
FACULTY OF SCIENCE
DEPARTMENT OF CHEMICAL SCIENCE
JALAN UNIVERSITY BANDAR BARAT,
KAMPAR PERAK
MALAYSIA

Date of Issue: 2019-05-31
Date of Received: 2019-05-23
Date of Completion: 2019-05-31

Sample Description: Plant 15/5/19 CMY

Test Description	Unit	Result(s)	Method or Equipment Used
BOD-5 days @ 20°C	mg/L	9.4	APHA 5210 B & APHA 4500 - O G (2005)

– END OF REPORT –

MY CO2 SDN BHD (744438-M) | GST No. 000 462 401 536
MY CO2 (PG) SDN BHD (1256244-P) | GST No. 000 456 159 232 | SAMM No. 384
16, LENGKOK KIKIK 1, TAMAN INDERAWASIH, 13600 PERAI, PENANG, MALAYSIA.
Tel: +604 - 380 8282 Fax: +604 - 380 8280
MY CO2 (KL) SDN BHD (1155142-M) | GST No. 000 685 047 040 | SAMM No. 564
40, JALAN SEPADU B26/B, 40400 SHAH ALAM, SELANGOR, MALAYSIA.
Tel: +603 - 5122 3366 Fax: +603 - 5122 3366
MY CO2 (JB) SDN BHD (1155302-A) | GST No. 000 252 465 152 | SAMM No. 752
15, JALAN MOLEK 1/8, TAMAN MOLEK, 81100 JOHOR BAHRU, JOHOR.
Tel: +607 - 355 8811 Fax: +607 - 355 9808
enquiry@myco2.com.my www.myco2.com.my

myCO2 The Compliance Catalyst

Certificate of Analysis

Lab Ref No.: AL1905-B20972 SN: RS1152694400251083 Page 1 / 1

Siti Zaleha Ahmad
Chemist
IKM No.: M/4250/7117/15
AN1: RA2797115079703463

UNIVERSITI TUNKU ABDUL RAHMAN
FACULTY OF SCIENCE
DEPARTMENT OF CHEMICAL SCIENCE
JALAN UNIVERSITY BANDAR BARAT,
KAMPAR PERAK
MALAYSIA

Date of Issue: 2019-06-07
Date of Received: 2019-05-25
Date of Completion: 2019-06-07

Sample Description: CMY Plant 23/5/19

Remark: ND = Not Detected
BOD analyzed on sample receiving date and incubated for 5 days @ 20 Deg C.

Test Description	Unit	Result(s)	Method or Equipment Used
BOD-5 days @ 20°C	mg/L	12.8	APHA 5210 B & APHA 4500 - O G (2005)

– END OF REPORT –

MY CO2 SDN BHD (744438-M) | GST No. 000 462 401 536
MY CO2 (PG) SDN BHD (1256244-P) | GST No. 000 456 159 232 | SAMM No. 384
16, LENGKOK KIKIK 1, TAMAN INDERAWASIH, 13600 PERAI, PENANG, MALAYSIA.
Tel: +604 - 380 8282 Fax: +604 - 380 8280
MY CO2 (KL) SDN BHD (1155142-M) | GST No. 000 885 047 040 | SAMM No. 564
40, JALAN SEPADU B25/B, 40400 SHAH ALAM, SELANGOR, MALAYSIA.
Tel: +603 - 5122 3366 Fax: +603 - 5122 3386
MY CO2 (JB) SDN BHD (1155302-A) | GST No. 000 252 465 152 | SAMM No. 752
15, JALAN MOLEK 1/8, TAMAN MOLEK, 81100 JOHOR BAHRU, JOHOR.
Tel: +607 - 355 9811 Fax: +607 - 355 9806
enquiry@myco2.com.my www.myco2.com.my

myCO2 The Compliance Catalyst

Certificate of Analysis

Lab Ref No.: **AL1905-B21001** SN: **RS6674423321919374**

Siti Zaleha Ahmad
Chemist
IKM No.: M/4250/7117/15
AN1: RA4732089673536587

UNIVERSITI TUNKU ABDUL RAHMAN
FACULTY OF SCIENCE
DEPARTMENT OF CHEMICAL SCIENCE
JALAN UNIVERSITY BANDAR BARAT,
KAMPAR PERAK
MALAYSIA

Date of Issue:	2019-06-04
Date of Received:	2019-05-27
Date of Completion:	2019-06-04

Sample Description: CMY Plant 24/5/19

BOD analyzed on sample receiving date and incubated for 5 days @ 20 Deg C

Test Description	Unit	Result(s)	Method or Equipment Used
BOD-5 days @ 20°C	mg/L	11.2	APHA 5210 B & APHA 4500 - O G (2005)

– END OF REPORT –

APPENDIX 5

SPSS statistical analysis report for synthetic leachate characterization (one-way ANOVA and Tukey's HSD post-hoc test)

ANOVA

		Sum of Squares	df	Mean Square	F	Sig.
pH	Between Groups	1.863	2	.931	19.335	.002
	Within Groups	.289	6	.048		
	Total	2.152	8			
BOD	Between Groups	830.216	2	415.108	37.008	.000
	Within Groups	67.300	6	11.217		
	Total	897.516	8			
Colour	Between Groups	21088.889	2	10544.444	14.600	.005
	Within Groups	4333.333	6	722.222		
	Total	25422.222	8			
COD	Between Groups	6466.667	2	3233.333	.593	.582
	Within Groups	32733.333	6	5455.556		
	Total	39200.000	8			
DO	Between Groups	20.608	2	10.304	13.327	.006
	Within Groups	4.639	6	.773		
	Total	25.247	8			
ORP	Between Groups	5.447	2	2.723	2.880	.133
	Within Groups	5.673	6	.946		
	Total	11.120	8			
Conductivity	Between Groups	6088.222	2	3044.111	.452	.657
	Within Groups	40444.000	6	6740.667		
	Total	46532.222	8			
Turbidity	Between Groups	5452.487	2	2726.243	17.782	.003
	Within Groups	919.913	6	153.319		
	Total	6372.400	8			
TDS	Between Groups	.002	2	.001	3.429	.102
	Within Groups	.001	6	.000		
	Total	.003	8			
Ammonia	Between Groups	20.777	2	10.389	.166	.851
	Within Groups	375.630	6	62.605		
	Total	396.407	8			

Multiple Comparisons

Tukey HSD

Dependent Variable	(I) Treatment	(J) Treatment	Mean Difference (I-J)	Std. Error	Sig.	95% Confidence Interval	
						Lower Bound	Upper Bound
pH	Control	EAPR	-.97000*	.17920	.004	-1.5198	-.4202
		non-	-.96000*	.17920	.004	-1.5098	-.4102
	EAPR	Control	.97000*	.17920	.004	.4202	1.5198
		non-	.01000	.17920	.998	-.5398	.5598
	non-	Control	.96000*	.17920	.004	.4102	1.5098
		EAPR	-.01000	.17920	.998	-.5598	.5398
BOD	Control	EAPR	21.20000*	2.73455	.001	12.8096	29.5904
		non-	19.43333*	2.73455	.001	11.0430	27.8237
	EAPR	Control	-21.20000*	2.73455	.001	-29.5904	-12.8096
		non-	-1.76667	2.73455	.801	-10.1570	6.6237
	non-	Control	-19.43333*	2.73455	.001	-27.8237	-11.0430
		EAPR	1.76667	2.73455	.801	-6.6237	10.1570
Colour	Control	EAPR	93.33333*	21.94269	.013	26.0071	160.6595
		non-	110.00000*	21.94269	.006	42.6738	177.3262
	EAPR	Control	-93.33333*	21.94269	.013	-160.6595	-26.0071
		non-	16.66667	21.94269	.739	-50.6595	83.9929
	non-	Control	-110.00000*	21.94269	.006	-177.3262	-42.6738
		EAPR	-16.66667	21.94269	.739	-83.9929	50.6595
COD	Control	EAPR	16.66667	60.30785	.959	-168.3744	201.7077
		non-	-46.66667	60.30785	.731	-231.7077	138.3744
	EAPR	Control	-16.66667	60.30785	.959	-201.7077	168.3744
		non-	-63.33333	60.30785	.576	-248.3744	121.7077
	non-	Control	46.66667	60.30785	.731	-138.3744	231.7077
		EAPR	63.33333	60.30785	.576	-121.7077	248.3744

DO	Control	EAPR	3.21333*	.71795	.010	1.0105	5.4162
		non-	3.20667*	.71795	.010	1.0038	5.4095
	EAPR	Control	-3.21333*	.71795	.010	-5.4162	-1.0105
		non-	-.00667	.71795	1.000	-2.2095	2.1962
	non-	Control	-3.20667*	.71795	.010	-5.4095	-1.0038
		EAPR	.00667	.71795	1.000	-2.1962	2.2095
ORP	Control	EAPR	-1.63333	.79396	.179	-4.0694	.8027
		non-	-1.66667	.79396	.170	-4.1027	.7694
	EAPR	Control	1.63333	.79396	.179	-.8027	4.0694
		non-	-.03333	.79396	.999	-2.4694	2.4027
	non-	Control	1.66667	.79396	.170	-.7694	4.1027
		EAPR	.03333	.79396	.999	-2.4027	2.4694
Conductivity	Control	EAPR	-55.66667	67.03565	.700	-261.3504	150.0171
		non-	-54.66667	67.03565	.708	-260.3504	151.0171
	EAPR	Control	55.66667	67.03565	.700	-150.0171	261.3504
		non-	1.00000	67.03565	1.000	-204.6838	206.6838
	non-	Control	54.66667	67.03565	.708	-151.0171	260.3504
		EAPR	-1.00000	67.03565	1.000	-206.6838	204.6838
Turbidity	Control	EAPR	54.43333*	10.11002	.004	23.4130	85.4537
		non-	49.66667*	10.11002	.006	18.6463	80.6870
	EAPR	Control	-54.43333*	10.11002	.004	-85.4537	-23.4130
		non-	-4.76667	10.11002	.887	-35.7870	26.2537
	non-	Control	-49.66667*	10.11002	.006	-80.6870	-18.6463
		EAPR	4.76667	10.11002	.887	-26.2537	35.7870
TDS	Control	EAPR	-.03000	.01238	.113	-.0680	.0080
		non-	-.02567	.01238	.176	-.0637	.0123
	EAPR	Control	.03000	.01238	.113	-.0080	.0680
		non-	.00433	.01238	.935	-.0337	.0423
	non-	Control	.02567	.01238	.176	-.0123	.0637
		EAPR	-.00433	.01238	.935	-.0423	.0337
Ammonia	Control	EAPR	.72333	6.46040	.993	-19.0989	20.5456
		non-	3.52333	6.46040	.853	-16.2989	23.3456
	EAPR	Control	-.72333	6.46040	.993	-20.5456	19.0989
		non-	2.80000	6.46040	.903	-17.0223	22.6223
	non-	Control	-3.52333	6.46040	.853	-23.3456	16.2989
		EAPR	-2.80000	6.46040	.903	-22.6223	17.0223

*. The mean difference is significant at the 0.05 level.

APPENDIX 6

SPSS statistical analysis report for plant growth and chlorophyll contents (one-way ANOVA and Tukey's HSD post-hoc test)

ANOVA

		Sum of Squares	df	Mean Square	F	Sig.
Percentage_drop_weight	Between Groups	1289.921	2	644.961	14.011	.005
	Within Groups	276.194	6	46.032		
	Total	1566.115	8			
Total_chlorophyll	Between Groups	5.266	2	2.633	7.098	.026
	Within Groups	2.225	6	.371		
	Total	7.491	8			
Ratio_ab	Between Groups	.443	2	.221	6.416	.032
	Within Groups	.207	6	.035		
	Total	.650	8			

Post Hoc Tests

Multiple Comparisons

Tukey HSD

Dependent Variable	(I) Treatment	(J) Treatment	Mean Difference (I-J)	Std. Error	Sig.	95% Confidence Interval	
						Lower Bound	Upper Bound
Percentage_drop_weight	Control	EAPR	-26.88178*	5.53969	.007	-43.8791	-9.8845
		Phyto	-23.58920*	5.53969	.013	-40.5865	-6.5919
	EAPR	Control	26.88178*	5.53969	.007	9.8845	43.8791
		Phyto	3.29258	5.53969	.828	-13.7047	20.2899
	Phyto	Control	23.58920*	5.53969	.013	6.5919	40.5865
		EAPR	-3.29258	5.53969	.828	-20.2899	13.7047
Total_chlorophyll	Control	EAPR	1.14709	.49726	.131	-.3786	2.6728
		Phyto	1.85648*	.49726	.023	.3307	3.3822
	EAPR	Control	-1.14709	.49726	.131	-2.6728	.3786
		Phyto	.70939	.49726	.387	-.8164	2.2351
	Phyto	Control	-1.85648*	.49726	.023	-3.3822	-.3307
		EAPR	-.70939	.49726	.387	-2.2351	.8164
Ratio_ab	Control	EAPR	-.51820*	.15166	.033	-.9835	-.0529
		Phyto	-.40038	.15166	.085	-.8657	.0650
	EAPR	Control	.51820*	.15166	.033	.0529	.9835
		Phyto	.11782	.15166	.730	-.3475	.5832
	Phyto	Control	.40038	.15166	.085	-.0650	.8657
		EAPR	-.11782	.15166	.730	-.5832	.3475

*. The mean difference is significant at the 0.05 level.

APPENDIX 7

SPSS statistical analysis report for Bioconcentration Factor (BCF) of leaf and root (two-way ANOVA)

Tests of Between-Subjects Effects

Dependent Variable: BCF_leaves

Source	Type III Sum of Squares	df	Mean Square	F	Sig.	Partial Eta Squared
Corrected Model	160490.841[a]	11	14590.076	5.000	.000	.696
Intercept	1020295.276	1	1020295.276	349.684	.000	.936
Metal	133842.313	5	26768.463	9.174	.000	.657
Treatment	1974.025	1	1974.025	.677	.419	.027
Metal * Treatment	24674.503	5	4934.901	1.691	.175	.261
Error	70026.386	24	2917.766			
Total	1250812.503	36				
Corrected Total	230517.227	35				

a. R Squared = .696 (Adjusted R Squared = .557)

Tests of Between-Subjects Effects

Dependent Variable: BCF_root

Source	Type III Sum of Squares	df	Mean Square	F	Sig.	Partial Eta Squared
Corrected Model	1357314123[a]	11	123392193.0	4.483	.001	.673
Intercept	1147657904	1	1147657904	41.699	.000	.635
Metal	1168309823	5	233661964.7	8.490	.000	.639
Treatment	68055845.16	1	68055845.16	2.473	.129	.093
Metal * Treatment	120948454.5	5	24189690.91	.879	.510	.155
Error	660545382.1	24	27522724.25			
Total	3165517410	36				
Corrected Total	2017859505	35				

a. R Squared = .673 (Adjusted R Squared = .523)

APPENDIX 8

SPSS statistical analysis report for Translocation Factor (TF) (two-way ANOVA)

Tests of Between-Subjects Effects

Dependent Variable: TF

Source	Type III Sum of Squares	df	Mean Square	F	Sig.	Partial Eta Squared
Corrected Model	1.964[a]	11	.179	8.012	.000	.786
Intercept	1.069	1	1.069	47.970	.000	.667
Metal	1.943	5	.389	17.433	.000	.784
Treatment	.006	1	.006	.273	.606	.011
Metal * Treatment	.016	5	.003	.139	.981	.028
Error	.535	24	.022			
Total	3.568	36				
Corrected Total	2.499	35				

a. R Squared = .786 (Adjusted R Squared = .688)

APPENDIX 9

SPSS statistical analysis report for heavy metal removal (two-way ANOVA)

Tests of Between-Subjects Effects

Dependent Variable: Percentageremoval

Source	Type III Sum of Squares	df	Mean Square	F	Sig.	Partial Eta Squared
Corrected Model	13788.304[a]	11	1253.482	6.344	.000	.744
Intercept	30909.742	1	30909.742	156.445	.000	.867
Metal	13615.252	5	2723.050	13.782	.000	.742
Treatment	41.024	1	41.024	.208	.653	.009
Metal * Treatment	132.028	5	26.406	.134	.983	.027
Error	4741.806	24	197.575			
Total	49439.852	36				
Corrected Total	18530.110	35				

a. R Squared = .744 (Adjusted R Squared = .627)

APPENDIX 10

SPSS statistical analysis report for antioxidative enzyme activities of *P. stratiotes* (two-way ANOVA)

Tests of Between-Subjects Effects

Dependent Variable: SOD

Source	Type III Sum of Squares	df	Mean Square	F	Sig.	Partial Eta Squared
Corrected Model	8.211[a]	3	2.737	3.350	.076	.557
Intercept	47.045	1	47.045	57.587	.000	.878
Tissue_type	.770	1	.770	.943	.360	.105
Group	.691	1	.691	.846	.385	.096
Tissue_type * Group	6.750	1	6.750	8.263	.021	.508
Error	6.535	8	.817			
Total	61.792	12				
Corrected Total	14.747	11				

a. R Squared = .557 (Adjusted R Squared = .391)

Tests of Between-Subjects Effects

Dependent Variable: APX

Source	Type III Sum of Squares	df	Mean Square	F	Sig.	Partial Eta Squared
Corrected Model	.112[a]	3	.037	1.397	.313	.344
Intercept	3.774	1	3.774	140.749	.000	.946
Tissue_type	.017	1	.017	.629	.451	.073
Group	.023	1	.023	.873	.377	.098
Tissue_type * Group	.072	1	.072	2.688	.140	.251
Error	.215	8	.027			
Total	4.101	12				
Corrected Total	.327	11				

a. R Squared = .344 (Adjusted R Squared = .098)

Tests of Between-Subjects Effects

Dependent Variable: POX

Source	Type III Sum of Squares	df	Mean Square	F	Sig.	Partial Eta Squared
Corrected Model	11.770[a]	3	3.923	.726	.565	.214
Intercept	1195.145	1	1195.145	221.048	.000	.965
Tissue_type	3.098	1	3.098	.573	.471	.067
Group	.284	1	.284	.052	.825	.007
Tissue_type * Group	8.388	1	8.388	1.551	.248	.162
Error	43.254	8	5.407			
Total	1250.169	12				
Corrected Total	55.024	11				

a. R Squared = .214 (Adjusted R Squared = -.081)

APPENDIX 11

Gel electrophoresis for total RNA

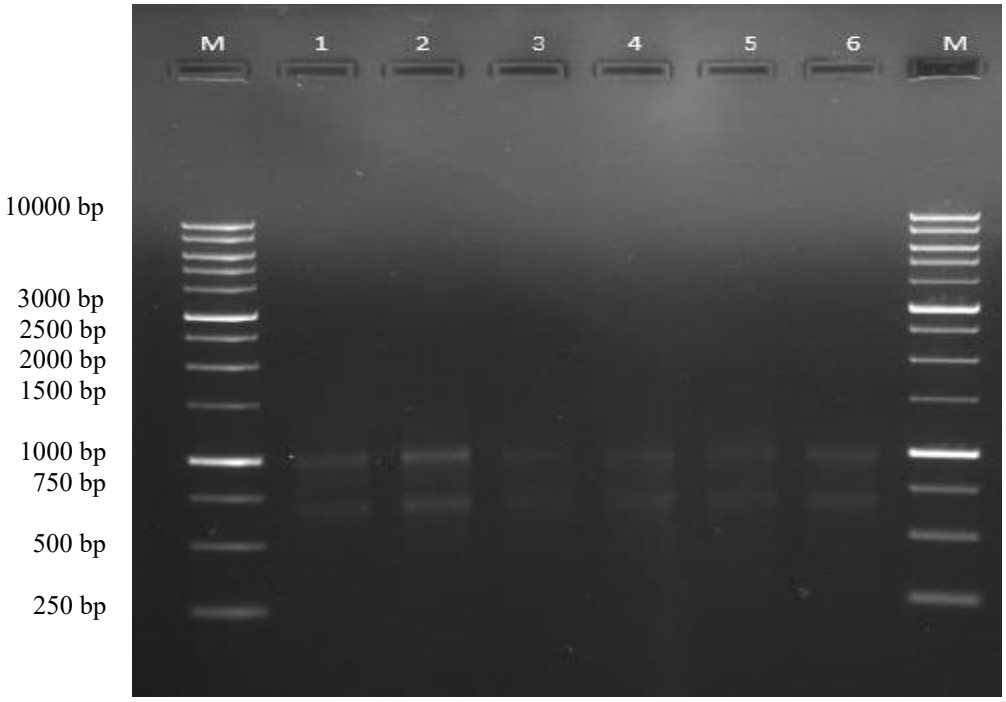

Line	Label	A260/280	Concentration (ng/ul)
M	1 kb DNA ladder	-	-
1	Total RNA of leaf sample *P. stratiotes* (control)	2.170	33.00
2	Total RNA of root sample *P. stratiotes* (control)	2.211	42.00
3	Total RNA of leaf sample *P. stratiotes* (non-EAPR)	2.255	24.00
4	Total RNA of root sample *P. stratiotes* (non-EAPR)	2.187	22.00
5	Total RNA of leaf sample *P. stratiotes* (EAPR)	2.263	32.00
6	Total RNA of root sample *P. stratiotes* (EAPR)	2.175	30.00

APPENDIX 12

qRT-PCR single reaction mixture

Component	Volume (µl)
2 X One Step SYBR Green mix	10.00
One Step SYBR Green Enzyme mix	1.00
Forward primer (10 µM)	0.40
Reverse primer (10 µM)	0.40
Distilled water	7.20
Total RNA (1 pg – 1 µg)	~1.00

APPENDIX 13

qRT-PCR reaction condition

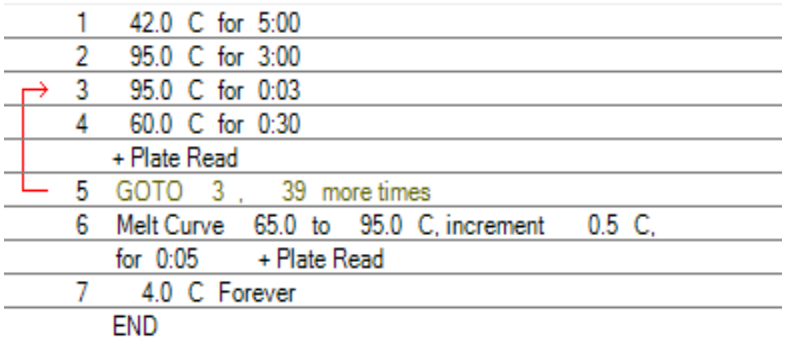

APPENDIX 14

qRT-PCR results

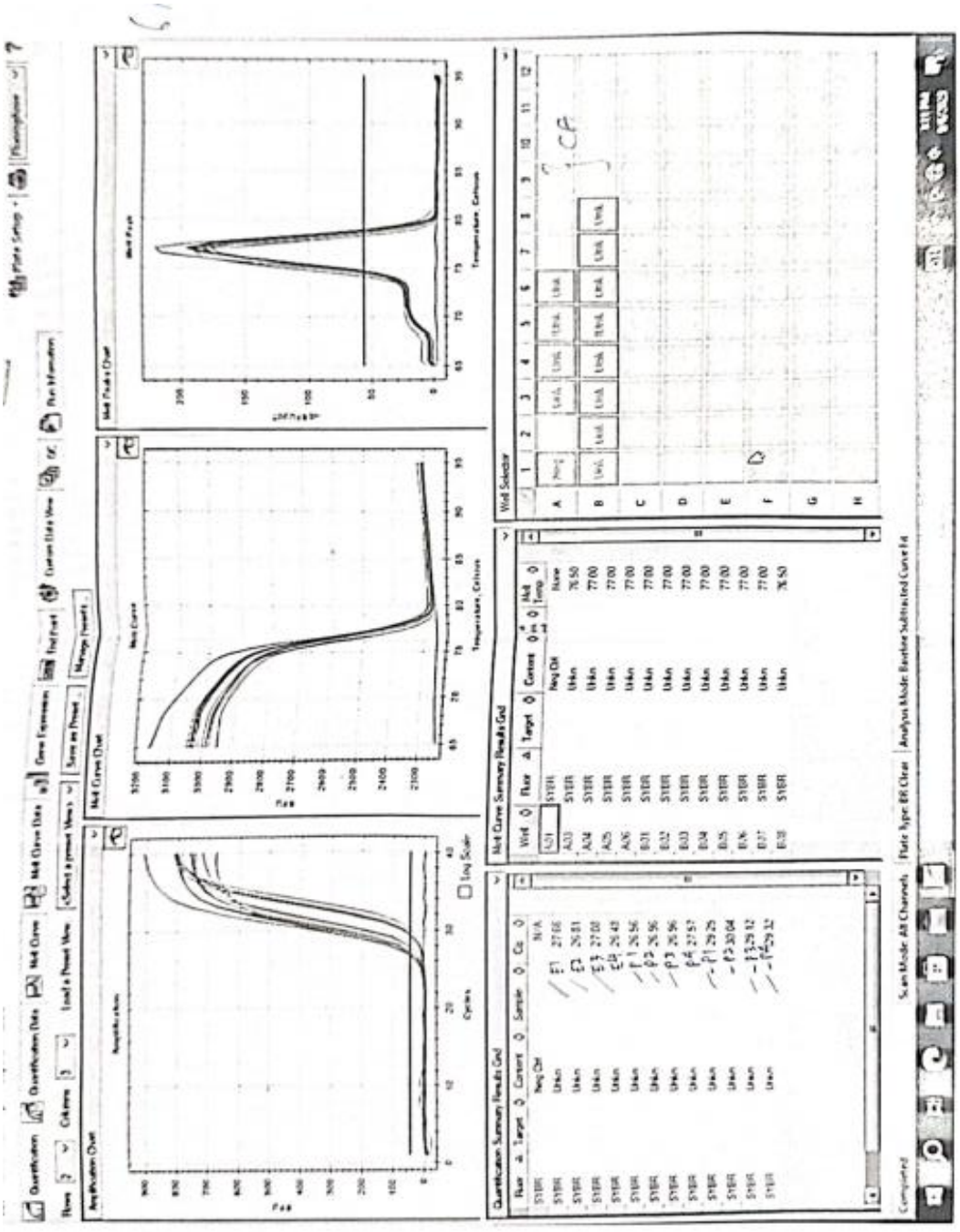

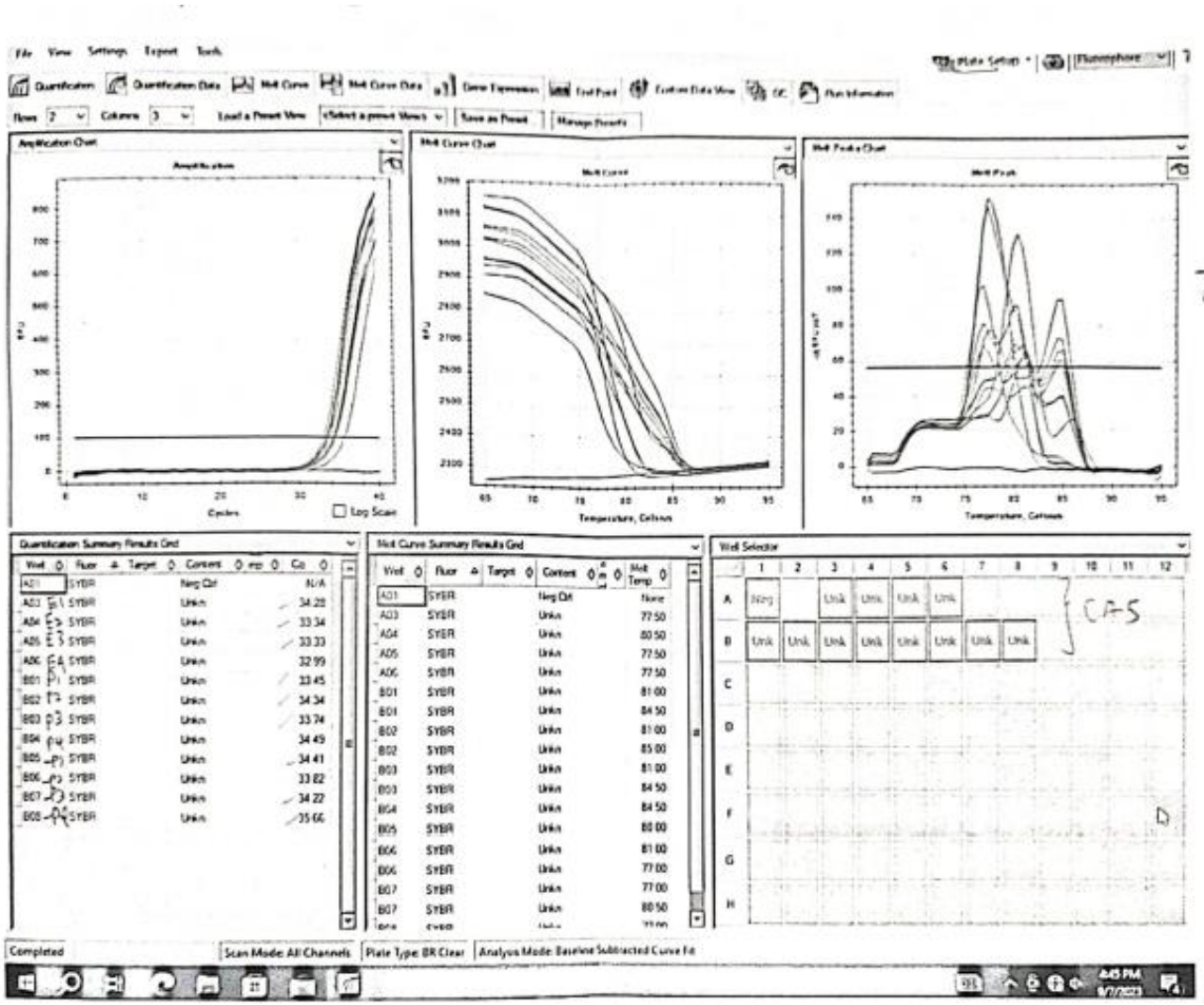
Amplification Chart
Melt Curve Chart
Melt Peaks Chart
Quantification Summary Results Grid
Melt Curve Summary Results Grid
Well Selector
Completed
Scan Mode: All Channels
Plate Type: BR Clear
Analysis Mode: Baseline Subtracted Curve Fit
719
CA-5

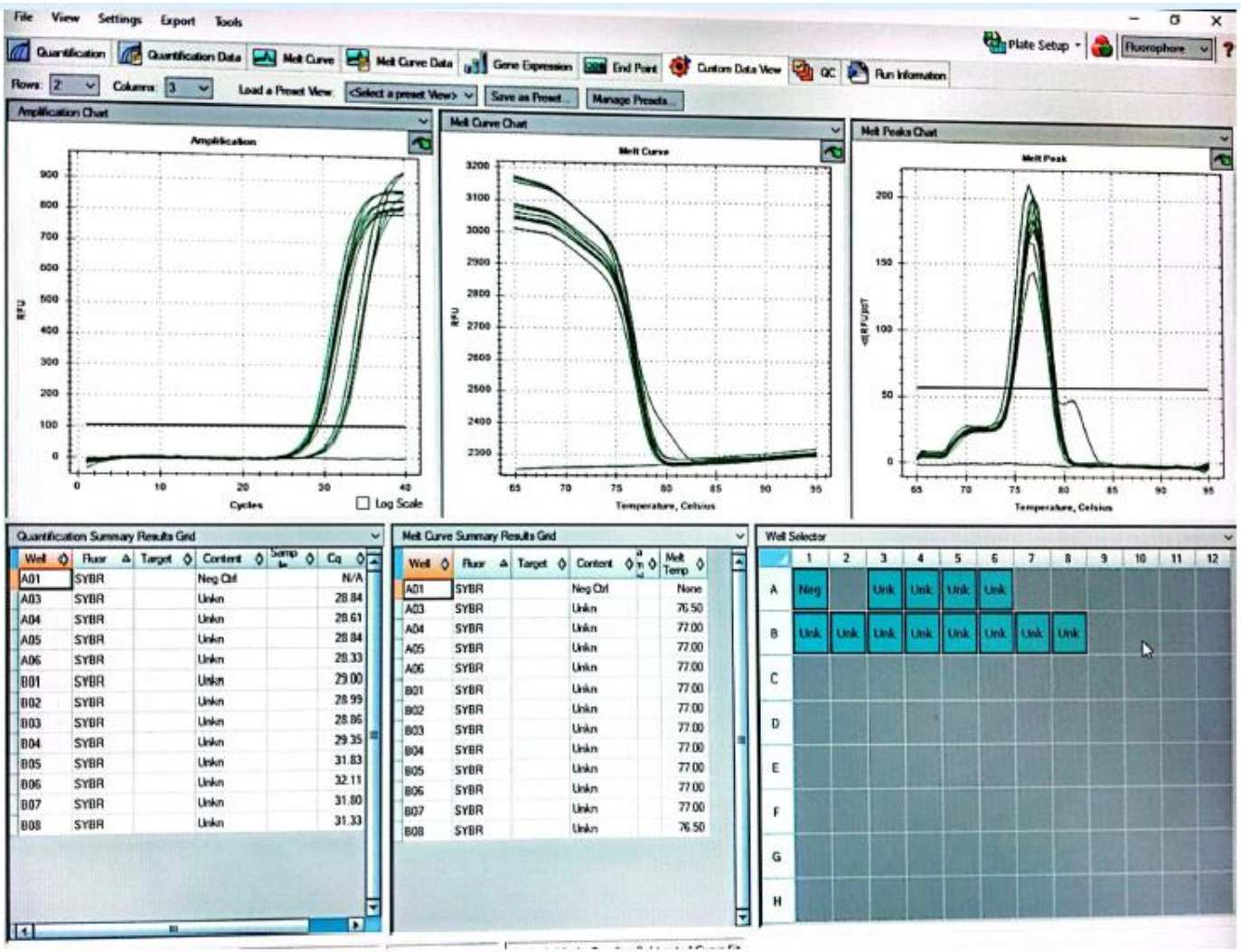
File View Settings Export Tools
Quantification
Quantification Data
Melt Curve
Melt Curve Data
Gene Expression
End Point
Custom Data View
QC
Run Information
Plate Setup
Fluorophore
Flows: 2
Columns: 3
Load a Preset View
<Select a preset View>
Save as Preset...
Manage Presets...
Amplification Chart
Amplification
RFU
Cycles
Log Scale
Melt Curve Chart
Melt Curve
RFU
Temperature, Celsius
Melt Peaks Chart
Melt Peak
-d(RFU)/dT
Temperature, Celsius
Quantification Summary Results Grid
Well | Fluor | Target | Content | Cq
A01 SYBR Neg Ctrl N/A
A03 SYBR Unkn 28.84
A04 SYBR Unkn 28.61
A05 SYBR Unkn 28.84
A06 SYBR Unkn 28.33
B01 SYBR Unkn 29.00
B02 SYBR Unkn 28.99
B03 SYBR Unkn 28.86
B04 SYBR Unkn 29.35
B05 SYBR Unkn 31.83
B06 SYBR Unkn 32.11
B07 SYBR Unkn 31.80
B08 SYBR Unkn 31.33
Melt Curve Summary Results Grid
Well | Fluor | Target | Content | Melt Temp
A01 SYBR Neg Ctrl None
A03 SYBR Unkn 76.50
A04 SYBR Unkn 77.00
A05 SYBR Unkn 77.00
A06 SYBR Unkn 77.00
B01 SYBR Unkn 77.00
B02 SYBR Unkn 77.00
B03 SYBR Unkn 77.00
B04 SYBR Unkn 77.00
B05 SYBR Unkn 77.00
B06 SYBR Unkn 77.00
B07 SYBR Unkn 77.00
B08 SYBR Unkn 76.50
Well Selector
1 2 3 4 5 6 7 8 9 10 11 12
A Neg Unk Unk Unk Unk
B Unk Unk Unk Unk Unk Unk Unk Unk
C
D
E
F
G
H

CAL

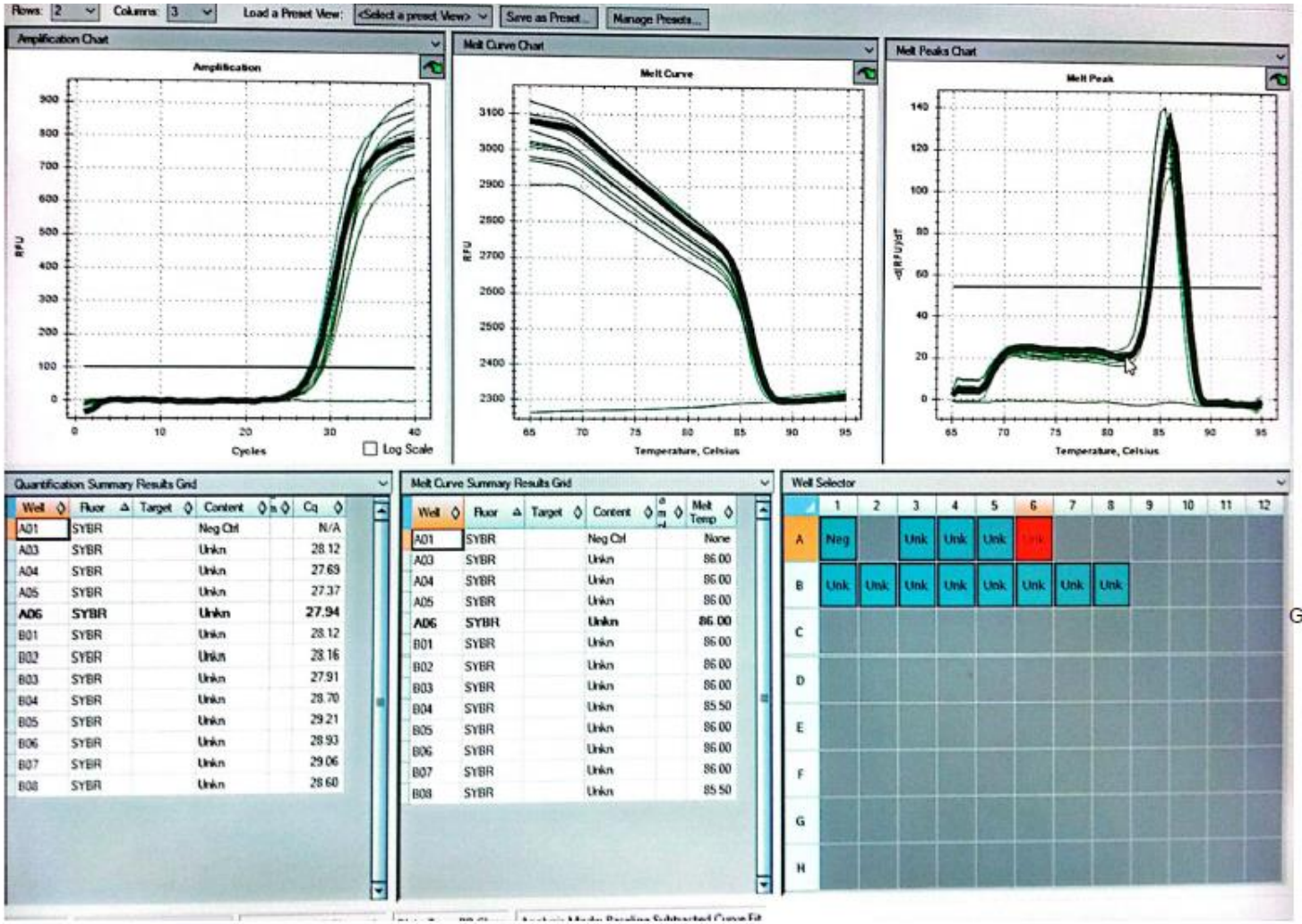
Rows: 2
Columns: 3
Load a Preset View:
<Select a preset View>
Save as Preset...
Manage Presets...
Amplification Chart
Amplification
RFU
Cycles
Log Scale
Melt Curve Chart
Melt Curve
RFU
Temperature, Celsius
Melt Peaks Chart
Melt Peak
-d(RFU)/dT
Temperature, Celsius
Quantification Summary Results Grid
Well | Fluor | Target | Content | Cq
A01 SYBR Neg Ctrl N/A
A03 SYBR Unkn 28.12
A04 SYBR Unkn 27.69
A05 SYBR Unkn 27.37
A06 SYBR Unkn 27.94
B01 SYBR Unkn 28.12
B02 SYBR Unkn 28.16
B03 SYBR Unkn 27.91
B04 SYBR Unkn 28.70
B05 SYBR Unkn 29.21
B06 SYBR Unkn 28.93
B07 SYBR Unkn 29.06
B08 SYBR Unkn 28.60
Melt Curve Summary Results Grid
Well | Fluor | Target | Content | Melt Temp
A01 SYBR Neg Ctrl None
A03 SYBR Unkn 86.00
A04 SYBR Unkn 86.00
A05 SYBR Unkn 86.00
A06 SYBR Unkn 86.00
B01 SYBR Unkn 86.00
B02 SYBR Unkn 86.00
B03 SYBR Unkn 86.00
B04 SYBR Unkn 85.50
B05 SYBR Unkn 86.00
B06 SYBR Unkn 86.00
B07 SYBR Unkn 86.00
B08 SYBR Unkn 85.50
Well Selector
1 2 3 4 5 6 7 8 9 10 11 12
A Neg Unk Unk Unk
B Unk Unk Unk Unk Unk Unk Unk Unk
C
D
E
F
G
H

GT

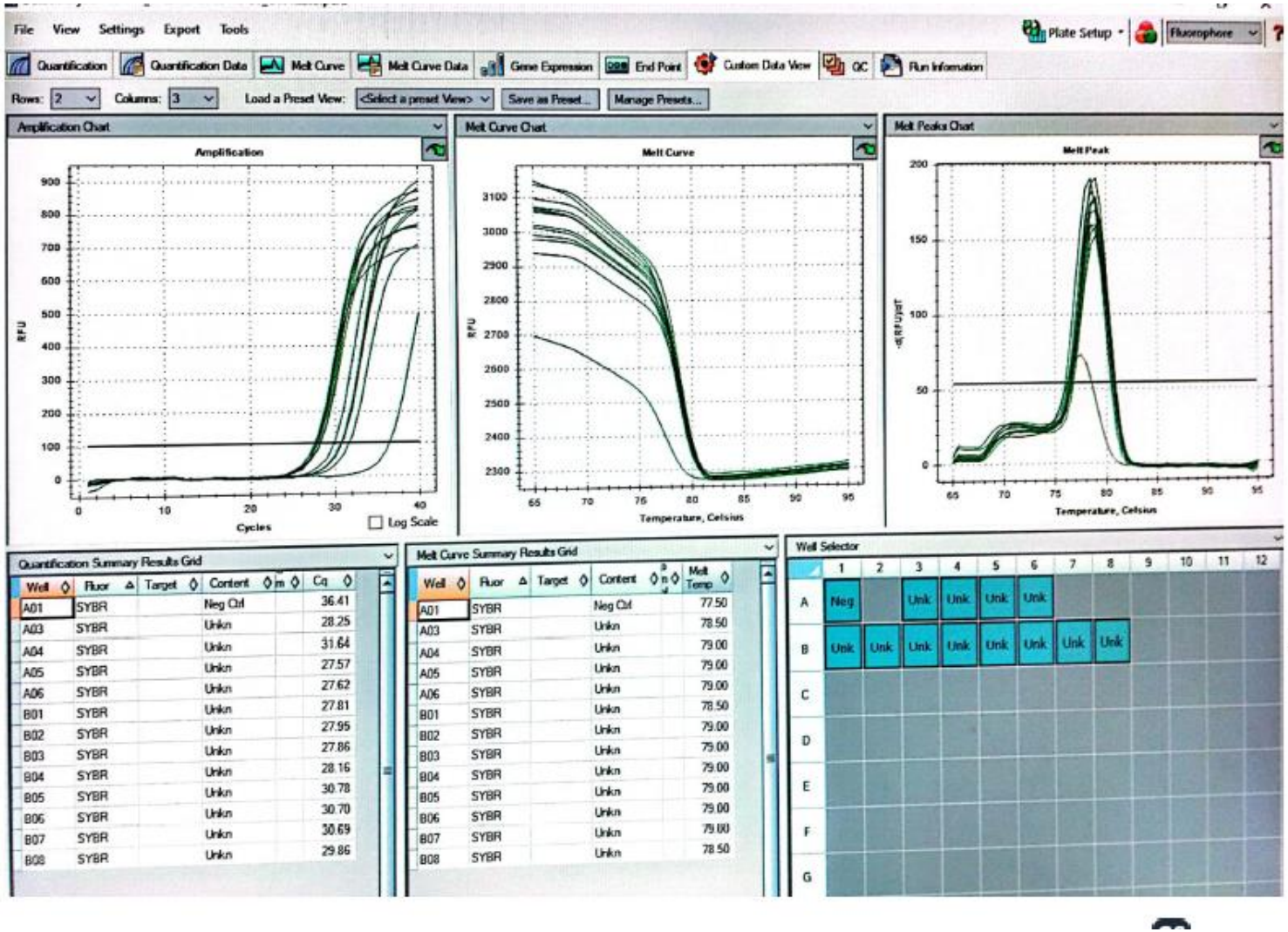
File View Settings Export Tools
Plate Setup
Fluorophore
Quantification
Quantification Data
Melt Curve
Melt Curve Data
Gene Expression
End Point
Custom Data View
QC
Run Information
Rows: 2
Columns: 3
Load a Preset View: <Select a preset View>
Save as Preset...
Manage Presets...
Amplification Chart
Amplification
RFU
Cycles
Log Scale
Melt Curve Chart
Melt Curve
RFU
Temperature, Celsius
Melt Peaks Chart
Melt Peak
-d(RFU)/dT
Temperature, Celsius
Quantification Summary Results Grid
Well Fluor Target Content Cq
A01 SYBR Neg Ctrl 36.41
A03 SYBR Unkn 28.25
A04 SYBR Unkn 31.64
A05 SYBR Unkn 27.57
A06 SYBR Unkn 27.62
B01 SYBR Unkn 27.81
B02 SYBR Unkn 27.95
B03 SYBR Unkn 27.86
B04 SYBR Unkn 28.16
B05 SYBR Unkn 30.78
B06 SYBR Unkn 30.70
B07 SYBR Unkn 30.69
B08 SYBR Unkn 29.86
Melt Curve Summary Results Grid
Well Fluor Target Content Melt Temp
A01 SYBR Neg Ctrl 77.50
A03 SYBR Unkn 78.50
A04 SYBR Unkn 79.00
A05 SYBR Unkn 79.00
A06 SYBR Unkn 79.00
B01 SYBR Unkn 78.50
B02 SYBR Unkn 79.00
B03 SYBR Unkn 79.00
B04 SYBR Unkn 79.00
B05 SYBR Unkn 79.00
B06 SYBR Unkn 79.00
B07 SYBR Unkn 79.00
B08 SYBR Unkn 78.50
Well Selector
1 2 3 4 5 6 7 8 9 10 11 12
A Neg Unk Unk Unk Unk
B Unk Unk Unk Unk Unk Unk Unk Unk
C
D
E
F
G

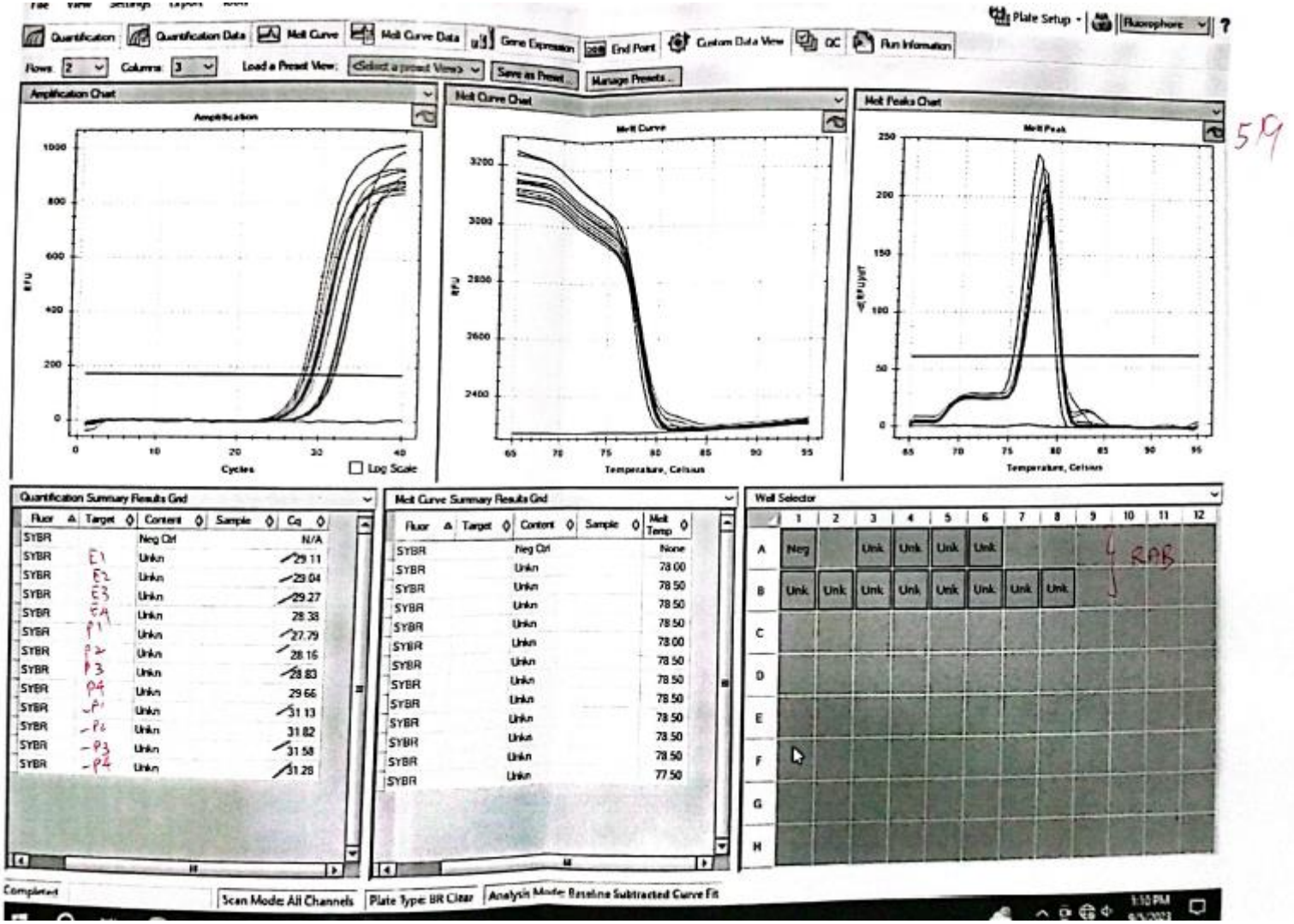
Quantification
Quantification Data
Melt Curve
Melt Curve Data
Gene Expression
End Point
Custom Data View
QC
Run Information
Plate Setup
Fluorophore
Amplification Chart
Melt Curve Chart
Melt Peaks Chart
Cycles
Log Scale
Temperature, Celsius
Quantification Summary Results Grid
Melt Curve Summary Results Grid
Well Selector
Scan Mode: All Channels
Plate Type: BR Clear
Analysis Mode: Baseline Subtracted Curve Fit

APPENDIX 15

The MAPK signaling pathway – plant

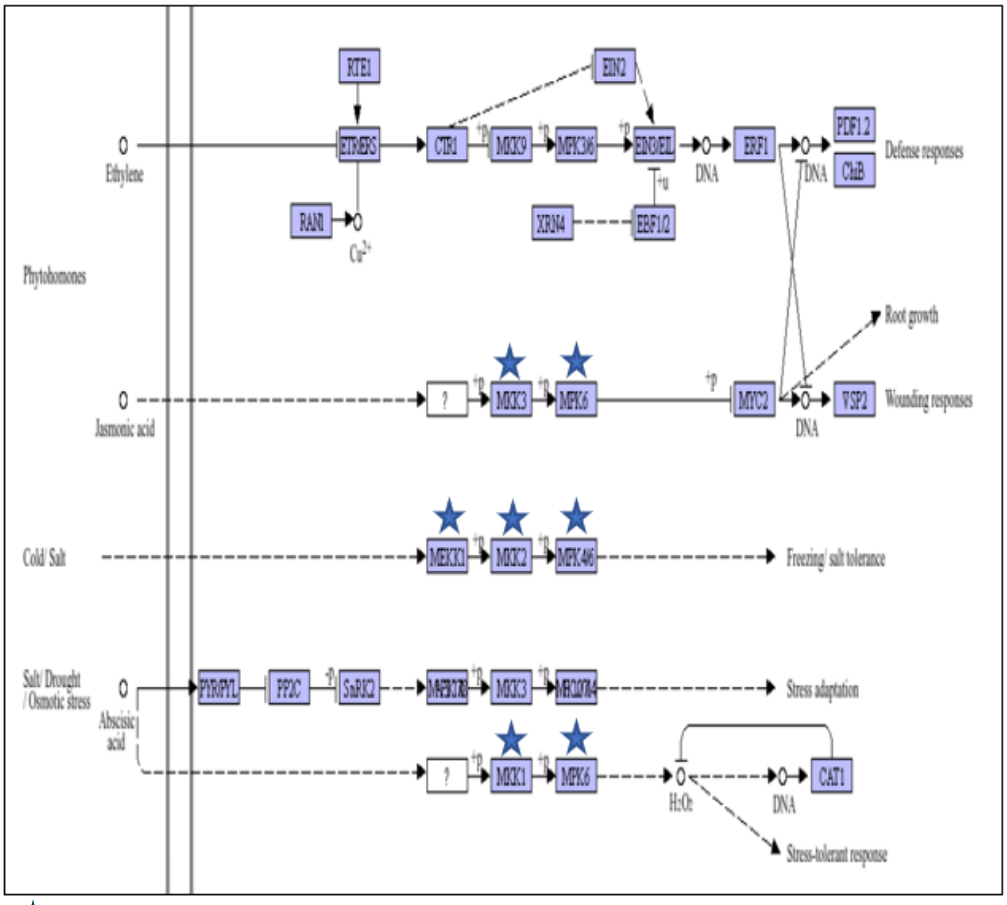

[★ sign corresponds to the encoded enzymes from the KEGG database ko04016 (adopted from KEGG BRITE Database, 2025)]

APPENDIX 16

List of MKK3 enzymes

No	GeneID	With_Pb_root_readcount	No_Pb_root_readcount	log2FoldChange	pval	padj	Gene Length
1	Cluster-109234.0	1.745424371	0.110459206	3.946187334	6.45E-09	1.22E-07	713
2	Cluster-147115.2335	0.84704418	0	8.161725386	8.20E-08	1.27E-06	347
3	Cluster-20134.0	0.539028115	0	7.512524626	1.27E-05	0.0001207	1111
4	Cluster-20881.0	0.539028115	0	7.512524626	1.27E-05	0.0001207	588

List of MPK6 enzymes

No	GeneID	With_Pb_root_readcount	No_Pb_root_readcount	log2FoldChange	pval	padj	Gene Length
1	Cluster-142041.0	1.052388224	0.220918413	2.236889874	0.000518548	0.00291808	1159
2	Cluster-37226.0	2.156112458	0.022091841	6.428881443	8.85E-13	3.18E-11	1126
3	Cluster-108412.0	4.876921037	0.243010254	4.310244243	1.31E-13	5.32E-12	1136
4	Cluster-16681.0	0.308016065	0	6.71108328	0.00085757	0.00442168	409
5	Cluster-124463.0	2.977488633	0.088367365	5.028212095	1.70E-13	6.82E-12	1560
6	Cluster-73563.0	0.821376175	0.022091841	5.039783425	1.30E-06	1.58E-05	802
7	Cluster-7414.0	0.513360109	0.044183683	3.45289991	0.000739506	0.00406026	659
8	Cluster-49763.0	3.721860791	0.552296032	2.745927701	1.43E-07	2.12E-06	1701

List of MEKK1enzymes

No	GeneID	With_Pb_root_readcount	No_Pb_root_readcount	log2FoldChange	pval	padj	Gene Length
1	Cluster-13494.2	6.904693468	0	11.18436697	2.92E-24	5.45E-22	1174
2	Cluster-147115.2334	3.644856775	0	10.26320607	2.45E-18	2.04E-16	341
3	Cluster-13494.1	3.080160655	0	10.02056475	6.31E-17	4.21E-15	1042
4	Cluster-21412.1	3.054492649	0	10.00850359	8.55E-17	5.60E-15	685
5	Cluster-8666.0	1.617084344	0	9.092210188	7.81E-12	2.39E-10	758
6	Cluster-13402.0	1.540080327	0	9.021953019	1.63E-11	4.76E-10	688
7	Cluster-25375.0	1.001052213	0	8.401958214	7.89E-09	1.46E-07	602
8	Cluster-14516.0	1.001052213	0	8.401958214	7.89E-09	1.46E-07	633
9	Cluster-11374.0	0.667368142	0	7.819126707	1.09E-06	1.34E-05	668
10	Cluster-23487.0	0.616032131	0	7.704181747	3.61E-06	3.99E-05	473
11	Cluster-19179.0	0.616032131	0	7.704181747	3.61E-06	3.99E-05	434
12	Cluster-14936.0	0.616032131	0	7.704181747	3.61E-06	3.99E-05	544
13	Cluster-27772.0	0.590364125	0	7.643081957	5.45E-06	5.77E-05	727
14	Cluster-17888.0	0.539028115	0	7.512524626	1.27E-05	0.00012071	429
15	Cluster-25178.2	0.539028115	0	7.512524626	1.27E-05	0.00012071	415
16	Cluster-20567.0	0.539028115	0	7.512524626	1.27E-05	0.00012071	397
17	Cluster-4834.0	0.487692104	0	7.368966156	3.05E-05	0.00026017	499
18	Cluster-27424.0	0.385020082	0	7.030254722	0.000193974	0.0012831	369
19	Cluster-24208.0	0.385020082	0	7.030254722	0.000193974	0.0012831	669
20	Cluster-20932.0	0.385020082	0	7.030254722	0.000193974	0.0012831	544
21	Cluster-22759.0	0.359352076	0	6.931507201	0.000315208	0.00193211	385
22	Cluster-28789.0	0.333684071	0	6.82550087	0.000517265	0.00291222	479
23	Cluster-16698.0	0.308016065	0	6.71108328	0.00085757	0.00442168	377
24	Cluster-3009.0	0.308016065	0	6.71108328	0.00085757	0.00442168	418

List of MKK2 enzymes

No	GeneID	With_Pb_root_readcount	No_Pb_root_readcount	log2FoldChange	pval	padj	Gene Length
1	Cluster-109234.1	1.155060246	0.088367365	3.66434935	5.57E-07	7.33E-06	1053
2	Cluster-116901.0	1.540080327	0.419744984	1.868032284	0.000851639	0.00442168	1420
3	Cluster-5296.0	0.513360109	0	7.442530292	1.96E-05	0.00017659	537
4	Cluster-83348.0	0.436356093	0.022091841	4.131822627	0.000575412	0.00321408	396
5	Cluster-72543.0	4.2352209	0.662755238	2.670452993	1.26E-07	1.88E-06	1480
6	Cluster-18642.0	1.69408836	0	9.159204229	3.82E-12	1.23E-10	1029
7	Cluster-26083.0	1.617084344	0	9.092210188	7.81E-12	2.39E-10	738
8	Cluster-139752.0	3.336840709	0.839489968	1.987088533	6.42E-05	0.00051007	1501
9	Cluster-89921.0	3.978540846	0.044183683	6.399854508	8.27E-18	6.32E-16	1438
10	Cluster-6946.2	4.337892922	0	10.51415082	6.87E-20	7.15E-18	1369
11	Cluster-156182.0	14.78477114	1.259234953	3.550385425	2.01E-13	7.96E-12	2572
12	Cluster-66562.0	3.798864807	1.082500222	1.808377356	0.000178085	0.00123237	1666

List of MEK1, MKK1 enzyme

No	GeneID	With_Pb_root_readcount	No_Pb_root_readcount	log2FoldChange	pval	padj	Gene Length
1	Cluster-3350.0	5.903641255	0	10.95849977	9.18E-23	1.41E-20	1038

List of MPK4 enzyme

No	GeneID	With_Pb_root_readcount	No_Pb_root_readcount	log2FoldChange	pval	padj	Gene Length
1	Cluster-18696.0	12.2436386	0	12.01047971	6.09E-30	2.08E-27	1369

APPENDIX 17

Read count for genes in the root samples of EAPR and non-EAPR

Gene	Read count		
	Control	Non-EAPR	EAPR
CA	0.40	6.03	1.65
CA5	1.09	25.87	0.11
CAL	0.13	3.77	0.94
GT	4.02	20.64	8.29
GUA	1.44	23.02	7.13
RAB	0.91	9.37	2.70

APPENDIX 18

List of Publication

Chan, M.Y., Tee, C.S., Chai, T.T., Sim, Y.L. and Beh, W.L., 2022. Evaluation of electro-assisted phytoremediation (EAPR) system for heavy metal removal from synthetic leachate using *Pistia stratiotes. International Journal of Phytoremediation*, [e-journal] 24(13), pp.1376-1384. https://dx.doi.org/10.1080/15226514.2022.2031863.